



HAL
open science

Plant photodynamic stress: study of molecular and cellular mechanisms in plant and plant cells upon porphyrin treatment

Mohammad Issawi

► **To cite this version:**

Mohammad Issawi. Plant photodynamic stress: study of molecular and cellular mechanisms in plant and plant cells upon porphyrin treatment. Agronomy. Université de Limoges, 2018. English. NNT : 2018LIMO0081 . tel-02150080

HAL Id: tel-02150080

<https://theses.hal.science/tel-02150080v1>

Submitted on 7 Jun 2019

HAL is a multi-disciplinary open access archive for the deposit and dissemination of scientific research documents, whether they are published or not. The documents may come from teaching and research institutions in France or abroad, or from public or private research centers.

L'archive ouverte pluridisciplinaire **HAL**, est destinée au dépôt et à la diffusion de documents scientifiques de niveau recherche, publiés ou non, émanant des établissements d'enseignement et de recherche français ou étrangers, des laboratoires publics ou privés.



Université de Limoges

ED 614 - Chimie, Environnement, Géosciences, Agrosiences (CEGA)

Peirene EA 7500

Thèse pour obtenir le grade de
Docteur de l'Université de Limoges

Discipline/spécialité : Biosciences de l'environnement et de la santé/Sciences agronomiques et écologiques

Présentée et soutenue par
Mohammad ISSAWI

Le 6 juin 2018

Plant photodynamic stress: study of molecular and cellular mechanisms in plant and plant cells upon porphyrin treatment

Thèse dirigée par Catherine RIOU

JURY:

Rapporteurs

M. Tim Maisch, Pr., Department of dermatology, University Hospital Regensburg, Allemagne
Mme. Magali Gary-Bobo, Dr., Institut des biomolécules Max Mousseron, Université de Montpellier, France

Examineurs

M. Henri Batoko, Pr., Institute of life sciences, University of Louvain, Belgique
M. Vincent Sol, Pr., Peirene EA 7500, Université de Limoges, France
Mme. Stéphanie Leroy-Lhez, Dr., Peirene EA 7500, Université de Limoges, France
Mme. Catherine Riou, Dr., Peirene EA 7500, Université de Limoges, France

“Properly speaking, there are in the world no such men as self-made men.”

Frederick Douglass

“My philosophy of life is that if we make up our mind what we are going to make of our lives, then work hard toward that goal, we never lose. Somehow we win out.”

Ronald Reagan

“I am not a perfectionist, but I like to feel that things are done well. More important than that, I feel an endless need to learn, to improve, to evolve.”

Cristiano Ronaldo

Droits d'auteurs

Cette création est mise à disposition selon le Contrat :

« **Attribution-Pas d'Utilisation Commerciale-Pas de modification 3.0 France** »

disponible en ligne : <http://creativecommons.org/licenses/by-nc-nd/3.0/fr/>



Dedication

To the memory of my father who passed away 15 years ago... Dad, you are missed...
To my mother who knew it would be a long and hard road, but encouraged and supported me
along the way...
To my brother, Ahmad...
To my sister, Mariam...

Acknowledgements

Due to the lack of support to local PhD programs in science and the major challenge in seeking funding in my country Lebanon, I have applied for a PhD in plant biology in Limoges-France. I was accepted when I was still in Iran, doing my M2 internship (September 2014) thanks to my brother Ahmad Issawi, Dr. Catherine Riou and Pr. Vincent Sol for their help and support.

Over the past three years of my PhD (2015-2018) I have witnessed unforgettable memories that will remain engraved in my heart. All the work presented in the present manuscript involves many different people, from different places, but all of them contributed in various but important ways. This journey would not have been possible without the support of my family, mentors, and friends.

First of all, I owe a special debt of gratitude to all members of the jury starting with Pr. Tim Maisch and Dr. Magali Gary-bobo as referees. I had the honor to meet Pr. Maisch at Coimbra and I appreciate his discussion there and his acceptance to be a part of my thesis jury. I also thank Pr. Henri Batoko, Pr. Vincent Sol, Dr. Stéphanie Lery-Lhez and Dr. Catherine Riou for accepting to review my manuscript.

With a deep sense of gratitude, I would like to convey thanks to Pr. Vincent Sol, our lab-head, for accepting me to join his group. Monsieur Sol, it was my pleasure to be a member in your team, known for your humbleness despite your prestigious status as a professor in organic chemistry and a group leader. Scientists in Coimbra (Portugal) - where I have attended the international photodynamic association world congress - were very interested when they have realized that I am working within Pr. Sol's research team.

My sincerest thanks are extended to my PhD advisor Dr. Catherine Riou. Catherine, I cannot express to what extent I was lucky when you replied me by e-mail on September 3rd, 2014 confirming your acceptance to start a PhD under your guidance. Thereafter, I highly appreciated your patience and support facing the complications of the Lebanese university. I have always remembered my first day in the lab (March 3rd, 2015) when I started to measure the hypocotyl and root length of in vitro growing tomato plantlets. I also remember our first meeting when you said that I must have three publications at the end of my thesis. And here I am ending with five publications as first author and two others as co-author. Over my three years I have always fascinated by your good mood and your funny jokes "à la Bretonne". Your strategical thinking and insightful leadership have inspired me, and I hope to work with you more and more. The Time wents so fast! (PS: Dorénavant je vais vous tutoyer).

I would like to thank Stephanie Leroy-Lhez whose "chemical" instructions and contributions always enlightening a lot our work. Special thanks for Céline Faugeron, I have gained a lot of experimental knowledge from her experience concerning GC and sugar analysis. I would like to thank also Yann Launay for his patience and his helpful contribution concerning starch granule microscopy.

Next, I am so grateful to Dr. Ahmad Kobeissi for his valuable cooperation and I am pleased that Mohammad Muhieddine (M2 student at the Lebanese university) has been contributed to my work.

I will never forget that wonderful time in Coimbra with Guillaume, Florent, Tan and the greatest Bertrand. "Come on!"

Thanks to Robert Granet, Olivier, Frédérique, Mark-Arthur, Shihong for your help concerning organic chemistry. Mark-Arthur, "ici c'est Madrid, Hala Madrid! y Viva CR7".

Thanks to Jeremy for your "phenalenonic" gifts and Cedric for sharing your knowledge about HPLC.

My next thanks are addressed to members of our lab: Nico, Amandine, CRICRI, Gaele, Idelette, Anais, Florian, Zineb, Soukaina, Roger, Dorothée and Michèle.

I also thank all Master 1 students who contributed to my work: Francois, David, Candice and Amy.

For Salim (my lab-mate) and Hajar, I will always remember our great moments and beautiful gatherings. Mec! rappelles toi toujours "Hala Madrid y nada mas". On va s'inscrire à la gym t'inquiète!

For Veronica, the dynamo of our lab and my "successor" working on plant-microbes-photosensitizers, you have all the ingredients for success. Hang in there!

For to the one and the only one, the greatest ever Holm Mustapha Amara! Words always fail to say something enough for you! Very and very briefly, your unique name fits you well.

I especially thank my family: Mom, Ahmad and Mariam, the true and the great supporters. Thank you for supporting me emotionally and financially, you should know that your support and encouragement was worth more than I can express on paper. I always knew that you believed in me and wanted the best for me. I would not have made it this far without you.

Table of content

Dedication	III
Acknowledgements.....	IV
Table of content.....	VI
List of figures.....	VIII
List of tables	IX
List of abbreviations.....	X
I. Introduction.....	1
I.1. Photosensitizers.....	1
I.1.1. General overview.....	1
I.1.2. Mechanisms of PS activation under light	1
I.1.3. Classification of PS.....	3
I.1.4. A great category of PS: the porphyrins.....	9
I.1.4.1. Porphyrin overview	9
I.1.4.2. Natural porphyrins and tetrapyrrole biosynthesis	12
I.2. Applications of PS	15
I.2.1. Photodynamic treatment in medicine.....	15
I.2.1.1. Photodynamic therapy against cancers	15
I.2.1.2. Photodynamic therapy against non-oncological diseases	16
I.2.1.3. Photodynamic therapy limitations	16
I.2.2. Antimicrobial photodynamic treatment (APDT).....	17
I.2.2.1. APDT in medical environment.....	17
I.2.2.2. APDT for water sewage	18
I.2.2.3. APDT for food decontamination.....	18
I.2.2.4. APDT in industrial domain	19
I.2.2.5. APDT in agronomy.....	19
I.2.3. PUBLICATION 1: Review “Plant photodynamic stress: what's new?”, Frontiers in Plant Science ..	20
II. PhD objectives	30
II. 1. APDT for plants: Is it a joke?	30
II. 2. Application of charged porphyrins on tobacco cell suspension: a help to understand how PS are photoactivated in plant cells	31
II. 3. Manuscript presentation	32
III. Results.....	33
Chapter I. APDT in agronomy: Dream or reality?	33
PUBLICATION 2: “Synergistic enhancement of tolerance mechanisms in response to photoactivation of cationic tetra (N-methylpyridyl) porphyrins in tomato plantlets”, Journal of Photochemistry and Photobiology B: Biology.....	34

PUBLICATION 3: “Responses of an adventitious fast-growing plant to photodynamic stress: comparative study of anionic and cationic porphyrin effect on <i>Arabidopsis thaliana</i> ”, <i>Physiologia Plantarum</i>	75
Discussion and perspectives	104
Chapter II. TBY-2 cells: a helpful tool to understand the cellular responses to photoactivated anionic porphyrin treatment from A to Z.....	106
PUBLICATION 4: “Unexpected features of exponentially growing Tobacco Bright Yellow-2 cell suspension culture in relation to excreted extracellular polysaccharides and cell wall composition”, <i>Glycoconjugate Journal</i>	107
PUBLICATION 5: “Characterization of pH dependent charge states and physico-chemical properties of anionic porphyrins” (Submitted to <i>Photochemical & Photobiological Sciences</i>).....	122
PUBLICATION 6: “Crossing the first threshold: New insights in the influence of chemical structure of anionic porphyrins from cell wall interactions to photodynamic cell death induction in TBY-2 suspension culture” (in preparation for submission to <i>The Plant Journal</i>).....	139
Discussion and perspectives	170
IV. General conclusion	173
V. Perspectives and outlook	174
References	177
Annex 1	188
Annex 2	189
Annex 3	190
Annex 4	191
Curriculum Vitae	192

List of figures

Figure 1. Photodynamic reactions of PS.	2
Figure 2. Porphyrinoids compounds.	3
Figure 3. Pigments of life: heme and chlorophyll.	10
Figure 4. Porphyrin absorption spectrum.	11
Figure 5. Structure of endogenous tetrapyrrolic photosensitizers.	13
Figure 6. Tetrapyrrole biosynthetic pathways in plants.	14
Figure 7. PDT application in cancer treatment.	16
Figure 8. APDT application for food decontamination.	18
Figure 9. APDT mechanism and its possible multiple targets in agronomy.	20
Figure 10. Schematic representation of the “two-in-one” strategy based on the use of PS in agronomy.	104
Figure 11. Structure of molecular dyad coupling TPPC with fluorescein via alkyne linker.	175

List of tables

Table 1. PS classification according to their origin.	9
Table 2. Cell wall composition of TBY-2 cells.	170

List of abbreviations

ALA: 5-aminolevulinic acid
APDT: Antimicrobial Photodynamic Treatment
BODIPY: Boron-dipyrromethene
CPO: Coproporphyrinogen oxidase
FeCH: Fe-chelatase
GluTS: Glutamyl t-RNA synthetase
GluTR: Glutamyl-tRNA reductase
GSA: Glutamate-1- semialdehyde aminotransferase
HP: Hematoporphyrin
HPD: Hematoporphyrin derivative
ISC: Intersystem Crossing
MgCH: Mg-chelatase
m-THPC: Metat-tetra (hydroxyphenyl) chlorin
PACT: Photoantimicrobial Chemotherapy
PBGD: Porphobilinogen deaminase
PDI: Photodynamic Inactivation
PDT: Photodynamic Therapy
PPO: Protoporphyrinogen oxidase
PS: Photosensitizer
ROS: Reactive Oxygen Species
S₀: Ground state
S₁: Excited singlet state
T₁: Excited triplet state
TBY-2: Tobacco Bright Yellow-2
THPP: Tetra-hydroxyphenyl porphyrin
TMPyP: Tetra (N-methylpyridyl) porphyrin

TPyP: tetra-pyridyl porphyrin

TPPC: Tetra (carboxyphenyl) porphyrin

TPPP: Tetra (phosphonatophenyl) porphyrin

TPPS: Tetra (sulfonatophenyl) porphyrin

TRX: Thioredoxin

UROD: Uroporphyrinogen decarboxylase

UROS: Uroporphyrinogen synthase

I. Introduction

I.1. Photosensitizers

I.1.1. General overview

Photosensitizers (PS) are conjugated chromophores that absorb ultraviolet or visible radiations and transfer energy to adjacent molecules (oxygen or other molecules) through photochemical reactions. Approximately 1000 B.C., Egyptians treated the skin pigment loss disease using a plant dried powder that contained psoralens which belong to furocoumarins, family of natural PS (Table 1, Joshi and Saenz 2013). In the beginning of the 20th century, PS and their applications became more and more investigated (Berg et al. 2005). The first photosensitization reaction was reported in 1900 when a German student called Oskar Raab discovered that acridine orange was toxic to the protozoan (*Paramecium caudatum*) in the presence of light (Van Straten et al. 2017). Four years later, his teacher Professor Hermann von Tappeiner demonstrated that the presence of oxygen was a prerequisite for the occurrence of photosensitization coining the term “photodynamic reaction”.

In parallel, Hill's studies on plant photosynthesis allowed to understand how the green pigments called chlorophylls could be excited by sunlight (Hill 1937). Afterward, the photosensitization mechanisms of chlorophyll were intensively studied and explored in the context of photosynthesis knowledge (Krasnovsky and Brin 1947, Evstigneev 1965, Krieger-liszkay 2004). There is no doubt that in the global process of photosynthesis, the photoreaction triggered by photoreceptors or PS named chlorophylls localized in chloroplasts of land plants and algae or cyanobacteria, has allowed life on earth with changes of atmosphere composition enriched in oxygen (Bassham 1959, Hohmann-marriott and Blankenship 2011).

From 1970s onwards, photodynamic reaction was largely investigated as potential tool for applications in medicine and struggle against microorganisms.

I.1.2. Mechanisms of PS activation under light

As a first step and to understand the potential applications of the PS in biological systems, the mechanism of PS photoactivation must be briefly described. Under light (UV-Visible), PS molecule jumps from a stable to an excited state. In presence of molecular oxygen, PS causes oxidative damages within biological systems. Illumination of a PS leads to the absorption of a photon and promotes the PS to its excited singlet state S₁. From this unstable and typically short-lived state, the

PS can return to its ground state S_0 by converting its energy into heat or fluorescence, a feature which can be used for the purposes of detection and optical monitoring. Alternatively, PS undergo intersystem crossing yielding PS in excited triplet state T_1 . In this T_1 state, the PS can relax through phosphorescence or react with other molecules to create chemically reactive species via two types of reactions (Figure 1). PS in T_1 can react with biological substrates and transfer an electron to generate radical anion or cation species. Typically, the PS reacts with an electron donating substrate to form PS that subsequently reacts with oxygen to form superoxide anion radicals, hydroxyl radicals and hydrogen peroxide. This is called type I reaction. In a type II reaction, excited PS reacts directly with molecular oxygen by transfer of energy to form singlet oxygen (1O_2) which is a highly reactive oxygen species.

Singlet oxygen and hydroxyl radical can directly react with nearly all biomolecules leading to oxidative damage. Hydrogen peroxide can be a part of a reaction that produces hydroxyl radical when it reacts with a metal via Fenton reaction ($Fe^{2+} + H_2O_2 \rightarrow \cdot OH + Fe^{3+} + ^-OH$). Most of PSs are thought to act through type II reactions where singlet oxygen is the main molecule causing oxidative cellular damage (Figure 1, Ding et al. 2012, Baptista et al. 2017).

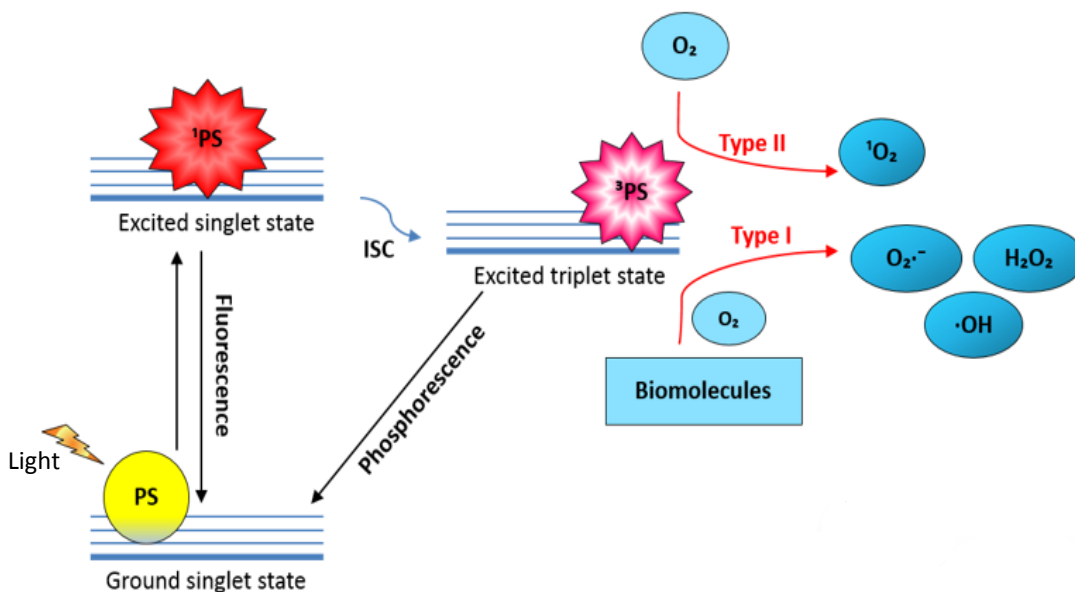


Figure 1. Photodynamic reactions of PS.

ISC: intersystem crossing, 1O_2 : singlet oxygen, $O_2^{\cdot-}$: superoxide anion, H_2O_2 : hydrogen peroxide, $\cdot OH$: hydroxyl radical, PS: photosensitizer in its ground state, 1PS : photosensitizer in its excited singlet state, 3PS : photosensitizer in its excited triplet state.

I.1.3. Classification of PS

PS can be distinguished between synthetic and naturally occurring compounds. Natural compounds are found in nature and can be extracted and modulated whereas synthetic compounds encompass all types of molecules that can be synthesized by chemical reactions such as porphyrins and derivatives, phthalocyanines, phenothiazines, xanthenes, corroles, squaraines and BODIPY.

PS can be classified into porphyrinoid and non-porphyrin molecules (Table 1).

- Porphyrinoid compounds have tetrapyrrolic backbone and are the most useful PS in medicine and in the perspective of environmental applications due to their highly conjugated structure and absorption of light in the visible region (Figure 2).

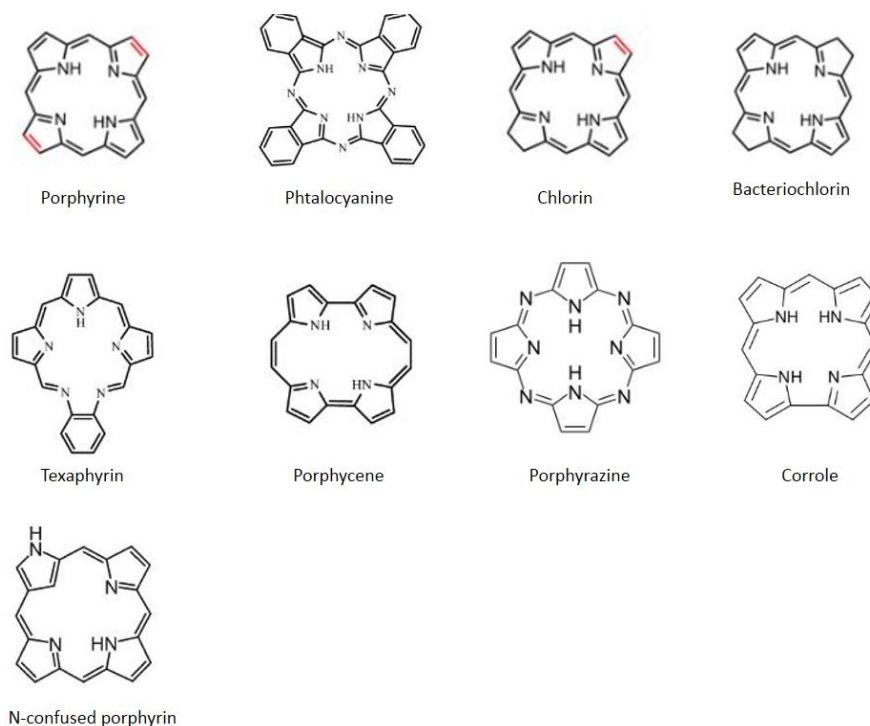
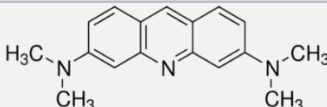
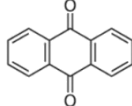
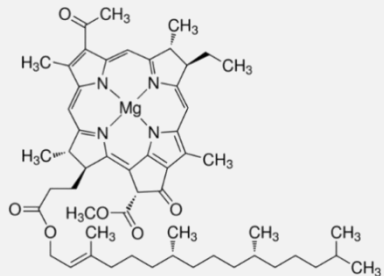
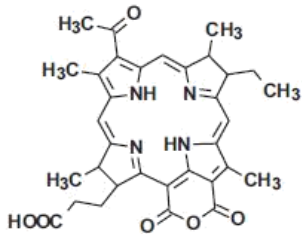
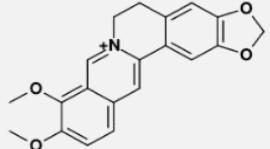
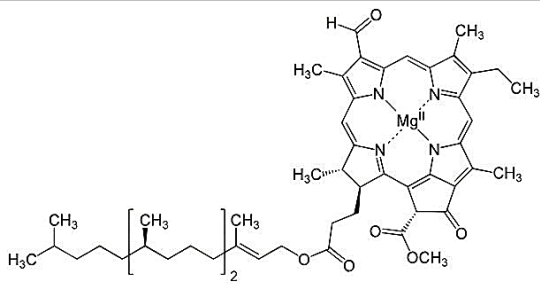
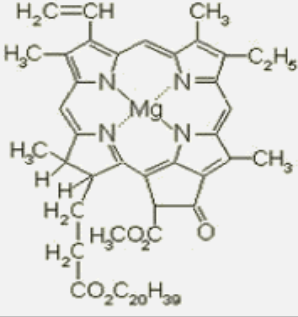
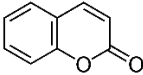
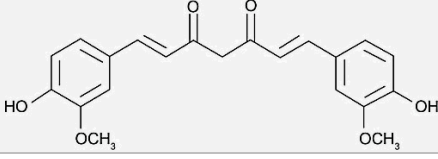

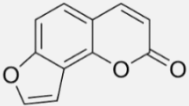
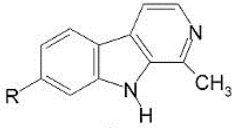
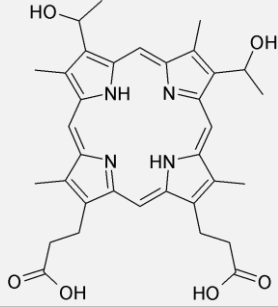
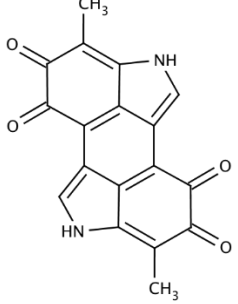


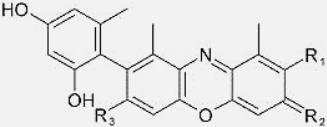
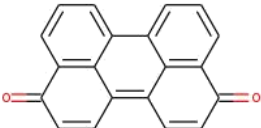
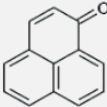
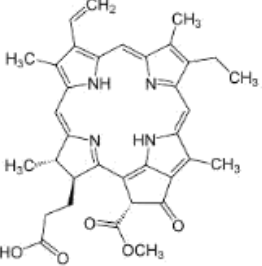
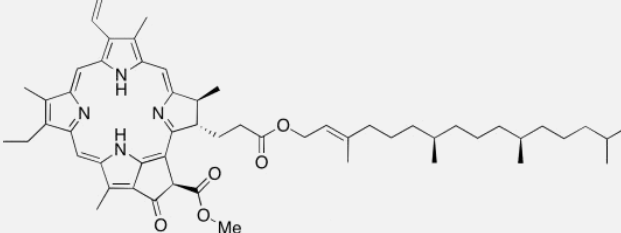
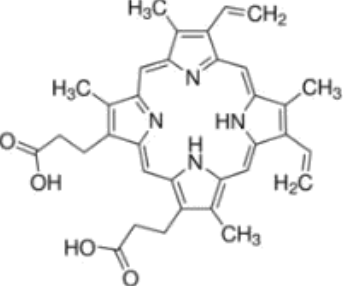
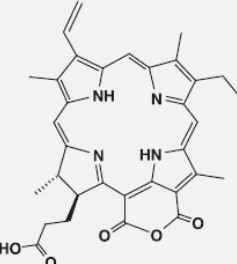
Figure 2. Porphyrinoids compounds.

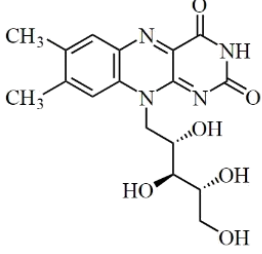
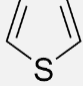
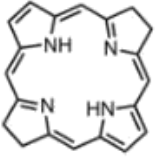
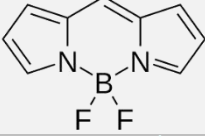
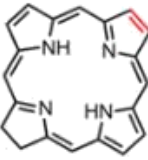
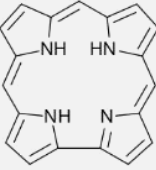
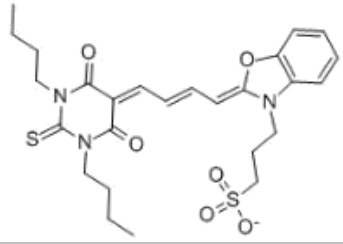
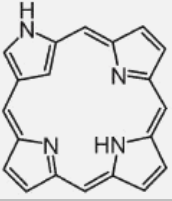
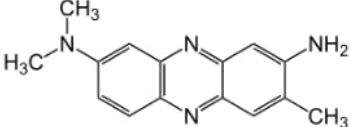
An extended family of photosensitizers bearing a tetrapyrrole macrocycle and show different structural features as N distribution, group substitution and redox state. They have the most useful applications as photodynamic compounds.

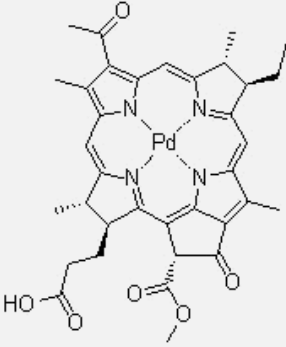
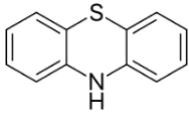
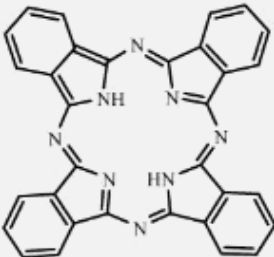
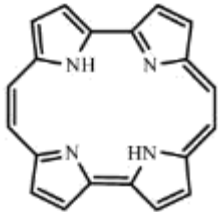
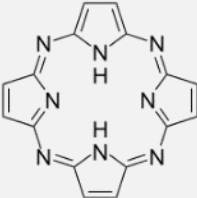
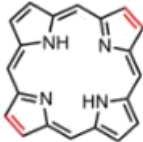
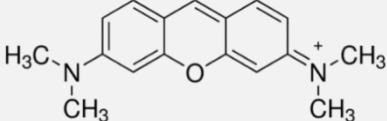
- Non-porphyrin compounds encompass among others anthraquinone, phenothiazine, xanthene, curcumine, and phenalenone. Although these compounds are not yet clinically approved, they were tested in clinical trials in addition to their efficient use as antimicrobials (Table 1).

	Name	Structure	References
Natural	Acridine orange		Matsubara et al. 2010
	Anthraquinone		Montoya et al. 2005
	Bacteriochlorophyll		Henderson et al. 1991
	Bacteriopurpurin 18 (semisynthetic)		Drogat et al. 2013
	Berberine		Molero et al. 1985
	Chlorophyll		Song et al. 2014

Chlorophyllin (semi synthetic)		Azizullah et al. 2014, Hader et al. 2016
Coumarin		De menezes et al. 2014a , Fracarolli et al. 2016
Curcumin		Spaeth et al. 2017
Fullerene		Dagani 1992
Furocoumarin		De Menezes et al. 2014a , Fracarolli et al. 2016
Harmine		Hazen and Gutierrez- Gonzalves 1988
Hematoporphyrin (semi synthetic)		Hazen et al. 1987
Melanin		Liu et al. 2015

Orcein		Molero and Hazen 1988
Perylenequinone		Daub et al. 2005
Phenalenone		Nazir et al. 2015 Song et al. 2017 Muehler et al. 2017
Pheophorbide		Yoon et al. 2014
Pheophytin		Hsu et al. 2010
Protoporphyrin IX		Yoshida et al. 2017, Delcanale et al. 2016
Purpurin 18 (semi synthetic)		Drogat et al. 2011

	Riboflavin		Maisch et al. 2014
	Thiophene		Dicosmo et al. 1982, Ebermann et al. 1996
Synthetic	Bacteriochlorin		Juzenienne 2009
	BODIPY		Durantini et al. 2018
	Chlorine		Juzenienne 2009
	Corrole		Pohl et al. 2014
	Merocyanine		Sieber et al. 1989
	N-confused porphyrin		Thomas et al. 2012
		Neutral red	

<p>Pd-Bacteriopheophorbide (Tookad®)</p>		<p>Azzouzi et al. 2013</p>
<p>Phenothiazine dyes</p>		<p>Monteiro et al. 2017</p>
<p>Phthalocyanine</p>		<p>Dumoulin et al. 2010</p>
<p>Porphycene</p>		<p>Ormond and Freeman 2013</p>
<p>Porphyrazine</p>		<p>Horne and Cronjé 2014</p>
<p>Porphyrin</p>		<p>Ormond and Freeman 2013, Abrahamse and Hamblin 2016, Almeida et al. 2011</p>
<p>Pyronin Y</p>		<p>Salci and Toprak 2015</p>

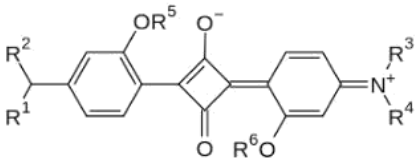
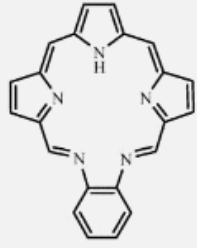
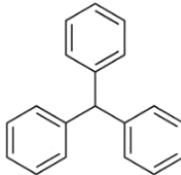
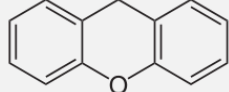
Squaraine		Babu et al. 2017
Texaphyrin		Sessler and Miller 2000
Triphenylmethane dyes		Tanaka et al. 2012, Junqueira et al. 2010, Davis et al. 2016
Xanthene dyes		Buck et al. 2017

Table 1. PS classification according to their origin.

Perylenquinone family including cercosporin and hypericin, phenothiazine family including methylene blue, toluidine blue, new methylene blue and xanthene family including rose Bengal, erythrosine, eosin Y, triphenylmethane dyes including crystal violet, malachite green, rhodamine have useful antimicrobial applications.

Although naturally occurring porphyrins like myoglobin, protoporphyrin IX are well employed as photosensitizing agents, porphyrin have been subjected to be synthesized and conjugated; synthetic porphyrins include Photofrin[®], TMPyP, TPPS etc. Chlorophyll, pheophorbide, pheophytine are naturally occurring chlorins meanwhile chlorin encompass several synthetic compounds as Foscan[®], Talaporphin[®] and Verteporphin[®]. As well, bacteriochlorin includes bacteriochlorophyll as natural compound and redaporphin[®] as synthetic drug. Anthraquinone, hypericin, phenalenone and fullerene can also be synthesized and functionalized yielding nuclear fast red, SGX301[®], SAPYR and cationic fullerene respectively. Although thiophenes are naturally synthesized photosensitizers by plants against fungi, synthetic thiophene-based organic dyes are used in PDT.

I.1.4. A great category of PS: the porphyrins

Among PS, porphyrins are remarkable complex chromophores and largely used for usual and recent applications from their first approved formulation (Photofrin[®] in 1970's) in medicine to environmental and industrial issues (Ormond and Freeman 2013).

I.1.4.1. Porphyrin overview

Porphyrins present unique structure consisting of a macrocycle core of four pyrrole rings linked by four methyne bridges. Porphyrins have an important characteristic, they have the capacity

to bind metal, very commonly iron and magnesium, in this form the metalloporphyrins gain their function as the key molecules of life. Indeed, heme, an iron-containing porphyrin, is the active cofactor for oxygen transport and storage (hemoglobin, myoglobin) and for the incorporation of molecular oxygen in organic substrates (cytochrome P450). Chlorophylls have a magnesium-chlorin playing role in light absorption and conversion for photosynthesis (Figure 3).

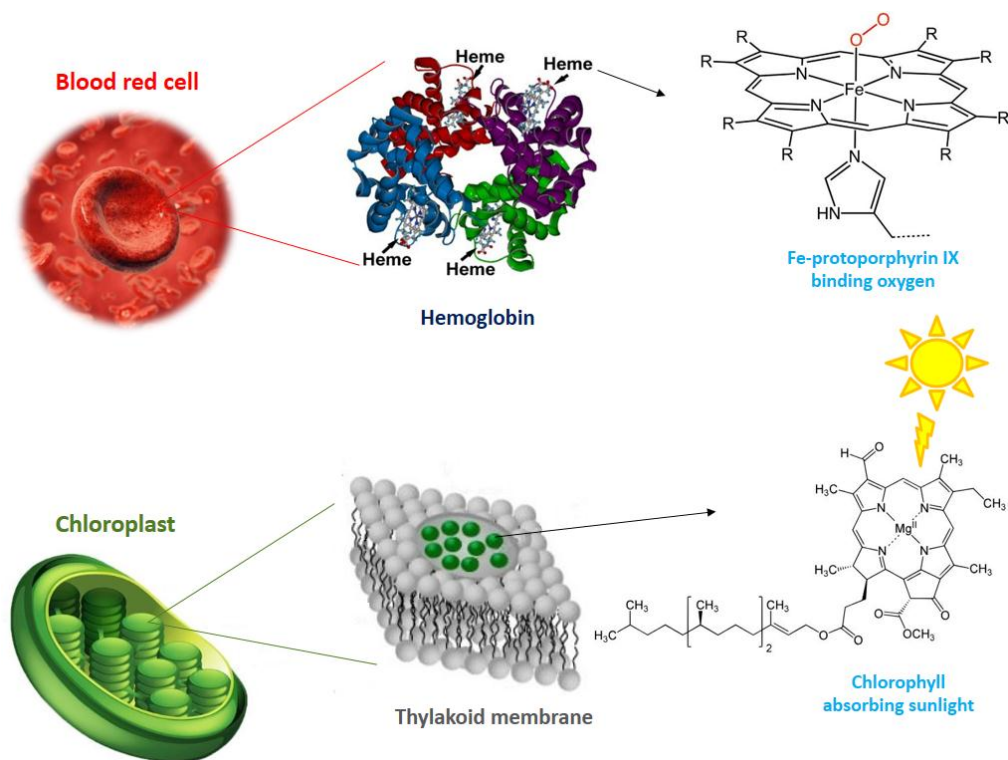


Figure 3. Pigments of life: heme and chlorophyll.

Heme b also known as Fe protoporphyrin IX is the prosthetic group of hemoglobin, a metalloprotein in blood red cells exerting their main role as oxygen transport. Chlorophylls are found in the membrane of thylakoids in chloroplasts of plants and algae, their role involve light absorption for photosynthesis.

Regarding synthetic porphyrins, metal coordination influences physicochemical properties as photon absorption, fluorescence, intersystem crossing, singlet oxygen quantum yield, photostability, lipophilicity and redox state. Therefore, biological outcomes are strongly correlated to metal magnetism, chemistry and size. Porphyrins complexed to paramagnetic metal fail to be useful in PDT due to their low fluorescence and poor ROS production. Hence the most used porphyrins in PDT are

Zn and Pd-coordinated. Moreover, these metalloporphyrins show some differences. For example, Pd-porphyrins are highly uptaken by biological cells comparing to Zn analogs owing to palladium small size and the absence of axial bonding. Moreover, Pd-porphyrins are more efficient to produce hydroxyl radical because they are better electron acceptor. In addition, subcellular localization and DNA photocleavage efficacy were not the same when comparing metalloporphyrins to their free-base counterparts (Guldi et al. 2000, Josefsen and Bowle 2008, Skwor et al. 2016, Dabrowski et al. 2016).

Porphyrins, either metalated or free base, exhibit a very characteristic absorption spectrum in the visible range (from 400 nm to 800 nm) due to several electronic transitions. Indeed, their UV-Visible spectrum shows an intense absorption band called Soret band in the near UV followed by four other absorption bands in the visible range called Q bands for free base porphyrin or two for metalloporphyrins (Figure 4).

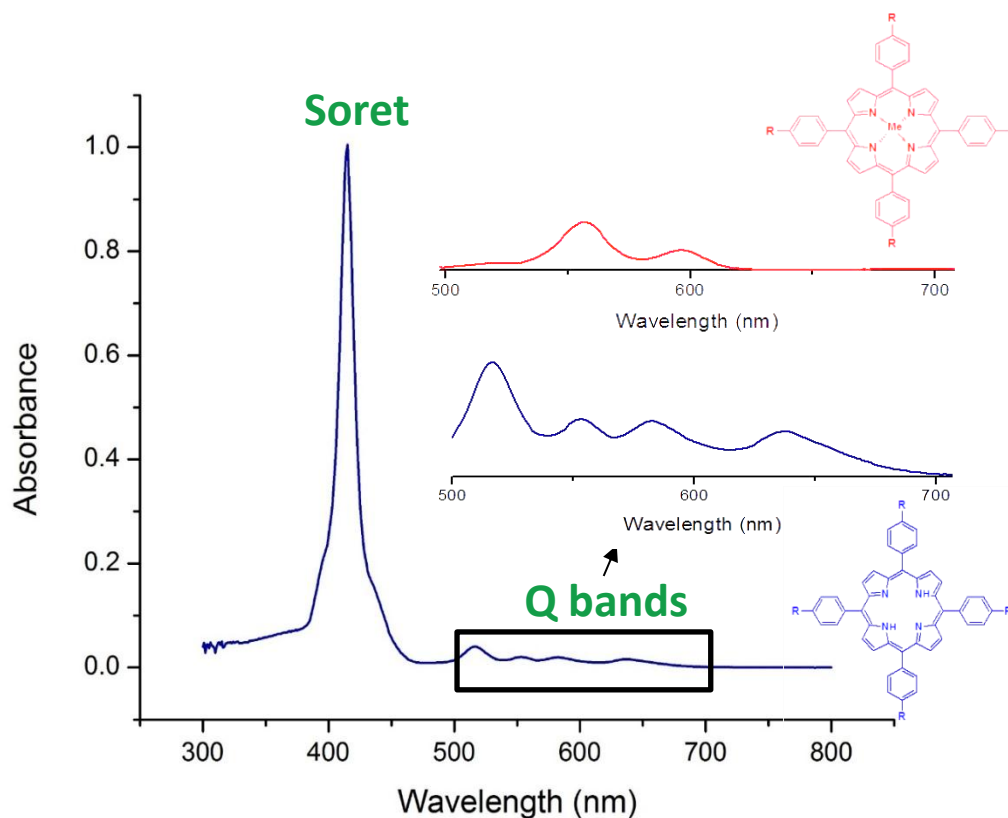


Figure 4. Porphyrin absorption spectrum.

Free base porphyrins (blue) show intensive absorption in the blue range assigned to soret band and 4 bands of lower intensity called Q bands in the visible range. Metalated porphyrins (red) show two Q bands instead of four bands.

Porphyrin emission is centered in the range 550-800 nm and metalloporphyrins show blueshifted fluorescence bands comparing to their free-base analogs (Valicsek and Horvath 2013). Most of porphyrins, mainly metalloporphyrins, exhibit poor quantum yields (usually lower than 0.2) relatively to other PS such as chlorins, bacteriochlorins and phthalocyanines (Barker et al. 2007, Mandal et al. 2016).

1.1.4.2. Natural porphyrins and tetrapyrrole biosynthesis

Endogenous tetrapyrroles are macrocyclic molecules playing crucial role in the vital process that are mandatory for diverse organism viability including light harvesting (chlorophylls), oxygen transport, oxidative phosphorylation, oxygen storage, nitrogen fixation, ROS scavenging (heme) (Battersby et al. 1980; Senge et al. 2015). Due to their chemical structure consisting of conjugated double bonds, metal coordination and the variation of external side chains, they acquire the capacity to absorb light and accept different redox state (Brzezowski et al. 2015). Their biosynthetic pathway is well established in mammals, plants as well as in microorganisms. The source of 5-aminolevulinic acid (5-ALA) which is the first common precursor can be either glycine plus succinyl-CoA (shemin pathway) or glutamate (C5 pathway), depending on the organisms. The shemin pathway operates in some bacteria, humans and yeast whereas C5 pathway exists in plants and most of bacteria.

The biosynthesis pathway presents two branching points. Firstly, serial enzymatic reactions - including the action of UROS - that convert ALA to uroporphyrinogen III, the first cyclic tetrapyrrole. Uroporphyrinogen III is at the first crossroad that leads to siroheme (synthesized in bacteria, yeast, and plants) and cobalamin B12 (synthesized in bacteria and archaea) and cofactor F430 (exists only in methanogenic bacteria) and coproporphyrinogen III through the intervention of coproporphyrinogen oxidase (Rodionov et al. 2003, Tripathy et al. 2010, Senge et al. 2014). Secondly, dominant reactions - including the action of protoporphyrinogen oxidase - lead to the production of protoporphyrin IX which is the first photoactive PS at the second branch point between iron branch leading to heme and magnesium branch leading to chlorophyll synthesis. The magnesium branch is unique for photosynthetic organisms and involves Mg-photosensitizers as Mg-protoporphyrin IX, Mg-protoporphyrin IX methylester, Mg-protochlorophyllide. Uroporphyrinogen III and coproporphyrinogen III become potent PS if any disturbance of that metabolic pathways takes place. Hence, it should be of importance to note that tetrapyrrole biosynthetic pathways are tightly

regulated and adjusted to the requirements of plants in order to avoid the generation of harmful PS (Figure 5 and Figure 6).

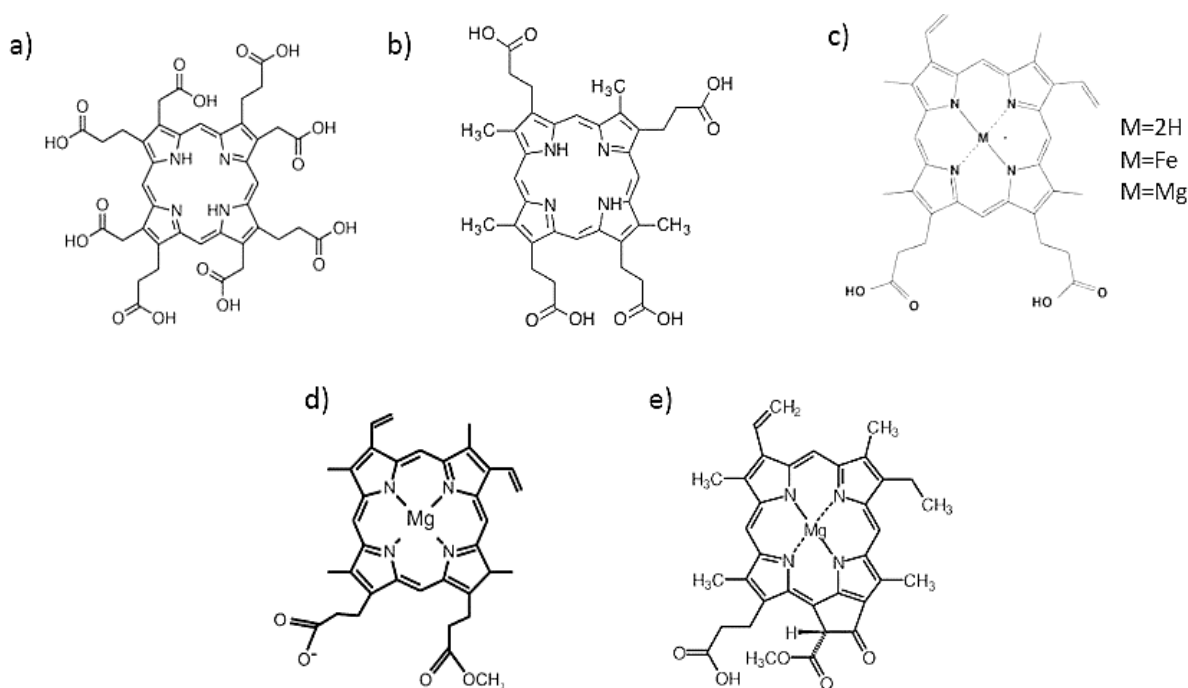


Figure 5. Structure of endogenous tetrapyrrolic photosensitizers.

a) uroporphyrin b) coproporphyrin c) protoporphyrin IX d) Mg-protoporphyrin IX methyl ester e) protochlorophyllide. These deleterious photosensitizers accumulate once disturbance in the tetrapyrrole biosynthetic pathway occurs. A metal M like iron and magnesium can be coordinated to the core of protoporphyrin IX to generate Fe-protoporphyrin IX in heme biosynthetic pathway and Mg-protoporphyrin IX in chlorophyll biosynthetic pathway. Mg-protoporphyrin IX, Mg-protoporphyrin IX methyl ester and protochlorophyllide exist mainly in plants.

The regulation of tetrapyrrolic pathway is mainly occurred at posttranslational level via modulating enzyme activities. Key regulators steps exist at the beginning, at the branching point heme/chlorophyll and at the end of this metabolic pathway. Moreover, the rate-limiting step is ALA synthesis, more specifically the activity of glutamyl t-RNA reductase GLUTR (Brzezowski et al. 2015, Publication 1 submitted) which is encoded by a small gene family called *Hem A*. It was argued that there was a lack in regulation via transcription control despite of the well-known plastid-to-nucleus retrograde signaling occurrence. This is since transcription regulation takes longer than enzymatic activity modulation. Indeed, plants must keep enzymes in higher amount even under normal conditions in such anticipated way to keep tetrapyrrole metabolites under control if stress

would occur (Tanaka and Tanaka 2007). The first regulation point is the feedback inhibition of GLUTR by heme, regulating therefore ALA formation and prevents the generation of deleterious PS. In addition, at the second branching point heme/chlorophyll, protoporphyrinogen oxidase and Mg chelatase are subjected to redox regulation via thioredoxin. Furthermore, in the Mg-branch, ALA synthesis is under negative control through protochlorophyllide (Figure 6, Beale 1990, Grimm 1998, Tanaka and Tanaka 2007, Richter and Grimm 2013, Brzezowski et al. 2015).

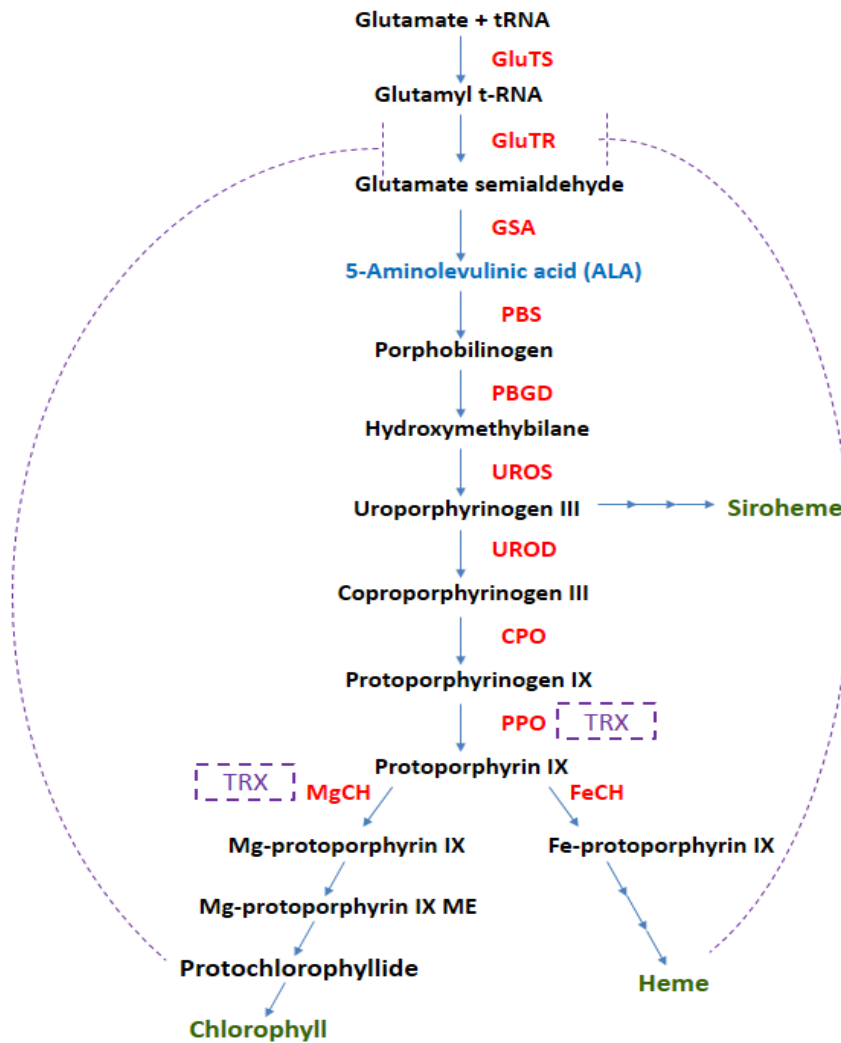


Figure 6. Tetrapyrrole biosynthetic pathways in plants.

Enzymes are shown in red. End products of the pathway are shown in green preceded by multi-arrows. The first common precursor 5-aminolevulinic acid is shown in blue. Dashed boxes indicate thioredoxin-base regulation and dashed arrows point out feedback regulation. GluTS: glutamyl t-RNA synthetase, GluTR: glutamyl-tRNA reductase, GSA: glutamate-1-semialdehyde aminotransferase, PBGD: porphobilinogen deaminase, UROS: uroporphyrinogen synthase, UROD:

uroporphyrinogen decarboxylase, CPO: coproporphyrinogen oxidase, PPO: protoporphyrinogen oxidase, FeCH: Fe-chelatase, MgCH: Mg-chelatase, TRX: thioredoxin.

I.2. Applications of PS

In the present manuscript we develop biological PS applications. Thus, energetic applications such as solar energy conversion, electrochemistry and organic electronics will be out of context and are not discussed (reader can refer to Zhao et al. 2013).

I.2.1. Photodynamic treatment in medicine

To date, the main application of PS is their use in photodynamic therapy (PDT) which is a worldwide clinically approved cancer therapy relying on a photochemical reaction between three components: PS, light, and molecular oxygen. PDT is a non-invasive procedure for the treatment of cancers and other diseases. In this paragraph we will develop the PDT applications from cancer to non-cancerous diseases in medical domains like dermatology, odontology, etc.

I.2.1.1. Photodynamic therapy against cancers

Forty years ago, a new treatment based on the combination effects of three harmless elements: light-oxygen-PS was imagined and investigated to struggle against cancer cells. Thus, the most famous and commercial PS introduced in the 1970's was the Photofrin® that is a mixture of dimers and oligomers of hematoporphyrin derivatives linked by ether, ester and C-C bonds (Ormond and Freeman 2013). The drawbacks of Photofrin® as skin sensitivity and weak absorption at 630 nm lead scientists to synthesize and design new molecules that could act as improved PS (Abrahamse and Hamblin 2016). Within PDT context, PS were ranged into 3 generations basing on the time of development and physico-chemical characteristics. photofrin® represents the first-generation PS, second generation regroup all porphyrinoid PS with improved features and third generation designates modified PS with biological conjugates as antibodies and carriers.

Researchers seek for the ideal PS that must fulfill the following requirements: it should have: no dark toxicity, natural fluorescence which is important for diagnostics, low photobleaching and high chemical stability, high singlet oxygen quantum yield, high absorption in “therapeutic window” between 620 and 850 nm (Figure 7).

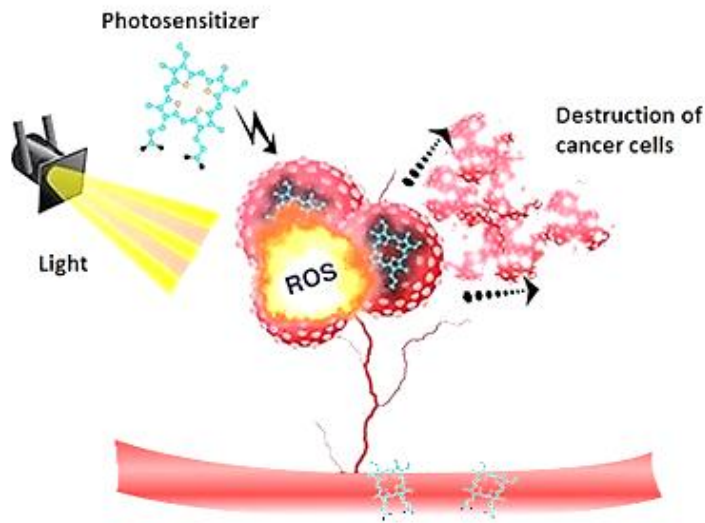


Figure 7. PDT application in cancer treatment.

(modified from <https://hope4cancer.com/our-therapies/sono-photo-dynamic-therapy/>). PS is transported and released into the tumor via blood circulation in the case of deep tumor where it exerts photochemical reactions leading to ROS generation that bring about cancer reduction under light. ROS: Reactive oxygen species.

I.2.1.2. Photodynamic therapy against non-oncological diseases

PDT applications reached therapies for non-malignancies and include several domains such as ophthalmology, dentistry, dermatology as well as cosmetics. It treats disease like age-related macular degeneration, psoriasis, actinic keratosis and rheumatoid arthritis using clinically approved PS as Photofrin®, Verteporphin®, and Levulan®-mediated protoporphyrin IX. Very recently, PDT using methyl aminolevulinic acid was employed for the removal of non-pigmented hair in the domain of cosmetics since laser therapies failed to remove blond or white hair due to the lack of chromophores (Babilas and Szeimies 2005, Uebelhoer and Dover 2005, Konopka et al. 2007, Rishi and Agarwal 2015, Shin et al. 2016).

I.2.1.3. Photodynamic therapy limitations

The difficulties or the limits of PDT in cancer or other diseases remain to optimize PS that must be photoactivated to be efficient to induce cell death. This treatment is efficient for superficial diseases but is not uploaded for deep tissue alterations. Researchers developed second generation PS as phtalocyanin and chlorin having stronger Q band absorption in order to the best deal with possible wavelength for ideal tissue penetration (therapeutic window). Furthermore, optical processes were

enhanced by exciting PS that have intense absorption in the blue range with two photons in the wavelength range from 800 to 1000 nm. Thus, that methodology dealt with light tissue penetration. Moreover, as advances have been made successfully in nanoengineering, researchers tended to target carcinoma that are deeply buried in human body via PS integration with nanocarriers as liposomes, quantum dots, carbon and inorganic nanomaterials (Ogawa and Kobuke 2008, Ormand and freeman 2013, Hong et al. 2016).

It is worthy to note that the promising PDT can be considered as an alternative modality to conventional cancer therapies like surgery, chemo- and radiotherapy and should be combined with these therapies to boost cancer control. Nevertheless, one of its current drawbacks is that PDT is ineffective against metastatic cancers which are the most frequent cause of death.

I.2.2. Antimicrobial photodynamic treatment (APDT)

Antimicrobial photodynamic treatment is derived from PDT and describes the use of PDT to inactivate microbial cells. Indeed, photodynamic inactivation (PDI) or Photo-Antimicrobial chemotherapy (PACT) or APDT are similar terms or acronyms. Their applications are widely expanded beyond medical scope to reach industrial, environmental and agricultural domains (Alves et al. 2010).

I.2.2.1. APDT in medical environment

PS was also used in order to inactivate virus and microorganisms such as bacteria, yeast and fungi in the present time witnessing the rise of multidrug resistant superbugs and therefore, the end of antibiotic era (Huang et al. 2010). APDT was clinically approved mainly in the field of dermatology and dentistry using 5-aminolevulinic acid (ALA)-mediated protoporphyrin IX and phenothiazinium dyes. Since skin and mouth infections are localized and superficial contrarily to systemic infections, APDT emerges as highly successful methodology in order to struggle against periodontitis, acne and other oral and skin infections. Moreover, APDT was used efficiently to reduce hospital-acquired infections such as nosocomial infections through PS applications on medical devices (Maisch et al. 2005, Kharkwal et al. 2011, McCoy et al. 2014, Yin et al. 2015).

I.2.2.2. APDT for water sewage

Water disinfection through APDT is seen as efficient, eco-friendly and cost-effective treatment against bacteria as *Enterococcus faecalis*, virus as bacteriophage (T4-like sewage bacteriophage) and parasites as *Ascaris lumbricoides* (nematode). APDT for this purpose relies mainly on the use of porphyrins, methylene blue and rose Bengal (Table 1). Its applications include aquaculture, crop irrigation and hospital water disinfection (Costa et al. 2008, Carvalho et al. 2009, Arrojado et al. 2011, Thandu et al. 2015, Bartolomeu et al. 2017).

I.2.2.3. APDT for food decontamination

The use of APDT in food industry has dealt with food-borne pathogens destruction without modification in organoleptic properties. The efficacy of such treatment was demonstrated using ALA and different PS as protoporphyrin IX, hematoporphyrin derivative, curcumin and chlorophyllin against bacteria, yeast and molds. The main applications include packaging materials, vegetables, fruits and seeds and involve grafting PS on organic materials, food soaking with PS solutions and PS dropping at the surface of fruits (Figure 8, Luksiene 2007; Luksiene and Brovko 2013; Buchovec et al 2016; Gluek et al. 2017).

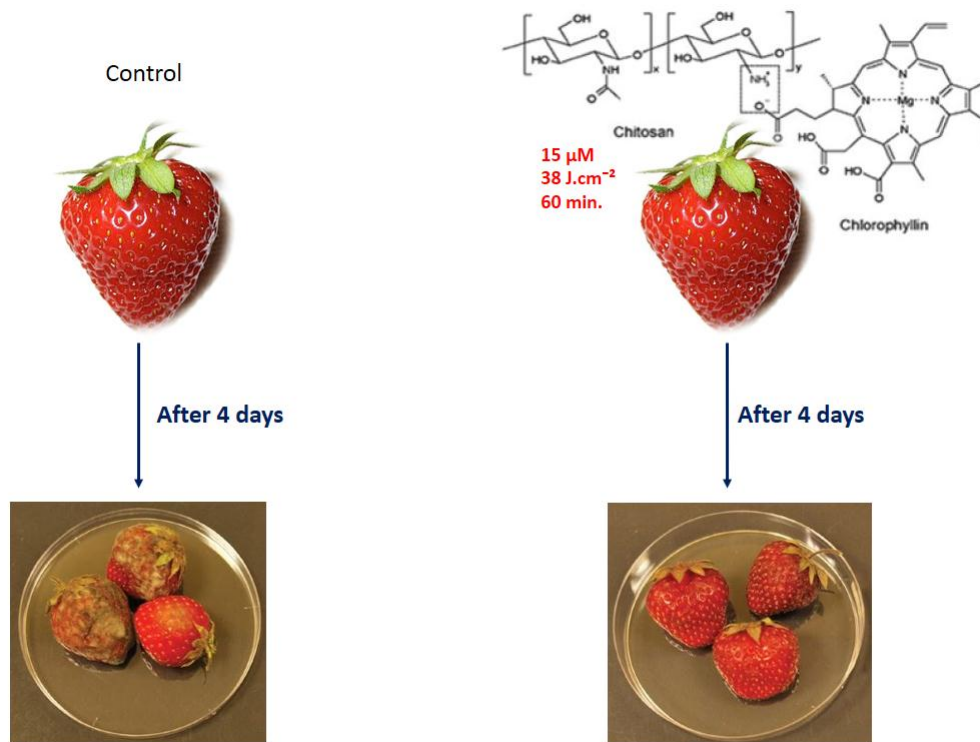


Figure 8. APDT application for food decontamination.

Strawberries were soaked with 0.1% chitosan (nutritional supplement) and 15 μM chlorophyllin then exposed to 405 nm light at fluence equal to 38 $\text{J}\cdot\text{cm}^{-2}$ for 60 min. whereas strawberries that are not treated served as control. 4 days after treatment, control strawberries were totally infected whereas treated strawberries with chlorophyllin–chitosan were not spoiled (Buchovec et al. 2016)

I.2.2.4. APDT in industrial domain

It consists in incorporation of cationic porphyrins or protoporphyrin IX into different textile materials to create protective clothing. Another application involves the grafting of porphyrins on cellulose to create sanitized packaging materials as cardboard, as well as embedding them into paper, fabrics and plastics. (Ringot et al. 2010, Feese et al. 2011; Lhotakova et al. 2012). Recently, APDT using methylene blue and cationic corrole PS was employed for the restauration of historic constructions that were colonized by photosynthetic biofilms (McCullagh and Robertson 2006, Pohl et al. 2014).

I.2.2.5. APDT in agronomy

In the last four years, the use of PS acquires new potential aiming to eradicate plant pathogens as well as unwanted vegetation without affecting crops (Figure 9). This particular aspect is largely developed in the review (Publication 1 submitted) and will be further deeply discussed later in the present manuscript. Briefly APDT applications reach agricultural domain as potential approach to fight against plant pathogens. Indeed, it was recently shown that perennial plants like citrus and kiwi trees were not affected after PS treatment whereas strawberry plants were damaged (De Menezes et al. 2014 a,b, Fracarolli et al. 2016, De Menezes et al. 2016, Gonzales et al. 2017, Jesus et al. 2018).

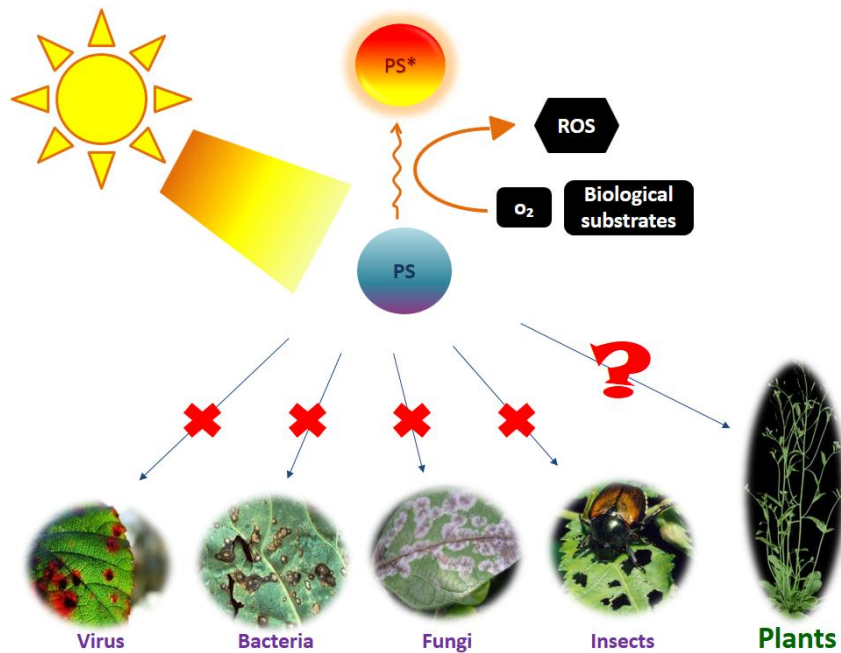


Figure 9. APDT mechanism and its possible multiple targets in agronomy.

With a double challenge: being safe for plants but lethal for their pathogens from virus to insects. It has been reported that APDT is highly efficient against plant pathogens including virus such as Tobacco Mosaic Virus (TMV), bacteria such as *Pseudomonas syringae* and fungi such as *Colletotrichum*, *Fusarium* and *Aspergillus*. Thus, we were wondering whether APDT has side effects on plants and how plants respond to such photodynamic treatment (Annex 3).

I.2.3. PUBLICATION 1: Review “Plant photodynamic stress: what's new?”, *Frontiers in Plant Science*



Plant Photodynamic Stress: What's New?

Mohammad Issawi, Vincent Sol and Catherine Riou*

Laboratoire Peirene (EA7500), Faculté des Sciences et Techniques, Université de Limoges, Limoges, France

In the 1970's, an unconventional stressful photodynamic treatment applied to plants was investigated in two directions. Exogenous photosensitizer treatment underlies direct photodynamic stress while treatment mediating endogenous photosensitizer over-accumulation pinpoints indirect photodynamic stress. For indirect photodynamic treatment, tetrapyrrole biosynthesis pathway was deregulated by 5-aminolevulinic acid or diphenyl ether. Overall, photodynamic stress involves the generation of high amount of reactive oxygen species leading to plant cell death. All these investigations were mainly performed to gain insight into new herbicide development but they were rapidly given up or limited due to the harmfulness of diphenyl ether and the high cost of 5-aminolevulinic acid treatment. Twenty years ago, plant photodynamic stress came back by way of crop transgenesis where for example protoporphyrin oxidases from human or bacteria were overexpressed. Such plants grew without dramatic effects of photodamage suggesting that plants tolerated induced photodynamic stress. In this review, we shed light on the occurrence of plant photodynamic stress and discuss challenging issues in the context of agriculture focusing on direct photodynamic modality. Indeed, we highlighted applications of exogenous PS especially porphyrins on plants, to further develop an emerged antimicrobial photodynamic treatment that could be a new strategy to kill plant pathogens without disturbing plant growth.

Keywords: 5-aminolevulinic acid, diphenyl ether herbicides, photosensitizers, plant photodynamic stress, porphyrins, tetrapyrroles

OPEN ACCESS

Edited by:

Paula Casati,
Consejo Nacional de Investigaciones
Científicas y Técnicas (CONICET),
Argentina

Reviewed by:

Raquel Esteban,
University of the Basque Country
(UPV/EHU), Spain
Nejat Duzgunes,
University of the Pacific, United States

*Correspondence:

Catherine Riou
catherine.riou@unilim.fr

Specialty section:

This article was submitted to
Plant Abiotic Stress,
a section of the journal
Frontiers in Plant Science

Received: 13 February 2018

Accepted: 03 May 2018

Published: 23 May 2018

Citation:

Issawi M, Sol V and Riou C (2018)
Plant Photodynamic Stress: What's
New? *Front. Plant Sci.* 9:681.
doi: 10.3389/fpls.2018.00681

INTRODUCTION

Almost all abiotic stresses induce oxidative stress underlying imbalance between reactive oxygen species (ROS) production and plant defense systems (Ramel et al., 2012; Müller-Xing et al., 2014; Hu et al., 2015; Loreti et al., 2016; Vian et al., 2016; Chakradhar et al., 2017; Hasan et al., 2017; Jaleel et al., 2017; Ohama et al., 2017; Rihan et al., 2017; Yang and Guo, 2017). Often, photo-oxidative and photodynamic stresses are confused whereas they bear two distinct meanings. The former points out a light-driven generation of ROS in chloroplasts through the photosensitization of excited chlorophyll molecules that are embedded in antennae complex and reaction center or via electron leakage from overloaded electron transport chain within photosystem apparatus. However, photodynamic stress involves the accumulation of exogenous or endogenous PS at various subcellular compartments and subsequently photochemical ROS production via two types of photochemical reactions under light conditions. In the type I, redox state change of excited sensitizer occurs upon reactions with biological molecules and oxygen resulting in hydrogen peroxide and free radical generation while In the Type II, energy from excited PS is transferred directly to oxygen leading to singlet oxygen production (**Figure 1**; Foyer et al., 1994; Pospíšil, 2016; Kashef et al., 2017).

In plants, occurrence of photodynamic stress corresponds to two distinct artificial situations. The first one involves deregulations of plant tetrapyrrole biosynthetic pathway using molecules such as 5-aminolevulinic acid (ALA), diphenyl ether (DPE) or genetic tools. Tetrapyrroles play numerous roles from light harvesting, oxygen transport, oxidative phosphorylation, oxygen storage, nitrogen fixation to ROS scavenging (heme) (**Figure 1A**; Battersby et al., 1980; Senge et al., 2014, 2015). Under normal conditions, this primary biosynthetic pathway is tiny regulated and mainly confined to plastidial organelles that protect cells from potential or accidental oxidative burst. Nevertheless, when this pathway is not anymore regulated by for instance exogenous supply of ALA or DPE or genetic modifications, some intermediates such as protoporphyrin IX (PPIX) and Mg-porphyrins become powerful photosensitizers that could trigger carbohydrates, proteins, lipids and nucleic acids damages (Rebeiz, 2014). In the second situation, photodynamic stress is induced through plant exposure to exogenous PS which are able to produce high amount of ROS inside cells under irradiation. Applications of exogenous PS such as phenothiazinium dyes, coumarins and furocoumarins, porphyrins were performed and summarized in **Table 1**. A new application of photodynamic treatment on plants is raising up as efficient weapon to struggle against pathogens essentially bacteria and fungi in the context of the so-called antimicrobial photodynamic treatment (APDT) (**Figure 1B**). Indeed, within APDT, plants of agronomic interest will normally grow protecting themselves from deleterious effect of photoactivated PS via setting up powerful antioxidant machinery. This review will develop photodynamic stress in plants and focus on the direct photodynamic stress regarding APDT to gain insight in improving agronomic practices with high crop yield and environmental protection goals. Photodynamic strategy applied to pathogens or microorganisms is subject of numerous reviews and will not be developed here (Ben Amor and Jori, 2000; Jori and Brown, 2004; Maisch, 2007, 2009; Donnelly et al., 2008; Almeida et al., 2011; Jori, 2011; Alves et al., 2015; Liu et al., 2015; Tim, 2015; Hamblin, 2016; Wainwright et al., 2016; Kashef et al., 2017).

INDIRECT PHOTODYNAMIC STRESS

Forcing plants to accumulate excessive amount of endogenous tetrapyrrolic photosensitizers induce photodynamic stress conditions such as ALA feeding, DPE treatment as well as by transgenesis experiments leading to growth and development impediment. In this review, we will not develop the crop transgenesis tools because they do not fit with plant photodynamic treatment. The reader should refer to these references for more informations (Li, 2003; Lee et al., 2004; Li and Nicholl, 2005; Jung et al., 2008; Ayliffe et al., 2009; Jung, 2011; Quesada et al., 2013; Yun et al., 2013; Kim et al., 2014).

5-aminolevulinic Acid (ALA) Feeding

5-aminolevulinic acid is not a PS *per se*. Instead, it is a non-protein amino acid and the first common precursor of the tetrapyrrole (chlorophylls, heme, and derivatives) pathway

(**Figure 1A**). Its supply lead to PPIX and/or other intermediates over-accumulation. From the 70's, exogenous application of ALA on yeast, insects, plants and in mammal cells was shown to induce high accumulation of tetrapyrroles (**Figure 1A**; Brouillet et al., 1975; Rebeiz et al., 1984, 1995; Matsumoto et al., 1994; Juzeniene et al., 2002; Fotinos et al., 2006; Xu et al., 2015). When tetrapyrroles were over-accumulated by ALA feeding, plants could not anymore struggle against induced photodynamic stress and died (Rebeiz et al., 1984, 1990; Matsumoto et al., 1994). When cucumber fields were sprayed with ALA, it was found that seedlings accumulated massive amount of endogenous porphyrins especially the potential singlet oxygen generator "protochlorophyllide" under 5,000 foot candle (Rebeiz et al., 1988). A similar result was obtained on duckweed (*Lemna paucicostata* Hegelm.) that showed rapid membrane damage after light irradiation and increase in both protochlorophyllide and PPIX contents suggesting herbicidal effect of ALA (Matsumoto et al., 1994). In the other hand, ALA-treated plants significantly upregulated transcript levels of genes encoding superoxide dismutase and serine/threonine kinase receptors but the induction of antioxidative components lacked capacity to withstand ROS generation (Phung and Jung, 2014, 2015). In 2004, Jung and co-workers shed light on "photodynamic stress" as they showed that rice plants suffered from severe oxidative damage upon the ectopic expression of the bacterial ALA synthase gene bringing about the accumulation of harmful photosensitizers PPIX and protochlorophyllide under $350 \mu\text{mol}\cdot\text{m}^{-2}\cdot\text{s}^{-1}$ (Jung et al., 2004). ALA feeding was performed in order to look for a new herbicide. However, there was no commercial formulation of ALA as field effective herbicide owing to the high amount required ($\geq 5 \text{ mM}$) and the cost-effective treatment (Sasikala et al., 1994; Phung and Jung, 2014; Xu et al., 2015; Nguyen et al., 2016).

Diphenyl Ether (DPE) Treatment

Since 1960's, DPE essentially oxyfluorfen and acifluorfen were introduced as commercial herbicides to control weeds (Yang et al., 2006). They constitute the main class of PPO-inhibiting herbicides that are widely investigated. Phung and Jung (2015) reported the different responses of photodynamically stressed rice plants undergoing ALA (5 mM) and oxyfluorfen (50 μM) herbicidal treatment. In term of phenotype under illumination, ALA induced bleached necrotic spots while oxyfluorfen caused bronzed necrotic spots on the leaves. This difference in photodynamic symptoms was due to PPIX overaccumulation in cytoplasm in DPE-treated plants whereas the photodynamic destruction of chlorophyll by Mg-porphyrins was responsible of the white spot appearance. Beyond the phenotypical effects, the brown necrosis in DPE-treated plants exhibited a more dispersed H_2O_2 production and was accompanied by an increase in H_2O_2 -scavenging enzymes, catalase and peroxidase activities as well as dehydroascorbate content, a strong stress marker compared to those of ALA-treated plants (Phung and Jung, 2015). Their mode of action was established and consisted in the inhibition of protoporphyrinogen oxidase (PPO) the last enzyme at the branching point between heme and

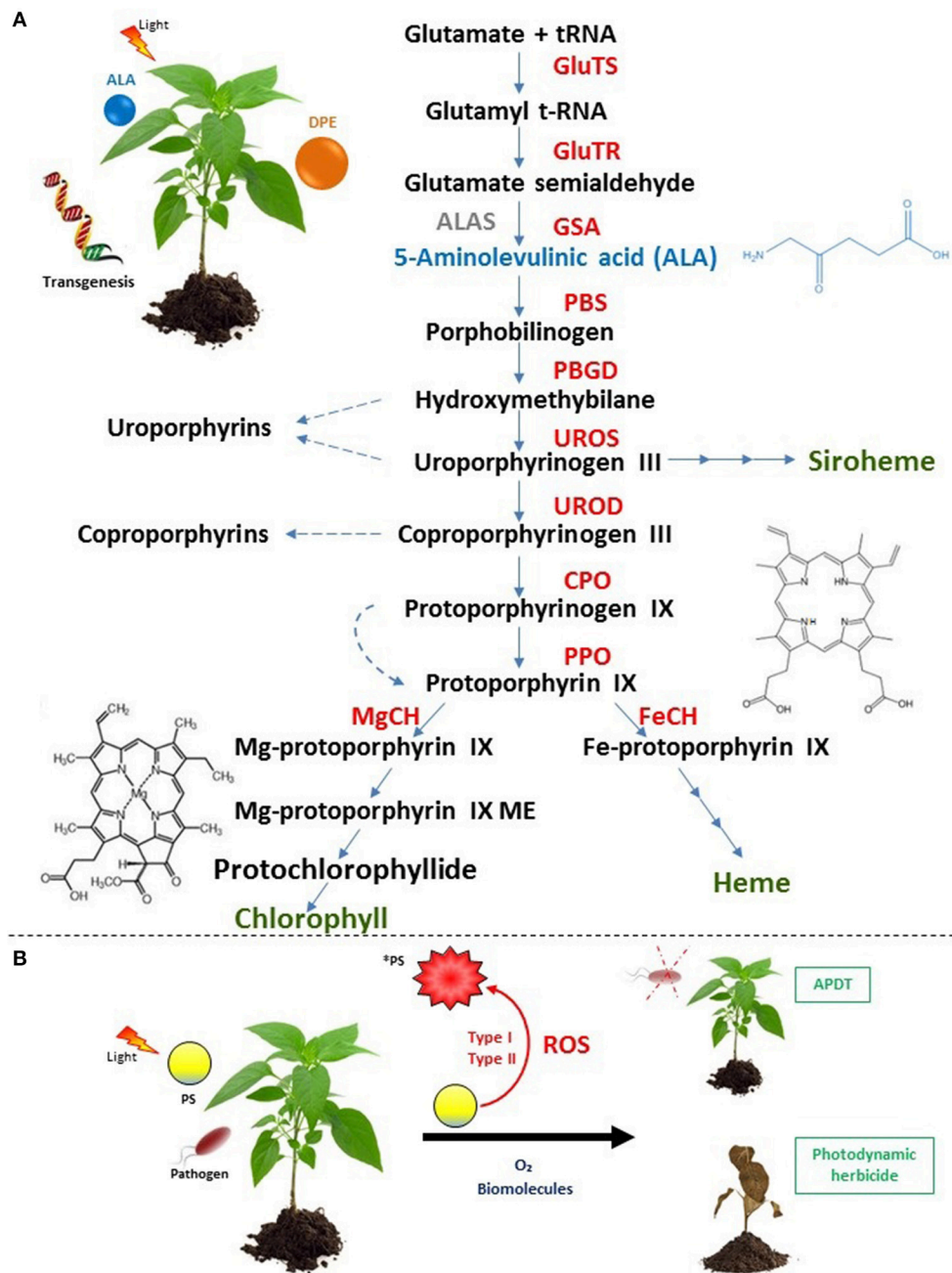


FIGURE 1 | Occurrence of plant photodynamic stress. **(A)** Indirect photodynamic stress occurs through forcing plants to over-accumulate endogenous PS upon tetrapyrrole biosynthetic pathway deregulation by ALA or DPE treatments as well as by transgenesis. Enzymes (capital letters) are shown in red. End products of the pathway are shown in green preceded by multi-arrows. Dashed arrows indicate the generation of endogenous PS (uroporphyrins, coproporphyrins, protoporphyrin IX that can be free-base or Fe/Mg metalated or esterified and protochlorophyllide) with the corresponding structures of the main harmful PS: protoporphyrin IX and protochlorophyllide. The non-plant enzyme ALAS is shown in gray. The first common precursor ALA is shown in blue with its chemical structure. ALAS, 5-aminolevulinic acid synthase; CPO, coproporphyrinogen oxidase; FeCH, Fe-chelatase; GSA, glutamate-1-semialdehyde aminotransferase; GluTR, glutamyl-tRNA reductase; GluTS, glutamyl t-RNA synthetase; PBGD, porphobilinogen deaminase; MgCH, Mg-chelatase; Mg-protoporphyrin IX ME, Mg-protoporphyrin IX methyl ester; PPO, protoporphyrinogen oxidase; UROD, uroporphyrinogen decarboxylase; UROS, uroporphyrinogen synthase. **(B)** Direct photodynamic stress is carried out via the use of exogenous PS such as porphyrins, phenothiazinium dyes, coumarins, and furocoumarins leading to ROS generation via two types of photochemical reactions upon irradiation. It was recently investigated for applications in agronomy in the context of APDT and for new herbicide development. *PS, excited PS.

TABLE 1 | Exogenous PS and their characteristics and application in plant photodynamic treatment.

PS	Origin	Concentration	Light range	Light intensity	Plant material	Function*	References
Non-porphyrin compounds							
Procion yellow	Synthetic	4% solution	UV		Elodea leaf mesophyll cells	Intracellular ultrastructure staining	Goodwin, 1976
Cercosporin	Natural	Variable (0.5–18.7 μM)	Various types of lamps	Variable	Potato, carrot, red beet, tobacco leaf discs, maize roots and NT575 tobacco suspension cells	Phytotoxin	Macri and Vianello, 1979; Daub, 1982a,b; Daub and Briggs, 1983
Rose bengal	Synthetic	10mM	White	100 and 350 $\mu\text{mol.m}^{-2}.\text{s}^{-1}$	Pea leaf discs	Membrane and nucleus staining	Knox and Dodge, 1984
Hypericin	Natural	100 μM	White	400 $\mu\text{mol.m}^{-2}.\text{s}^{-1}$	Pea leaf discs	Plant defense	Knox and Dodge, 1985a
Eosin Y	Synthetic	5 μM and 1 mM	White and green	350 $\mu\text{mol.m}^{-2}.\text{s}^{-1}$ and 5.26 mW.cm ⁻²	Pea leaf discs and onion bulb roots	Protein staining, DNA binding	Knox and Dodge, 1985b; Molero and Hazen, 1988
Berberine	Natural	Variable (1 nM to 10 μM)	Violet	195 KW.m ⁻²	Roots of onion bulbs	Antimicrobial, heparin staining, DNA binding	Molero et al., 1985
Pyronin Y	Synthetic	1 and 5 μM	Green	129.9 KW.m ⁻²	Roots of onion bulbs	DNA binding	Armas-Portela et al., 1985
Acridin orange	Synthetic	5 μM	Green	5.26 mW.cm ⁻²	Roots of onion bulbs	Mitochondria staining and DNA binding	Molero and Hazen, 1988
Orcein	Natural	5 μM	Green	5.26 mW.cm ⁻²	Roots of onion bulbs	Chromosome staining	Molero and Hazen, 1988
Harimine	Natural	500nM	UV	2.5 mW.cm ⁻²	Roots of onion bulbs	enzymatic inhibition and DNA binding	Hazen and Gutierrez-Gonzalez, 1988
Coumarins and furocoumarins	Natural	Variable	Solar radiation		Citrus tree leaves and strawberry leaves	Plant defense	de Menezes et al., 2014a; Fracaroli et al., 2016
Phenothiazinium dyes	Synthetic	Variable (5, 25, and 50 μM)	Solar radiation		Citrus tree leaves (healthy and combinated with fungal pathogen)	DNA/RNA staining and bacterial staining	de Menezes et al., 2014b; Gonzales et al., 2017
Porphyrins							
HPD	Synthetic	25 $\mu\text{g.ml}^{-1}$	Near UV	9 W.m ⁻²	<i>Vicia faba</i> leaf protoplasts	Usage in PDT as PHOTOFRIN	Kjeldstad et al., 1986
TPyP and HP	Synthetic	100nM	Red	0.001 J.m ⁻²	Roots of onion bulbs	DNA binding	Hazen et al., 1987
TMPyP/Zn-TMPyP	Synthetic	Variable (10nM to 100 μM)	Red, blue, white and solar radiation	Variable	Onion bulb roots, TBY-2 cells, kiwi leaves (healthy and contaminated), tomato and <i>Arabidopsis thaliana</i> plantlets	DNA binding	Villaneuva et al., 1986, 1989; Riou et al., 2014; Guillaumot et al., 2016; Issawi et al., 2018; Jesus et al., 2018
TPPS/Zn-TPPS	Synthetic	3.5 μM	White	95 and 250 $\mu\text{mol.m}^{-2}.\text{s}^{-1}$	TBY-2 suspension cells, tomato and <i>Arabidopsis thaliana</i> plantlets		Riou et al., 2014; Guillaumot et al., 2016; Issawi et al., 2018

TPyP, Tetra(4-pyridyl) porphyrin; TMPyP, Tetra (N-methylpyridyl) porphyrin; TPPS, meso-tetra (4-sulphophenyl) porphyrin; HPD, Hematoporphyrin derivative; HP, Hematoporphyrin; TBY-2, Tobacco Bright Yellow-2. *Other properties of PS that are not related to their photodynamic action.

chlorophyll synthesis (Figure 1A; Matringe and Scalla, 1987; Matringe et al., 1989a,b). Thus, triggering leakage of PPO substrate, the non-fluorescent protoporphyrinogen IX that was converted by unknown peroxidase to the first effective PS of this pathway PPIX. Indeed, when PPIX absorbs light, it induces photochemical reactions and vital processes are affected (Figure 1A).

DIRECT PHOTODYNAMIC STRESS: AN OLD STORY WITH NOVEL DEVELOPMENT

Plant exposure to exogenous PS could induce tissue damage and subsequently cell death. First studies relative to direct application of PS on plant materials were reported four decades ago (Table 1). Concerning porphyrins, the most used PS, Kjeldstad and co-workers showed the photodamage of plasma membrane of *Vicia faba* leaf protoplasts subjected to hematoporphyrin derivative treatment under near UV light (Kjeldstad et al., 1986). Moreover, other studies showed mutagenic effect of porphyrins which were able to bind DNA in root meristematic cells of onion bulbs (Table 1; Villaneuva et al., 1986, 1989; Hazen et al., 1987). The aims of testing exogenous PS on plant materials were to study the symplastic intracellular movement, decipher the mode of action of fungal toxin as well as the effects of singlet oxygen on plant cells and exploring sister chromatid exchange upon dye DNA-intercalation in fast-rate dividing cells (Table 1; Goodwin, 1976; Macri and Vianello, 1979; Daub, 1982a,b; Daub and Briggs, 1983; Knox and Dodge, 1984, 1985a,b; Armas-Portela et al., 1985; Molero et al., 1985; Kjeldstad et al., 1986; Villaneuva et al., 1986, 1989; Hazen et al., 1987; Hazen and Gutierrez-Gonzalez, 1988; Molero and Hazen, 1988).

For agronomic issues, the use of exogenous PS as powerful photoactivated molecules was not anymore investigated because the undesirable effects described above. Hence, any potential application of whatever PS in the aim to fight plant pathogens requires a risk assessment on plant hosts. It was reported that natural photosensitizers such as coumarins and furocoumarins or synthetic ones such as phenothiazinium and porphyrins inactivated pathogenic agents as virus (Tobacco mosaic virus), bacteria (*Pseudomonas syringae*) and fungi (*Collectotrichum abscissum*, *Colletotrichum gloeosporioides*, *Collectotrichum acutatum*, *Aspergillus nidulans*, *Fusarium oxysporum*, *Fusarium moniliforme*, *Fusarium solani*) (Table 1). However, when spotted on orange tree and strawberry plants, or on kiwi contaminated leaves under solar radiation, the leaves and flowers were not affected by either natural/synthetic photosensitizers excepted for strawberry leaves that were damaged upon treatment with 100 μ M phenothiazinium (Orlob, 1967; de Menezes et al., 2014a,b; Fracarolli et al., 2016; Gonzales et al., 2017; Jesus et al., 2018). In another extended context, Issawi and co-workers conceived a double target strategy that could eradicate in the same time unwanted vegetation and plant pathogens without killing plants of agronomic interest (Figure 1B). To fulfill that purpose, they studied the effect of exogenous water-soluble cationic and anionic porphyrins on tomato, plant of agronomic interest and on *Arabidopsis thaliana*, weed-like

plant. Thus, they showed that cationic porphyrins were able to eradicate *Arabidopsis* plantlets without killing tomato plantlets (Guillaumot et al., 2016; Issawi et al., 2018). Favorably, Riou and co-workers treated TBV-2 cells with these same porphyrins aiming to find out new herbicides because no new herbicide modes of action were discovered since the last 3 decades (Duke, 2012; Heap, 2014; Riou et al., 2014).

DETERMINANTS OF PLANT PHOTODYNAMIC STRESS

Plants exposed to various stressors respond by involving mechanisms of sensing and signaling (Tuteja and Sopory, 2008; Mittler and Blumwald, 2010; Suzuki et al., 2012; Pandey et al., 2016; Zhu, 2016; Mittler, 2017). Although plant stress signaling pathways were abundantly investigated, stress sensors remain largely unknown so it is much difficult to detect sensing systems in plants subjected to direct photodynamic stress under unconventional conditions. However, Phung and collaborators outlined the switch photodynamic/drought-tolerance in PPO-transgenic rice under drought conditions explaining how drought determinants reduced porphyrin level in order to elaborate tolerance response through gene expression modulation upon sensing change in tetrapyrrole amount (Phung et al., 2011). Nonetheless seeking for photodynamic sensors represents serious challenge. Exogenous PS exert photodynamic function through the production of ROS including singlet oxygen and hydrogen peroxide which are well known signaling molecules, it is worthwhile to distinguish between primary sensing that may be assigned to the PS *per se* and secondary sensing ascribed to ROS (Laloi et al., 2007; Niu and Liao, 2016; Wang et al., 2016). ABC transporters and TSPO receptor could play role in exogenous PS sensing since they were identified as endogenous tetrapyrrolic receptors (Theodoulou, 2000; Guillaumot et al., 2009). Interestingly, PPIX interacted with Toll-Like Receptor 4 (TLR-4) in mammals. Possible interaction with a putative TLR should be investigated in plant cells (Figueiredo et al., 2007; Tangudu and Spasic, 2017). In term of signaling, exogenous photodynamic action is likely to generate various secondary messengers holding signaling potential like ROS, modified proteins, lipid peroxidation by-products. In addition, photodynamic signaling may also involve cross-talk with phytohormones as abscissic acid, jasmonic acid, salicylic acid, calcium, protein kinases, transcription factors (Tuteja and Sopory, 2008; Suzuki et al., 2012; Zhu, 2016). Thus, studies involving transcription profiling, proteomic and metabolomic approaches should be envisaged upon photodynamic administration of exogenous PS in plants.

CHALLENGES AND PERSPECTIVES

In the present review, two ways to carry out photodynamic action on plants were emphasized (i) indirect photodynamic reaction via ALA or DPE treatments and transgenesis, (ii) direct photodynamic reaction through the use of exogenous PS. Comparing to conventional weed management methods using

photodynamic DPE herbicides that are commercially available, it was reported that this kind of herbicides were not only toxic to weeds but wildlife was also affected as DPE herbicides were toxic to nestling birds and fresh water polyp, also, they could be toxic to humans. In addition, DPE alone were not expected to control weeds and need the combinational use of chemicals or mulch. Indeed, there are several reported weeds that developed DPE-resistance (Hoffman et al., 1991; Rio et al., 1997; Li and Nicholl, 2005; Beckie and Tardif, 2012; Reed et al., 2018). Thus, we conclude that direct photodynamic treatment holding herbicidal potential via exogenous PS could be a promising approach relying on the fact that weeds cannot induce resistance against PS because they exert a multi-targeted photodynamic action damaging cellular DNA, lipids, carbohydrates and proteins. Taken together, we support the application of exogenous PS as weed control alternative and further studies are required as far as we know that studies concerning that task are very few (Riou et al., 2014; Issawi et al., 2018).

In regard to antimicrobial strategies, APDT was recently envisaged as promising approach to strike against plant pathogens without side effects on plant hosts and environment. In this context, we think that several aspects must be taken into consideration such as whole study of a defined pathosystem should be considered including biological life cycle of pathogen, growth and reproduction phenology of plants and timing of PS application. Moreover, PS administration methods as inclusion in soil aqueous phase, spotting on leaves and field spraying should not be neglected although spraying is the most convenient and reasonable.

REFERENCES

- Almeida, A., Cunha, A., Faustino, M. A. F., Tome, A. C., and Neves, M. G. P. M. S. (2011). "Porphyrins as antimicrobial photosensitizing agents" in *Photodynamic Inactivation of Microbial Pathogens: Medical and Environmental Applications*, eds M. R. Hamblin and G. Jori (Cambridge, UK: RCS Publishing), 83–160.
- Alves, E., Faustino, M. A. E., Neves, M. S., Cunha, A., Nadaisc, H., and Almeida, A. (2015). Potential applications of porphyrins in photodynamic inactivation beyond the medical scope. *J. Photochem. Photobiol. B Biol.* 22, 34–57. doi: 10.1016/j.jphotochemrev.2014.09.003
- Armas-Portela, R., Hazen, M. J., and Stockert, J. C. (1985). Increase in sister-chromatid exchanges in BrdU-substituted chromosomes of *Allium cepa* induced by the combined effect of pyronin Y and green light. *Mutat. Res. Genet. Toxicol.* 158, 77–80. doi: 10.1016/0165-1218(85)90100-4
- Ayliffe, M. A., Agostino, A., Clarke, B. C., Furbank, R., Von Caemmerer, S., and Pryor, A. J. (2009). Suppression of the barley uroporphyrinogen III synthase gene by a Ds activation Tagging element generates developmental photosensitivity. *Plant Cell* 21, 814–831. doi: 10.1105/tpc.108.063685
- Battersby, A. R., Fooks, C. J. R., Matcham, G. W. H., and McDonald, E. (1980). Biosynthesis of the pigments of life: formation of the macrocycle. *Nature* 285, 17–21. doi: 10.1038/285017a0
- Beckie, H. J., and Tardif, F. J. (2012). Herbicide cross resistance in weeds. *Crop Prot.* 35, 15–28. doi: 10.1016/j.cropro.2011.12.018
- Ben Amor, T., and Jori, G. (2000). Sunlight-activated insecticides: historical background and mechanisms of phototoxic activity. *Insect Biochem. Mol. Biol.* 30, 915–925. doi: 10.1016/S0965-1748(00)00072-2

CONCLUSION

In conclusion, plant photodynamic stress is considered as abiotic stress linked to ROS production as the first cause of cell death. It is still poorly studied regarding characterization of photodynamic stress determinants and outcomes especially at molecular level in plants. Besides, plant photodynamic stress has not been exploited yet, especially as valuable exogenous treatment for the purposes we mentioned above. Nevertheless, we are confident that in the near future, this approach based on PS and especially porphyrins could be relevant to respond to the Directive 2009/128/EC of the European Parliament plans that aim to reduce the use of pesticides while maintaining high yield as well as high quality in agricultural production. PS are photodegradable and non-toxic under dark as well as they were used at micromolar concentrations therefore they could be promising candidates to fulfill the task of European projects for environment sustainability in respect to wildlife, water sources and human health.

AUTHOR CONTRIBUTIONS

MI and CR prepared and wrote the present manuscript. MI designed the figure and the table. VS reviewed the manuscript.

ACKNOWLEDGMENTS

MI was supported by a Grant from the Municipality of Sharkieh (Lebanon).

- Brouillet, N., Arselin-De Chateaubodeau, G., and Volland, C. (1975). Studies on protoporphyrin biosynthetic pathway in *Saccharomyces cerevisiae*; characterization of the tetrapyrrole intermediates. *Biochimie* 57, 647–655. doi: 10.1016/S0300-9084(75)80146-5
- Chakradhar, T., Mahanty, S., Reddy, R. A., Divya, K., Reddy, P. S., and Reddy, M. K. (2017). "Biotechnological perspective of reactive oxygen species (ROS)-mediated stress tolerance in plants," in *Reactive Oxygen Species and Antioxidant Systems in Plants: Role and Regulation under Abiotic Stress*, eds M. Khan and N. Khan (Singapore: Springer), 53–87.
- Daub, M. E. (1982a). Cercosporin, a photosensitizing toxin from *Cercospora species*. *Phytopathology* 72, 370–374. doi: 10.1094/Phyto-72-370
- Daub, M. E. (1982b). Peroxidation of tobacco membrane lipids by the photosensitizing toxin, cercosporin. *Plant Physiol.* 69, 1361–1364. doi: 10.1104/pp.69.6.1361
- Daub, M. E., and Briggs, S. P. (1983). Changes in tobacco cell membrane composition and structure caused by cercosporin. *Plant Physiol.* 71, 763–766. doi: 10.1104/pp.71.4.763
- de Menezes, H. D., Pereira, A. C., Brancini, G. T. P., Leão, H. C., Massola Júnior, N. S., Bachmann, L., et al. (2014a). Furocoumarins and coumarins photoinactivate *Colletotrichum acutatum* and *Aspergillus nidulans* fungi under solar radiation. *J. Photochem. Photobiol. Biol.* 131, 74–83. doi: 10.1016/j.jphotobiol.2014.01.008
- de Menezes, H. D., Rodrigues, G. B., Teixeira, S. P., Massola, N. S., Bachmann, L., Wainwright, M., et al. (2014b). *In vitro* photodynamic inactivation of plant-pathogenic fungi *colletotrichum acutatum* and *colletotrichum gloeosporioides* with novel phenothiazinium photosensitizers. *Appl. Environ. Microbiol.* 80, 1623–1632. doi: 10.1128/AEM.02788-13

- Donnelly, R. F., McCarron, P. A., and Tunney, M. M. (2008). Antifungal photodynamic therapy. *Microbiol. Res.* 163, 1–12. doi: 10.1016/j.micres.2007.08.001
- Duke, S. O. (2012). Why have no new herbicide modes of action appeared in recent years? *Pest Manag. Sci.* 68, 505–512. doi: 10.1002/ps.2333
- Figueiredo, R. T., Fernandez, P. L., Mourao-Sa, D. S., Porto, B. N., Dutra, F. F., Leticia, L. S., et al. (2007). Characterization of heme as activator of toll-like receptor 4. *J. Biol. Chem.* 282, 20221–20229. doi: 10.1074/jbc.M610737200
- Fotinos, N., Campo, M. A., Popowycz, F., Gurny, R., and Lange, N. (2006). 5-Aminolevulinic acid derivatives in photomedicine: characteristics, application and perspectives. *J. Photochem. Photobiol.* 82, 994–1015. doi: 10.1562/2006-02-03-IR-794
- Foyer, C. H., Lelandais, M., and Kunert, K. J., (1994). Photooxidative stress in plants. *Physiol. Plant* 92, 696–717. doi: 10.1111/j.1399-3054.1994.tb03042.x
- Fracarolli, L., Rodrigues, G. B., Pereira, A. C., Massola Júnior, N. S., Silva-Junior, G. J., Bachmann, L., et al. (2016). Inactivation of plant-pathogenic fungus *Colletotrichum acutatum* with natural plant-produced photosensitizers under solar radiation. *J. Photochem. Photobiol. Biol.* 162, 402–411. doi: 10.1016/j.jphotobiol.2016.07.009
- Gonzales, J. C., Brancini, G. T. P., Rodrigues, G. B., Silva-Junior, G. J., Bachmann, L., Wainwright, M., et al. (2017). Photodynamic inactivation of conidia of the fungus *Colletotrichum abscessum* on *Citrus sinensis* plants with methylene blue under solar radiation. *J. Photochem. Photobiol. Biol.* 176, 54–61. doi: 10.1016/j.jphotobiol.2017.09.008
- Goodwin, P. B. (1976). “Physiological and electrophysiological evidence for intercellular communication in plant symplasts,” in *Intercellular Communication in Plants: Studies on Plasmodesmata*, eds B. E. S. Gunning and A. W. Robards (Berlin; Heidelberg; New York, NY: Springer), 121–129. doi: 10.1007/978-3-642-66294-2_6
- Guillaumot, D., Guillon, S., Morsomme, P., and Batoko, H. (2009). ABA, porphyrins and plant TSP0-related protein. *Plant Signal. Behav.* 4, 1087–1090. doi: 10.4161/psb.4.11.9796
- Guillaumot, D., Issawi, M., Da Silva, A., Leroy-Lhez, S., Sol, V., and Riou, C. (2016). Synergistic enhancement of tolerance mechanisms in response to photoactivation of cationic tetra (N-methylpyridyl) porphyrins in tomato plantlets. *J. Photochem. Photobiol. Biol.* 156, 69–78. doi: 10.1016/j.jphotobiol.2016.01.015
- Hamblin, M. R. (2016). Antimicrobial photodynamic inactivation: a bright new technique to kill resistant microbes. *Curr. Opin. Microbiol.* 33, 67–73. doi: 10.1016/j.mib.2016.06.008
- Hasan, M. K., Cheng, Y., Kanwar, M. K., Chu, X. Y., Ahammed, G. J., and Qi, Z. Y. (2017). Responses of plant proteins to heavy metal stress—a review. *Front. Plant Sci.* 8:1492. doi: 10.3389/fpls.2017.01492
- Hazen, M. J., and Gutierrez-Gonzalez, M. G. (1988). UV-mediated toxic bioactivity of harmine in the meristematic cells of *Allium cepa*. *Mutagenesis* 3, 333–335. doi: 10.1093/mutage/3.4.333
- Hazen, M. J., Villaneuva, A., and Stockert, J. C. (1987). Induction of sister chromatid exchanges in *Allium cepa* meristematic cells exposed to meso-tetra (4-pyridyl) porphine and hematoporphyrin photoradiation. *J. Photochem. Photobiol. Biol.* 46, 463–467. doi: 10.1111/j.1751-1097.1987.tb04796.x
- Heap, I. (2014). Global perspective of herbicide-resistant weeds. *Pest Manag. Sci.* 70, 1306–1315. doi: 10.1002/ps.3696
- Hoffman, D. J., Spann, J. W., LeCaptain, L. J., Christine, M. B., and Rattner, B. A. (1991). Developmental toxicity of diphenyl ether herbicides in nestling American kestrels. *J. Toxicol. Environ. Health* 34, 323–336. doi: 10.1080/15287399109531571
- Hu, B., Wang, W., Deng, K., Li, H., Zhang, Z., Zhang, L., et al. (2015). MicroRNA399 is involved in multiple nutrient starvation responses in rice. *Front. Plant Sci.* 6:188. doi: 10.3389/fpls.2015.00188
- Issawi, M., Guillaumot, D., Sol, V., and Riou, C. (2018). Responses of an adventitious fast-growing plant to photodynamic stress: comparative study of anionic and cationic porphyrin effect on *Arabidopsis thaliana*. *Physiol. Plant* 162, 379–390. doi: 10.1111/ppl.12666
- Jaleel, C. A., Manivannan, P., Wahid, A., Farooq, M., Al-juburi, H. J., Somasundaram, R., et al. (2017). Drought stress in plants: a review on morphological characteristics and pigments composition. *Int. J. Agric. Biol.* 11, 100–105.
- Jesus, V., Martins, D., Branco, T., Valério, N., Neves, M. G. P. M. S., Faustino, M. A. F., et al. (2018). An insight into the photodynamic approach versus copper formulations in the control of *Pseudomonas syringae* pv. actinidiae in kiwi plants. *Photochem. Photobiol. Sci.* 17, 180–191. doi: 10.1039/C7PP00300E
- Jori, G. (2011). “Antimicrobial photodynamic therapy: basic principles,” in *Photodynamic Inactivation of Microbial Pathogens: Medical and Environmental Applications*, eds M. R. Hamblin and G. Gori (Cambridge, UK: RCS Publishing), 83–160.
- Jori, G., and Brown, S. (2004). Photosensitized inactivation of microorganisms. *Photochem. Photobiol. Sci.* 3, 403–405. doi: 10.1039/b311904c
- Jung, S. (2011). Level of protoporphyrinogen oxidase activity tightly correlates with photodynamic and defense responses in oxyfluorfen-treated transgenic rice. *J. Pestic. Sci.* 36, 16–21. doi: 10.1584/jpestics.G10-46
- Jung, S., Lee, H. J., Lee, Y., Kang, K., Kim, Y. S., Grimm, B., et al. (2008). Toxic tetrapyrrole accumulation in protoporphyrinogen IX oxidase-overexpressing transgenic rice plants. *Plant Mol. Biol.* 67, 535–546. doi: 10.1007/s11103-008-9338-0
- Jung, S., Yang, K., Lee, D. E., and Back, K. (2004). Expression of Bradyrhizobium japonicum 5-aminolevulinic acid synthase induces severe photodynamic damage in transgenic rice. *Plant Sci.* 167, 789–795. doi: 10.1016/j.plantsci.2004.05.038
- Juzeniene, A., Juzenas, P., Iani, V., and Moan, J. (2002). Topical application of 5-aminolevulinic acid and its methylester, hexylester and octylester derivatives: considerations for dosimetry in mouse skin model. *J. Photochem. Photobiol.* 76, 329–334. doi: 10.1562/0031-8655(2002)076<0329:TAOAAA>2.0.CO;2
- Kashef, N., Huang, Y. Y., and Hamblin, M. R. (2017). Advances in antimicrobial photodynamic inactivation at the nanoscale. *Nanophotonics* 6, 853–879. doi: 10.1515/nanoph-2016-0189
- Kim, J. G., Back, K., Lee, H. Y., Lee, H. J., Phung, T. H., Grimm, B., et al. (2014). Increased expression of Fe-chelatase leads to increased metabolic flux into heme and confers protection against photodynamically induced oxidative stress. *Plant Mol. Biol.* 6, 271–287. doi: 10.1007/s11103-014-0228-3
- Kjeldstad, B., Olsten, M. L., Christensen, T., and Johnsson, A. (1986). Photodynamic damage to protoplasts with a hematoporphyrin derivative. *Plant Sci.* 44, 139–143. doi: 10.1016/0168-9452(86)90083-X
- Knox, J. P., and Dodge, A. D. (1984). Photodynamic damage to plant leaf tissue by rose bengal. *Plant Sci. Lett.* 37, 3–7. doi: 10.1016/0304-4211(84)90194-9
- Knox, J. P., and Dodge, A. D. (1985a). Isolation and activity of the photodynamic pigment hypericin. *Plant Cell Environ.* 8, 19–25. doi: 10.1111/j.1365-3040.1985.tb01204.x
- Knox, J. P., and Dodge, A. D. (1985b). The photodynamic action of eosin, a singlet-oxygen generator. *Planta* 164, 22–29. doi: 10.1007/BF00391021
- Laloi, C., Stachowiak, M., Pers-Kamczyc, E., Warzych, E., Murgia, I., and Apel, K. (2007). Cross-talk between singlet oxygen- and hydrogen peroxide-dependent signaling of stress responses in *Arabidopsis thaliana*. *Proc. Natl. Acad. Sci. U.S.A.* 104, 672–677. doi: 10.1073/pnas.0609063103
- Lee, Y., Jung, S., and Back, K. (2004). Expression of human protoporphyrinogen oxidase in transgenic rice induces both a photodynamic response and oxyfluorfen resistance. *Pest. Biochem. Physiol.* 80, 65–74. doi: 10.1016/j.pestbp.2004.06.008
- Li, X. (2003). Development of protoporphyrinogen oxidase as an efficient selection marker for agrobacterium tumefaciens-mediated transformation of maize. *Plant Physiol.* 133, 736–747. doi: 10.1104/pp.103.026245
- Li, X., and Nicholl, D. (2005). Development of PPO inhibitor-resistant cultures and crops. *Pest Manag. Sci.* 61, 277–285. doi: 10.1002/ps.1011
- Liu, Y., Qin, R., Zaat, S., Breukink, E., and Heger, M. (2015). Antibacterial photodynamic therapy: overview of a promising approach to fight antibiotic-resistant bacterial infections. *J. Clin. Transl. Res.* 1, 140–167. doi: 10.18053/jctres.201503.002
- Loreti, E., Van veen, H., and Perata, P. (2016). Plant responses to flooding stress. *Curr. Opin. Plant Biol.* 33, 64–71. doi: 10.1016/j.pbi.2016.06.005
- Macri, F., and Vianello, A. (1979). Photodynamic activity of cercosporin on plant tissues. *Plant Cell Environ.* 2, 267–271. doi: 10.1111/j.1365-3040.1979.tb00078.x
- Maisch, T. (2007). Anti-microbial photodynamic therapy: useful in the future? *Lasers Med. Sci.* 22, 83–91. doi: 10.1007/s10103-006-0409-7

- Maisch, T. (2009). A new strategy to destroy antibiotic resistant microorganisms: antimicrobial photodynamic treatment. *Mini Rev. Med. Chem.* 9, 974–983. doi: 10.2174/138955709788681582
- Matringe, M., Camadro, J., Labbe, P., and Scalla, R. (1989a). Protoporphyrinogen oxidase as a molecular target for diphenyl ether herbicides. *Biochem. J.* 260, 231–235. doi: 10.1042/bj2600231
- Matringe, M., Camadro, J., Labbe, P., and Scalla, R. (1989b). Protoporphyrinogen oxidase inhibition by three peroxidizing herbicides: oxadiazon, LS 82-556 and M&B 39279. *FEB Lett.* 245, 35–38. doi: 10.1016/0014-5793(89)80186-3
- Matringe, M., and Scalla, R. (1987). Photoreceptors and respiratory electron flow involvement in the activity of acifluorfen-methyl and LS 82-556 on non chlorophyllous soybean cells. *Pest. Biochem. Physiol.* 27, 267–274. doi: 10.1016/0048-3575(87)90056-3
- Matsumoto, H., Tanida, Y., and Ishizuka, K. (1994). Porphyrin intermediate involved in herbicidal action of 5-Aminolevulinic acid on duckweed (*Lemna paucicostata* Hegelm.). *Pest. Biochem. Physiol.* 48, 214–221. doi: 10.1006/pest.1994.1022
- Mittler, R. (2017). ROS are good. *Trends Plant Sci.* 22, 11–19. doi: 10.1016/j.tplants.2016.08.002
- Mittler, R., and Blumwald, E. (2010). Genetic engineering for modern agriculture: challenges and perspectives. *Annu. Rev. Plant Biol.* 61, 443–462. doi: 10.1146/annurev-arplant-042809-112116
- Molero, M. L., and Hazen, M. J. (1988). Photodynamic effect of acridine orange, eosin Y and orcein in a plant system *in vivo* measured by the sister chromatid exchanges test. *J. Plant Physiol.* 132, 636–637. doi: 10.1016/S0176-1617(88)80268-2
- Molero, M. L., Hazen, M. J., and Stockert, J. C. (1985). Photodynamic effect of berberine sulfate on the growth rate of *Allium cepa* roots. *J. Plant Physiol.* 120, 91–94. doi: 10.1016/S0176-1617(85)80126-7
- Müller-Xing, R., Xing, Q., and Goodrich, J. (2014). Footprints of the sun: memory of UV and light stress in plants. *Front. Plant Sci.* 5:474. doi: 10.3389/fpls.2014.00474
- Nguyen, A. H., Kim, H.-S., and Jung, S. (2016). Altered tetrapyrrole metabolism and transcriptome during growth-promoting actions in rice plants treated with 5-aminolevulinic acid. *Plant Growth Regul.* 78, 133–146. doi: 10.1007/s10725-015-0080-8
- Niu, L., and Liao, W. (2016). Hydrogen peroxide signaling in plant development and abiotic responses: crosstalk with nitric oxide and calcium. *Front. Plant Sci.* 7:230. doi: 10.3389/fpls.2016.00230
- Ohama, N., Sato, H., Shinozaki, K., and Yamaguchi-Shinozaki, K. (2017). Transcriptional regulatory network of plant heat stress response. *Trends Plant Sci.* 22, 53–65. doi: 10.1016/j.tplants.2016.08.015
- Orlob, G. B. (1967). Inactivation of purified plant viruses and their nucleic acids by photosensitizing dyes. *Virology* 31, 402–413. doi: 10.1016/0042-6822(67)90219-X
- Pandey, G. K., Pandey, A., Prasad, M., and Böhmer, M. (2016). Editorial: abiotic stress signaling in plants: functional genomic intervention. *Front. Plant Sci.* 7:681. doi: 10.3389/fpls.2016.00681
- Phung, T. H., Jung, H. I., Park, J. H., Kim, J. G., Back, K., and Jung, S. (2011). Porphyrin biosynthesis control under water stress: sustained porphyrin status correlates with drought tolerance in transgenic rice. *Plant Physiol.* 157, 1746–1764. doi: 10.1104/pp.111.188276
- Phung, T. H., and Jung, S. (2014). Perturbed porphyrin biosynthesis contributes to differential herbicidal symptoms in photodynamically stressed rice (*Oryza sativa*) treated with 5-aminolevulinic acid and oxyfluorfen. *Pest. Biochem. Physiol.* 116, 103–110. doi: 10.1016/j.pestbp.2014.10.002
- Phung, T. H., and Jung, S. (2015). Differential antioxidant defense and detoxification mechanisms in photodynamically stressed rice plants treated with the deregulators of porphyrin biosynthesis, 5-aminolevulinic acid and oxyfluorfen. *Biochem. Biophys. Res. Commun.* 459, 346–351. doi: 10.1016/j.bbrc.2015.02.125
- Pospíšil, P. (2016). Production of reactive oxygen species by photosystem II as a response to light and temperature stress. *Front. Plant Sci.* 7:1950. doi: 10.3389/fpls.2016.01950
- Quesada, V., Sarmiento-Manus, R., Gonzalez-Bayon, R., Hricova, A., Ponce, M. R., and Micol, J. L. (2013). Porphobilinogen deaminase deficiency alters vegetative and reproductive development and causes lesions in *Arabidopsis*. *PLoS ONE* 8:53378. doi: 10.1371/journal.pone.0053378
- Ramel, F., Sulmon, C., Serra, A. A., Gouesbet, G., and Couée, I. (2012). Xenobiotic sensing and signalling in higher plants. *J. Exp. Bot.* 63, 3999–4014. doi: 10.1093/jxb/ers102
- Rebeiz, C. A. (2014). *Chlorophyll Biosynthesis and Technological Applications*. Dordrecht; Heidelberg; New York, NY; London: Springer. doi: 10.1007/978-94-007-7134-5
- Rebeiz, C. A., Gut, L. J., Lee, K., Juvik, J. A., Rebeiz, C. C., and Bouton, C. E. (1995). Photodynamics of porphyrin insecticides. *Crit. Rev. Plant Sci.* 14, 329–366. doi: 10.1080/07352689509382363
- Rebeiz, C. A., Montazer-Zouhoor, A., Hopen, H. J., and Wu, S. M. (1984). Photodynamic herbicides: 1. concept and phenomenology. *Enzyme Microb. Technol.* 6, 390–396. doi: 10.1016/0141-0229(84)90012-7
- Rebeiz, C. A., Montazer-Zouhoor, A., Mayasich, J. M., Tripathy, B. C., Wu, S., Rebeiz, C. C., et al. (1988). Photodynamic herbicides. Recent developments and molecular basis of selectivity. *Crit. Rev. Plant Sci.* 6, 385–436. doi: 10.1080/07352688809382256
- Rebeiz, C. A., Reddy, K. N., Nandihalli, U. B., and Velu, J. (1990). Tetrapyrrole-dependent photodynamic herbicides. *Photochem. Photobiol. Sci.* 52, 1099–1117. doi: 10.1111/j.1751-1097.1990.tb08451.x
- Reed, T. V., Boyd, N. S., Wilson, P. C., and Dittmar, P. J. (2018). Effect of plastic mulch type on fomesafen dissipation in florida vegetable production systems. *Weed Sci.* 66, 142–148. doi: 10.1017/wsc.2017.48
- Rihan, H. Z., Al-Issawi, M., and Fuller, M. P. (2017). Advances in physiological and molecular aspects of plant cold tolerance. *J. Plant Interact.* 12, 143–157. doi: 10.1080/17429145.2017.1308568
- Rio, B., Parent-Massin, D., Lautraite, S., and Hoellinger, H. (1997). Effects of a diphenyl-ether herbicide, oxyfluorfen, on human BFU-E/CFU-E development and haemoglobin synthesis. *Hum. Exp. Toxicol.* 16, 115–122. doi: 10.1177/096032719701600207
- Riou, C., Calliste, C. A., Da Silva, A., Guillaumot, D., Rezazgui, O., Sol, V., et al. (2014). Anionic porphyrin as a new powerful cell death inducer of Tobacco Bright Yellow-2 cells. *Photochem. Photobiol. Sci.* 13, 621–625. doi: 10.1039/c3pp50315a
- Sasikala, C. H., Ramana, C. V., and Rao, P. R. (1994). 5-Aminolevulinic acid: a potential herbicide/insecticide from microorganisms. *Biotechnol. Prog.* 10, 451–459. doi: 10.1021/bp00029a001
- Senge, M. O., MacGowan, S. A., and O'Brien, J. M. (2015). Conformational control of cofactors in nature – the influence of protein-induced macrocycle distortion on the biological function of tetrapyrroles. *ChemComm* 51, 17031–17063. doi: 10.1039/C5CC06254C
- Senge, M., Ryan, A., Letchford, K., MacGowan, S., and Mielke, T. (2014). Chlorophylls, symmetry, chirality, and photosynthesis. *Symmetry (Basel)* 6, 781–843. doi: 10.3390/sym6030781
- Suzuki, N., Koussevitzky, S., Mittler, R., and Miller, G. (2012). ROS and redox signaling in the response of plants to abiotic stress: ROS and redox signaling in plants. *Plant Cell Environ.* 35, 259–270. doi: 10.1111/j.1365-3040.2011.02336.x
- Tangudu, N. K., and Spasic, M. V. (2017). Heme activates macrophage hepcidin expression via toll like receptor 4 and extracellular signal-regulated kinases signaling pathway. *J. Clin. Pharmacol. Biopharm.* 6, 1–6. doi: 10.4172/2167-065X.1000166
- Theodoulou, F. L. (2000). Plant ABC transporters. *Biochim. Biophys. Acta* 1465, 79–103. doi: 10.1016/S0005-2736(00)00132-2
- Tim, M. (2015). Strategies to optimize photosensitizers for photodynamic inactivation of bacteria. *J. Photochem. Photobiol. Biol.* 150, 2–10. doi: 10.1016/j.jphotobiol.2015.05.010
- Tuteja, N., and Sopory, S. K. (2008). Chemical signaling under abiotic stress environment in plants. *Plant Signal. Behav.* 3, 525–536. doi: 10.4161/psb.3.8.6186
- Vian, A., Davies, E., Gendraud, M., and Bonnet, P. (2016). Plant responses to high frequency electromagnetic fields. *Biomed Res. Int.* 2016:1830262. doi: 10.1155/2016/1830262
- Villaneuva, A., Hazen, M. J., and Stockert, J. C. (1986). Photodynamic effect of porphyrin derivative meso-tetra (4-N-methylpyridyl) porphine on sister chromatid exchanges in meristematic cells. *Experientia* 42, 1269–1271. doi: 10.1007/BF01946418
- Villaneuva, A., canete, M., and Hazen, M. J. (1989). Uptake and DNA photodamage induced in plant cells *in vivo* by two cationic porphyrins. *Mutagenesis* 4, 157–159. doi: 10.1093/mutage/4.2.157

- Wainwright, M., Maisch, T., Nonell, S., Plaetzer, K., Almeida, A., Tegos, G. P., et al. (2016). Photoantimicrobials—are we afraid of the light? *Lancet Infect. Dis.* 17, 49–55. doi: 10.1016/S1473-3099(16)30268-7
- Wang, L., Kim, C., Xu, X., Piscurewicz, U., Dogra, V., Singh, S., et al. (2016). Singlet oxygen- and EXECUTER1-mediated signaling is initiated in grana margins and depends on the protease FtsH2. *Proc. Natl. Acad. Sci. U.S.A.* 113, 1–9. doi: 10.1073/pnas.1603562113
- Xu, L., Zhang, W., Ali, B., Islam, F., Zhu, J., and Zhou, W. (2015). Synergism of herbicide toxicity by 5-aminolevulinic acid is related to physiological and ultra-structural disorders in crickweed (*Malachium aquaticum* L.). *Pest. Biochem. Physiol.* 125, 53–61. doi: 10.1016/j.pestbp.2015.06.002
- Yang, K., Jung, S., Lee, Y., and Back, K. (2006). Modifying Myxococcus xanthus protoporphyrinogen oxidase to plant codon usage and high level of oxyfluorfen resistance in transgenic rice. *Pest. Biochem. Physiol.* 86, 186–194. doi: 10.1016/j.pestbp.2006.04.003
- Yang, Y., and Guo, Y. (2017). Elucidating the molecular mechanisms mediating plant salt-stress responses. *New Phytol.* 2, 523–539. doi: 10.1111/nph.14920
- Yun, Y. B., Park, J. I., Choi, H. S., Jung, H., Jang, S. J., Back, K., et al. (2013). Protoporphyrinogen oxidase-overexpressing transgenic rice is resistant to drought stress. *Crop Sci.* 53, 1076–1085. doi: 10.2135/cropsci2012.07.0452
- Zhu, J. K. (2016). Abiotic stress signaling and responses in plants. *Cell* 167, 313–324. doi: 10.1016/j.cell.2016.08.029

Conflict of Interest Statement: The authors declare that the research was conducted in the absence of any commercial or financial relationships that could be construed as a potential conflict of interest.

Copyright © 2018 Issawi, Sol and Riou. This is an open-access article distributed under the terms of the Creative Commons Attribution License (CC BY). The use, distribution or reproduction in other forums is permitted, provided the original author(s) and the copyright owner are credited and that the original publication in this journal is cited, in accordance with accepted academic practice. No use, distribution or reproduction is permitted which does not comply with these terms.

II. PhD objectives

In the introduction, the notion of APDT based on the combinatorial effect of the harmless trilogy: PS-light-oxygen was developed. Until recently, APDT for agronomic approaches was not seriously envisaged especially because plants need light to grow (Gest 1988). Thus, an exogenous spreading of PS on plants in regard to their effects after photoactivation is nonsense. Nevertheless, as demonstrated above, PS are relevant tools to fight against large panel of pathogens from virus to fungi (Figure 9). Therefore, they could also be efficient against plant pathogens (bacteria, fungi and virus) that seriously damage crops.

In order to deal with sustainable development and maintenance of crop protection, there is an upward trend to reduce the use of pesticides that have many drawbacks: harmful effects on non-target organisms including crops, human health risks and pollution. Hence, PS seem to be eco-friendly effective molecules against pathogens for many reasons: 1-PS can be used at low concentrations (micromolar), 2-pathogenic agents cannot develop resistance to PS treatment.

II.1. APDT for plants: Is it a joke?

Our aim was to investigate the plant or “green” side of APDT regarding its possible application as farming practice in the near future. Therefore, we needed to understand how plants themselves respond to PS-mediated photosensitization as we called it photodynamic treatment.

To do so, we chose the worldwide plant model *Arabidopsis thaliana* ecotype Wassilewskija (WS) which is an annual small flowering plant having some weed characteristics and a plant of economic interest *lycopersicum esculentum* (tomato) which is one of the most vegetable plants in the world. Then we studied their responses to water soluble porphyrins that differ by their external charges and groups (cationic or anionic). First of all, none of tested PP was cytotoxic and/or genotoxic when tested under dark condition on seed germination. This result was really promising because it did not disturb germination that is of importance in term of agriculture and probably did not affect soil microlife in agreement to environmental protection. Curiously, both plant species showed different responses to porphyrin treatment at post-emergence stage; although anionic porphyrins had no effect on both plantlets, the cationic ones eradicated *Arabidopsis* but only delayed the growth of tomato plantlets that showed tolerance to such

photodynamic treatment. All these results are largely developed and discussed in two publications and constitute the first chapter of the present manuscript (Publications 2 and 3).

II. 2. Application of charged porphyrins on tobacco cell suspension: a help to understand how PS are photoactivated in plant cells

These studies on plants were not suitable to reveal the fine regulations at molecular level that drives cell and therefore plantlet to death. Indeed, plants are complex multicellular organisms and their responses to drugs and/or PS are multifactorial depending on their genetic background, annual or perennial, stage of development and age, organs or tissues... Thus, we decided to use a simpler model to explore molecular mechanisms of plant photodynamic stress at cellular level: Tobacco Bright Yellow-2 suspension culture, that is one of the most used plant cell cultures for cellular biology research (Nagata 1992). The second reason to choose TBV-2 cells was their ability to grow under dark conditions. Therefore, it is not difficult to induce PS in contact with TBV-2 under light to gain insight in their effects on plant cells. Before I came into the lab, a previous study based on TBV-2 cells and charged porphyrins that are water-soluble, showed that anionic porphyrins were much more efficient to induce cell death than cationic ones (Riou et al., 2014). This first result was in contradiction to the results obtained in *planta*. Thus, we wanted to understand why anionic porphyrins were so efficient to induce TBV-2 cell death while it was cationic porphyrins in *Arabidopsis* and tomato plantlets. Young plantlet cells as well as TBV-2 cells are surrounded by a primary cell wall. Our hypothesis was stated following cell wall composition of TBV-2 cells. It was suspected to be different in term of pectins, hemicellulose and cellulose contents from that of plantlet cells. In a first attempt and as preliminary data needed to understand porphyrin interaction with plant cell, we established TBV-2 cell wall composition and their polysaccharide secretion in the spent medium during TBV-2 cell growth phases (Publication 4).

This work was a pre-requisite for further experiments with porphyrins. Indeed, we needed to know cell wall composition (largely negatively charged) to be able to understand potential porphyrin-cell wall interactions. Here, we try to tackle two questions: 1-how do porphyrins induce cell death in relation to their chemical structure and interact with the first barrier, the plant cell wall? 2- what are the molecular mechanisms in term of ROS production and cell responses underlying plant photodynamic treatment?

II.3. Manuscript presentation

We chose to present our PhD manuscript as accepted and/or submitted (or in preparation) publications with general introduction and discussion relative to the multiple aspects of this work. In the Chapter I, two publications deal with APDT feasibility in Plants (Guillaumot et al., 2016; Issawi et al. 2018). In the Chapter II, one publication was accepted in Glycoconjugate journal (Issawi et al. 2017) relative to TBY-2 characterization: cell wall and polysaccharide secretion in spent medium. The two other publications cover separately chemical and biological aspects that will help to answer to the fundamental question: how anionic porphyrins are able to strongly induce TBY2 cell death? The chemical structure of anionic porphyrins and their behavior in organic solvent or aqueous solutions were investigated in Leroy-Lhez et al. submitted to Photochemical & photobiological science. Porphyrin and cell wall interaction and induction of photodynamic stress in TBY-2 cells were developed and studied in a manuscript in preparation for the Plant Journal. The end of the manuscript will be devoted to a large discussion with open up perspectives followed by a completed bibliography and a CV of the PhD candidate.

Chapter I. APDT in agronomy: Dream or reality?

Response to photoactivated PS is linked to plant species and physicochemical properties of PS. Thus, it was recommended to study the responses of plant to photodynamic treatment in a case-by-case way depending on plant species. In order to fulfill that task, we focused on annual plants that could show tolerance to photoactivated porphyrins unlikely to perennial trees that are protected by thick cuticle preventing efficiently the PS photodamage. Firstly, we focused on plant of agronomic interest: *Lycopersicon esculentum*, commonly known as tomato. Response to cationic or anionic porphyrin was opposite. While anionic porphyrin (TPPS) tested at 50 μM did not alter plantlet growth, cationic porphyrins (Zn-TMPyP or free-base TMPyP) significantly reduced growth at low concentration (3.5 μM). Nevertheless, tomato plantlets were able to resist to cationic porphyrins via induction of antioxidative systems (enzymes such as catalase, peroxidase and superoxide dismutase and antioxidant molecules) (Publication 2). To enlarge our expertise, we chose *Arabidopsis thaliana*, ecotype Wassilewskija (WS). *Arabidopsis* is a “lab star” presenting special features as fast growth rate and invasiveness. Surprisingly, we showed that these plants were roughly killed under the action of cationic porphyrins. Thus, we conceived a dual strategy aiming to eradicate in the same way plant pathogens and weeds (Publication 3).

PUBLICATION 2: “Synergistic enhancement of tolerance mechanisms in response to photoactivation of cationic tetra (N-methylpyridyl) porphyrins in tomato plantlets”, *Journal of Photochemistry and Photobiology B: Biology*.

Accepted Manuscript

Synergistic enhancement of tolerance mechanisms in response to photoactivation of cationic tetra (N-methylpyridyl) porphyrins in tomato plantlets

Damien Guillaumot, Mohammad Issawi, Anne Da Silva, Stephanie Leroy-Lhez, Vincent Sol, Catherine Riou

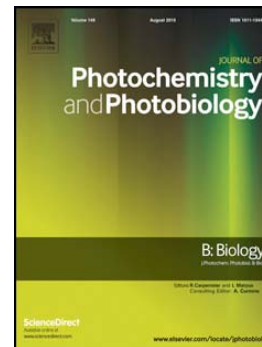
PII: S1011-1344(15)30093-2
DOI: doi: [10.1016/j.jphotobiol.2016.01.015](https://doi.org/10.1016/j.jphotobiol.2016.01.015)
Reference: JPB 10233

To appear in:

Received date: 13 October 2015
Revised date: 15 January 2016
Accepted date: 25 January 2016

Please cite this article as: Damien Guillaumot, Mohammad Issawi, Anne Da Silva, Stephanie Leroy-Lhez, Vincent Sol, Catherine Riou, Synergistic enhancement of tolerance mechanisms in response to photoactivation of cationic tetra (N-methylpyridyl) porphyrins in tomato plantlets, (2016), doi: [10.1016/j.jphotobiol.2016.01.015](https://doi.org/10.1016/j.jphotobiol.2016.01.015)

This is a PDF file of an unedited manuscript that has been accepted for publication. As a service to our customers we are providing this early version of the manuscript. The manuscript will undergo copyediting, typesetting, and review of the resulting proof before it is published in its final form. Please note that during the production process errors may be discovered which could affect the content, and all legal disclaimers that apply to the journal pertain.



Synergistic enhancement of tolerance mechanisms in response to photoactivation of cationic tetra (N-methylpyridyl) porphyrins in tomato plantlets

Damien Guillaumot^a, Mohammad Issawi^a, Anne Da Silva^b, Stephanie Leroy-Lhez^a, Vincent Sol^a and Catherine Riou^{a*}

^aLaboratoire de Chimie des Substances Naturelles (EA 1069), Université de Limoges, Faculté des Sciences et Techniques, 123 avenue Albert Thomas, 87060 Limoges Cedex, France

^b Unité de Génétique Moléculaire et Animale (UMR INRA 1061), Université de Limoges, Faculté des Sciences et Techniques, 123 avenue Albert Thomas, 87060 Limoges Cedex, France

* correspondence to: Catherine Riou, Laboratoire de Chimie des Substances Naturelles (EA 1069), Université de Limoges, Faculté des Sciences et Techniques, 123 avenue Albert Thomas, 87060 Limoges Cedex, France E-mail : catherine.riou@unilim.fr

Keywords: Photoactivation; cationic and anionic porphyrins; ROS production; *Solanum lycopersicum*.

Abstract

Antimicrobial photodynamic treatment (APDT) is largely used in medical domain and could be envisaged as a farming practice against crop pathogens such as bacteria and fungi that generate drops in agricultural yields. Thus as a prerequisite for this potential application, we studied the effect of water soluble anionic (TPPS and Zn-TPPS) and cationic (TMPyP and Zn-TMPyP) porphyrins tested on tomato (*Solanum lycopersicum*) plantlets grown *in vitro* under a 16h photoperiod. First of all, under dark conditions, none of the four porphyrins inhibited germination and induced cytotoxic effects on tomato plantlets as etiolated development was not altered. The consequences of porphyrin long term photoactivation (14 days) were thus studied on *in vitro*-grown tomato plantlets at phenotypic and molecular levels. Cationic porphyrins especially Zn-TMPyP were the most efficient photosensitizers and dramatically altered growth without killing plantlets. Indeed, tomato plantlets were rescued after cationic porphyrins treatment. To gain insight the different molecular ways implied in the plantlet tolerance to photoactivated Zn-TMPyP, lipid peroxidation, antioxidative molecules (total thiols, proline, ascorbate) and ROS detoxification enzymes were evaluated. In parallel to an increase in lipid peroxidation and hydrogen peroxide production, antioxidative molecules and enzymes (guaiacol peroxidase, catalase and superoxide dismutase) were up-regulated in root apparatus in response to photoactivated Zn-TMPyP. This study showed that tomato plantlets could overcome the pressure triggered by photoactivated cationic porphyrin by activating antioxidative molecule and enzyme arsenal and confining Zn-TMPyP into cell wall and/or apoplasm, suggesting that APDT directed against tomato pathogens could be envisaged in the future.

1. Introduction

Molecules such as porphyrins, naturally present in all living kingdom, are photoexcitable by sunlight and able to produce reactive oxygen species (ROS) such as superoxide anion radical, hydrogen peroxide, hydroxyl radical and singlet oxygen which, in turn, lead to cell damage and ultimately cell death^{1,2}. Under dark, porphyrins do not exhibit significant cyto or genotoxicity.^{1,4} Two studies performed on root meristematic cells of *Allium cepa* and tobacco Bright Yellow cell suspensions showed opposite results with photoactivated porphyrins^{4,5}. Study performed on *Allium cepa* root apex demonstrated that cationic porphyrins, either free or Zn-metallated, induce DNA photodamage whereas in tobacco cell suspension, anionic and cationic porphyrins were not cytotoxic and anionic porphyrin was the most efficient death inducer compared to cationic one upon illumination. According to literature, this last result was quite surprising taking into account that cationic or neutral porphyrins are always the most efficient to induce cell death from bacteria to mammal cells and/or tissues. Previous work showed that derivatives of cationic porphyrin were more efficient than neutral and anionic porphyrins on Gram-negative bacteria (*Escherichia coli*) and that these effects were less pronounced on Gram-positive bacteria such as *Enterococcus hirae* or *Staphylococcus aureus*^{2,6-10}. Likewise, exogenous supply of cationic porphyrin in cultures of cyanobacteria and green microalgae showed that the latter were more photosensitive than the former.¹¹ Upon illumination, protoporphyrin IX and other derivatives were proved to be strongly cytotoxic to the yeasts *Saccharomyces cerevisiae* and *Candida albicans*.^{1,12-14} Furthermore, tested on mosquito or fly larvae, photoactivated cationic porphyrins also possess an insecticidal power.¹⁵⁻¹⁷ Finally, strategies known as photodynamic therapy including antimicrobial photodynamic treatment are based on the use of photoactivated porphyrins in a large variety of medical domains such as cancerology,

dermatology, ophthalmology or odontology^{1-3, 18}. This strategy is also envisaged to struggle plant-pathogens such as *Colletrichum acutatum* and *Aspergillus nidulans* fungi¹⁹

All these studies were focused on an optimization of a fatal issue such as death linked to photoactivation of porphyrins. Furthermore they were essentially performed on isolated cells or tissues from prokaryotic to eukaryotic cells, excepted on mosquito larvae. Nevertheless it should be of interest to understand the consequence of photoactivation of exogenous porphyrins in whole organisms especially in plants. Indeed as antimicrobial photodynamic treatment (APDT) could be considered as a potential agronomic strategy against plant pathogens (fungi and bacteria)¹⁹, it would be of interest to study the response of plants to photoactivated porphyrins. In that respect, our aim was to study the effect of two categories of water-soluble synthetic porphyrins: cationic and anionic porphyrins, either free base (TMPyP and TPPS, respectively) or zinc-metallated (Zn-TMPyP and Zn-TPPS) on tomato plantlets grown *in vitro*. Previous studies on plants were performed to set up modifications of endogenous porphyrins biosynthesis by transgenesis.²⁰⁻²⁴ Authors showed that an accumulation of protoporphyrin IX, common precursor of heme and chlorophylls, triggered lethal phenotypic alterations (growth inhibition, browning leaves, desiccation) after illumination.^{22,23}

Based on these studies and because porphyrins could be used as antimicrobial agents in agronomic practices, we studied the consequences of sunlight photoactivation of exogenous porphyrins on tomato plantlets at phenotypic and molecular levels. We supposed that defense mechanisms such as antioxidative machinery would be activated to allow plantlet tolerance to the presence of exogenous photosensitizer. We firstly showed that none of these porphyrins was able to inhibit germination and was cytotoxic under dark conditions. Thus, we compared the consequences of their photoactivation on phenotype of 14 day-old *in vitro* plantlets. Cationic porphyrins, especially Zn-TMPyP, induced the strongest altered phenotype.

Nevertheless, tomato plantlets could resist to high amounts of cationic porphyrins and also be completely rescued afterwards. Thus, taking into account these first results, we focused our study on the cellular and molecular mechanisms triggered in particularly by Zn-TMPyP in plantlets roots, trying to understand how tomato plantlets were able to resist to photoactivated Zn-TMPyP. Indeed, endogenous levels of total thiol, proline and ascorbate, considered as antioxidant molecules, and enzyme activities such as peroxidases and superoxide dismutase were significantly up-regulated in tomato roots. In conclusion we suggested that, in response to Zn-TMPyP photoactivation tomato plantlets were able to produce appropriate amounts of total thiol, proline and ascorbate as well as to sufficiently activate ROS detoxification enzymes to resist to photoactivated Zn-TMPyP.

2. Materials and methods

2.1 Porphyrins

All porphyrins are soluble in water and their chemical structures have been reported in Fig 1. Anionic porphyrin corresponds to TPPS and was purchased from Sigma-Aldrich (St Louis, MO, USA). Zn-TPPS was obtained by metallation of TPPS with zinc acetate.²⁵ Cationic porphyrins: Tetra (N-methylpyridyl) porphyrin tetrachloride or TMPyP and Zn-TMPyP were purchased from Frontier Scientific (Carnforth, UK).

To evaluate porphyrin photostability in the plant culture medium, they were added to the medium at the wanted concentration. For all experiments, plates were maintained for 15 days in a controlled growth chamber at 22 °C under a 16h photoperiod and a photon flux density of 250 $\mu\text{mol}\cdot\text{m}^{-2}\cdot\text{s}^{-1}$. Photostability was evaluated by Uv-Vis absorption method, monitoring decrease of the Soret Band at 437 and 414 for Zn-TMPyP and TPPS respectively. For each measurement, a square (1cm²) of medium with porphyrin was taken, suspended in 10 mL

water under vigorous agitation. Then absorption spectra was recorded. Initial value of Soret band absorbance was used to define 100% level.

2.2 Plant material

Seeds of tomato var Bali F1 hybrid purchased from Tézier (Portes-lès-Valence, France), were germinated *in vitro* on a Gamborg B5 culture medium (Duchefa Biochemie, Haarlem, Netherlands) at pH 5.8 supplemented with 2% (w/v) sucrose and 0.8% (w/v) agar (Difco, Dallas, USA).²⁶ Porphyrins were added to the medium after autoclaving. For all experiments, plants were grown on 25 mL of B5 alone or supplemented with porphyrin in a controlled growth chamber at 22 °C under a 16h photoperiod and a photon flux density of 250 $\mu\text{mol. m}^{-2} \text{s}^{-1}$. Cool daylight lamps (OSRAM Lumilux 24W) were used in the growth chamber. After 14 days of growth, tomato plantlets were harvested and used for phenotypic and biochemical analyses. Germination ratio was evaluated after 4 days of culture using a binocular microscope. Under these conditions, 8 tomato seeds were sown on the same plate. The experiments were performed three time independently. Pictures from the last experiment were taken with a digital camera and/or under a Leica binocular microscope.

For cytotoxicity assessment, plates containing 8 seeds and surrounding by aluminium foil in order to avoid any light source were maintained vertically for 4 days in growth chamber. The experiments were performed three time independently.

Roots and shoots from tomato plantlets isolated from 14 day-old plantlets were harvested, weighed and frozen at -20 °C until used. For the determination of the ratio dry weight on fresh weight, tomato organs were fresh weighed (FW), dried at 42 °C for 4 days and weighed again (DW).

2.3 Confocal microscopy analysis

We incubated 14 day-old plantlets in B5 medium containing or not 3.5 μM Zn-TMPyP for 20 h in the dark and rinsed them 3 times with B5 new medium before observation under a LSM510META Zeiss confocal microscope. For analysis, two ways of data acquisition were performed: a spectral acquisition to check signal specificity of Zn-TMPyP and a channel mode for calcofluor and Zn-TMPyP. For spectral acquisition, samples were excited at 458 nm and fluorescence was monitored between 476 and 732 nm. Zn-TMPyP specific emission peak was detected around 640 nm as its fluorescence emission maxima is at 634 nm⁴. For channel mode acquisition, we used an excitation wavelength at 405 nm and emission wavelength between 420 and 450 nm for calcofluor and excitation wavelength at 458 nm and a long pass filter (cut off at 560 nm) for Zn-TMPyP.

2.4 *In situ* DAB and NBTZ stainings

3,3-diaminobenzidine (DAB) staining on tomato roots was performed using DAB Kit (Sigma-Aldrich, St Louis, MO, USA) following manufacturer's instructions. Nitro blue tetrazolium (NBTZ) staining was performed as followed: roots were dived into 10 mM phosphate buffer pH7.8, 10 mM NaNO_3 and 0.1 % (w/v) NBTZ. Roots were vacuum infiltrated for 5 min and placed in the dark for 2 h for DAB and 30 min for NBTZ respectively. DAB or NBTZ solutions were replaced by 70% (v/v) ethanol and stored at 4 °C until examination under a binocular microscope.

2.5 Hydrogen peroxide (H_2O_2) quantification

The H_2O_2 measurement was performed according to ²⁷ with some modifications. 1 mL of sodium phosphate buffer (25 mM, pH 7) was added to the frozen samples ground with liquid nitrogen. The homogenate was centrifuged at $10,000 \times g$ at 4 °C for 15 min. 335 μl of 0.1%

titanium III sulfate in 20% (w/v) H₂SO₄ was added in extracted solution. The absorbance was measured at 415 nm and H₂O₂ level was expressed as nM.g⁻¹ proteins. Proteins were quantified by Bradford assay using BSA as standard²⁸.

2.6 Antioxidant molecule assays

2.6.1 Proline content

Free proline contents of tomato roots were assayed according to a previous work.²⁹

2.6.2 Ascorbate content

Ascorbate was quantified as previously reported³⁰ with some minor modifications. Frozen plant tissues (between 50 and 200 mg FW) were ground into powder using liquid nitrogen. The resulting powder was weighed before addition of 200 µL of 6% TCA solution. Samples were then incubated for 10 minutes on ice and centrifuged at 16 000 g for 25 minutes at 4 °C. Supernatant was completed to 500 µL with 6% TCA and centrifuged 16 000 g for 10 minutes at 4 °C. 100 µL of each sample were then transferred to 150 µL 0.2 M phosphate buffer pH 7.4 and supplemented with 250 µL 10 % TCA, 200 µL 42 % H₃PO₄, 200 µL 2,2'-dipyridyl and 100 µL 3% FeCl₃. Similarly, standards containing 0 to 70 µmoles of ascorbate were realized. After 40 minute incubation in a 42 °C water bath, absorbance of standards and samples were read at 525 nm.

2.6.3 Total thiol assay

Total thiol assay was performed according to³¹. Frozen samples were ground in liquid nitrogen and then extracted into 1 mL of 0.2 N HCl. After centrifugation at 16000 x g for 4 min, 500 µL of extracted solution were neutralized with 400 µL NaOH (0.2M) and 50 µL NaH₂PO₄ (0.2M). 0.7 mL of 0.12 M NaH₂PO₄ (pH 7.5), 6 mM EDTA, 0.1 ml of 6 mM Dithiobis 2 nitro benzoic acid (DTNB) were added to 0.2 mL extract. For standards, extract

was replaced by 0, 10, 20, 50, and 100 nmol GSH (total volume 1mL). Absorbance at 412 nm was read 5 min after the addition of standard or extract.

2.7 Determination of malondialdehyde (MDA) content

Around 100 mg of fresh or frozen plant materials were ground in liquid nitrogen. The resulting powder was suspended into 1.5 mL of 20% TCA. After centrifugation, supernatants were collected and analyzed for their MDA content as described by ³² with minor modifications. 500 μ L of each sample were added to either 500 μ L 20 % TCA alone (-TBA) or 20% of TCA supplemented with 0.5% thiobarbituric acid (+TBA). Samples were then boiled in a water bath for 30 minutes. The samples were cooled on ice and absorbances were read at 440, 560 and 600 nm. Owing to the possible presence of porphyrin in the extract and subsequent interference with absorbance readings at 440 nm, some modifications were brought to the calculation formula proposed by ³²

$$1) [(Abs\ 532_{+TBA} - Abs\ 600_{+TBA}) - (Abs\ 532_{-TBA} - Abs\ 600_{-TBA})] = A$$

$$2) \{[(Abs\ 440_{+TBA} - Abs\ 600_{+TBA}) - (Abs\ 440_{-TBA} - Abs\ 600_{-TBA})] 0.0571\} = B$$

$$3) \text{MDA equivalents (nmol.L}^{-1}\text{)} = [(A-B)/157\ 000] \cdot 10^6$$

2.8 Determination of enzymatic activities

Frozen plant samples were ground to a fine powder in liquid nitrogen. Proteins were solubilized into 1 mL of extraction buffer containing 50 mM phosphate buffer pH 7.8, 1 mM EDTA, 1% (w/v) PVP and 10 % (v/v) glycerol and centrifuged at 16 100 g for 10 minutes at 4 °C. Protein concentration of the resulting supernatant was quantified according to Bradford (1976)²⁸.

2.8.1 Catalase

Catalase activity was measured according to Aebi's protocol.³³ 20 µg of total soluble proteins were diluted into a 50 mM phosphate potassium buffer (pH 6.5). The reaction was initiated by addition of H₂O₂ to a final concentration of 20 mM and for a final volume of 1 mL. Absorbance decrease at 240 nm was monitored during 3 minutes and H₂O₂ disappearance was calculated on the slope of the linear portion of the resulting curve using a molar extinction coefficient of 43.6 M⁻¹cm⁻¹.

2.8.2 Guaiacol peroxidase

Guaiacol peroxidase activity was monitored at 436 nm due to the formation of tetraguaiacol and calculated using a molar extinction coefficient of 25.5 mM⁻¹.cm⁻¹. 10 µg of total soluble proteins were diluted into 50 mM phosphate potassium buffer pH 6.5 and supplemented with 0.25% guaiacol (5 % stock solution in 95 % ethanol w/v). Reaction was initiated by addition of H₂O₂ to a final concentration of 2.5 mM and absorbance was immediately monitored during 2 minutes.

2.8.3 Ascorbate peroxidase

Ascorbate peroxidase activity was analyzed by adapting the microplate protocol to tubes.³⁴ 20 µg of soluble protein extracts of tomato roots were diluted into 50 mM phosphate buffer pH 7.0 supplemented with 0.25 mM ascorbic acid. The reaction started by addition of H₂O₂ up to 5 mM in a final reaction volume of 1 mL. The decrease in absorbance at 290 nm corresponding to the formation of ascorbate was then monitored during 3 minutes. Activity was calculated on the slope of the linear section of the resulting curve using a molar extinction coefficient of 2.8 mM⁻¹.cm⁻¹.

2.8.4 Superoxide dismutase

Superoxide dismutase (SOD) activity protocol was performed in absence of bathocuproine sulfonate.³⁵ Standard curve was set so that the increase in absorbance at 560 nm was between

0.02 and 0.03 absorbance unit per minute and was monitored for 5 minutes. One unit of SOD was defined as the amount of enzyme required for a 50% inhibition of NBT reduction. 5 μ L of enzyme extract were used. SOD specific enzyme activity was determined according to the protein concentration of each sample.

2.9 Statistical analysis

Germination percentage was assessed according to generalized linear models with quasibinomial proportional distribution of errors to correct overdispersed data. All results were expressed as mean \pm SEM (Standard Error of the mean). Data were analyzed by t-student test and one-way ANOVA followed by the Dunnett multiple comparison test³⁶ using the Control group as reference, while p-value < 0.05 was considered statistically significant. All tests were performed in R statistical software (R Developmental Core Team 2012).

3. RESULTS

3.1 Seed germination in presence of 80 μ M anionic and cationic porphyrins

Germination of tomato seeds sown on media containing each tested porphyrin at high concentration was examined (Table 1). As none of the photosensitizers significantly inhibited tomato seed germination, anionic or cationic porphyrins could definitely not be considered as cytotoxic at pre-emergence state.

3.2 Phenotype analyses of tomato plantlets in the dark and under illumination.

3.2.1 Porphyrins did not altered tomato seedling development under dark

To gain insight porphyrins cytotoxicity during post-germination event, seedling growth was tested and observed in the dark in presence of 80 μ M porphyrins for both species (Fig. 2). Tomato seedlings grown in the dark did not show any significant growth alteration after 4 days treatment (Fig. 1) suggesting that the four photosensitizers were neither cytotoxic nor genotoxic for tomato seedlings.

3.2.2 Phenotype alterations under 16h photoperiod

As porphyrins are photoexcitable by visible light, light exposure effects of porphyrins, tomato seeds were allowed to germinate on each compounds for 14 days (Fig. 3A). Although phenotypic alterations were not really obvious in contact of 50 μ M TPPS or Zn-TPPS compared to control condition, plantlets showed significant reduction in hypocotyl and root length while no new leave did appeared in presence of 3.5 μ M TMPyP or Zn-TMPyP. We determined the ratio of dry to fresh weight; this ratio significantly increased in all the tested conditions in comparison to the controls. Taking together, these results suggested that cationic porphyrin especially the metalated form induced a strong abiotic stress (Fig. 3B). Intriguingly Zn-TPPS seemed to be the less stressful photoactivated porphyrins in regard to its effect on

plant phenotype of plantlets (Fig. 3A). To gain insight into the selection of the most efficient photosensitizers with the aim of a future APDT application, we gave up the anionic porphyrins (Zn-TPPS and TPPS) that are not enough efficient to kill fungi and bacteria. In another way, we showed that they did not alter tomato plantlet growth.

3.3 Plantlet rescue after treatment with photoactivated cationic porphyrins TMPyP and Zn-TMPyP

As high concentration of cationic photosensitizers induced important alterations of developmental trait of tomato plantlets under light but did not seem to be cytotoxic in the dark, we checked whether tomato plantlets could be rescued after 14 days on 80 μM cationic porphyrins. Such tomato plantlets were thus transferred on medium without porphyrins for one week and then allowed to grow in soil for 6 more weeks (Fig. 4). In light of our results, we could assume that tomato plants were rescued since they had recovered a growth similar to control plant, meaning that 14 days contact with cationic porphyrins did not fatally disturb growth and development of tomato plantlets to prevent further normal development, which was quite surprising after 80 μM Zn-TMPyP treatment. Thus in order to understand the reason behind such tolerance, we decided to further analyze the defense mechanisms in presence of photoactivated TMPyP and Zn-TMPyP. We decided to work with a very lower concentration of cationic porphyrins corresponding to 3.5 μM which was able to sufficiently stress plants.

3.4 Zn-TMpyP localization in root apparatus

As under illumination, Zn-TMPyP clearly induced phenotypic effects on plantlets; it was of importance to check Zn-TMPyP localization in root apparatus although it was already shown that cationic porphyrins (free metal or not) were located in meristematic root cells of *Allium*

cepa and more precisely into nucleus¹⁹. As photoactivated Zn-TMPyP treatment strongly affected plants tissues, root incubation was performed in the dark in order to study its localization in tomato healthy roots. In tomato thick sections performed in elongation zone, Zn-TMPyP seemed to be confined to cell wall and/or apoplast as shown by co-localization with calcofluor used as cell wall marker (Fig. 5). Contrary to previous work⁵, our result strongly suggested that Zn-TMPyP stayed outside of cell cytoplasm of tomato root epidermis. This result could be also well correlated to the non cytotoxicity or genotoxicity described above.

3.5 Lipid peroxidation and ROS production as a consequence of cationic porphyrin photoactivation

Because photoactivated porphyrins generate reactive oxygen species (ROS), cell membranes containing high amounts of polyunsaturated lipids represent a target for these powerful reactive molecules leading to lipid peroxidation, degradation, and further malondialdehyde production (MDA). Thus we checked MDA level in roots and shoots of tomato plantlets. A significant increase in MDA content was found in roots and shoots of cationic porphyrins treated plantlets compared to control (Fig. 6). This was probably linked to Zn-TMPyP localization in root cells. As shown by confocal microscopy, Zn-TMPyP preferentially accumulates into cell wall rather than in apoplasm, thus preventing its lethal effect under illumination. Nevertheless DAB and NBTZ stainings showed that ROS such as hydrogen peroxide (H_2O_2) and in a lesser extent anion superoxide (O_2^-) were produced in root apparatus in particularly root apex of treated plantlets (Fig. 7 A and B). This was also confirmed by the detection of a high amount of H_2O_2 in roots by comparison in shoots (Fig. 6C). As H_2O_2 is more stable than the other ROS and diffuses into cells, we supposed that photoactivation of Zn-TMPyP probably led to type I rather than type II reactions in root cells.

3.6 Antioxidant molecule productions in treated tomato plantlets

To gain insight into ROS generated pathway upon porphyrins illumination, we determined ascorbate, proline and total thiol contents in plantlets considering them as antioxidant molecules. The abiotic stress triggered by photoactivated Zn-TMPyP induced, in tomato roots, a huge increase in proline (around 40 fold) and to a lesser extent in ascorbate and total thiol (around twice) contents (Fig. 8). These results could explain why tomato plantlets were able to better resist to photoactivated Zn-TMPyP by generating a large amount of proline and to a lesser extent thiol and ascorbate in order to offset ROS production triggered by its photoactivation.

3.7 Pattern of antioxidative stress enzymes in response to photoactivated Zn-cationic porphyrin

Finally, the question of enzymes involved in superoxide radicals and hydrogen peroxide take off was considered as another way to fight against ROS production induced by photoactivated Zn-TMPyP. Thus we determined guaiacol and ascorbate peroxidases, catalase and superoxide dismutase activities in tomato roots growing in presence of 3.5 μ M Zn-TMPyP. Guaiacol peroxidase and catalase activities were clearly up-regulated, reaching, respectively, three-fold and around two-fold enhancement compared to the control (Fig. 9). Strikingly, ascorbate peroxidase did not show any increase although intracellular ascorbate content was shown to increase (Fig. 8 and 9). Superoxide dismutase activity also increased, suggesting its implication in transformation of superoxide radicals overproduced by photoactivated Zn-TMPyP treated roots into hydrogen peroxide that could be essentially transformed by catalase and not by ascorbate peroxidase that, in turn, did not change (Fig. 9).

4 DISCUSSION

In this work, we studied the effect of two categories of synthetic porphyrins on tomato plantlets (*Solanum lycopersicum* var. Bali). The choice of tomato plants as experimental model was triggered by two main reasons: this plant represents a wide cultured species over the world and it is mainly attacked by pathogens such as bacteria (*Xanthomonas campestris* and *Pseudomonas syringae*) and fungi (*Phytophthora infectans*).³⁷ These pathogens could be eradicated by using the PACT strategy^{1-3,7,8,19}. From that perspective, it should be of interest to understand how plants could resist to such a future potential treatment. We are confident that these preliminary data performed *in vitro* reflected what could happen in green houses or soil. To our knowledge this is the first study that address this type of issue in regard to the use of photosensitizers as pesticides. Thus our aim was not to describe a new herbicide but to try to understand how plants are able to fight against a photoactivated antimicrobial agent potentially used in agriculture. Previous study and experiments in our laboratory were monitored to test the effect of anionic and cationic porphyrins on *Pseudomonas aeruginosa* and showed that cationic porphyrins were also the most efficient (data not shown)³⁷.

Currently, the phototoxicity property of porphyrins and their herbicidal effect were indirectly described in plants. The first approach was to feed cultures or spread plants with precursor of tetrapyrrole compounds biosynthesis such as 5-aminolevulinic acid (ALA).³⁹⁻⁴¹ Although presenting a true herbicide property, ALA treatment required high concentrations (around 20 mM) that was very much higher to 3.5 μ M cationic porphyrins described in this study.^{40,41} The other approach using transgenesis targeted to porphyrin oxidase activity, showed that modifications in porphyrins metabolism in rice and maize plants led to fatal issue.²⁰⁻²⁴ Culture on exogenous cationic porphyrins also induced dramatic effects on tomato plantlets similar to the described phenotype of porphyrin oxidase overproducer. Nevertheless

in regard to plant rescue when the porphyrin pressure was removed and their rapid photobleaching (Table 2), cationic porphyrins could not be considered as potential post-emergence herbicide.

Under dark conditions porphyrins did not lead to phenotypic alterations of tomato plantlets. This result confirmed the no-cytotoxicity and genotoxicity effect of porphyrins as already shown for tobacco plant cells.⁴

Upon illumination, porphyrins generate radicals such as superoxide anion ($O_2^{\bullet-}$) and hydroxyl radical (OH^{\bullet}) by electron transfer (type I process) or singlet oxygen (1O_2) by energy transfer to dioxygen (type II process). As singlet oxygen lifetime is very short (order of the nanosecond), its scope is limited to the formation site.^{1,42} Nevertheless it remains still very difficult to detect this species *in vivo*. Generation of free radicals as superoxide anion radical ($O_2^{\bullet-}$) or hydroxyl radical (OH^{\bullet}) could also lead to the formation of hydrogen peroxide (H_2O_2) and other reactive oxygen species. The significant increase in H_2O_2 detected in tomato roots treated with Zn-TMPyP could at least correspond to a pool coming from type I reaction and anion superoxide and from the transformation of singlet oxygen into H_2O_2 , the most stable ROS. All these ROS damage a large number of cellular constituents such as nucleic acids, proteins and lipids, leading to cell death by necrosis and more often by apoptosis.⁴³⁻⁴⁵ As a consequence of porphyrin photoactivation, cell death was shown in animal cells, fungi, bacteria and recently in tobacco BY-2 cells.^{1,4,6-17}

One of the consequences of Zn-TMPyP photoactivation was supposed to be superoxide anion radical and hydroxyl radical productions. Thus because lipid peroxidation is thought to be mainly triggered by these ROS, we performed a MDA quantification on tomato roots. Tomato roots and especially shoot cells showed an increase in MDA, suggesting that cell membranes were damaged. Nevertheless as Zn-TMPyP seemed to be only accumulated in cell

wall and/or apoplast and not in the nucleus as shown in *Allium* root cells⁵, we suggested that Zn-TMPyP were able to produce ROS close to plasma membrane under illumination. Furthermore the Zn-TMPyP localization could explain its no-genotoxicity in tomato plantlets although DNA damages could also be triggered by MDA; this molecule has been shown to be highly mutagenic for bacteria and mammal cells as well.⁴⁵

Another way for the plantlets to tolerate to photoactivated Zn-TMPyP and to protect themselves against ROS, is to produce antioxidant molecules that could neutralize ROS. Thus we determined proline and ascorbate contents in tomato roots. Clearly, tomato plantlets were able to co-activate the production of total thiol, proline and ascorbate. In plants, the role of proline as free radical scavenger in response to a large range of abiotic and biotic stresses was proposed.^{47,48} Proline can act as singlet oxygen quencher and as scavenger of hydroxyl radicals⁴⁷. We can suppose that proline (40 fold increase) assumes these two roles in tomato roots in response to photoactivated Zn-TMPyP. Additionally, ascorbate can rapidly react with singlet oxygen resulting in hydrogen peroxide production and has therefore been suggested to be a good sink of this ROS.⁴⁹ Both amounts of these ROS scavengers and/or quenchers were significantly overproduced in Zn-TMPyP treated tomato roots to counteract its photoactivation. It should be also interesting to quantify other scavengers such as α tocopherol to refine the different ROS triggered by Zn-TMPyP under illumination in roots.

As for ascorbate and proline, a significant increase in total thiol content was detected in treated roots in response to Zn-TMPyP. Total thiol quantification was envisaged as a link between its potential role as scavenger and ROS enzymes especially peroxidases. Previous work showed that protoporphyrin IX was able to be degraded by plant peroxidases associated to thiol substrates such as glutathione and cysteine⁵⁰. Furthermore this reaction was inhibited by ascorbate⁵⁰. This could explain why we did not detected any change in ascorbate peroxidase activity in tomato roots but around a two fold increase in ascorbate content. Thus

we envisage to address this issue by measuring glutathione content and glutathione relative activities. In the other hand, we might suppose that Zn-TMPyP could also be degraded by this way which should be also relevant to its non fatal effect after a 14-day treatment.

In parallel, we investigated ROS detoxification enzyme activities such as peroxidases, catalases and superoxide dismutases. In plantlets, these enzymes with exception of ascorbate peroxidases were clearly up regulated to counter balance ROS production induced by Zn-TMPyP photoactivation. GPX and catalase could scavenge H_2O_2 produced in one way by SOD and in other way by Zn-TMPyP photoactivation (type I reaction). Furthermore, GPX activity is known to be regulated by biotic and abiotic stresses that corresponded to our situation.^{27,53} A possible explanation could arise from Zn-TMPyP subcellular localization in apoplast and/or cell wall of tomato root cells. Indeed GPX that are class III peroxidases are mainly located into cytoplasm and apoplast while class I peroxidases such as ascorbate peroxidases are essentially intracellular^{51,52}. Thus, it seems relevant that GPX would preferentially be activated in order to detoxify the cells from the oxidative stress generated by photoactivated Zn-TMPyP. Additionally the effect of GPX in preventing membrane lipid peroxidation has also been reported and is consistent with the lower amount of MDA found in Zn-TMPyP treated tomato plantlets⁵³. Our study based on tomato plantlets grown *in vitro* in contact to Zn-TMPyP revealed that tomato plantlets were able to protect themselves from this abiotic stress using three different and concomitant ways: Zn-TMPyP accumulation in cell wall and potentially its degradation, antioxidant molecules production and activation of ROS detoxification enzymes.

Although photoactivated Zn-TMPyP was efficient to dramatically slow down plantlet growth, plantlets did not die. We supposed that while the enzymatic activities and anti-oxidative molecules significantly increased, it was not sufficient to assume a normal growth of the plantlets grown in contact to photoactivated Zn-TMPyP. One hypothesis could be that a

proportion of H_2O_2 amount stay into cell and interfered with root growth. Another hypothesis should be that primary metabolism and anti-oxidative molecules synthesis activated in response to Zn-TMPyP affected the other metabolisms linked to normal root growth. Indeed, root apparatus was really and deeply altered showing a typical reduction of main root growth and multiple lateral root formation linked to an escape strategy. Such behaviour was also described in resistance to abiotic stress. Plant growth and development suffered from the fact that it focused on coping with such oxidative stress and efficiently activating its defense mechanisms. Considering the ability of photoactivated cationic porphyrins to rapidly kill bacteria at low concentration⁷ (decrease in bacterial population by a 10^5 factor in 30 min) and their inefficiency to kill tomato plants after a longer and higher treatment, we think that cationic porphyrin and especially Zn-TMPyP, might be promising candidates as antimicrobial agents in agronomic practices.

ACKNOWLEDGEMENTS

Authors thank the région Limousin for financial supports of Dr Guillaumot as post doctoral fellowship and the French National Research Agency (ANR Porphy-Plant), Dr F. Brevier for providing Zn-TPPS, Dr C. Carrion for confocal microscopy analysis and Dr. Michel Guilloton for help in manuscript editing.

Conflict of interest the authors declare that they have no conflict of interest.

Author contribution statement

Damien Guillaumot, Mohammad Issawi and Catherine Riou designed research and conducted all plant experiments. Stephanie Leroy-Lhez performed the photostability measurements and Anne Da Silva all statistical tests. Vincent Sol helped in the reflection and writing of the manuscript. All authors read and approved the manuscript.

REFERENCES

- [1] Donnelly RF, McCarron PA, Tunney M, Antifungal photodynamic therapy. *Microbiol. Res.* 163 (2008) 1-12. DOI: 10.1016/j.micres.2007.08.001
- [2] Benov L, Photodynamic therapy: Current status and future directions. *Med. Princ. Pract.* 24 (2015) 14-28, DOI: 10.1159/000362416.
- [3] Maisch T, Resistance in antimicrobial photodynamic inactivation of bacteria. *Photochem. Photobiol. Sci.* (2015) DOI: 10.1039/c5pp00037h.
- [4] Riou C, Calliste CA, Da Silva A, Guillaumot D, Rezazgui O, Sol V, Leroy-Lhez S, Anionic porphyrin as a new powerful cell death inducer of Tobacco Bright Yellow-2 cells. *Photochem Photobiol. Sci.* (2014) DOI: 10.1039/c3pp50315a.
- [5] Villanueva A, Canete M, Hazen MJ, Uptake and DNA photodamage induced in plant cells *in vivo* by two cationic porphyrins. *Mutagenesis* 4 (1989) 157-159.
- [6] Jori G, Brown SB, Photosensitized inactivation of microorganisms. *Photochem. Photobiol. Sci* 3 (2004) 403-405. DOI:10.1039/b311904c
- [7] Merchat M, Bertoloni G, Giacomoni P, Villanueva A, Jori G, Meso-substituted cationic porphyrins as efficient photosensitizers of gram-positive and gram-negative bacteria. *J. Photochem. Photobiol* 32 (1996) 153-157.
- [8] Gábor F, Szocs K, Maillard P, Csík G, Photobiological activity of exogenous and endogenous porphyrin derivatives in *Escherichia coli* and *Enterococcus hirae* cells *Radiat Environ Biophys* 40 (2001) 145–151.
- [9] Ringot C, Sol V, Barrière M, Saad N, Bressollier P, Granet R, Couleaud P, Frochot C, Krausz P, Triazinyl porphyrin-based photoactive cotton fabrics: preparation, characterization and antibacterial activity. *BioMacromol* 12 (2012) 1716-1723. dx.doi.org/10.1021/bm200082d
- [10] Mbakidi JP, Herke K, Alvès S, Chaleix V, Granet R, Krausz P, Leroy-Lhez S, Ouk T, Sol V, Synthesis and photobiocidal properties of cationic porphyrin-grafted paper. *Carbohydrate Polymers* 91 (2013) 333-338. <http://dx.doi.org/10.1016/j.carbpol.2012.08.013>
- [11] Drabkova M, Marsalek B, Admiraal W, Photodynamic therapy against cyanobacteria. *Environ. Toxicol.* 22 (2007) 112-117. DOI:10.1002/tox.20240

- [12] Carré V, Gaud O, Sylvain I, Bourdon O, Spiro M, Blais J, Granet R, Krausz P, Guilloton M, Fungicidal properties of meso-arylglycosylporphyrins : influence of sugar substituents on photoinduced damage in the yeast *Saccharomyces cerevisiae*. J. Photochem. Photobiol. 48 (1999) 57-62.
- [13] Cormick MP, Alvarez MG, Rovera M, Durantini E, Photodynamic inactivation of *Candida albicans* sensitized by tri and tetra-cationic porphyrin derivatives. Eur. J. Med. Chem. 44 (2009) 1592-1599. DOI:10.1016/j.ejmech.2008.07.026
- [14] Funes MD, Caminos DA, Alvarez MG, Fungo F, Otero LA, Durantini EN, Photodynamic properties and photoantimicrobial action of electrochemically generated porphyrin polymeric films Environ. Sci. Technol 43 (2009) 902-908. DOI: 10.1021/es802450b
- [15] Ben Amor T, Jori G, Sunlight-activated insecticides: Historical background and mechanisms of phototoxic activity. Insect Biochem. Mol. Biol. 30 (2000) 915-925.
- [16] Dondji B, Duchon S, Diabate A, Hervé J-P, Corbel V, Hougard J-M, Santus R, Schrevel J, Assessment of Laboratory and Field Assays of Sunlight-Induced Killing of Mosquito Larvae by Photosensitizers. J. Med. Entomol. 42 (2005) 652-656.
- [17] Lucantoni L, Magaraggia M, Lupidi G, Ouedraogo R, Coppellotti O, Esposito F, Fabris C, Jori G, Habluetzel A, Novel Meso-substituted cationic porphyrin molecule for photo mediated larval control of the dengue vector *Aedes aegypti*. Plos Neglected Tropical Diseases 5 (2011) 1434-1445. DOI:10.1371/journal.pntd0001434
- [18] Robertson CA, Hawkins Evans D, Abrahamse H, Photodynamic therapy (PDT): a short review on cellular mechanisms and cancer research applications for PDT. J. Photochem. Photobiol 96 (2009) 1-8. DOI:10.1016/j.photobiol.2009.04.001
- [19] Menezes HD, Pereira AC, Brancini GTP, de Leão HC, Massola Junior NS, Bachmann L, Wainwright M, Bastos JK, Braga GUL, Furocoumarins and coumarins photoinactivate *Colletrichum acutatum* and *Aspergillus nidulans* fungi under solar radiation. J. Photochem. Photobiol. B: Biol. 131 (2014) 74-83. DOI 10.1016/j.jphotobiol.2014.01.008
- [20] Kuk Y, Lee H, Chung J, Kim K., Lee S, Ha S, Back K, Guh J, Expression of a *Bacillus subtilis* protoporphyrinogen oxidase gene in rice plants reduces sensitivity to peroxidizing herbicides. Biol. Plantarum 49 (2005) 557-583. DOI 10.1007/s10535-005-0052-3

- [21] Li X, Nicholl D, Development of PPO inhibitor-resistant cultures and crops. *Pest Manag Sci.* 61 (2005) 277-285. DOI:10.1002/ps.1011
- [22] Jung S, Lee H, Lee Y, Kang K, Kim YS, Grimm B, Back K, Toxic tetrapyrrole accumulation in protoporphyrinogen IX oxidase-overexpressing transgenic rice plants. *Plant Mol Biol.* 67(2008) 535-546.
- [23] Phung T-A, Jung H, Park J-H, Kim J-G, Back K, Jung S, Porphyrin biosynthesis control under water stress: sustained prophyrin status correlates with drought tolerance in transgenic rice. *Plant Physiol.* 157 (2011) 1746-1764. DOI:10.1104/pp.111.188276
- [24] Yun YB, Park J-I, Choi HS, Jung H-I, Jang SJ, Back K, Kuk YI, Protoporphyrinogen oxidase-overexpressing transgenic rice is resistance to drought stress. *Crop Sci.* 53 (2013) 1076-1085. doi:10.2135/cropsci2012.07.0452
- [25] Barbat A, Gloaguen V, Sol V, Krausz P, Aqueous extraction of glucuronoxylans from chestnut wood: new strategy for lignin oxidation using phthalocyanine or porphyrin/H₂O₂ system. *Bioresource Tech.* 101 (2010) 6538-6543. doi:10.1016/j.biortech.2010.03.054
- [26] Gamborg OL, Miller RA, Ojima K, Nutrient requirements of suspension cultures of soybean root cells. *Exp. Cell Res.* 50 (1968) 151-158.
- [27] Pandey VP, Singh S, Jaiswal N, Awasthi M, Pandey B, Dwivedi UN, Papaya fruit ripening: ROS metabolism, gene cloning, characterization and molecular docking of peroxidase. *J. Mol. Catal. B: Enzymatic* 98 (2013) 98-105. <http://dx.doi.org/10.1016/j.molcatb.2013.10.005>
- [28] Bradford MM, A rapid and sensitive method for the quantitation of microgram quantities of protein utilizing the principle of protein-dye binding. *Anal biochem* 72 (1976) 248-254.
- [29] Moudouma CFM, Gloaguen V, Riou C, Forestier L, Saladin G, High concentration of cadmium induces AtPCS2 gene expression in *Arabidopsis thaliana* (l.) heynh ecotype Wassilewskija seedlings. *Acta Physiol. Plantarum* 34 (2012) 1083-1091. DOI 10.1007/s11738-011-0905-7
- [30] Kampfenkel K, Van Montagu M, Inze D, Effects of Iron Excess on *Nicotiana plumbaginifolia* Plants (Implications to Oxidative Stress). *Plant Physiol.* 107 (1995) 725-735.

- [31] Queval G, Noctor G, A plate reader method for the measurement of NAD, NADP, glutathione, and ascorbate in tissue extracts: Application to redox profiling during *Arabidopsis* rosette development. *Anal. Biochem.* 363 (2007) 58–69.
- [32] Hodges DM, DeLong JM, Forney CF, Prange RK, Improving the thiobarbituric acid-reactive-substances assay for estimating lipid peroxidation in plant tissues containing anthocyanin and other interfering compounds. *Planta* 207 (1999) 604-607.
- [33] Aebi H, Catalase *in vitro*. *Methods Enzymol* 105 (1984) 121-126.
- [34] Murshed R, Lopez-Lauri F, Sallanon H, Microplate quantification of enzymes of the plant ascorbate–glutathione cycle. *Anal. biochem.* 383 (2008) 320-322. doi:10.1016/j.ab.2008.07.020
- [35] Weydert CJ, Cullen JJ, Measurement of superoxide dismutase, catalase and glutathione peroxidase in cultured cells and tissue. *Nature protocols* 5 (2010) 51-66.
- [36] Dunnett CW, A multiple comparisons procedure for comparing several treatments with a control. *J. Am Stat. Ass.* 50 (1955) 1096-1121.
- [37] Bergougnot V, The history of tomato: from domestication to biopharming. *Biotech. Adv* 32 (2014) 170-189. doi:10.1016/j.biotechadv.2013.11.003
- [38] Merchan M, Ouk TS, Kubat P, Lang K, Coelho C, Verbey V, Commereuc S, Leroux F, Sol V, Taviot-Gueho C, Photostability and photobactericidal properties of porphyrin-layered double hydroxide-polyurethane composite films. *J. Mater. Chem. B* 8 (2013) 2139-2146. DOI:10.1039/c3tb20070a
- [39] Duke SO, Rebeiz CA, Porphyrin biosynthesis as a tool in pest management: An overview. In: Duke SO, Rebeiz CA (eds) *Porphyric Pesticides: Chemistry, Toxicology and pharmaceutical Applications*, ACS Symp Ser 559. American Chemical Society, Washington DC, pp 1–17 (1994).
- [40] Chakraborty N, Tripathy BC. Involvement of Singlet Oxygen in 5-Aminolevulinic Acid-Induced Photodynamic Damage of Cucumber (*Cucumis sativus* L.) Chloroplasts. *Plant Physiol.* 98(1) (1992) 7-11.
- [41] Sasikala C, Ramana CV, Rao PR, 5-Aminolevulinic acid: a potential herbicide/insecticide from microorganisms. *Biotechnol Progress* 10 (1994) 451–459.
- [42] Moan J, On the diffusion length of singlet oxygen in cells and tissues. *J. Photochem. Photobiol.* 6 (1990) 343-344.
- [43] Gil SS, Tuteja N, Reactive oxygen species and antioxidant machinery in abiotic stress

- tolerance in crop plants. *Plant Physiol. Biochem.* 48 (2010) 909-930.
doi:10.1016/j.plaphy.2010.08.016
- [44] Avery SV, Molecular targets of oxidative stress. *Biochem J.* 434 (2011) 201-210.
- [45] Marnett LJ, Oxy radicals, lipid peroxidation and DNA damage. *Toxicol.* 181-182 (2002) 219-222.
- [46] Beckie HJ, Tardif FJ, Herbicide cross resistance in weeds. *Crop Protect.* 35 (2012) 15-28.
doi:10.1016/j.cropro.2011.12.018
- [47] Szabados L, Savoure A, Proline: a multifunctional amino acid, *Trends Plant Sci.* 15 (2010) 89-97. DOI:10.1016/j.tplants.2009.11.009
- [48] Rejeb KB, Abdelly C, Savoure A, How reactive oxygen species and proline face stress together, *Plant Physiol. Biochem.* 80 (2014) 278-284.
<http://dx.doi.org/10.1016/j.plaphy.2014.04.007>
- [49] Kramarenko GG, Hummel SG, Martin SM, Buettner GR, Ascorbate reacts with singlet oxygen to produce hydrogen peroxide, *Photochem Photobiol* 82 (2006) 1634-1637.
- [50] Dayan FE, Rimando AM, Duke SO, Jacobs NJ, Thiol-dependent degradation of protoporphyrin IX by plant peroxidases. *FEBS* 444 (1999) 227-230.
- [51] Kärkönen A, Kuchitsu K, Reactive oxygen species in cell wall metabolism and development in plants, *Phytochem.* 112 (2015) 22-32.
<http://dx.doi.org/10.1016/j.phytochem.2014.09.016>
- [52] Mathé C, Barre A, Jourda C, Dunand C. Evolution and expression of class III peroxidases. *Arch Biochem Biophys.* 500(1) (2010) 58-65.
doi:10.1016/j.abb.2010.04.007
- [53] Tayefi-Nasrabadi H, Dehghan G, Daeihassani B, Movafegi A, Samadi A, Some biochemical properties of guaiacol peroxidases as modified by salt stress in leaves of salt-tolerant and salt-sensitive safflower (*Carthamus tinctorius* L.cv.) cultivars, *African J. Biotech.* 10(5) (2011) 751–763.

Table 1: No pre-emergence inhibitory effect of porphyrins was observed on tomato seed germination. Anionic porphyrin (TPPS) and its metallated form (Zn-TPPS), cationic porphyrin (TMPyP) and its metallated form (Zn-TMPyP) were tested at 80 μM . Results are expressed as percentage of germination and the mean of 4 independent experiments \pm sem. p-value was 0.29.

	Control	TPPS	Zn-TPPS	TMPyP	Zn-TMPyP
Tomato	87.76 \pm 4.73	94.29 \pm 3.98	88.89 \pm 4.74	95.56 \pm 3.10	89.19 \pm 5.17

Table 2: Photostability of Zn-TMPyP and TPPS in plantlet growth medium after irradiation with white light ($250 \mu\text{E}\cdot\text{s}^{-1}\cdot\text{m}^{-2}$) under 16h photoperiod per day during 15 days. TPPS was tested at 50 μM and Zn-TMPyP at 3.5 μM . Results are expressed as percentage of Soret band absorption and are the mean of 3 independent experiments \pm sem.

porphyrins	Illumination time exposure (days)				
	0	1	2	6	15
Zn-TMPyP	100 \pm 0	97.2 \pm 2.45	93.8 \pm 3.1	68.6 \pm 4.9	15.4 \pm 1.6
TPPS	100 \pm 0	72.0 \pm 8.9	61.6 \pm 3.0	33.7 \pm 0.3	8.2 \pm 6.0

FIGURES LEGEND

Figure 1: Structures of different porphyrins tested in this study

Figure 2: Porphyrins tested at 80 μM are not cytotoxic for tomato plantlets grown in the dark. Tomato seed germination took place for 4 days on media supplemented with 80 μM porphyrins. B5 represented the control without porphyrins. Experiments were repeated at least 3 times. Representative pictures of one of these biological repeats were reported. Scale bar represents 1 cm.

Figure 3: Cationic porphyrins, especially Zn-TMPyP, altered growth and development. A) Tomato seeds germinated on different media supplemented with 50 μM of TPPS/Zn-TPPS and 3.5 μM TMPyP/Zn-TMPyP for 14 days under 16 h photoperiod. B5 corresponded to the control medium without porphyrins. Experiments were repeated at least 3 times and representative pictures were taken. Scale bar represents 1 cm for tomato. B) Dry to fresh weight ratio (DW/FW) determined in 14 day-old tomato plantlets (cf mat and meth). Tomato seeds germinated on different media supplemented with 50 μM TPPS/Zn-TPPS and 3.5 μM TMPyP/Zn-TMPyP for 14 days under 16 h photoperiod. Results are the mean of 4 independent experiments \pm sem. ***: $P < 0.001$

Figure 4: Tomato plantlets placed on high concentrations of TMPyP/Zn-TMPyP for 14 days could be rescued and recovered a phenotype similar to control plants. Tomato seed germination took place on media supplemented with 80 μM PP for 14 days (D14). Plantlets

were placed for one week on B5 medium (D21) and then transferred to soil and green house for 6 weeks (D63). C represented the control without cationic porphyrins. Scale bar for D14 and D21 represents 1 cm, scale bar for D63 represent 3 cm.

Figure 5: Zn-TMPyP localization in tomato root sections. Pictures were taken from spectral mode acquisition. Left panel: calcofluor staining and Right panel: Zn-TMPyP treated roots. Labelling and detection are described in mat and meth. Scale bar represents 50 μm .

Figure 6: Photoactivated cationic porphyrins induce lipid peroxidation in 14 day-old tomato roots and shoots. Black box corresponded to control parts of plantlets, 3.5 μM TMPyP and Zn-TMPyP to grey and dark grey respectively. Results are the mean of 4 independent experiments \pm sem (ns: not significant; *** $P < 0.001$).

Figure 7: H_2O_2 production in whole 14 day-old tomato plantlets. A) Control root apparatus was stained by NBTZ (left) or root apex by DAB (right) (cf Mat and meth). B) Zn-TMPyP treated roots stained by NBTZ or DAB. Zn-TMPyP was tested at 3.5 μM . Scale bar represents 1 mm. C) H_2O_2 quantification was performed on isolated roots and shoots of no treated (B5) or treated plantlets. Results are the mean of 5 independent experiments \pm sem (*** $P < 0.001$; * $0.01 < P < 0.05$).

Figure 8: Antioxidant molecule contents in 14 day-old tomato roots. Black boxes corresponded to control roots and grey boxes to 3.5 μM Zn-TMPyP. Results are the mean of 4 independent experiments \pm sem (*** $P < 0.001$; ** $P < 0.01$).

Figure 9: Effect of photoactivated Zn-TMPyP on antioxidant enzyme specific activities in 14 day-old tomato roots. Activities were determined as described in mat and meth. GPX: guaiacol peroxidase, APX: ascorbate peroxidase, CAT: catalase, SOD: superoxide dismutase. Results are the mean of 4 independent biological experiments \pm sem (ns: not significant; a: $0.05 < P < 0.1$; *: $0.01 < P < 0.05$; ***: $P < 0.001$)

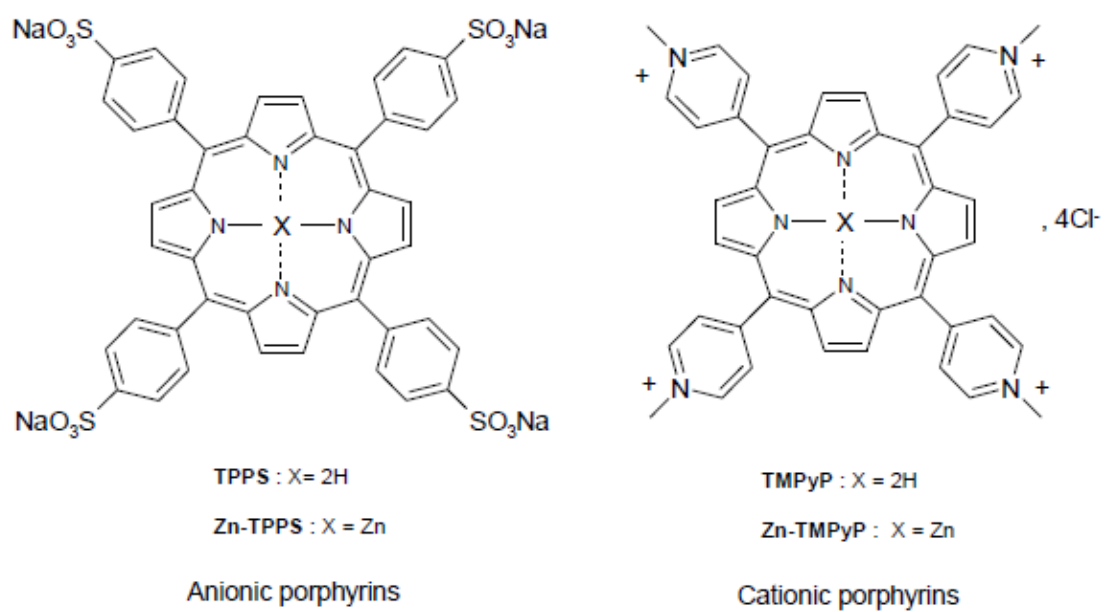


Figure 1

ACCEPTED

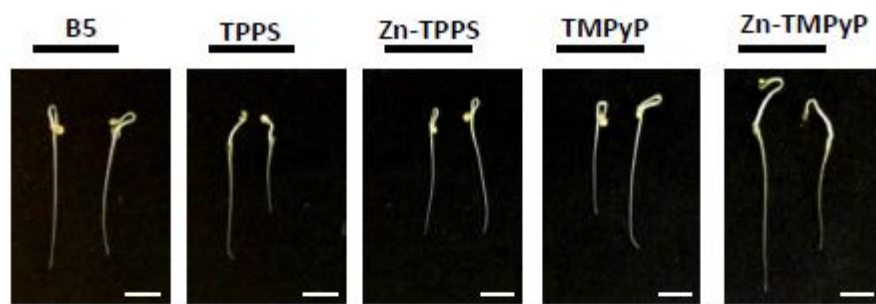


Figure 2

ACCEPTED MANUSCRIPT

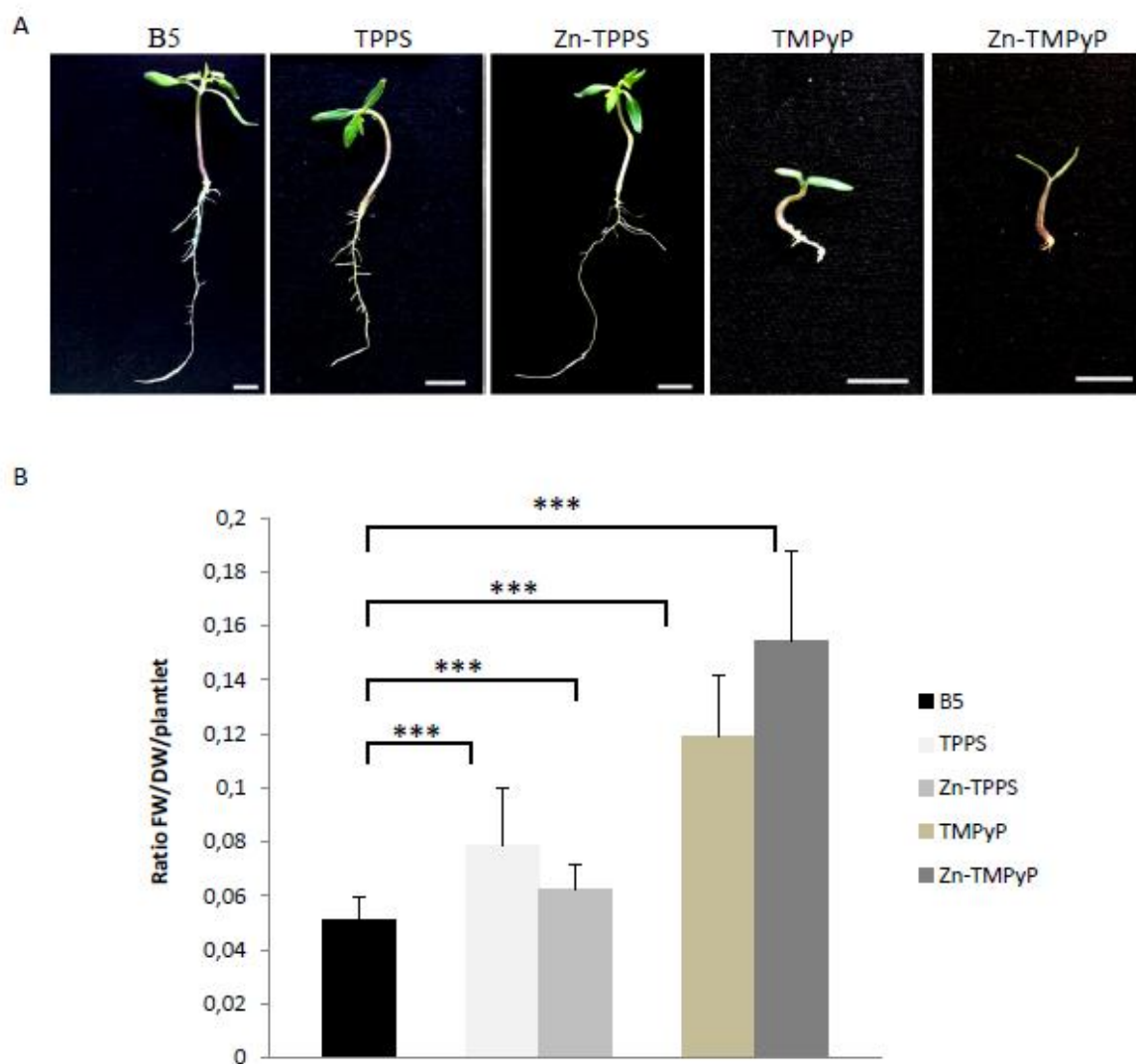


Figure 3

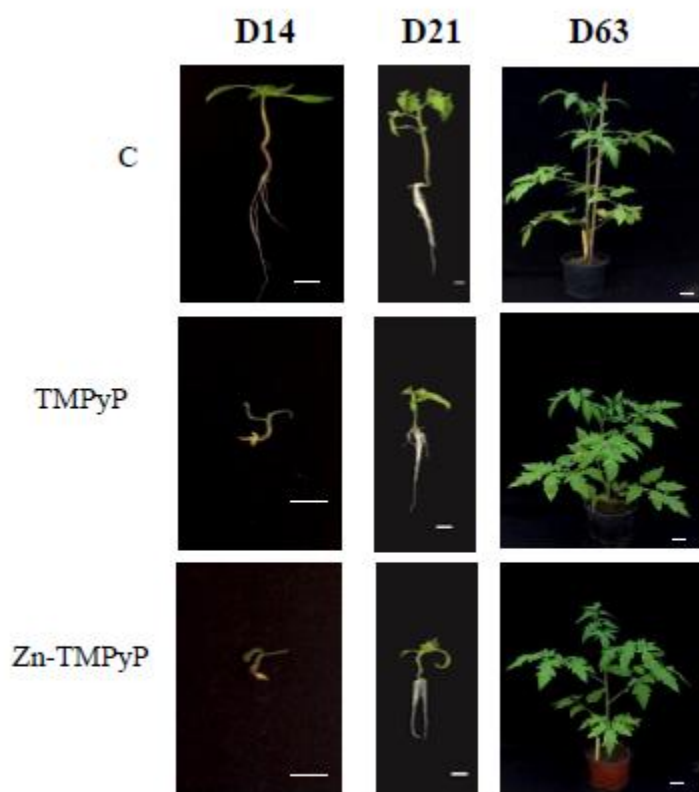


Figure 4

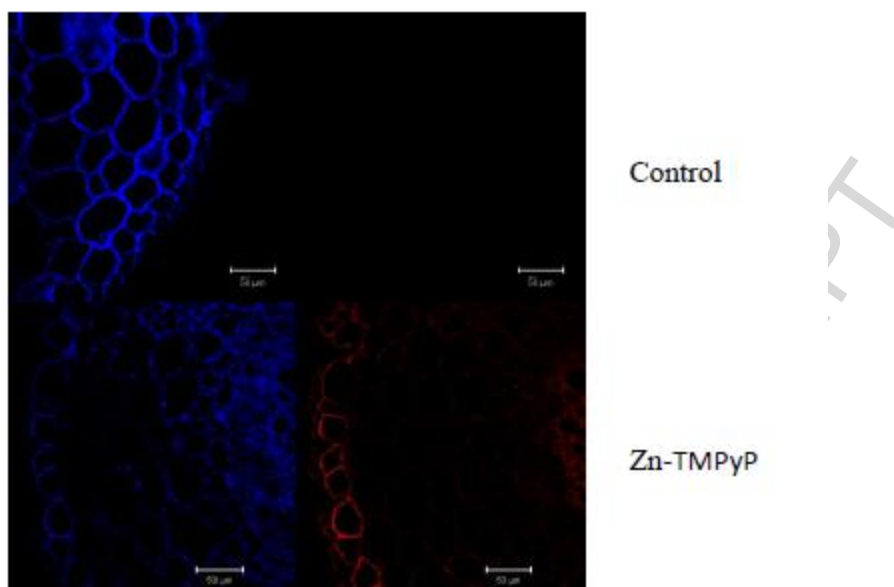


Figure 5

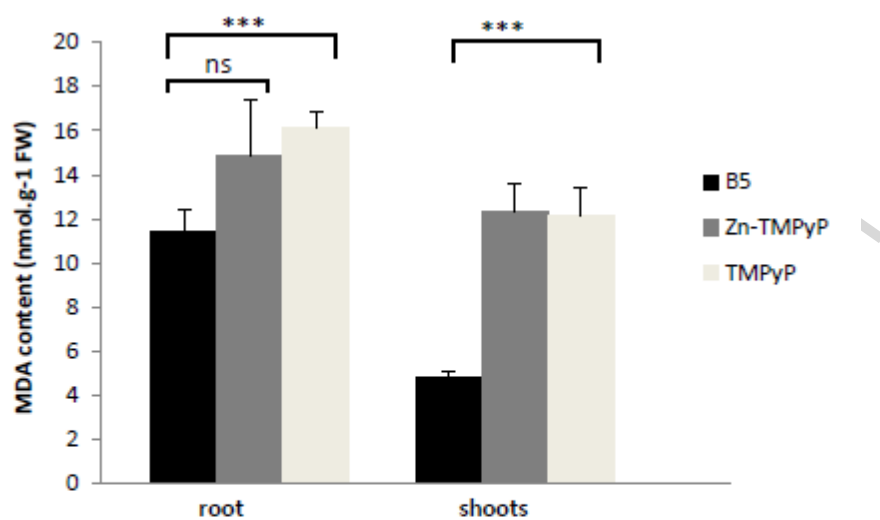


Figure 6

ACCEPTED MANUSCRIPT

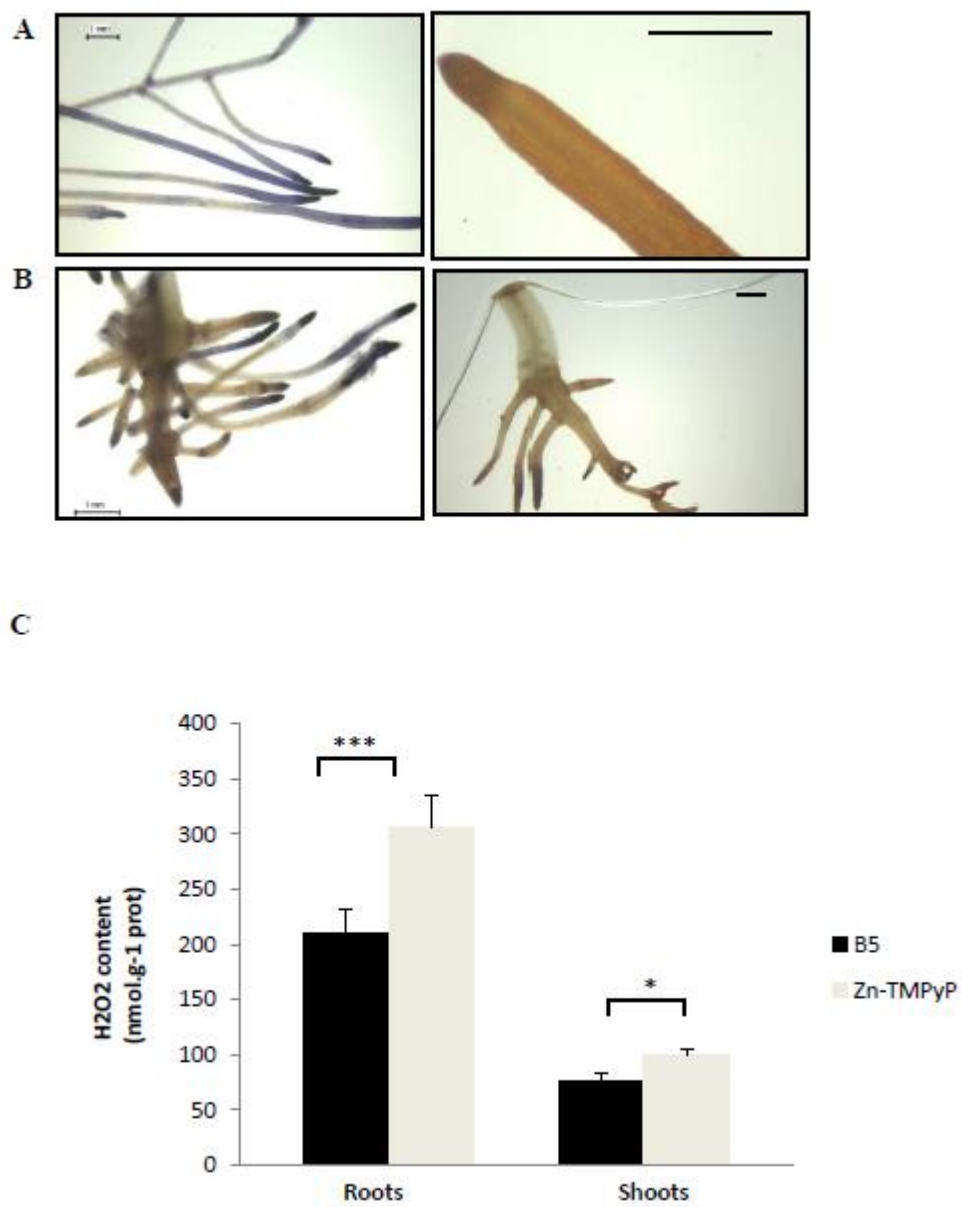


Figure 7

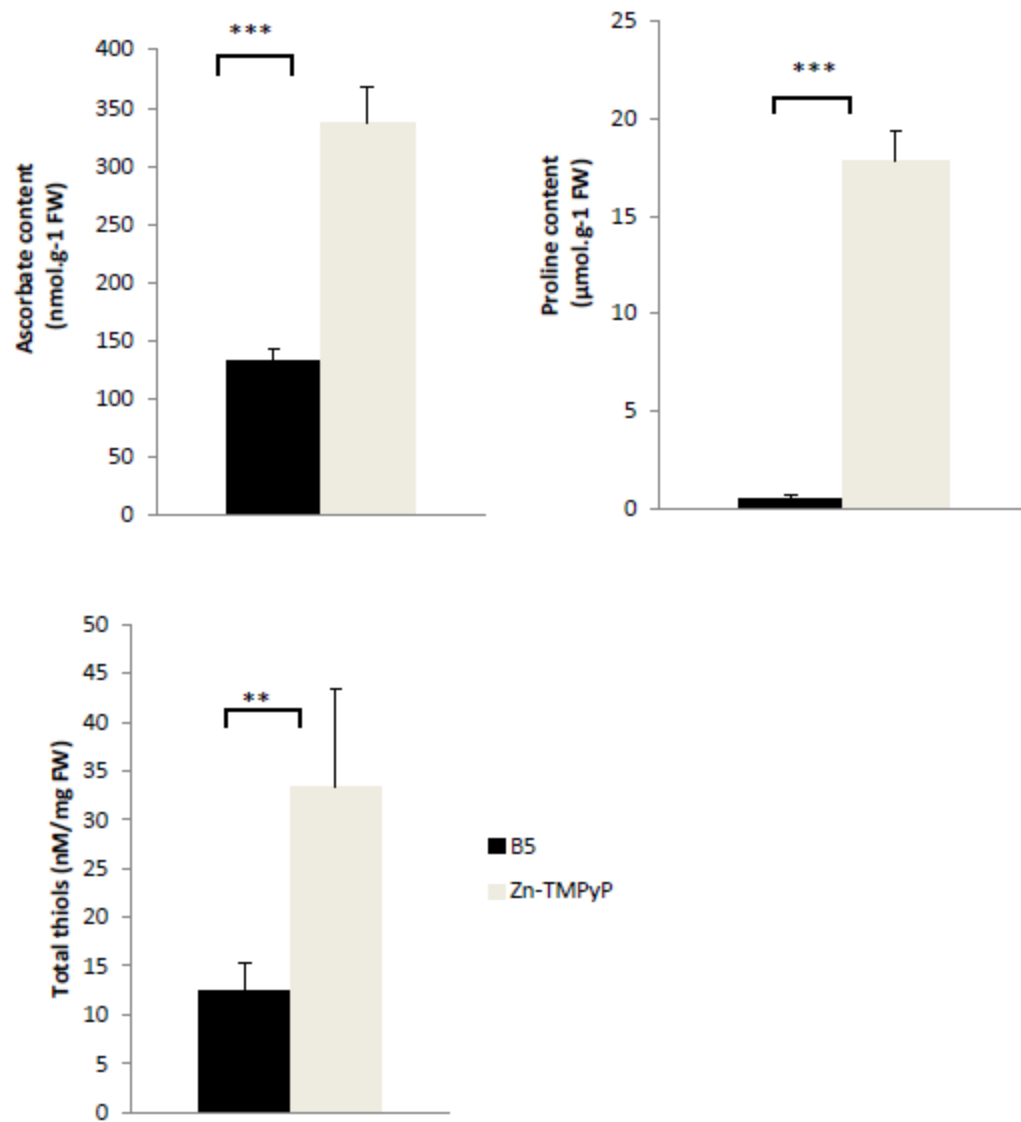


Figure 8



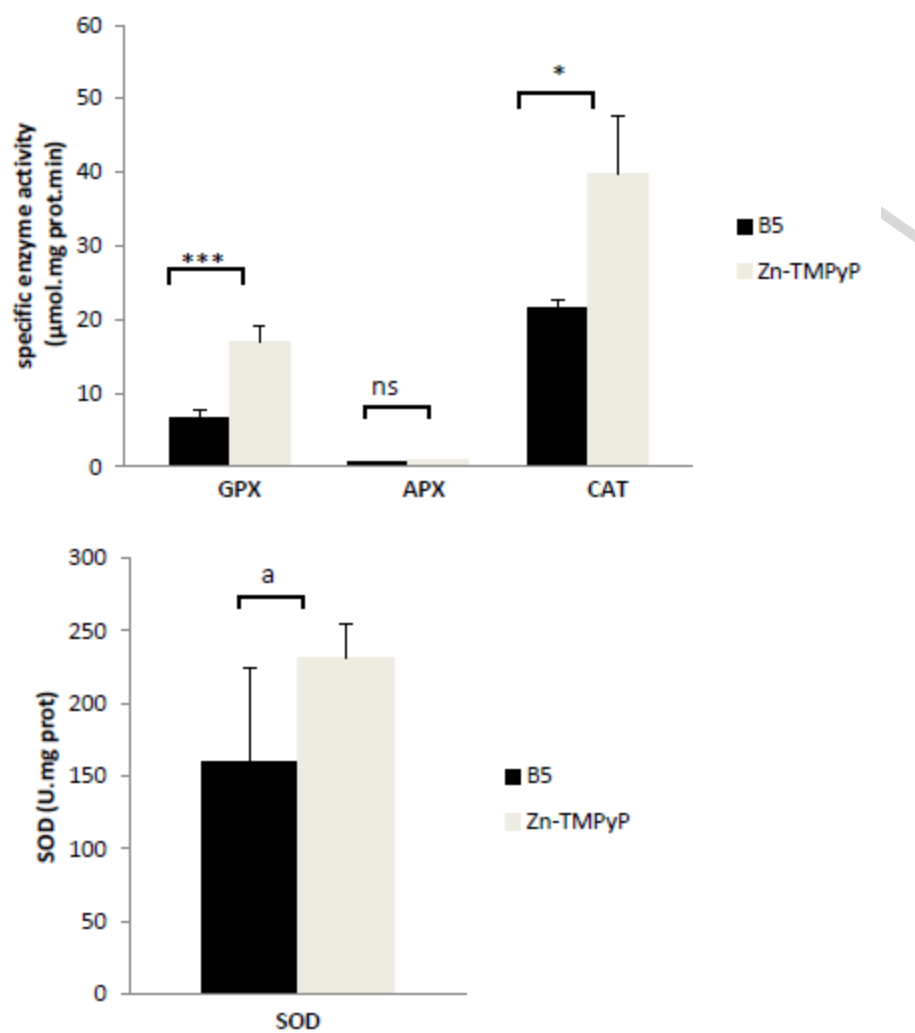


Figure 9

Y

Highlights

- * Zn-TMPyP altered vegetative development of tomato plantlets without killing them.
- * Anti-oxidative molecules and enzymes involved in ROS detoxification increased
- * Zn-TMPyP is proposed as a valuable APDT molecule with no-killer effect on plants.

ACCEPTED MANUSCRIPT

PUBLICATION 3: “Responses of an adventitious fast-growing plant to photodynamic stress: comparative study of anionic and cationic porphyrin effect on *Arabidopsis thaliana*”, *Physiologia Plantarum*.

Responses of an adventitious fast-growing plant to photodynamic stress: comparative study of anionic and cationic porphyrin effect on *Arabidopsis thaliana*

Mohammad Issawi, Damien Guillaumot, Vincent Sol and Catherine Riou*

Laboratoire de Chimie des Substances Naturelles (EA 1069), Université de Limoges, Faculté des Sciences et Techniques, 123 avenue Albert Thomas, 87060 Limoges Cedex, France

Correspondence

* corresponding author,

e-mail : catherine.riou@unilim.fr

Abbreviations – APDT, antimicrobial photodynamic treatment; AP, Meso-Tetra (4-sulfophenyl) Porphyrin; CP, Tetra (N-methylpyridyl) porphyrin tetrachloride.

Antimicrobial Photodynamic Treatment based on the use of a photosensitizer to produce reactive oxygen species that induce cell death could be envisaged to fight against plant pathogens. For setting this strategy, we want to study how plants themselves respond to photodynamic treatment. In a previous work we showed that tomato plantlets were able to resist to photoactivated tetra (N-methylpyridyl) porphyrin (CP) or Zinc metalated form (CP-Zn). To enlarge our plant expertise related to exogenous porphyrins treatment and to further defend this approach, we studied how an adventice like *Arabidopsis thaliana* responded to exogenous supply of anionic and cationic porphyrins. Both types of photosensitizers had no negative effect on seed germination and did not hamper *Arabidopsis* etiolated plantlet development under dark conditions. Thus, post-emergence effects of porphyrin photoactivation on 14 day-old in vitro *Arabidopsis* plantlet development under light were observed. CP-Zn was the most efficient photosensitizer to kill *Arabidopsis* plantlets while anionic tetra (4-sulfonatophenyl) porphyrin only delayed their growth and development. Indeed only 7 % of plantlets could be rescued after CP-Zn treatment. Furthermore, non-enzymatic and enzymatic defense components involved in detoxification of ROS generated by CP-Zn under illumination were down-regulated or stable with the exception of seven fold increase in proline content. As previously demonstrated in the literature for microbial agents and in the present work for *Arabidopsis*, CP-Zn was efficient enough to eradicate in the same time unwanted vegetation and plant pathogens without killing plants of agronomic interest such as tomato plantlets.

This article has been accepted for publication and undergone full peer review but has not been through the copyediting, typesetting, pagination and proofreading process, which may lead to differences between this version and the Version of Record. Please cite this article as doi: 10.1111/ppl.12666

Introduction

The light-based approach antimicrobial photodynamic treatment (APDT) that is used in several domains such as medicine, food and water decontamination could be used beyond (Alves et al 2015). It could be envisaged as a farming practice in order to eradicate plant pathogens as bacteria and fungi that cause serious threats by drastically reducing crops yield. Studies focusing on the side effects of APDT directly on plants are rare (De Menezes et al 2014a,b, Fracarolli et al 2016, Guillaumot et al 2016). However, such studies are required to evaluate the efficiency of APDT. Recently, it was reported that natural photosensitizers such as coumarins and fucocoumarins or synthetic such as phenothiazinium inactivated pathogenic fungi (*Colletotrichum*, *Aspergillus* and *Fusarium*). When spotted on orange tree or strawberry plants, orange tree leaves were not affected by either natural/synthetic photosensitizers whereas they damaged strawberry leaves when tested at 100 μM (De Menezes et al 2014a,b, Fracarolli et al 2016). Our aim is to explore, the phenotypic and molecular responses of plantlets growing in vitro under photodynamic stress induced by photoactivated porphyrins included in growth medium. In the present work we want to know how *Arabidopsis thaliana*, an adventitious fast-growing plants respond to such photodynamic treatment.

Molecules such as porphyrins, naturally present in all living kingdom, seem to be good candidates for APDT. Indeed, these systems, photo-excitabile by sunlight, are able to induce cell death by the mean of reactive oxygen species (ROS) such as superoxide anion radical, hydrogen peroxide, hydroxyl radical and singlet oxygen. Under dark conditions, porphyrins do not exhibit significant cyto- or genotoxicity (Donnelly et al 2008). Until now applications for porphyrins were essentially performed on cancer cells for photodynamic therapy or on microorganisms as antimicrobial agents (Plaetzer et al 2013, Maish 2015, Pérez-Lagunal et al 2017, Zampini et al 2017). For example, upon illumination, protoporphyrin IX and other derivatives induced a strong cytotoxic effect in yeasts *Saccharomyces cerevisiae* and *Candida albicans* (Donnelly et al 2008, Carré et al 1999, Cormick et al 2009, Funes et al 2009, Quiroga et al 2015). Another study showed that the derivatives of cationic porphyrin were more efficient than neutral and anionic porphyrins on Gram-negative bacteria (*Escherichia coli*) than on Gram-positive bacteria such as *Enterococcus hirae* or *Staphylococcus*

aureus (Merchat et al 1996, Gabor et al 2001, Ringot et al 2012, Fayyaz 2015). As well, the exogenous supply of cationic porphyrin on cyanobacteria and green microalgae cultures showed that microalgae were more sensitive to the effect of the photosensitizer than cyanobacteria (Drabkova et al 2007). Furthermore, tested on mosquito or fly larvae, it would appear that photoactivated porphyrins also have an insecticidal effect (Ben Amor and Jori 2000, Dondji et al 2005, Lucantoni et al 2011). Over the last three decades, it was of interest to modify the endogenous porphyrin pathway in order to overproduce protoporphyrin IX, the first natural photosensitizer, by supplying 5-aminolevulinic acid on plants (5-ALA). 5-ALA induced herbicidal and negative effect on wildlife when tested at high concentration around 5 mM (Rebeiz et al, 1984, Chakraborty and Tripathy 1992, Matsumoto et al 1994, Sasikala et al 1994). To our knowledge, only two studies were conducted on plants. On *Allium cepa* root meristematic cells it was reported that zinc metalated/free base cationic porphyrins were able to be up-taken by cells and induce DNA photodamage (Villanueva et al 1989). More recently, study on tomato plantlets showed that they were able to withstand the damaging effects of photoactivated cationic porphyrins (Guillaumot et al. 2016). As pointed by these studies, we supposed that exogenous photoactivated porphyrins could seriously alter plant development leading to preferentially death of fast growing species such as *Arabidopsis thaliana*. *Arabidopsis* is a cosmopolitan small flowering plant that is widely used as a model organism in plant biology research. It is the “darling” of plant science but it is neither grown for food nor to feed animals and it is not of major agronomic significance. In the contrary, *Arabidopsis* plants have some weedy traits and may be considered as unwanted vegetation in a farm field. Responses of such plants to photodynamic treatment is required in order to cover all aspects of APDT as a future commercial tool in the field. (Meyerowitz 1989, Provar and Meyerowitz 2016). Moreover, as discussed by De Menezes (2014a), this type of treatment required a case-by-case analysis because its outcome depends on plant species.

For this work, we tested two categories of water-soluble porphyrins: cationic and anionic synthetic porphyrins respectively that were free-base or zinc-metalated. We showed that none of the porphyrins was able to produce a pre-emergence lethal phenotype of *Arabidopsis*. Thus, we compared the consequences of their photoactivation on phenotypes of 14 day-old *Arabidopsis* plantlets and showed that cationic porphyrin especially CP-Zn tested at 3.5 μM induced the strongest phenotypic

alterations. Thus, taking into account these first results, we focused our study on cellular and molecular mechanisms triggered by CP-Zn in plantlets roots, trying to understand why tomato plantlets were less sensitive than *Arabidopsis*. Indeed, *Arabidopsis* presented very high H₂O₂ and MDA productions leading to biomembrane damages. Moreover, endogenous levels of proline, ascorbate and total thiols considered as antioxidant molecules and enzyme activities such as peroxidases, catalase and superoxide dismutase were clearly down-regulated in *Arabidopsis* plantlets. In conclusion, we suggested that *Arabidopsis* plantlets were photodynamically damaged by photoactivated cationic porphyrins that impair enzymatic defense machinery and rendering them unable to produce sufficient amount of antioxidative molecules such as ascorbate and total thiols to withstand this stressful conditions.

Materials and methods

Plant material

Seeds of *Arabidopsis thaliana* ecotype Wassilewskija (Ws-4) were germinated in vitro on a Gamborg B5 culture medium (Duchefa Biochemie, Haarlem, Netherlands) at pH 5.8 supplemented with 2% (w/v) sucrose and 0.8% (w/v) agar (Difco, Dallas, TX (Gamborg et al 1968)). For all experiments, plates were maintained for 14 days in a controlled growth chamber at 22°C under a 16h photoperiod and a photon flux density of 250 $\mu\text{mol m}^{-2} \text{s}^{-1}$. Germination ratio was evaluated after 4 days of culture using binocular microscope. Under these conditions, around 100 *Arabidopsis* seeds were tested on the same square plate. Pictures were taken under binocular microscope (Leica EZ4D stereo microscope W/ digital camera, Jena, Germany) and Leica LAS EZ software. For cytotoxicity, plates were maintained vertically under same conditions without illumination for 7 days. After 14 day culture, plantlets were harvested, weight and frozen at -20°C until used. For determination of dry weight, plantlets were placed in an oven at 42°C for 4 days and weight.

Porphyrins

All porphyrins were soluble in water and their chemical structures were reported (Riou et al 2014). Briefly, anionic porphyrin (AP and AP-Zn) correspond to the free zinc sulfonated tetraphenylporphyrin (H₂TPPS) and Zinc-TPPS, respectively. AP was purchased from Sigma-Aldrich (St Louis, MO) and AP-Zn from Porphychem (Dijon, France). Cationic porphyrins: Tetra (N-methylpyridyl) porphyrin tetrachloride or H₂TMPyP (CP) and Zinc TMPyP (CP-Zn) were purchased from Frontier Scientific (Carnforth, United Kingdom).

Confocal microscopy analysis

We incubated 14 day-old plantlets in B5 medium with or without 3.5 μ M CP-Zn overnight under dark conditions and rinsed them 3 times before observations under a Zeiss confocal microscope (LSM 510-META, Jena, Germany). For analysis, two ways of acquisition were performed: a spectral acquisition to verify signal specificity of CP-Zn and a channel mode for root apex stained by calcofluor (Sigma-aldrich, St Louis, MO). For spectral acquisition, samples were excited at 458 nm and fluorescence was followed between 476 and 732 nm. CP-Zn emission peak was detected around 640 nm (Guillaumot et al 2016). For channel mode acquisition and calcofluor, we used an excitation wavelength at 405 nm and emission wavelength between 420 and 450 nm.

In situ DAB staining

3,3-diaminobenzidine (DAB) staining on Arabidopsis whole plantlets was performed using DAB Kit (Sigma-Aldrich, St Louis, MO) following manufacturer's instructions. Plant material was vacuum-infiltrated for 5 min and placed under dark conditions for 2 h. DAB solution was replaced by 70% (v/v) ethanol and conserved at 4°C until observations under binocular microscope.

Antioxidant molecule assays

The proline content was analyzed as follow. Frozen samples of plantlets were ground in liquid nitrogen then homogenized in 1 ml of 5% (w/v) 5-sulfosalicylic acid. After centrifugation for 15 min at 13 000 g and 4°C, 250 μ l of supernatants were mixed with 1ml of 1% (w/v) ninhydrin in 60% (v/v) acetic acid. The samples were incubated at 100°C for 20 min and cooled at room temperature before

addition of 1.25 ml toluene. After 4 h incubation at room temperature, the upper phase was collected and absorbance was read at 520 nm. A standard curve was performed with proline and the content was expressed in $\mu\text{mol g}^{-1}$ FW.

Total thiol assay was performed according to (Guillaumot et al 2016). Frozen samples were ground in liquid nitrogen and then extracted into 1 ml of 0.2 N HCl. After centrifugation at 16 000 g for 4 min, 500 μl of extracted solution were neutralized with 400 μl NaOH (0.2M) and 50 μl NaH_2PO_4 (0.2 M). 0.7 ml of 0.12 M NaH_2PO_4 (pH 7.5), 6 mM EDTA, 0.1 ml of 6 mM Dithiobis 2-nitro benzoic acid (DTNB) were added to 0.2 ml extract. For standards, extract was replaced by 0, 10, 20, 50, and 100 nmol GSH (total volume 1 ml). Absorbance at 412 nm was read 5 min after the addition of standards or extract.

Ascorbate was quantified as reported by Kampfenkel et al (1995). Briefly, frozen plant tissues (around 100 mg fresh weight) were ground in liquid nitrogen with a mortar and pestle. The resulting powder was weighted before addition of 200 μl of 6 % TCA solution. Samples were then incubated for 10 min on ice and centrifuged at 16 000 g for 25 min at 4°C. Supernatant was completed to 500 μl with 6% TCA and centrifuged 16 000 g for 10 min. at 4°C. 100 μl of each sample were then transferred to 150 μL 0.2 M phosphate buffer pH 7.4 and supplemented with 250 μl 10 % TCA, 200 μl 42% H_3PO_4 , 200 μl 2,2'-dipyridyl and 100 μl 3% FeCl_3 . Standards ranged from 0 to 70 nmoles of ascorbate were run. After 40 min incubation at 42°C, absorbance of standards and samples was read at 525 nm.

Determination of MDA content

MDA content was determined by the thiobarbituric acid (TBA) reaction as described by Hodges (1999), with minor modifications. Around 100 mg of fresh or frozen plant materials were ground with liquid nitrogen. The resulting powder was suspended into 1.5 ml of 20% TCA. After centrifugation, supernatants were collected and analyzed for their MDA content. 500 μl of each sample were added to either 500 μl 20% TCA alone (-TBA) or 20% of TCA supplemented with 0.5% thiobarbituric acid (+TBA). Samples were then boiled in a water bath for 30 min. The samples were cooled on ice and absorbances were read at 440, 560 and 600 nm. Corrections for interfering compounds were made and the MDA content was calculated as follow:

$$(1) [(Abs\ 532_{+TBA} - Abs\ 600_{+TBA}) - (Abs\ 532_{-TBA} - Abs\ 600_{-TBA})] = A$$

$$(2) \{[(Abs\ 440_{+TBA} - Abs\ 600_{+TBA}) - (Abs\ 440_{-TBA} - Abs\ 600_{-TBA})] \cdot 0.0571\} = B$$

$$(3) \text{MDA equivalents (nmol}\cdot\text{mL}^{-1}) = [(A-B)/157\ 000] \cdot 10^6$$

Enzymatic activities determination

Frozen plant samples were ground to a fine powder in liquid nitrogen using a mortar and pestle. Proteins were solubilized into 1 ml of extraction buffer containing 50 mM phosphate buffer pH 7.8, 1 mM EDTA, 1% (w/v) PVP and 10% (v/v) glycerol and centrifuged at 16 000 g for 10 min at 4°C. The resulting supernatant was used for protein quantification according to Bradford (Bradford 1976) and then for antioxidant enzyme analysis.

The activity of catalase (CAT) was measured by monitoring H₂O₂ decomposition at 240 nm during 3 min according to Aebi's protocol (Aebi 1984). 50 or 20 µg of total soluble proteins from each sample were diluted in 50 mM phosphate potassium buffer (pH 6.5). The reaction was initiated by the addition of H₂O₂ to a final concentration of 20 mM. Amount of H₂O₂ was calculated based on a molar extinction coefficient of 43.6 M⁻¹ cm⁻¹.

Guaiacol peroxidase activity was quantified following the increase in absorbance at 436 nm during 2 min due to the formation of tetraguaiacol and calculated with a molar extinction coefficient of 25.5 mM⁻¹ cm⁻¹. 10 µg of total soluble proteins were diluted into 50 mM phosphate potassium buffer pH 6.5 and supplemented with 0.25% of guaiacol (5% stock solution in 95% ethanol w/v). Reaction started by addition of H₂O₂ to a final concentration of 2.5 mM.

Ascorbate peroxidase activity was analyzed by adapting the microplate protocol to tubes by estimating the rate of ascorbate oxidation (extinction coefficient: 2.8 mM⁻¹·cm⁻¹) (Murshed et al. 2008). 50 µg of soluble protein extracts were diluted in 50 mM phosphate buffer pH 7.0 supplemented with 0.25 mM ascorbic acid. The reaction started by addition of H₂O₂ to the final concentration of 5 mM. The decrease in absorbance at 290 nm was then measured during 3 min.

The activity of superoxide dismutase (SOD) was assayed by measuring its ability to inhibit the photochemical reduction of nitro blue tetrazolium (NBT) according to (Weydert and Cullen 2010).

Standard curve was set so that the increase in absorbance at 560 nm was between 0.02 and 0.03

absorbance unit per minutes and was monitored for 5 min. One unit of SOD was defined as the amount of enzyme required for an inhibition of 50% of NBT reduction. 10 μ l of enzyme extract were used and further converted to an amount of proteins according to their respective concentration.

Statistical analysis

All biological experiments were performed at least three times independently. Results were expressed as mean \pm SD (Standard Deviation). Data were analyzed by *t*-student test and one-way ANOVA using the PAST free software.

Results

We tested two categories of porphyrins: cationic and anionic because of their solubility in water and culture medium. Furthermore, anionic or cationic porphyrins were free base or zinc metalated. Our aim was to describe the effect of low concentration of photoactivated porphyrins at pre and post emergence levels.

High concentration of anionic or cationic porphyrins does not affect seed germination

Arabidopsis seeds were placed in darkness for 7 days on media containing each porphyrin tested at high concentration. Photosensitizer concentrations were 50 μ M for anionic compounds and 5 μ M for cationic species. As none of these tested concentrations inhibited Arabidopsis seed germination (Table 1), anionic or cationic porphyrins could definitively not be considered as a pre-emergent inhibitor. Moreover, it seemed that 5 μ M CP promoted seed germination (Table 1). Thus, we studied subsequent effects of porphyrins at the post-germination level.

Photoactivated cationic porphyrins efficiently affect Arabidopsis growth

In regard to potential cytotoxicity of PP described in mammal cells (Magnieto et al 2014), post-germination events under dark conditions were assayed. Thus we tested the same concentrations for AP/AP-Zn and CP/CP-Zn that tested in Table 1 and monitored etiolated plantlet development during 7 days (Fig. 1). Indeed, 7 day-old etiolated plantlets seemed very similar to control ones in term of root

and hypocotyls growth (Fig. 1). This result showed that under dark conditions, the four porphyrins did not lead to significant cytotoxicity and/or genotoxicity which is a great advantage for further agronomic investigations. Thus, under darkness prevailing conditions in the soil, porphyrins would not be cytotoxic for living systems as seedlings and soil microorganisms.

Using large spectrum illumination that mimic summer sunlight for 16h per day, we then tested porphyrin effect on seedlings grown at light. In a first attempt, 14 day-old *Arabidopsis* whole plantlets grown *in vitro* were transferred for a short time light exposure (72h experiment corresponds to 48h light) into a new liquid culture medium containing porphyrins (Fig. 2). In contact to AP/AP-Zn, *Arabidopsis* plantlets did not show leaf alterations compared to control plants whereas on 3.5 μM CP/CP-Zn, yellowish leaves and nearly dead plantlets were observed (Fig. 2). This first result suggested a greater efficiency of cationic porphyrins to induce cell and plantlet death.

To gain insight to the effects of long time exposure to porphyrins, *Arabidopsis* seedlings were grown in contact to each porphyrin for 14 days under 16 h photoperiod. Although phenotypic alterations were not obviously observed in contact to 50 μM AP or AP-Zn compared to control condition, plantlets placed on 3.5 μM CP or CP-Zn showed significant reduction of root length, asymmetry in cotyledon expansion, that could become white, and no formation of new leaves (Fig. 3A). We determined dry on fresh weight ratio in control and treated plantlets. A significant increase in this ratio was observed for all tested conditions (Fig 3B). It was probably linked to plantlet dehydration that could be also correlated to the 7-fold proline increase in CP-Zn treated plantlets (Fig. 3B, Table 2). Nevertheless, those results confirm that anionic porphyrins (free or zinc metaled forms) had almost no effect on *Arabidopsis* plantlets (Fig. 3). Since previous studies on microbial agents showed higher efficiency of cationic porphyrins and *Arabidopsis* plantlets treated with cationic porphyrins were prone to pronounced photodynamic stress, we did not pursue with anionic porphyrins that did not effectively inhibit *Arabidopsis* vegetative growth while tested at nearly 15 times more concentrated than cationic porphyrins.

Few plantlets could be rescued after photoactivation of CP-Zn treatment

Another focus for agronomic traits was to rescue plantlets that grew on photoactivated porphyrins. Only few green plantlets obtained on CP-Zn were rescued whereas the white plantlets could not be rescued (Fig 4). Tested at the same concentration (5 μM) it was also shown that photoactivated CP was less efficient than CP-Zn to induce the death of Arabidopsis plantlets (Fig. 4). Nevertheless, CP-Zn worked at dose dependent manner and we tested a range of CP-Zn concentrations from 1 to 10 μM on Arabidopsis seedling development (Fig. 4C) as 3.5 μM CP-Zn already induced lethal phenotype for 60% of Arabidopsis plantlets. Whereas on 1 μM CP-Zn, nearly 100% plantlets were green and could undergo further development, on 10 μM CP-Zn this proportion fall to less than 5% of surviving plantlets. According to our results, we decided to continue with an intermediary concentration of CP-Zn corresponding to 3.5 μM that was an effective concentration for killing Arabidopsis seedlings. .

H₂O₂ production and lipid peroxidation strongly increase in treated Arabidopsis plantlets

Because photoactivated porphyrins generate reactive oxygen species, we monitored H₂O₂ production in plantlets in situ by DAB staining and biochemical assay. In parallel we determined membrane lipid peroxidation by MDA assay in treated plantlets compared to control ones (Fig. 5). A significant increase in both H₂O₂ and MDA contents was determined suggesting that H₂O₂ over-production and lipid peroxidation were together responsible for plantlet death (Fig. 5). Our hypothesis was that CP-Zn was probably able to accumulate in the cell wall and/or cytoplasm of Arabidopsis root, thereby inducing ROS over-production under illumination.

Antioxidant arsenal is overwhelmed in treated Arabidopsis plantlets

As antioxidant molecules, total thiol, proline and ascorbate contents in CP-Zn treated plantlets were assayed. The photodynamic stress triggered by photoactivated CP-Zn induced a 7-fold increase in proline content in Arabidopsis whole plantlets while ascorbate amount did not significantly change and total thiol content fall down in response to CP-Zn (Table 2). These results could explain why plantlets were not able to fight against ROS production triggered by CP-Zn photoactivation. Furthermore, while ascorbate and guaiacol peroxidases were not activated, superoxide dismutase and

catalase were down-regulated (Fig 6). Taken together, it could explain why DAB staining was so intense in the treated plantlets (Fig.5A).

CP-Zn is localized in Arabidopsis root apex

As CP-Zn seemed to be a good weed killer candidate, it was also of importance to check CP-Zn localization in Arabidopsis root apparatus. Previous study already showed that cationic porphyrin was able to get in *Allium cepa* root meristematic cells (Villanueva et al., 1989). Confocal microscopy analysis, using the natural fluorescence of CP-Zn and calcofluor as a contrast marker of the cell wall, showed that CP-Zn was strongly localized in the first external layers of root (epidermis and parenchyma cells) in Arabidopsis root apex (Fig. 7). Furthermore, it seemed that CP-Zn was in cell wall and/or cytoplasm of these cells but further analysis are required to distinguish between the two localizations. Nevertheless this result suggested that CP-Zn could cross cell wall, get in the cytoplasm where it could be photoactivated and induced a strong oxidative burst leading to plantlet death.

Discussion

To our knowledge, this approach of supplying exogenous porphyrin on Arabidopsis plantlets was the first although it was extensively studied on bacteria, fungi, insects and mammal cells (Donnelly et al 2008, Plaetzer et al 2013, Maish 2015, Pérez-Lagunal et al 2017). Furthermore, cationic porphyrins were able to reach root meristematic cell nucleus and induced DNA photodamage (Villanueva et al 1989). Recently and in the present work, we showed that cationic porphyrins at 3.5 μM were able to inhibit Arabidopsis early vegetative development whereas tomato plantlets treated with 80 μM CP/CP-Zn were also affected but could be rescued (Guillaumot et al 2016). This result was in agreement to the necessity of a case-by-case study because photosensitizer effects depend on the ability to be uptaken by plants and to enter into cells. Indeed, observation of CP-Zn localization in Arabidopsis treated roots showed an intense labelling from epidermis cells to vessels while in tomato roots labelling was confined to external layers suggesting a differential root interaction and uptake of the photosensitizer between the two distant species (Guillaumot et al., 2016). This also was observed

between citrus and strawberry leaves in contact to coumarins and fucocoumarins where citrus leaf cuticle prevents photosensitizer to cross epidermis whereas it could diffuse through strawberry epidermis and induce oxidative damages (De Menezes et al 2014a). Thus, the future use of APDT in environment must consider plant species and their anatomical traits such as thickness and/or interaction between epidermis cells and photosensitizers. Moreover, the effects of photosensitizer will be also more or less important depending on the way of its administration, e.g. soil feeding and spraying. Soil feeding supposes that photosensitizer should be up-taken by roots and translocated to the leaves where they become photoactivated. In the present study, we also showed that translocation occurred in 14 day-old CP-Zn treated plantlets through H₂O₂ cotyledon accumulation linked to CP-Zn photoactivation. This result was also in agreement to previous work with Mg-ProtoIX feeding in *Arabidopsis* (Kindgren et al., 2012; Larkin, 2016). The spraying method is probably less harmful for plants than the constant photosensitizer inclusion in culture medium as we did, explaining why a low CP-Zn (3.5 μ M) was so efficient to kill *Arabidopsis* plantlets in vitro. We supposed that in the field such concentration will have no effect on plants treated by spraying. Nevertheless, studies on plant pathogens as fungi showed that a concentration up to 50 μ M of natural and synthetic photosensitizers was required to eradicate fungi (De Menezes et al 2014a,b, Fracarolli et al 2016). At this threshold concentration of cationic porphyrins, *Arabidopsis* and pathogens will be most likely eradicated whereas this concentration does not kill tomato plantlets (Guillaumot et al 2016). Further study on plants in greenhouse alone and against pathogens under porphyrin spreading are now required to test this hypothesis.

In the other hand, we showed that under dark condition, photosensitizers did not affect germination and post-germinative development of *Arabidopsis* and tomato plantlets (Guillaumot et al 2016). Thus it does not affect soil micro-wildlife where darkness takes over.

Under light conditions, post-emergence effect of porphyrins was investigated and we showed that cationic porphyrins were able to inhibit *Arabidopsis* early vegetative development. When illuminated, photosensitizers, especially porphyrins, generate radicals such as superoxide anion (O₂⁻) and hydroxyl radical (OH) by electron transfer (type I process) or singlet oxygen (¹O₂) by energy transfer to dioxygen (type II process). All these ROS damage cellular constituents such as nucleic

acids, proteins, lipids leading to cell death by necrosis and more often by apoptosis (Gill and Tuteja 2010, Avery 2011). As a consequence of porphyrin photoactivation, cell death was shown in animal cells, fungi, bacteria and recently in tobacco BY-2 cells (Donnelly et al 2008, Ringot et al 2012, Plaetzer et al 2013, Riou et al 2014, Maish 2015). Because lipid peroxidation is thought to be mainly triggered by these ROS, we performed MDA quantification on Arabidopsis whole plantlets (Gill and Tuteja 2010, Avery 2011). A significant increase in MDA was detected suggesting that cell membranes were seriously damaged, presumably leading to cell death and ultimately to plantlet death. Our result strongly suggested that CP-Zn was able to get inside root cells (Villanueva et al 1989) and produce ROS close to the different membrane systems (endoplasmic reticulum, mitochondria) under illumination. Nevertheless, photoactivation of CP-Zn and CP was also shown to induce DNA photodamage (Villanueva et al 1989). Altogether, lipid peroxidation and DNA damage are seen as consequences of CP-Zn photoactivation in root cells and led to a fatal issue in Arabidopsis. Moreover, DNA damages could also be induced by MDA itself which was shown to be highly mutagenic in bacteria and mammal cells (Marnett 2002). Further investigations should be performed to check whether DNA photodamage also occurs in Arabidopsis.

Another way for the plantlets to resist to photoactivated CP-Zn and to protect themselves against ROS, is to produce antioxidant molecules that could scavenge ROS. Thus, we determined proline, total thiol and ascorbate contents and ROS detoxification enzyme activities such peroxidases, catalase and superoxide dismutase. Arabidopsis plantlets did not show any increase in these enzyme activities but only a 7-fold increase in proline content that is mainly considered as a stress marker. Moreover, it was argued that proline accumulation is a consequence to tissue dehydration under abiotic stress injuries more than being an induced radical scavenger or singlet oxygen quencher (De Lacerda et al 2003). Thus, we considered that the high amount of proline in treated plantlets was not sufficient enough to overcome photoactivated CP-Zn damages in plantlet cells. To efficiently cope with the photoactivated porphyrins all the molecular defenses must be activated as shown in tomato plantlets (Guillaumot et al 2016). In fact, we suggest that 3.5 μM CP-Zn was already too high, preventing Arabidopsis plantlets from triggering defense mechanisms. Indeed, at 1 μM CP-Zn, Arabidopsis plantlets survived and were probably able to activate these pathways. Further

investigations are needed at molecular level to confirm this hypothesis. Nevertheless, in the aim to find an efficient weed killer, we proposed to use CP-Zn at 3.5 μM that is able to kill approximately 90 % of plantlets.

Finally, we pointed out difference between CP and CP-Zn response to Arabidopsis. It was also shown that CP-Zn was a stronger photosensitizer than CP on DNA photodamage (Villanueva et al 1989) because of its binding mode that must be different to free Zn complex form. Until now it is quite difficult to understand why the metalation of cationic porphyrin lead to a fatal issue for Arabidopsis compared to CP without Zn metalation. We supposed that it could be linked to CP-Zn greater stability than CP. Study on photobleaching and photostability of CP-Zn compared to CP would be soon engaged.

In conclusion, we demonstrated that adventitious Arabidopsis plantlets were irreversibly damaged by photoactivated cationic porphyrins that inhibit enzymatic defense machinery and rendering them unable to produce sufficient amount of antioxidative molecules to withstand this photodynamic stressful conditions. This data should be kept in mind for further investigation related to APDT use in the farming practical approach that aims to eradicate plant pathogens without deleterious effects on plants of agronomic interest. Additionally, we can imagine a double target strategy that could eradicate in the same time unwanted vegetation and plant pathogens without killing plants of agronomic interest such as tomato plantlets under sunlight.

Author contributions

MI, DG and CR designed research and conducted experiments. VS helped in the reflection and writing of the manuscript. All authors read and approved the manuscript.

Acknowledgments –

Mohammad Issawi was supported by a Grant from the municipality of Sharkieh (Lebanon). Authors thank Dr C. Carrion for confocal microscopy analysis.

References

- Aebi H (1984) Catalase in vitro. *Methods Enzymol* 105: 121-126
- Alves E, Faustino MAE, Neves MS, Cunha A, Nadaisc H, Almeida A (2015) Potential applications of porphyrins in photodynamic inactivation beyond the medical scope. *J Photochem Photobiol B Biol* 22: 34-57
- Avery S (2011) Molecular targets of oxidative stress. *Biochem J* 434: 201–210
- Ben Amor TB, Jori G (2000) Sunlight-activated insecticides: historical background and mechanisms of phototoxic activity. *Insect Biochem.Mol Biol* 30: 915–925
- Bradford MM (1976) A rapid and sensitive method for the quantitation of microgram quantities of protein utilizing the principle of protein-dye binding. *Anal.Biochem* 72: 248–254
- Carré V, Gaud O, Sylvain I, Bourdon O, Spiro M, Biais J, Granet R, Krausz P, Guilloton M (1999) Fungicidal properties of meso-arylglycosylporphyrins: influence of sugar substituents on photoinduced damage in the yeast *Saccharomyces cerevisiae*. *J Photochem Photobiol B Biol* 48: 57–62
- Chakraborty N, Tripathy BC (1992) Involvement of Singlet Oxygen in 5-Aminolevulinic Acid-induced Photodynamic Damage of Cucumber (*Cucumis sativus* L.) Chloroplasts. *Plant Physiol* 98: 7-11
- Chu ES, Wu RW, Yow CM, Wong TK, Chen JY (2006) The cytotoxic and genotoxic potential of 5-aminolevulinic acid on lymphocytes: a comet assay study, *Cancer Chemother Pharmacol* 58: 408–414
- Cormick MP, Alvarez MG, Rovera M, Durantini EN (2009) Photodynamic inactivation of *Candida albicans* sensitized by tri- and tetra-cationic porphyrin derivatives. *Eur J.Med Chem* 44: 1592–1599
- De Lacerda CF, Cambraia J, Oliva MA, Ruiz HA, Prisco JT (2003) Solute accumulation and distribution during shoot and leaf development in two sorghum genotypes under salt stress. *Environ Exp Bot* 49: 107-120
- De Menezes HD, Tonani L, Bachmann L, Wainwright M, Braga UL G, von Zeska Kress MR (2014a) Furocoumarins and coumarins photoinactivate *Colletotrichum acutatum* and *Aspergillus nidulans* fungi under solar radiation. *J Photochem Photobiol B Biol* 131: 74-83
- De Menezes HD, Rodrigues GB, Teixeira SDP, Massola NS, Bachmann L, Wainwright M, Bragaa ULG (2014b) In Vitro Photodynamic Inactivation of Plant-Pathogenic Fungi *Colletotrichum acutatum* and *Colletotrichum gloeosporioides* with Novel Phenothiazinium Photosensitizers. *Appl Environ Microb* 80: 1623-1632
- De Menezes HD, Tonani L, Bachmann L, Wainwright M, Gilberto Braga ULG, Von Zeska Kress MR (2016) Photodynamic treatment with phenothiazinium photosensitizers kills both

- ungerminated and germinated microconidia of the pathogenic fungi *Fusarium oxysporum*, *Fusarium moniliforme* and *Fusarium solani*. J photochem Photobiol 164:1-12
- Dondji B, Duchon S, Diabate A, Herve JP, Corbel V, Hougard JM, Santus R, Schrevel J (2005) Assessment of laboratory and field assays of sunlight-induced killing of mosquito larvae by photosensitizers. J Med Entomol 42: 652–656
- Donnelly RF, McCarron PA, Tunney MM (2008) Antifungal photodynamic therapy. Microbiol Res 163: 1–12
- Drabkova M, Marsalek B, Admiraal W (2007) Photodynamic therapy against cyanobacteria. Environ Toxicol 22: 112–115
- Fayyaz F, Rahimi R, Rassa M, Yaghoobi RZ (2015) Photodynamic Antimicrobial Chemotherapy, A Pathway for Photo-Inactivation of Bacteria by Porphyrin Compounds., 1st International Electronic Conference on Molecular Science Cell Signaling, Survival and Growth .
- Fracarolli L, Rodrigues GB, Pereira AC, Massola Júnior NS, José Silva-Junior G, Bachmann L, Wainwright M, Kenupp Bastos J, Braga GUL (2016) Inactivation of plant pathogenic fungus *Colletotrichum acutatum* with natural plant-produced photosensitizers under solar radiation. J Photochem Photobiol B Biol 162 : 402-411
- Funes MD, Caminos DA, Alvarez MG, Fungo F, Otero LA, Durantini EN (2009) Photodynamic Properties and Photoantimicrobial Action of Electrochemically Generated Porphyrin Polymeric Films. Environ Sci Technol 43: 902–908
- Gabor F, Szocs K, Maillard P, Csik G (2001) Photobiological activity of exogenous and endogenous porphyrin derivatives in *Escherichia coli* and *Enterococcus hirae* cells. Radiat Environ Biophys 40: 145–151.
- Gamborg OI, Miller RA, Ojima K (1968) Nutrient requirements of suspension cultures of soybean root cells. Exp. Cell Res 50:151-158
- Gill SS, Tuteja N (2010) Reactive oxygen species and antioxidant machinery in abiotic stress tolerance in crop plants. Plant Physiol Biochem 48: 909–930
- Guillaumot D, Issawi M, Da Silva A, Leroy-Lhez S, Sol V, Riou C (2016) Synergistic enhancement of tolerance mechanisms in response to photoactivation of cationic tetra (N-methylpyridyl) porphyrins in tomato plantlets. J Photochem Photobiol B Biol. 156: 69-78
- Heap I (2014) Global perspective of herbicide-resistant weeds. Pest Manag 70: 1306–1315
- Hodges DM, DeLong JM, Forney CF, Prange RK (1999) Improving the thiobarbituric acid-reactive-substances assay for estimating lipid peroxidation in plant tissues containing anthocyanin and other interfering compounds. Planta 207: 604–611
- Kampfenkel K, Van Montagu M, Inzé D (1995) Effects of iron excess on *Nicotiana plumbaginifolia* plants (implications to oxidative stress). Plant Physiol 107: 725–735
- Kindgren P, Norén L, Lopez GDB, Shaikhali J, Strand A (2012) Interplay between HEAT SHOCK PROTEIN 90 and HY5 Controls PhANG Expression in Response to the GUN5 Plastid Signal.

- Mol. Plant 5:901-913
- Larkin, R.M. (2016) Tetrapyrrole signaling in plants. *Front. Plant Sci.* 7:1586-1603
- Lucantoni L, Magaraggia M, Lupidi G, Ouedraogo K, Coppellotti O, Esposito F, Fabris C, Jori G, Habluetzel A (2011) Novel, Meso-Substituted Cationic Porphyrin Molecule for Photo-Mediated Larval Control of the Dengue Vector *Aedes aegypti*. *PLoS Negl Trop Dis* 5:1434-1446
- Magnieto JR, Di Meo F, Delcourt MC, Clément S, Norman P, Richete S, Linares M, Surin M (2014) Binding modes of a core-extended metalloporphyrin to human telomeric DNA G-quadruplexes. *Org Biomol Chem* 13: 2453-63
- Maish T (2015) Strategies to optimize photosensitizers for photodynamic inactivation of bacteria, *Photochem Photobiol B Biol* 150: 2-10
- Marnett LJ (2002) Oxy radicals, lipid peroxidation and DNA damage. *Toxicol* 181-182: 219-222
- Matsumoto H, Tanida Y, Ishizuka K (1994) Porphyrin Intermediate Involved in Herbicidal Action of δ -Aminolevulinic Acid on Duckweed (*Lemna paucicostata* Hegelm.), *Pestic Biochem and Physiol* 48: 214-221.
- Merchat M, Bertolini G, Giacomini P, Villaneuva A, Jori J (1996) Meso-substituted cationic porphyrins as efficient photosensitizers of gram-positive and gram-negative bacteria. *J Photochem Photobiol B Biol* 32: 153–157.
- Meyerowitz EM (1989) Arabidopsis, a useful weed. *Cell* 56: 263–269.
- Murshed R, Lopez-Lauri F, Sallanon H (2008) Microplate quantification of enzymes of the plant ascorbate glutathione cycle. *Anal Biochem* 383: 320–322.
- Pérez-Laguna¹ V, Pérez-Artiaga L, Lampaya-Pérez V, García-Luque I, Ballesta S, Nonell S, Paz-Cristobal MP, Gilaberte Y, Rezusta A (2017) Bactericidal Effect of Photodynamic Therapy, Alone or in Combination with Mupirocin or Linezolid, on *Staphylococcus aureus*. *Front Microbiol* 8: 1002
- Plätzer k, Berneburg M, Kiesslich T, Maisch T (2013) New Applications of Photodynamic Therapy in Biomedicine and Biotechnology. *Biomed Res Int.* 2013:161362-161365
- Provart NJ and Meyerowitz EM (2016) 50 years of Arabidopsis research: highlights and future directions. *New Phytol.* 209: 921-944
- Quiroga ED, Mora SJ, Alvarez MG, Durantini EN (2016) Photodynamic inactivation of *Candida albicans* by a tetracationic tentacle porphyrin and its analogue without intrinsic charges in presence of fluconazole. *Photodiagnosis Photodyn Ther.* 13: 334-40
- Rebeiz, CA, Montazer-Zouhour A, Hopen HJ, Wu SM (1984). Photodynamic herbicides: 1. Concept and phenomenology. *Enzyme and Microbial Technology*, 6: 390-396
- Ringot C, Sol V, Barrière M, Saad N, Bressollier P, Granet R, Couleaud P, Frochot C, Krausz P (2012). Triazinyl porphyrin-based photoactive cotton fabrics: preparation, characterization and

- antibacterial activity. *BioMacromol* 12: 1716-1723
- Riou C, Calliste CA, Da Silva A, Guillaumot D, Rezazgui O, Sol V, Leroy-Lhez S (2014) Anionic porphyrin as a new powerful cell death inducer of Tobacco Bright Yellow-2 cells. *Photochem Photobiol Sci* 13: 621-625
- Sasikala C, Ramana CV, Rao PR (1994) 5-Aminolevulinic Acid: A Potential Herbicide/Insecticide from Microorganisms. *Biotechnol Prog* 10: 451-459
- Villanueva A, Cañete M, Hazen MJ (1989) Uptake and DNA photodamage induced in plant cells in vivo by two cationic porphyrins. *Mutagenesis* 4: 157-159
- Weydert CJ, Cullen JJ (2010) Measurement of superoxide dismutase, catalase and glutathione peroxidase in cultured cells and tissue. *Nat Protoc* 5: 51-66
- Zampini G, Planas O, Marmottini F, Gulias O, Agut M, Nonell S, Latterini L (2017) Morphology effects on singlet oxygen production and bacterial photoinactivation efficiency by different silica-protoporphyrin IX nanocomposites *RSC Advances* 7: 14422-14229

FIGURES LEGEND

Fig. 1. Porphyrins are not cytotoxic for Arabidopsis plantlets grown under dark conditions. Arabidopsis seeds (At) were placed on different media supplied with 50 μM anionic porphyrin (AP/AP-Zn) and 5 μM of cationic porphyrin (CP/CP-Zn) for 7 days. C represented the control without porphyrins. Scale bar represents 1 cm.

Fig. 2. Arabidopsis plantlet phenotypes placed on porphyrins for 3 days. 14 day-old Arabidopsis plantlets grown on B5 medium were transferred in liquid B5 supplemented with 50 μM AP/AP-Zn or 3.5 μM CP/CP-Zn for 72 h in growth chamber with 16 h photoperiod. C represented the control without porphyrins, T0: the beginning of experiment and T72h: 3 days after.

Fig. 3. Phenotypic effects of photoactivated cationic and anionic porphyrins on 14 day-old Arabidopsis plantlets. (A) Arabidopsis seeds germinated on different media supplied with 50 μM of AP/AP-Zn and 3.5 μM CP/CP-Zn for 14 days with 16 h photoperiod. Scale bar represents 1 mm for plantlets that were photographed under binocular microscope. Arrows indicated the white and green plantlets corresponding to Arabidopsis two phenotypes observed on CP-Zn. (B) Dry and fresh weight ratio Arabidopsis plantlets under photodynamic stress. Arabidopsis seeds germinated on different media supplemented with 50 μM AP/AP-Zn and 3.5 μM CP/CP-Zn for 14 days with 16 h photoperiod. DW: dry weight and FW: fresh weight. Results are the mean of 4 independent experiments \pm SD ($***P < 0.001$).

Fig. 4. 7% of the green 14 day-old Arabidopsis plantlets grown on CP-Zn could be rescued. Arabidopsis seed germination took place on media supplemented with 5 μM CP/CP-Zn for 14 days. Plantlets were then placed for 1 week on B5 medium. (A) Proportion of rescued plantlets. Green box for green plantlets and white box for white dead plantlets. C represented the control without porphyrins. (B) Pictures of the different plantlets after 1 week rescue. Scale bar corresponds to 1 mm and 1 cm for 14 day-old plantlets undergoing photodynamic stress and “rescued” plantlets respectively. (C) Increase in CP-Zn concentration clearly inhibits post-germination development of Arabidopsis plantlets. Four concentrations of CP-Zn were tested from 1 to 10 μM and the number of green (living) and white (dead) plantlets was determined. Results are the mean of 3 independent experiments \pm SD.

Fig. 5. Photoactivated CP-Zn induces ROS overproduction and lipid peroxidation in 14 day-old Arabidopsis seedlings. CP-Zn was tested at 3.5 μM . (A) Hydrogen peroxide production in whole plantlets qualitative (DAB staining). Left panel corresponds to control Arabidopsis plantlet and right panel to CP-Zn treated plantlet. Scale bar represents 1 mm. (B) Quantitative

H₂O₂ production. (C) Lipid peroxidation by MDA quantification assay. Results are the mean of 4 independent experiments \pm SD (***) $P < 0.001$).

Fig. 6. Effect of photoactivated CP-Zn on antioxidant enzyme specific activities in Arabidopsis whole plantlets. GPOX: guaiacol peroxidase, APX: ascorbate peroxidase, CAT: catalase, SOD: superoxide dismutase. Results are the mean of 4 independent experiments \pm SD (ns: not significant; * $P < 0.05$).

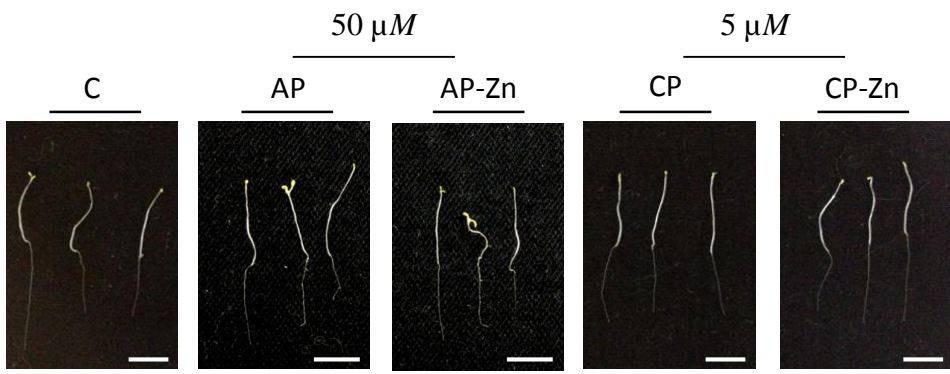
Fig. 7. CP-Zn localization in Arabidopsis roots. Pictures of root apex were obtained from channel mode acquisition. Roots were staining by calcofluor and observed under UV (left panel). Scale bar represents 50 μ m.

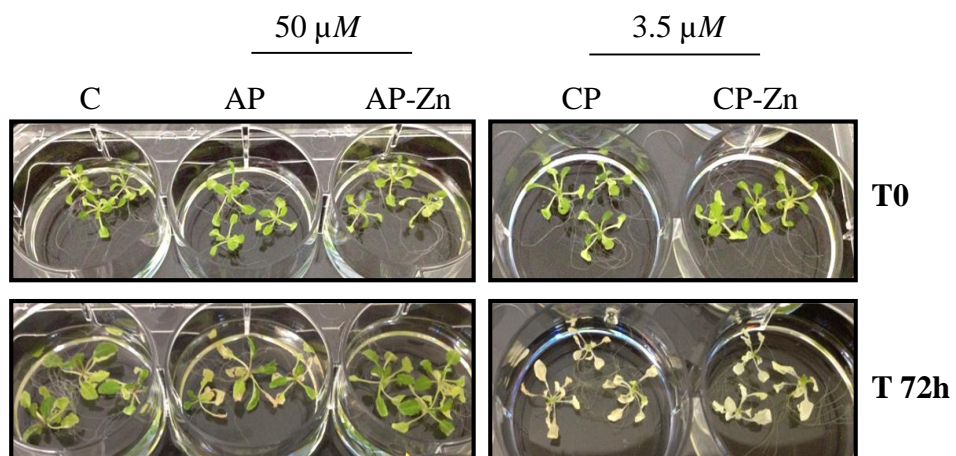
Table 1. Exogenous porphyrins do not have a pre-emergence effect on Arabidopsis seeds germination. Anionic porphyrin (AP) and its metalated form (AP-Zn) and cationic porphyrin (CP) and its metalated form (CP-Zn) were tested at 50 μ M or 5 μ M, respectively. Control corresponded to seed germination on medium without porphyrin. Results are expressed as percentage of germination and the mean of 4 independent experiments \pm SD.

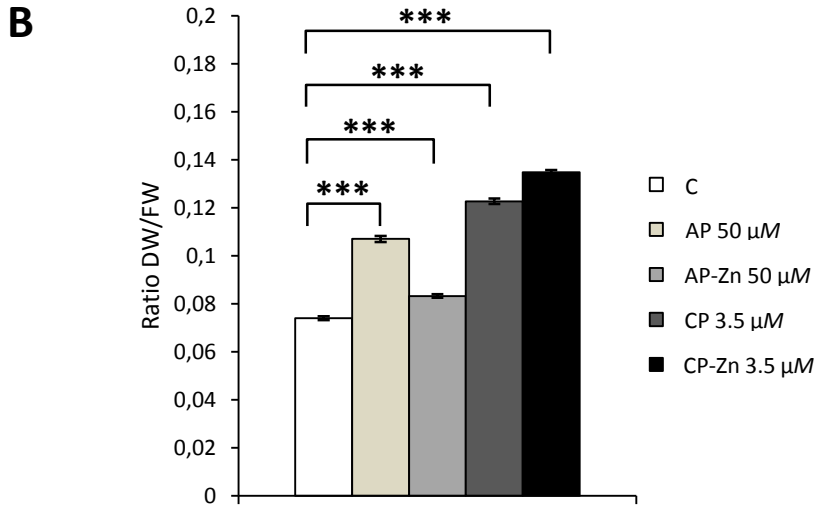
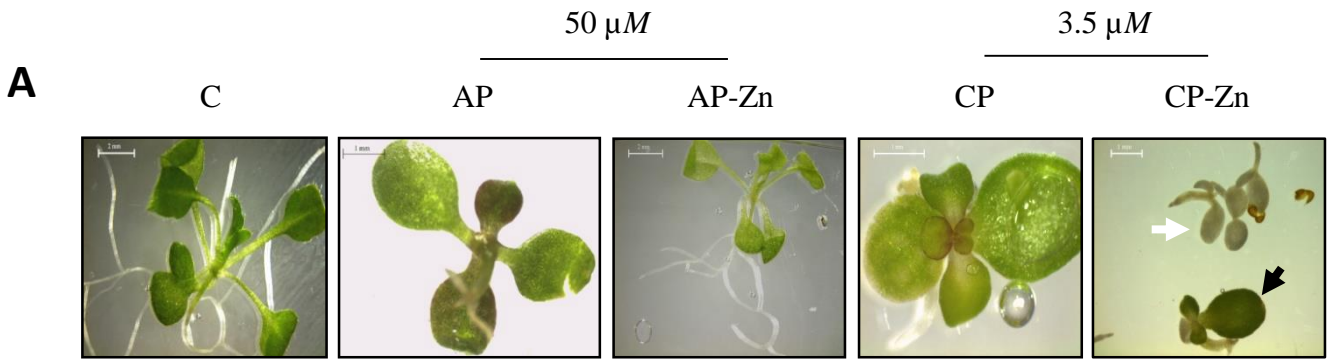
	Control	AP	AP-Zn	CP	CP-Zn
Arabidopsis	86.13 \pm 1.09	88.25 \pm 0.96	85.63 \pm 1.11	89.92 \pm 1.33	88.54 \pm 1.04
P value	-----	0.14	0.96	0.006	0.08

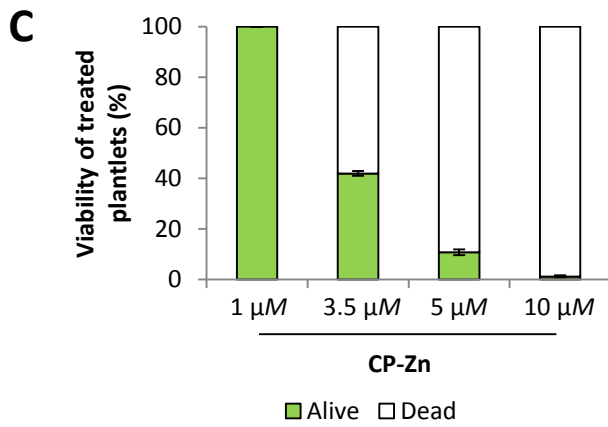
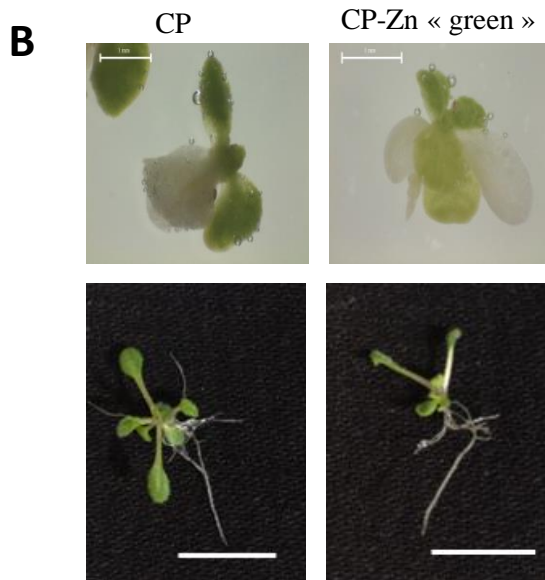
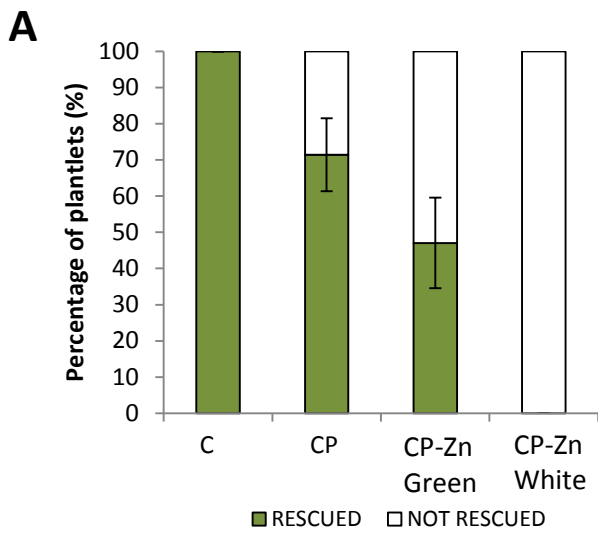
Table 2. Ratio of antioxidant molecule contents in Arabidopsis plantlets grown on medium containing 3.5 μM CP-Zn or medium without porphyrin (control) for 14 days under 16 h photoperiod. Results are the mean of 4 independent experiments \pm SD (ns: not significant, *** $P < 0.001$)

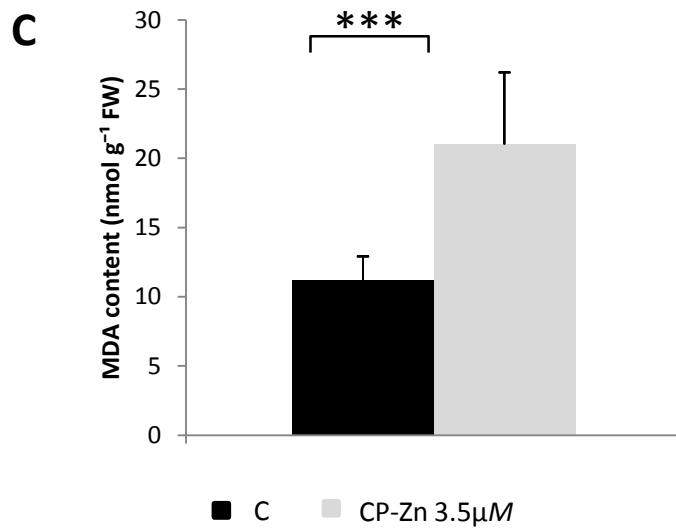
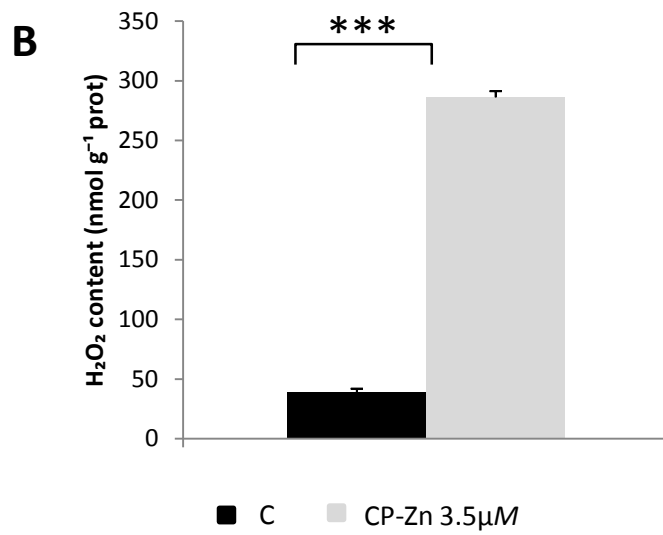
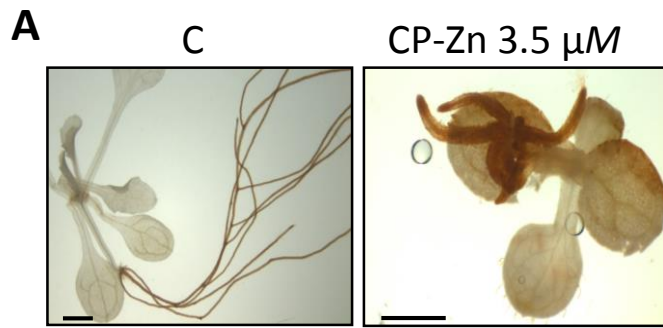
Proline content ($\mu\text{mol g}^{-1}$ FW)		Ascorbate content (nmol g^{-1} FW)		Total thiol content (nmol mg^{-1} FW)	
Control	CP-Zn 3.5 μM	Control	CP-Zn 3.5 μM	Control	CP-Zn 3.5 μM
0.72 \pm 0.1	4.9 \pm 1	185.2 \pm 10	209 \pm 27	58.67 \pm 1.6	32.37 \pm 2.6
***		ns		***	

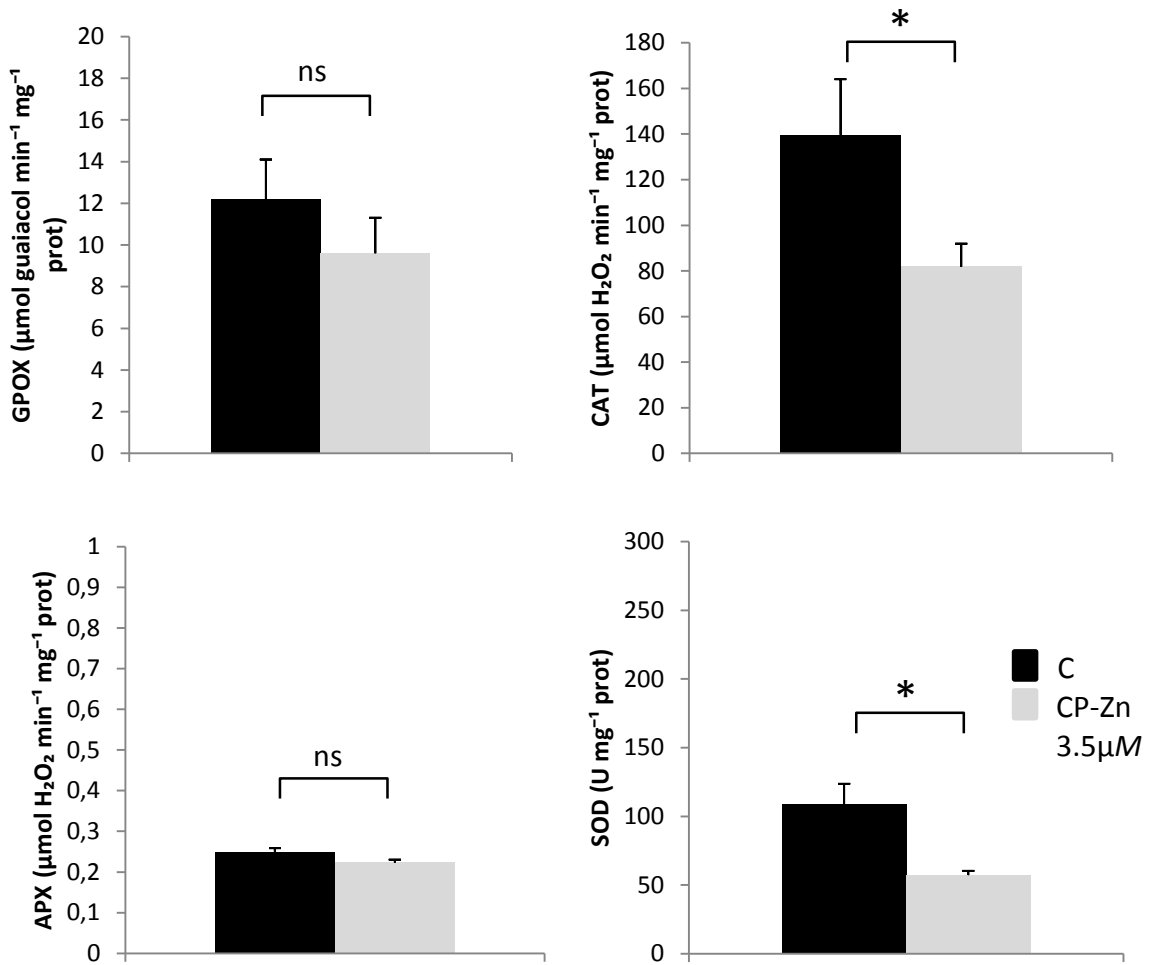


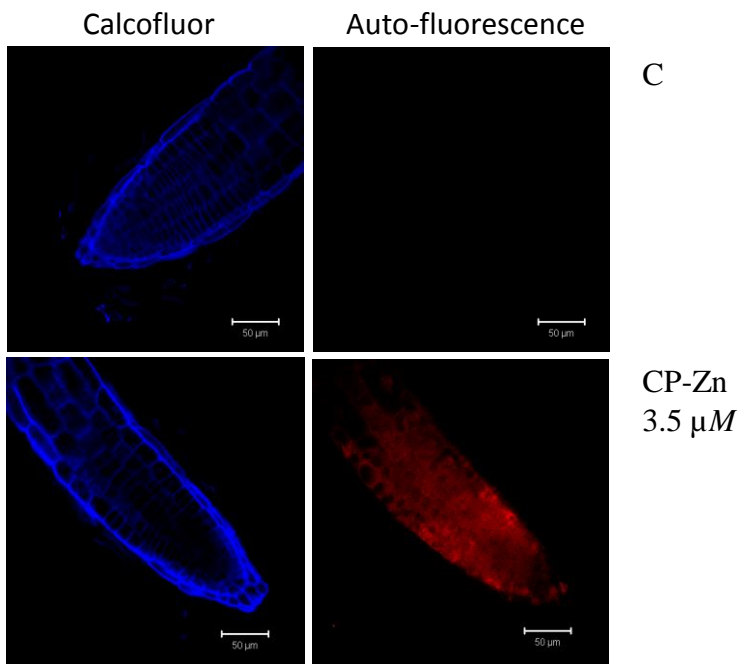












Discussion and perspectives

We showed that negatively charged porphyrins tested at 50 μM had no effects on both plantlets. Moreover, positively charged porphyrins (free base TMPyP or Zinc-metalated) were deleterious for *Arabidopsis* demonstrating an herbicide potential effect but they only delayed tomato plantlet growth. According to literature, this result was surprising for tomato plantlets that were also rescued after 14 days treatment. Indeed, cationic porphyrins are known as powerful PS against various types of microorganisms including plant pathogens (Orlob 1967, Fayyaz et al. 2015, Jesus et al. 2018). Taken together, we could imagine a double weapon modality aiming to struggle against plant pathogens and unwanted weeds (Figure 10). We only worked on plant side but the research team of Pr Gilberto Braga in Brazil showed the ability to apply this strategy using a PS, more specifically at the level of plant pathogens (De Menezes et al. 2014 a,b, Fracarolli et al. 2016, De Menezes et al. 2016, Gonzales et al. 2017). We are now enlarging our study testing PS treatments on perennial plant: *Vitis vinifera* var Chardonnay clones and a new annual species: potato explants (Veronica Ambrosini PhD work).

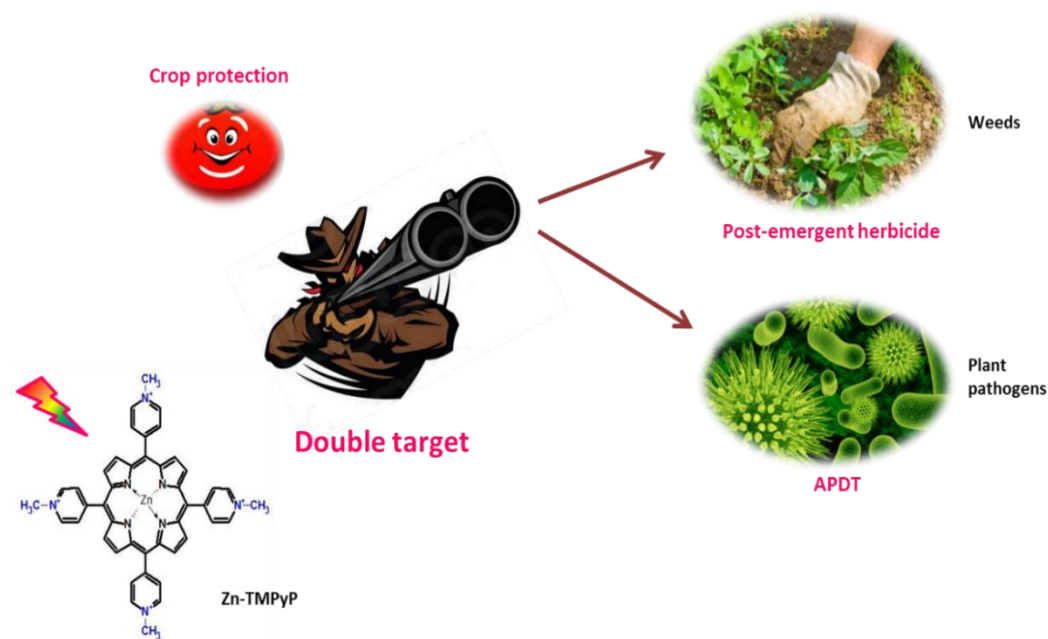


Figure 10. Schematic representation of the “two-in-one” strategy based on the use of PS in agronomy.

One of the most important perspective that should be taken in consideration to validate APDT in field areas is the requirement of whole study of a defined pathosystem including

biological life cycle of pathogen, phenology of growth and reproduction of plants and timing of PS application. For example, Gonzales et al. 2017 reported that to fight against *Colletotrichum* fungal species that cause orange crop damage in the Americas via photodynamic approach, methylene blue PS must be applied in the wet season because rain splash disperses conidia and citrus flowering coincides with rain events in tropical region. Other study conducted by Jesus et al, 2018 showed that in temperate region, porphyrin like TMPyP should be applied in the period when bacteria (*Pseudomonas syringae*) infect their host as kiwi plants in winter and early spring and especially after winter pruning and bud outbreak that facilitates infection process. In accordance with the last point, our laboratory is on the road to develop consistent pathosystem involving the mold (*Botrytis cinerea*) and its two plant hosts *Solanum tuberosum* (potato) and *Vitis vinifera* (grapevine) then trying to apply porphyrin molecular systems in agreement with APDT (Veronica Ambrosini PhD study).

This study also pointed out the potential use of photodynamic treatment to eradicate weeds by means of herbicide. Indeed, this could explain why developing such approach in agriculture was not envisaged due to its large spectrum targets including plants and more broadly wildlife (Figure 9). Nevertheless, based on our case-by-case study, we demonstrated that plant of agronomic interest can tolerate photodynamic stress and anionic porphyrins had no effects when tested on both plants. Moreover, orange and kiwi tree leaves and flowers were not affected by PS treatment. In addition, the demand for new herbicide is being to increase by the agricultural chemical industry because there are no new herbicide modes of action and up to 400 weeds evolved resistance in the last 30 years. Currently, the World Health Organization classified some Diphenyl ether (for more details see DPE in the review (Publication 1 submitted) as "substances of very high concern". Thus, some commercial herbicides will be soon banned, and agriculture is still missing some new herbicide molecules. Therefore, we think about the possibility to employ PS especially porphyrins as herbicide due to their multi-target sites at cellular level, their efficient application at very low (μM) concentration and micro-organisms subjected to PS treatment did not develop resistance yet.

We are aware that our studies represent a first preliminary step to examine the usefulness of plant photodynamic treatment at large scale level in the near future. Our studies constitute the cornerstone for sustainable agriculture and crop protection basing on the power of light-driven PS activation against pathogens and weeds.

**Chapter II. TBY-2 cells: a helpful
tool to understand the cellular
responses to photoactivated
anionic porphyrin treatment from
A to Z**

In order to study the cellular and molecular mechanisms underlying plant responses to photodynamic treatment by exogenously porphyrin supply, we looked out for plant cell suspension cultures that are intensively used in plant biology as reliable tool for the investigation of wide range of phenomena bypassing therefore whole plant structural complexity. We chose TBY-2 cell suspension showing high growth rate with good synchrony as well as easy and inexpensive culture.

In a previous study published in 2014, we showed that anionic porphyrin (TPPS) was more efficient than cationic ones (TMPyP) to induce high production of hydrogen peroxide leading to cell death. This result was in opposition to what the literature reported. Indeed, cationic porphyrins were more powerful than anionic forms to photodamage almost each living entity (Tegos et al. 2005, Guillaumot et al. 2016).

To gain insight in molecular mechanisms that occurred at cellular level in response to photoactivated three anionic porphyrins (TPPS, TPPC and TPPP), we tried to cover all aspects from extracellular porphyrin behaviour, cell wall interaction and penetration, photodynamic damage, cell responses to cell death. As already mentioned in introduction, a preliminary but necessary step for this exhaustive study was to get knowledge about TBY-2 cell wall (publication 4).

PUBLICATION 4: “Unexpected features of exponentially growing Tobacco Bright Yellow-2 cell suspension culture in relation to excreted extracellular polysaccharides and cell wall composition”, Glycoconjugate Journal.

Dear Dr. Riou:

We are pleased to inform you that your manuscript, "Unexpected features of exponentially growing Tobacco Bright Yellow-2 cell suspension culture in relation to excreted extracellular polysaccharides and cell wall composition" has been accepted for publication in Glycoconjugate Journal.

For queries regarding your accepted paper, please click the following link <http://www.springer.com/10719>; then click on "Contacts", and then "Production Editor", complete the query form and click "Submit".

Please remember to always include your manuscript number, #GLYC-D-17-00015R3, whenever inquiring about your manuscript. Thank you.

Best regards,

The Editorial Office
Glycoconjugate Journal

Unexpected features of exponentially growing Tobacco Bright Yellow-2 cell suspension culture in relation to excreted extracellular polysaccharides and cell wall composition

Mohammad Issawi, Mohammad Muhieddine, Celine Girard, Vincent Sol and Catherine Riou*

Université de Limoges, Laboratoire de Chimie des Substances Naturelles, EA 1069, 123 avenue Albert Thomas, 87060 Limoges, France.

*Corresponding author: catherine.riou@unilim.fr; Tel: +33 555457474; Fax: +33 555457202

ABSTRACT

This article presents a new insight about TBY-2 cells; from extracellular polysaccharides secretion to cell wall composition during cell suspension culture. In the medium of cells taken 2 days after dilution (end of lag phase), a two unit pH decrease from 5.38 to 3.45 was observed and linked to a high uronic acid (UA) amount secretion (47.8 %) while, in 4 and 7 day-old spent media, pH increased and UA amounts decreased 35.6 and 42.3 % UA, respectively. To attain deeper knowledge of the putative link between extracellular polysaccharide excretion and cell wall composition, we determined cell wall UA and neutral sugar composition of cells from D2 to D12 cultures. While cell walls from D2 and D3 cells contained a large amount of uronic acid (twice as more as the other analysed cell walls), similar amounts of neutral sugar were detected in cells from lag to end of exponential phase cells suggesting an enriched pectin network in young cultures. Indeed, monosaccharide composition analysis lead to an estimated percentage of pectins of 56% for D3 cell wall against 45% D7 cell walls indicating that the cells at the mid-exponential growth phase re-organized their cell wall linked to a decrease in secreted UA that finally led to a stabilization of the spent medium pH to 5.4. In conclusion, TBY-2 cell suspension from lag to stationary phase showed cell wall remodeling that could be of interest in drug interaction and internalization study.

Keywords:

cell wall composition; extracellular polysaccharides; Tobacco BY-2 suspension culture; uronic acid.

Abbreviations:

CW: cell wall; TBY-2: tobacco bright yellow-2 cells; UA: uronic acid.

INTRODUCTION

Amongst broad and numerous literature on plant cell suspensions, Tobacco Bright Yellow cell line (TBV-2) suspension remains largely well documented because of its extensive use in laboratories working from cell cycle regulation to programmed cell death or responses to biotic or abiotic stress [1-7]. TBV-2 cells mainly form chains of 2 to 8 cells, ovoid-like micro-colonies that are easy to observe, label and count. While they are usually cultivated in the dark in liquid medium, they could also grow on solidified medium under continuous light or dark. Moreover, the culture of these cells does not require sophisticated material and is feasible for a great variety of experiments from protoplast to transient DNA expression [8].

Moreover, TBV-2 cells have been also used as a model system for cell wall studies including the purification of enzymes involved in cell wall formation or regeneration from protoplasts of transformed TBV-2 cell lines [9-12]. However, TBV-2 cell wall composition *per se* has not been readily investigated. Until now, two studies were performed on TBV-2 rhamnogalacturonan-II, a component of the pectin network, in response to boron feeding and only one on whole secondary cell wall characterization [13-15]. Indeed, knowledge about TBV-2 cell wall (CW) will help to understand potential interactions between exogenous molecules (herbicides, elicitors, growth factors) and primary CW, their entry into cell and/or their accumulation into this compartment. This is of interest to model plant cell interaction with exogenous molecules such as in some abiotic stresses (drug, herbicide treatments). Furthermore, growing cells modify initial cell culture medium in term of chemical composition [16]. Both molecules from primary and secondary metabolisms (amino and organic acids, alkaloids), cell wall polysaccharides and enzymes and/or proteins were found in spent medium of suspension-cultured cells of *Lupinus polyphyllus*, *Pyrus communis* and *Arabidopsis thaliana* making cell medium similar to the vacuole for detoxification but also as a sink-source [16-18]. Particularly, the release of extracellular polysaccharides which are thought to be non-cellulosic cell wall matrix from plant cells in suspension culture into the medium has been intensively reported by several works [19-23]. As a consequence of sucrose uptake, ammonium assimilation and organic acid release, pH of medium was more and more acidic especially in the first days of culture [16, 24]. Since we also found a decrease in pH of culture medium during TBV-2 cell growth, just before the exponential phase starts, we aim to investigate polysaccharide secretion in spent medium of growing cells and try to link it to cell wall composition.

MATERIAL and METHODS

TBY-2 cell suspension

Tobacco Bright Yellow-2 cell suspension was maintained in the dark under continuous agitation (140 rpm) at 22 °C in modified Murashige and Skoog medium, supplemented with 0.27 mg.L⁻¹ 2,4-dichlorophenoxyacetic acid; 10 mg.mL⁻¹ thiamine-HCl; 100 mg.L⁻¹ myo-inositol; 30 g.L⁻¹ sucrose and 200 mg.L⁻¹ KH₂PO₄, pH 5.8. The suspension was subcultured every 7 days, by transferring 1.5 to 2 mL aliquot into 40 mL of fresh medium. Establishment of growth curve was performed by weighing the cell pellets obtained from 40 mL of suspension (4,500 g, 10 min); supernatants were either discarded or kept for analyses of excreted polysaccharides. Cells isolated at the end of lag phase (2 days after dilution), at the beginning (3 or 4 days after dilution) or the mid-exponential phase (7 or 8 days after dilution), and, at the stationary phase (9, 10 and 14 days after dilution) were used for cell wall isolation and analysis.

Cell wall extraction

Cell wall was extracted according to [15] with minor modifications. TBY-2 cells were ground in liquid nitrogen then homogenized in 0.5 M potassium phosphate buffer (pH 7.0) by sonication (50 pulses/min for 1 min, 4 times). Homogenates were centrifuged (4,500 g, 30 min at 4 °C) and pellets were washed twice with the same buffer and subsequently 3 times with cold distilled water. To remove lipids, cell walls were extracted 3 times with chloroform/methanol (1:1, v/v). Proteins were eliminated by three extractions with phenol/ acetic acid/water (2:1:1, v/v/v). After centrifugation (900 g, 10 min), cell walls were rinsed with sufficient ethanol and water to remove the solvent. Starch hydrolysis was performed by a treatment with type XII-A Bacillus α -amylase (50 U/ml) from Sigma-Aldrich (Mo, USA) for D2, D3 and D4 cell walls (1 h, 37°C). D7, D8, D9 and D12 cell walls were incubated with XII-A Bacillus α -amylase (100 U/ml) overnight at room temperature. After starch hydrolysis, cell wall fractions were centrifuged (4,500 g, 30 min at 4 °C) then freeze-dried for 24 hours.

Sugar content determination

Whole cell walls were solubilized in 10 ml distilled water. Neutral sugars and uronic acids were determined according to [25] and [26] respectively with glucose and glucuronic acid as standards. Absorbance values were corrected according to [27].

Monosaccharide composition

Monosaccharide composition was evaluated by gas liquid chromatography using methanolysis followed by trimethylsilylation according to [28] modified by [29].

Main polysaccharides estimation

We estimated the amount of cell wall major polysaccharides from the monosaccharide composition according to [30]. Pectin percentage was evaluated as following % pectin = GalA + Rha + Gal + Ara. Cellulose percentage was estimated arbitrarily by 50% Glc (cellulose = ½ Glc), the other half was attributed to hemicellulose that comprises in particular xyloglucans, xylans and mannans which can therefore be estimated by the sum ½ Glc + Xyl + GlcA + Man. Monosaccharides are expressed in molar percentage as determined in [29].

Extracellular polysaccharide quantification

According to [31], TBY-2 culture medium was concentrated by rotary evaporation then subjected to precipitation by ethanol 95% (v/v), 3 vol. at 4 °C overnight. After centrifugation (3,500g, 30 min), pellets were

Results

Mohammad ISSAWI | Thèse de doctorat | Université de Limoges | 2018

Licence CC BY-NC-ND 3.0

dialyzed (MWCO: 12,000-14,000 Da) against distilled water and represented the extracellular polymer fraction. Sugar content was evaluated according to [25] and [26] as described above.

Statistical analysis

All biological experiments were performed at least three times independently. Results were expressed as mean \pm SD (Standard Deviation). Data were analyzed by t-student test and one-way ANOVA using the PAST free software.

RESULTS and DISCUSSION

To gain insight into TBY-2 cells growth curve, we monitored, daily, the fresh weight of the whole culture (40 mL culture) until day 14 after dilution (Fig. 1A). Surprisingly TBY-2 cells taken 7 days after dilution were not in stationary phase as mainly described in the literature but rather in mid-exponential phase (Fig. 1A ; [2,7]). Nine days after dilution, the cells were still in “good health” with a high viability percentage ($> 92\%$ data not shown) but they progressively became elongated as shown in Fig1B for D14 cells and, while they increased in volume, granules appeared around the nucleus (Fig. 1A). We supposed that, for these reasons, and because 9 day-old cultures also became very viscus and difficult to dilute and to work with, most laboratories choose to work with D7 cells or even with very young cell suspensions (D3 and/or D4), as we previously did [32]. In fact, D3 or D4 cells were in very early exponential growth phase considering that D2 cells were at the end of the lag phase (Fig 1A). We placed the switch between lag (D2) and exponential (D3) phases not in regard to cell curve or cell size (no significant difference in fresh weights with $P=0.9081$; Fig 1A) but to pH variations: a two pH-unit decrease during the lag phase followed, after D2, by a slow return to the initial pH of the medium around 5.4 (Fig. 1B) as it had already been shown with lupinus cell suspension [16]. We noticed that this pH was reached for D7 cells and stayed constant after that point (Fig.1A).

To better understand this pH decrease observed 2 days after dilution, we measured the amount of extracellular polysaccharides excreted by the cells in the dried spent medium, especially uronic acids (UA), at D2, D4 and D7. Spent medium is a complex combination of culture medium basal components and sugars and/or proteins excreted by cells themselves. As shown in Table 1, dry weight of the extracellular fraction varied from nearly 1 mg for D2 and D4 supernatants to more than 4 mg for D7 suggesting very high molecule secretions of cells in mid-exponential phase. Nevertheless, determination of UA and neutral contents in D7 dry spent medium did not reflect an important polysaccharide secretion suggesting that D7 cells were rather able to secrete protein and/or lipid into the medium (Table 1). For D2 and D4 spent media, while UA secretion was significantly higher (0.285 and 0.258 g.g^{-1} DW extracellular fraction respectively) than in D7 medium (0.196 g.g^{-1} DW extracellular fraction), neutral sugar production for D4 cells was notably upregulated (Table 1). In TBY-2 cells, it was shown that cell invertase released fructose and glucose from sucrose breakdown into the culture medium that could also be the case for D4 cells [33]. Thus, it should be interesting to follow sucrose consummation during cell growth and establish extracellular fraction composition especially for D4 cells.

Our aim was firstly to understand the pH decrease in D2 spent medium (Fig. 1A). Although UA contents relative to DW extracellular fraction were similar in D2 and D4 media, percentage of UA in D2 spent medium (47.8%) was clearly higher to D4 one (35.6%) (Table 1). Thus, we supposed that the pH decrease was mainly due to excreted UA. Nevertheless, it could also be triggered by organic acid production such as malic and oxalic acids which is strongly linked to high oxidative metabolism that could strongly occur in D2 [16]. Indeed, D2 cells are

metabolically active because they doubled their fresh weight from 1.7 g to 3 g in D3. Thus, organic acid secretion could be envisaged at the end of lag phase linked to respiratory metabolism and energy production. It was also shown that sucrose uptake and ammonium assimilation led to acidification of culture media of *Lupinus polyphyllus* and *Ocotea catharinensis* suspensions suggesting a similar situation for TBY-2 cells [16,24]. Moreover, as rhamnogalacturonans II could also be excreted by TBY-2 cells, this could be similar in D2 supernatant leading to potential acidification [13,14]. Further studies have to be made in order to confirm these hypotheses.

As TBY-2 cells from the end of lag phase to mid exponential phase were able to excrete polysaccharides especially UA, it was of interest to characterize their cell wall in term of cellulose, hemicellulose and pectin networks as well as their sugar composition. We determined the cell wall composition of cells from D2 to D12 (Fig. 2). Surprisingly, concerning UA content, D2 and D3 cell walls were very similar and contained nearly 3 times less UA than D4 to D12 cell walls (Fig. 2A). On the contrary, neutral sugar contents from lag phase (D2) to end of exponential phase (D8) cell walls were very similar around 270 $\mu\text{g}\cdot\text{mg}^{-1}$ dried CW (Fig. 2B). In fact, D2 and D3 cell walls were enriched in UA-bearing polysaccharides such as pectins, compared to D7 and later cell walls (Fig.2). That was confirmed by monosaccharide analysis and percentage estimation of the three main cell wall polysaccharides from D3, D4 and D7 cell walls (Table 2). D3 and D4 were very similar in regard to pectin content although D3 had significantly more negatively charged sugars especially galacturonic acid than D4 (Table 2). On the opposite, D4 contained more neutral sugars as rhamnose and arabinose that are also parts of pectin network (Table 2). Taken together, D3 and D4 cell wall polysaccharide compositions were similar and different to D7 cell wall which is enriched in cellulose network, twice as much as D3 and D4 cell walls. Moreover, measurement of zeta potential showed that it was similar between D3 and D4 cell wall (around -30 mV, data not shown) while it was less negative for D7 cell wall (-20 mV) that was in good agreement with its rich neutral sugar content. For stationary phase D9 and D12 cell walls, neutral sugar content significantly increased (Fig2B). This could be linked to a thickening of cell wall with an extra-cellulose deposition that could be investigated by electronic microscopy.

In conclusion, TBY-2 cell suspension from D2 after dilution to stationary phase showed cell wall remodeling. For D7 cell wall, we showed that cells at mid-exponential phase that are usually used in the laboratories around the world, were still able to secrete UA in their spent medium. As reported by [34], UA-rich pectic polymers which were excreted by white campion (*Silene latifolia*) suspension culture were able to promote cell growth when added into new culture media. Thus, we suppose that a synergistic effect between cells after the mid-log growth phase induced by UA-rich polysaccharides excreted through a specific secretory pathway that could be linked to an unconventional secretory pathway [35]; [36]. This remains unclear and warrants to be further investigated.

Acknowledgements

Mohammad Issawi was supported by a Grant from the municipality of Sharkieh (Lebanon). Authors greatly thank Pr M. Guilloton for reading this manuscript.

References

1. Kato, K., Matsumoto, T., Koiwai, S., Mizusaki, S., Nishida, K., Nogushi, M., Tamaki, E.: Liquid suspension culture of tobacco cells. in *Fermentation Technology Today*. ed Terui G (Society of Fermentation Technology, Osaka) 689–695 (1972).
2. Nagata, T., Nemoto, Y., Hasezawa, S.: Tobacco BY-2 cell line as the “Hela” cell in the cell biology of higher plants. *Internal. Rev. Cytol.* 132, 1–30 (1992).
3. Kobayashi, I., Hakuno, H.: Actin-related defense mechanism to reject penetration attempt by a non-pathogen is maintained in tobacco BY-2 cells. *Planta* 217, 340–345 (2003).
4. de Pinto, M.C., Locato, V., Sgobba, A., Romero-Puertas, M. d. C., Gadaleta, C., Delledonne, M., De Gara, L.: S-Nitrosylation of Ascorbate Peroxidase Is Part of Programmed Cell Death Signaling in Tobacco Bright Yellow-2 Cells. *Plant Physiol.* 163, 1766–1775 (2013).
5. Takahashi, S., Kojo, K.H., Kutsuna, N., Endo, M., Toki, S., Isoda, H., Hasezawa, S.: Differential responses to high- and low-dose ultraviolet-B stress in tobacco Bright Yellow-2 cells. *Front. Plant Sci.* 6, 254–264 (2015).
6. Moscatiello, R., Baldan, B., Navazio, L.: Plant Cell Suspension Cultures. In: Maathuis, F.J.M. (ed.) *Plant Mineral Nutrients*. pp. 77–93. Humana Press, Totowa, NJ (2013).
7. Srba, M., Černíková, A., Opatrný, Z., Fischer, L.: Practical guidelines for the characterization of tobacco BY-2 cell lines. *Biol. Plant.* 60, 13–24 (2016).
8. Bratic, A., Majic, D., Samardzic, J., Kragl, M.W., Maksimovic, V.: Transient expression in tobacco Bright Yellow 2 cells and pollen grains: A fast, efficient and reliable system for functional promoter analysis of plant genes. *Arch. Biol. Sci.* 62, 57–62 (2010).
9. De Marco, A., Guzzardi, P., Jamet, É.: Isolation of tobacco isoperoxidases accumulated in cell-suspension culture medium and characterization of activities related to cell wall metabolism. *Plant Physiol.* 120, 371–382 (1999).
10. Nebenführ, A., Frohlick, J.A., Staehelin, L.A.: Redistribution of Golgi stacks and other organelles during mitosis and cytokinesis in plant cells. *Plant Physiol.* 124, 135–152 (2000).
11. Hong, Z., Delauney, A.J., Verma, D.P.S.: A cell plate-specific callose synthase and its interaction with phragmoplastin. *Plant Cell* 13, 755–768 (2001).
12. Yokoyama, R., Tanaka, D., Fujino, T., Itoh, T., Nishitani, K.: Cell wall dynamics in tobacco BY-2 cells. In: *Tobacco BY-2 Cells*. 53, 217–230 (2004).
13. Kobayashi, M., Ohno, K., Matoh, T.: Boron nutrition of cultured tobacco BY-2 cells. II. Characterization of the boron-polysaccharide complex. *Plant Cell Physiol.* 38, 676–683 (1997).
14. Matoh, T., Takasaki, M., Kobayashi, M., Takabe, K.: Boron nutrition of cultured tobacco BY-2 cells. III. Characterization of the boron-rhamnogalacturonan II complex in cells acclimated to low levels of boron. *Plant Cell Physiol.* 41, 363–366 (2000).
15. Goué, N., Mortimer, J.C., Nakano, Y., Zhang, Z., Josserand, M., Ohtani, M., Dupree, P., Kakegawa, K., Demura, T.: Secondary cell wall characterization in a BY-2 inductive system. *PCTOC* 115, 223–232 (2013).
16. Wink, M.: The cell culture medium—a functional extracellular compartment of suspension-cultured cells. In: *Primary and Secondary Metabolism of Plants and Cell Cultures III*. pp. 307–319. Springer (1994).

17. Jamet, E., Canut, H., Boudart, G., Pont-Lezica, R.F.: Cell wall proteins: a new insight through proteomics. *Trends Plant Sci.* 11, 33–39 (2006).
18. Webster, J.M., Oxley, D., Pettolino, F.A., Basic, A.: Characterisation of secreted polysaccharides and glycoproteins from suspension cultures of *Pyrus communis*. *Phytochem.* 69, 873–881 (2008).
19. Becker, G.E., Hui, P.A., Albersheim, P.: Synthesis of extracellular polysaccharide by suspensions of *Acer pseudoplatanus* cells. *Plant Physiol.* 39, 913 (1964).
20. Olson, A.C., Evans, J.J., Frederick, D.P., Jansen, E.F.: Plant suspension culture media macromolecules—pectic substances, protein, and peroxidase. *Plant Physiol.* 44, 1594–1600 (1969).
21. Liao, D.-F., Boll, W.G.: Extracellular polysaccharide from cell suspension cultures of bush bean (*Phaseolus vulgaris* cv. Contender). *Can. J. Bot.* 50, 2031–2037 (1972).
22. Moore, T.S.: An extracellular macromolecular complex from the surface of soybean suspension cultures. *Plant Physiol.* 51, 529–536 (1973).
23. Oliveira C.J.F., Cavalari, A.A., Carpita, N.C., Buckeridge, M.S., Braga, M.R.: Cell wall polysaccharides from cell suspension cultures of the Atlantic Forest tree *Rudgea jasminoides* (Rubiaceae). *Trees.* 24, 713–722 (2010).
24. Moser, J.R, Gonçalves Garcia, M., Maria Viana, A.: Establishment and growth of embryogenic suspension cultures of *Ocotea catharinensis* Mez.(Lauraceae). *PCTOC.* 78, 37–42 (2004).
25. Dubois, M., Gilles, K.A., Hamilton, J.K., Rebers P.A, Smith, F. : Colorimetric method for determination of sugars and related substances. *Analytical Chem.* 28, 350–356 (1956).
26. Blumenkrantz, N., Asboe-Hansen, G.: New method for quantitative determination of uronic acids. *Analytical Biochem.* 54, 484–489 (1973).
27. Montreuil, J., Bouquelet, S., Debray, H., Fournet, B., Spik, G., Strecker, G.: In: Chaplin MF, Kennedy JF. (Eds), *Carbohydrate analysis, a practical approach*, IRL Press, Oxford, Washington D.C 143-204. (1986).
28. Kamerling, J.P., Gerwig, G.J., Vliegthart, J.F.G., Clamp, J.R.: Characterization by gas-liquid chromatography-mass spectrometry and proton-magnetic-resonance spectroscopy of pertrimethylsilyl methyl glycosides obtained in the methanolysis of glycoproteins and glycopeptides. *Biochem. J.* 151, 491–495 (1975).
29. Marga, F., Freyssac, V., Morvan, H.: Rapid gas liquid chromatography microanalysis of carbohydrates in woody plant tissues. *J. Trace Microprobe Techn.* 13, 473–478 (1995).
30. Douchiche, O., Driouich, A., Morvan, C.: Impact of cadmium on early stages of flax fibre differentiation: Ultrastructural aspects and pectic features of cell walls. *Plant Physiol. Biochem.* 49, 592–599 (2011).
31. Muschitz, A., Faugeron, C., Morvan, H.: Response of cultured tomato cells subjected to excess zinc: role of cell wall in zinc compartmentation. *Acta Physiol. Plant.* 31, 1197–1204 (2009).
32. Riou, C., Calliste, C.A., Da Silva, A., Guillaumot, D., Rezazgui, O., Sol, V., Leroy-Lhez, S.: Anionic porphyrin as a new powerful cell death inducer of Tobacco Bright Yellow-2 cells. *Photochem. Photobiol. Sci.* 13, 621-625 (2014).
33. Yamanaka, A., Hashimoto, A., Matsuo, T., Kanou, M., Suehara, K.-I., Kameoka, T.: Analysis of kinetic uptake phenomena of monosaccharide and disaccharide by suspension TBV-2 cells using an FT-IR/ATR method. *Bioproc Biosystems Eng.* 30, 457–468 (2007).
34. Morvan, H., Priem, B., Verdus, M.C., Kwan, J.S., Morvan, C.: Relationship between the acidity of the

- pectic acid polymers from suspension cultured cells of white campion and their promoting effects on the growth. *Food Hydrocolloids*. 1, 501–503 (1987).
35. Ding, Y., Robinson, D.G., Jiang, L.: Unconventional protein secretion (UPS) pathways in plants. *Curr. Op. Cell Biol.* 29, 107–115 (2014).
 36. Kim, S.-J., Brandizzi, F.: The plant secretory pathway for the trafficking of cell wall polysaccharides and glycoproteins. *Glycobiol.* 26, 940–949 (2016).

Table 1: Estimations of UA and neutral sugars content in extracellular fractions of 3 culture points: 2 days (D2), 4 days (D4) and 7 days (D7) after dilutions. D2: end of lag phase, D4: rapid exponential growth phase and D7: mid-exponential phase. Uronic acid (UA) and neutral sugar (NS) contents were determined as described in material and methods. Each result is the mean of three independent experiments \pm SD.

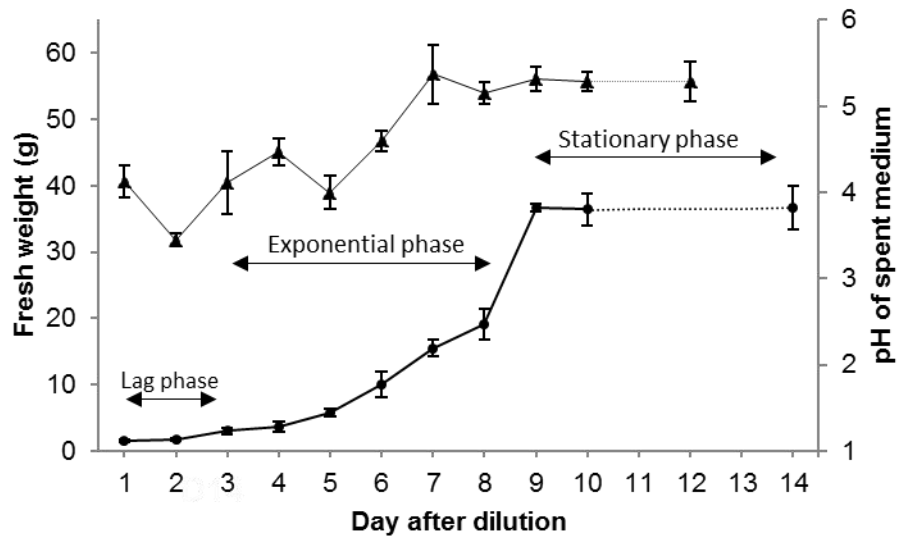
	Dry weight of the extracellular fraction (mg)	Percentage of UA in the extracellular fraction (%)	UA content ($\text{g}\cdot\text{g}^{-1}$ DW extracellular fraction)	NS content ($\text{g}\cdot\text{g}^{-1}$ DW extracellular fraction)
D2	0.76 ± 0.06	47.8 ± 1.6	0.285 ± 0.033	0.312 ± 0.035
D4	0.95 ± 0.04	35.6 ± 1.3	0.258 ± 0.035	0.468 ± 0.04
D7	4.3 ± 0.2	42.3 ± 1.3	0.196 ± 0.013	0.268 ± 0.049

Table 2: Estimations of monosaccharide compositions and deduced percentage of cellulose, hemicellulose and pectin fraction in cell wall from D3, D4 and D7 cell suspensions. Molar percentages and monosaccharide content were determined and calculated as described in material and methods section and represented the mean of three independent experiments \pm SD. CW: cell wall; nd: not detected.

		D3 CW	D4 CW	D7 CW
Monosaccharides (%)	Rhamnose	9.5 \pm 0.3	13 \pm 1.3	15.47 \pm 0.3
	Arabinose	5.1 \pm 0.4	8 \pm 0.2	21 \pm 0.7
	Fucose	2.1 \pm 0.1	3.2 \pm 0.5	3.57 \pm 0.04
	Xylose	7.4 \pm 0.4	8.75 \pm 0.7	3.09 \pm 0.07
	Mannose	8.65 \pm 0.15	10.3 \pm 1.1	5.42 \pm 0.2
	Galactose	7.35 \pm 0.9	7.26 \pm 1	2 \pm 0.02
	Galacturonic acid	32.65 \pm 0.2	24.1 \pm 1.2	5.77 \pm 0.3
	Glucose	20.95 \pm 1.1	19.20 \pm 0.8	43 \pm 0.7
	Glucuronic acid	5.7 \pm 0.1	4.25 \pm 0.6	nd
Polysaccharides (%)	Cellulose	10.7	10.1	21.5
	Hemicellulose	33.1	34.6	31
	Pectins	56.1	52.2	45

Figure 1: TBY-2 cell suspension characterization. **A)** TBY-2 suspension growth curve (circles) and pH variations of spent medium during growth (triangles). Fresh weights of independent cultures were determined in function of culture time after dilution. D: day after dilution. Each point is the mean of results from 5 independent cultures \pm SD. pH of the medium after autoclaving without cells used for cell dilution was measured (5.38 ± 0.14). Each pH value is the mean of four independent cultures \pm SD. **B)** Pictures of TBY-2 cells 4 days after dilution (D4) or early exponential phase; 7 days after dilution (D7) or mid-exponential phase and finally 14 days after dilution (D14) or stationary phase.

A)



B)

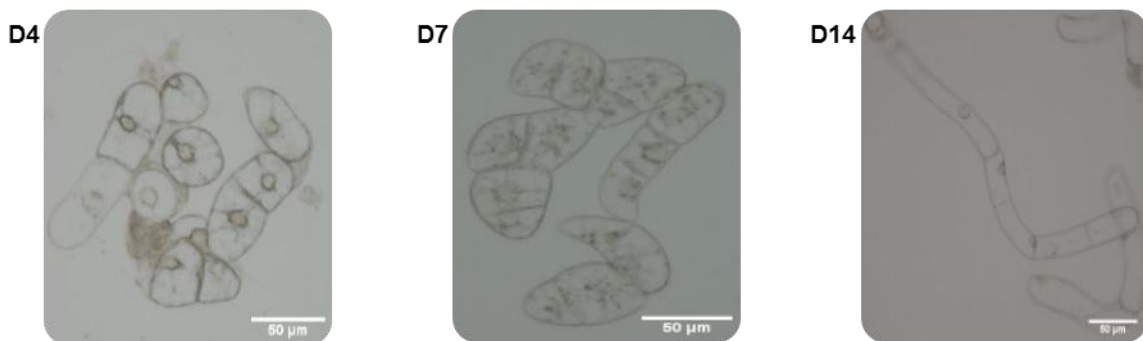
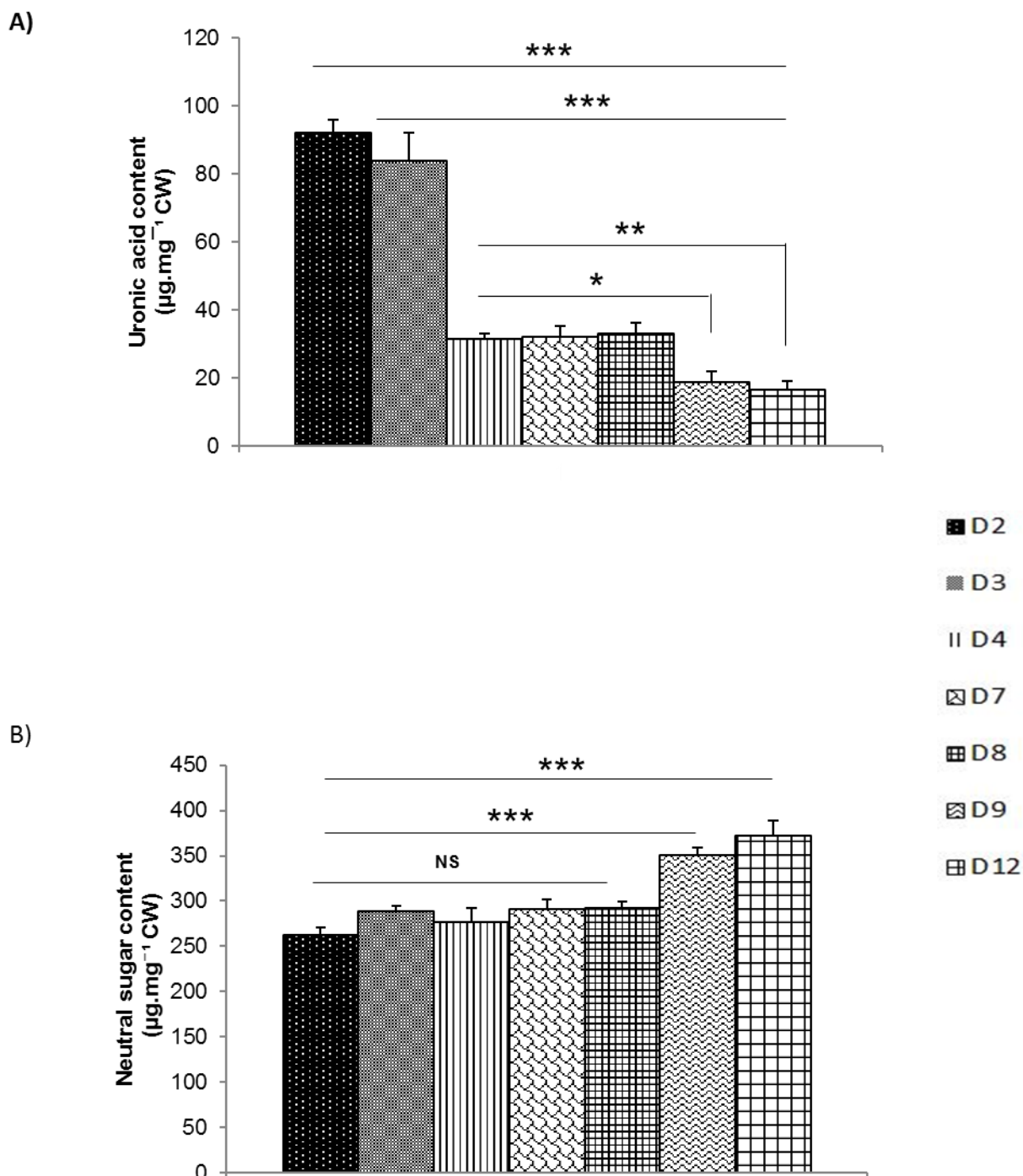


Figure 2: Sugar content determination of TBY-2 cell wall during growth. Isolated and purified cell walls (CW) were analyzed at the end of lag phase (2 days after dilution), at the beginning (3 or 4 days after dilution) or the mid-exponential phase (7 or 8 days after dilution), and, at the stationary phase (9 or 12 days after dilution). Determinations of UA **A)** and neutral sugar **B)** contents in different CW. Results are the mean \pm SD of three independent experiments (NS: not significant; *: $P < 0.05$; **: $P < 0.01$; ***: $P < 0.001$).



PUBLICATION 5: “Characterization of pH dependent charge states and physico-chemical properties of anionic porphyrins” (Submitted to Photochemical & Photobiological Sciences).

**Characterization of pH dependent charge states and physico-chemical properties of anionic porphyrins**

Journal:	<i>Photochemical & Photobiological Sciences</i>
Manuscript ID	PP-ART-04-2018-000152
Article Type:	Paper
Date Submitted by the Author:	10-Apr-2018
Complete List of Authors:	Leroy-Lhez, Stéphanie; PEIRENE EA7500, Faculté des Sciences et Techniques - Université de Limoges Rezazgui, Olivier; Laboratoire PEREINE Issawi, Mohammad; PEIRENE - EA 7500, Faculté des Sciences et techniques - université de Limoges Elhabiri, Mourad; CNRS, ECPM, UMR 7509 Calliste, Claude; PEIRENE EA 7500, Faculté de Pharmacie - Université de Limoges Riou, Catherine; PEIRENE EA7500, aculté des Sciences et Techniques - Université de Limoges



Journal Name

ARTICLE

Characterization of pH dependent charge states and physico-chemical properties of anionic porphyrins

Received 00th January 20xx,
Accepted 00th January 20xx

Stéphanie Leroy-Lhez,^{a*} Olivier Rezazgui,^a Mohammad Issawi,^a Mourad Elhabiri,^b Claude Alain Calliste,^a Catherine Riou.^a

DOI: 10.1039/x0xx00000x

www.rsc.org/

Surprisingly, we had shown in a previous report that anionic porphyrins are better cell death inducers under light irradiation than cationic ones. Thus, always for Antimicrobial PhotoDynamic Treatment applications in the agronomic domain, we investigated structure-activity relationship of a series of anionic porphyrins. Their charge states as a function of the pH medium, their abilities to generate reactive oxygen species as well as their spectroscopic and photophysical properties have been investigated. These data will be used to argue discussion on biological assays on Tobacco cells.

Introduction

In the tetrapyrrolic macrocycles' family, porphyrins are unquestionably the most studied.¹ Naturally present in living organisms (*i.e.*, both in animal and plants), crucial for many biological functions,² easy to be chemically functionalized,^{3,4} porphyrins exhibit a number of fascinating properties which allow targeting a wide range of applications.^{5,6} Thus, the recent scientific achievements in the synthesis and development of these molecules have made possible their use to a wide range of applications in fields as distinct as energy (solar panel⁷), microelectronics⁸ or even in industry as catalysts^{9,10} or analytical probes.¹¹ However, it is in the medical sector that their interest is highest, first as imaging probes¹² but above all as photosensitive drugs.^{13,14}

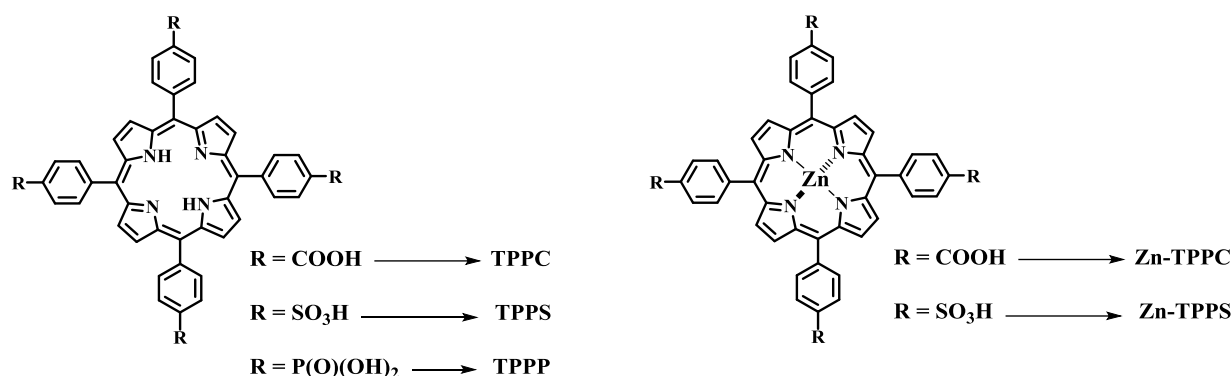
During the last decades, the porphyrins' capacity to generate Reactive Oxygen Species (ROS) under light irradiation was deeply explored in PhotoDynamic Therapy (PDT). This non-invasive technique uses light concomitantly to active compounds, the so-called photosensitizers, to treat, for example, precancerous lesions, various cancers or skin diseases.¹⁵ In response to new health issues that have emerged in recent years (nosocomial infections, groundwater contamination...), PDT's principle was successfully transposed to new targets.¹⁶ Always based on ROS production, porphyrins and others photosensitizers (PS) were used as photoactivable insecticides against devastating and invasive species,¹⁷ or disease vectors.^{18–20} However the most known is the Antimicrobial PhotoDynamic Treatment (APDT), focused on infections brought by deleterious pathogens such as bacteria,^{21,22} virus²³ and fungi.^{24–26}

Always to respond to crucial societal issues, APDT is increasingly used for agronomic issues. Without being exhaustive, the work of Braga *et al.*^{25–26} on plant pathogens fight can be cited. In this domain, porphyrins^{27–29} can also be used directly as photoactivable crop protection products to offer new and cleaner solutions for agronomy or even on an endogenous way.^{30–32} Whatever, to the best of our knowledge, there are still a few studies on such applications for porphyrins although it has been demonstrated that they were able to penetrate deep into the cells.^{33,34} To develop this field, a deeper understanding of interaction between porphyrins and plant cells is required. Indeed, it is of utmost importance to protect plants from further treatment and to enlarge efficiency of the PS towards plant pathogens while plants are kept safe. A first publication from our group in 2014 has demonstrated the potential of charged-porphyrins to induce cell death on Tobacco cells (Tobacco Bright Yellow-2 or TBY-2).²⁸ These preliminary results performed both on anionic and cationic porphyrins showed that the anionic ones were the more efficient to lead to hydrogen peroxide overproduction and thus to cells apoptosis.

In line with this previous investigation and in the frame of our research topic focused on APDT applications in agronomy, the main matter of this work was to evaluate the capacity of anionic porphyrins to induce cell death, depending on nature and number of anionic groups. For this purpose, we have chosen three commercially available compounds exhibiting different anionic functions as well as two of their zinc analogues (Scheme 1). Indeed, as their protonation and charge states intimately rely on the pH of the medium, the possibility (for free-base porphyrins) or not (metalloporphyrins under given conditions) to protonated the central nitrogen is of utmost importance. In the present study, we focused our attention on the UV-Vis absorption properties of a homogenous series of free-base or Zn(II) porphyrins as a function of pH to evaluate their charge pattern and the corresponding outcomes on TBY-2 cells.

^a PEIRENE – EA7500, Univ. Limoges, 123 Avenue Albert Thomas, 87060 Limoges, France.

^b Université de Strasbourg, Université de Haute-Alsace, CNRS, LIMA, UMR 7042, Equipe Chimie Bioorganique et Médicinale, ECPM, 25 Rue Becquerel, 67000 Strasbourg, France.



Scheme 1 Chemical structures of free-base or Zn-metallated porphyrins.

Results and discussion

UV-Visible absorption and fluorescence emission properties in aqueous medium

UV-Vis absorption as well as corrected fluorescence emission spectra of compounds **TPPC**, **TPSS**, **TPPP**, **Zn-TPPC** and **Zn-TPSS** (Scheme 1) were recorded in water, at room temperature and at concentration of *ca.* 2×10^{-6} M. Selected data have been collected and are depicted in Table 1. Apart from **TPSS** and **Zn-TPSS**, direct water solubilisation was not possible. Therefore, the same solubilisation protocol was used for all compounds, *i.e.* addition of an aliquot of a 1 M sodium hydroxide solution (3.75 equiv. by ionisable function, final pH= 8.7 \pm 0.2) to trigger deprotonation of the peripheral ionisable sites of the porphyrins, get the corresponding negatively charged functions and thus complete water solubility. All the results presented were from

at least 3 independent experiments. As expected,^{35,36} all investigated porphyrins showed a characteristic porphyrinic profile with the characteristic Soret band (from 415 to 425 nm) and the Q bands (*i.e.* four for the free-base and two for the metallated porphyrins, respectively) in the 500-650 nm spectral range. **TPPC**, **TPSS** and **TPPP** exhibited a characteristic *etio-type* ($\epsilon_{IV} > \epsilon_{III} > \epsilon_{II} > \epsilon_I$) spectrum. Interestingly, **TPPC** displayed the higher absorption intensity (*i.e.*, particularly the Soret band) with respect to the other free-base systems, especially **TPPP**. For zinc porphyrins, **Zn-TPSS** was found to display the higher absorptivity. Neither aggregation nor change in the protonation pattern was detected under these basic conditions for the concentrations tested (2 to 3.5 μM). Moreover, the excitation spectra were measured and exhibited similar profiles than the corresponding UV-Vis absorption spectra over the whole spectral range, thus confirming the degree of purity of all the investigated compounds.

Table 1 Selected spectroscopic and photophysical data for **TPPC**, **TPSS**, **TPPP**, **Zn-TPPC**, **Zn-TPSS** measured in water under basic conditions (pH 8.7, 2 μM , 298 K).

	Absorption		Emission	
	λ_{abs} (nm)	$\epsilon_{\text{abs}} (\times 10^5 \text{ M}^{-1} \text{ cm}^{-1})$	λ_{em} (nm)	$\Phi_{\text{f}}^{\text{a}}$
TPPC	416	3.740	644	0.15
	519	0.117		
	556	0.073		
	583	0.070		
	638	0.023		
TPSS	414	3.028	643	0.05
	517	0.104		
	553	0.047		
	582	0.041		
	636	0.025		
TPPP	416	0.642	648	0.09
	522	0.026		
	558	0.013		
	583	0.100		
	640	0.008		
Zn-TPPC	423	3.891	607	0.21
	558	0.146	658	
	598	0.081		
Zn-TPSS	422	5.350	606	0.03
	557	0.176	656	
	596	0.072		

^a Measured by using tetraphenylporphyrin, **TTP**, as a standard ($\Phi_{\text{f}} = 0.11$ in toluene), $\lambda_{\text{exc}} = 555 \text{ nm}$.³⁷

TPPC, **TPPS** and **TPPP** exhibited the typical free-base porphyrin emission profile, with an emission band centred at about 650 nm, and low fluorescence quantum yields. Similarly, fluorescence emission characteristics of **Zn-TPPC** and **Zn-TPPS** are those anticipated for metallated porphyrins. These expected features were compatible with the presence of preferential non-radiative de-excitation pathways such as Inter-System Crossing (ISC) towards a triplet state that would permit singlet oxygen production for all these compounds. Anyway, as these molecules have to be studied in the presence of TBY-2 cells and because the pH of the growth medium employed varies from 5.8 to 4.5, it was of utmost importance to monitor these properties as a function of pH. With respect to the UV-Vis absorption properties, spectra were as a first step recorded in 0.1 M phosphate buffers at different pH values (Figure 1). For the free-base compounds, protonation can occur either at the peripheral ionisable sites or at the central nitrogens. In the case of metallated porphyrins, this second protonation scheme is unlikely to occur as

nitrogens are already involved in zinc complexation, unless demetallation occurred. No change in the UV-Vis spectra of **Zn-TPPS** as a function of pH was observed (Figure 1). In the case of **Zn-TPPC**, marked modifications were observed with a decrease of the Soret band intensity and formation of a broad band between 400 and 460 nm (λ_{max} ca. 440 nm).

No modification was observed in the Q bands region. This behaviour, also observed for the free-base **TPPC**, is likely due to the protonation of the carboxylic functions, *vide infra*. For **TPPC**, we also noticed the modification of Q bands, especially an intensity increase of the Q_1 transitions which is characteristic of the protonation of central porphyrinic nitrogens.^{38,39} In the case of **TPPS**, its spectroscopic behaviour was exactly the same as described by Hollingsworth *et al.*,³⁶ i.e. red-shift of the Soret band with a clear isosbestic point at 423 nm and intensity increase of the Q_1 one. A new band, centred at 490 nm, also appeared at pH below 4 which is likely due, according to the same authors, to aggregation phenomenon. As expected, no

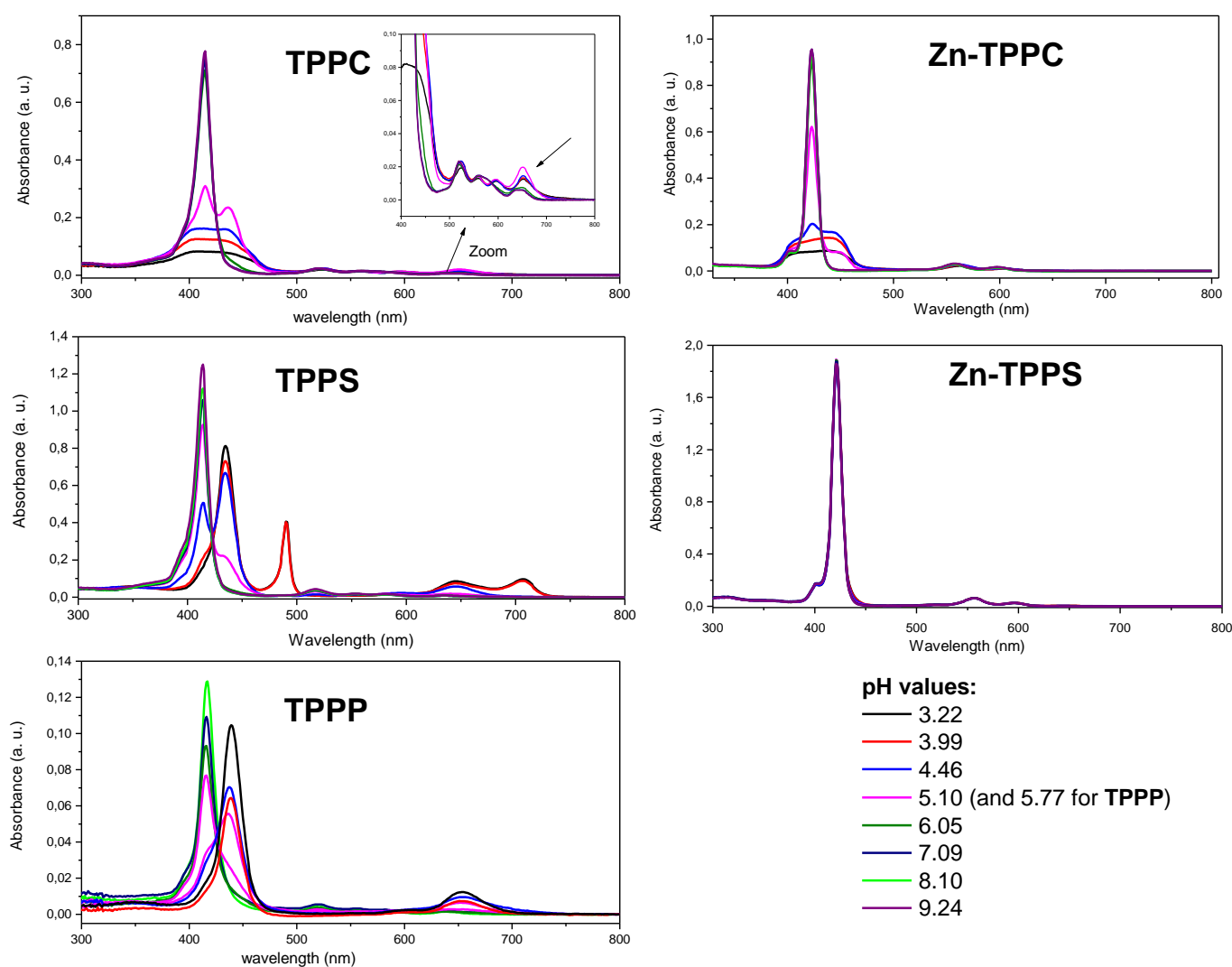


Figure 1 UV-Visible spectra of **TPPC**, **TPPS**, **TPPP**, **Zn-TPPC**, **Zn-TPPS** in phosphate buffer at different pH values (concentration = 2×10^{-6} M, except for **TPPS** and **Zn-TPPS**, concentration = 3.5×10^{-6} M; 298 K).

protonation of the sulfonic groups was evidenced as sulfonic acid is well-known to be a strong acid.⁴⁰ Finally, for **TPPP**, classical protonation of the central nitrogens (red-shift of Soret and Q_i bands as well as hyperchromic shift of the Q_i band) was observed. However, no clear isosbestic point (~ 425-430 nm) can be determined unlike **TPPS**. This behaviour could be due to the numerous protonation sites of **TPPP**. Indeed, each of the four phosphonic groups can be (de)protonated twice (pK_a values for substituted aryl-phosphonic acid in water in the range of 1-2 and 6-8, respectively)³⁸ whereas the free-base porphyrins remained dibasic compounds.

To further investigate the protonation patterns of these compounds (free-base and metallated porphyrins), the acid-basic properties were extensively studied using UV-Vis absorption spectrophotometric titrations as a function of pH of both the free-base porphyrins (**TPPS**, **TPPC** and **TPPP**) and the zinc(II)

metalloporphyrins (**Zn-TPPP** and **Zn-TPPS**). Indeed, while our preliminary approach allowed evaluating the pH effects on the absorption spectrophotometric properties of the systems herein investigated, these physico-chemical data allow predicting whether these compounds in TBY-2 growth medium predominate only in a single charged state (anionic, neutral, cationic or even zwitterionic) or otherwise as a pool of several protonated/charged species. Following this preliminary approach, a more accurate analysis of the structure-activity relationships with respect to the plant cells can be then undertaken.

Acido-basic properties probed by absorption spectrophotometric titration versus pH

Following this preliminary investigation, the acido-basic properties of the free-base porphyrins **TPPS**, **TPPC** and **TPPP** were thoroughly

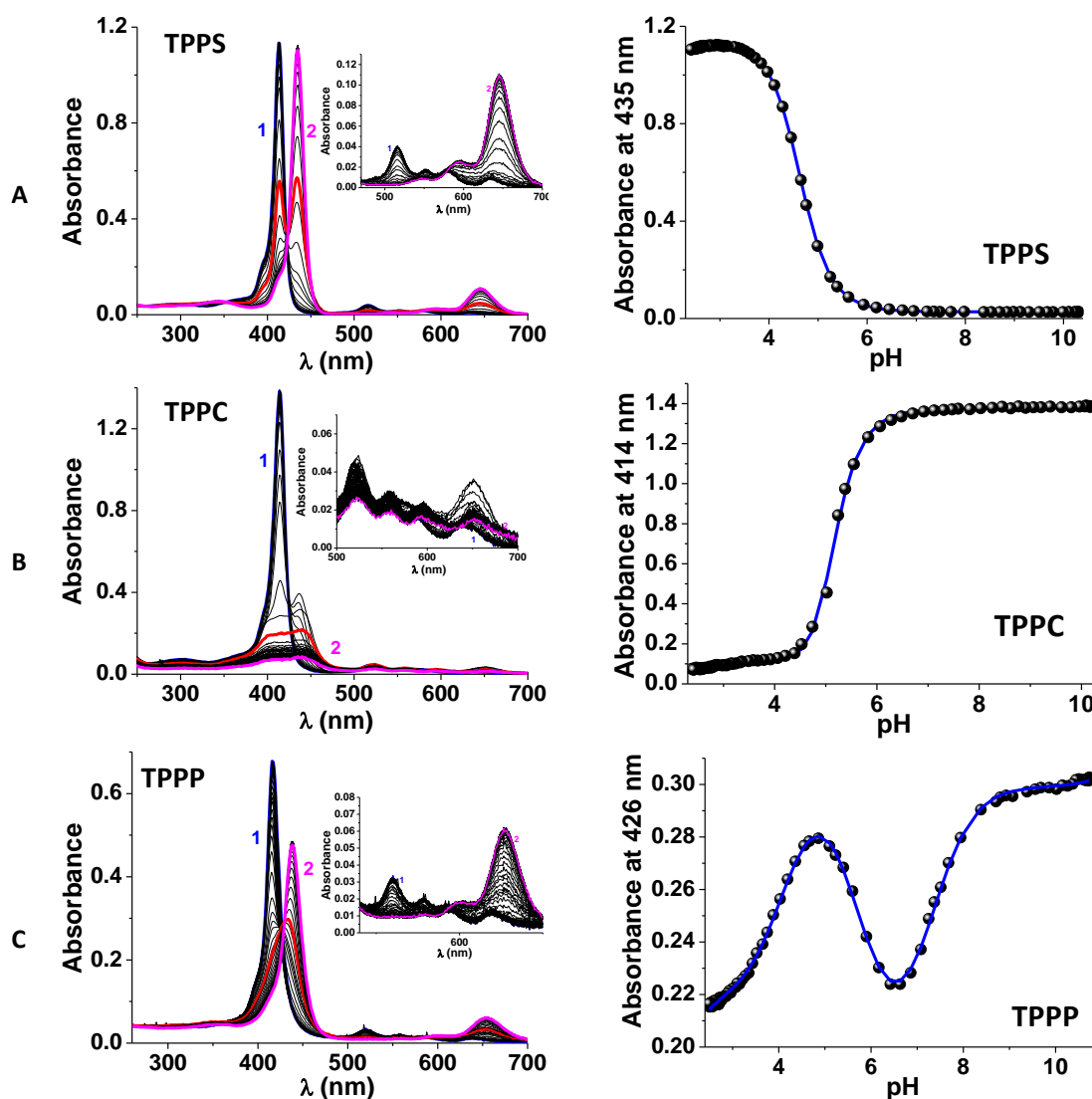


Figure 2 (left) UV-Visible absorption titrations versus pH of the free-base porphyrins and (right) corresponding absorbance variations of the Soret band as a function of pH (*i.e.*, the blue solid line corresponds to the theoretical curve from the Specfit program). (A) [**TPPS**]₀ = 3.50 × 10⁻⁶ M; (1) pH = 10.31; (2) pH = 2.41; **porphyrin**: pK_{a1} = 4.57 ± 0.02 and pK_{a2} = 4.66 ± 0.03. (B) [**TPPC**]₀ = 3.50 × 10⁻⁶ M; (1) pH = 10.29; (2) pH = 2.41; **porphyrin**: pK_{a1} = 4.5 ± 0.2 and pK_{a2} = 5.5 ± 0.3 & **benzoate**: pK_a* = 3.4 ± 0.3. (C) [**TPPP**]₀ = 3.50 × 10⁻⁶ M; l = 1 cm; (1) pH = 10.73; (2) pH = 2.49; **porphyrin**: pK_{a1} = 4.1 ± 0.2 and pK_{a2} = 5.7 ± 0.1 & **phosphonate**: pK_a* = 7.33 ± 0.07. Solvent: water; l = 0.1 NaCl; T = 25.0 ± 0.2°C, l = 1 cm. The spectra labelled in red correspond to the absorption data measured at pH ~ 4.5.

examined in water containing 0.1 M of NaCl as the supporting electrolyte. The absorption spectrophotometric titrations *versus* pH were first carried out by adding aliquots of HCl to a basic solution of the porphyrins to ensure appropriate solubilisation of these macrocycles in water. Figure 2A first depicts the absorption titration *versus* pH of **TPPS**. Under basic conditions, **TPPS** is characterized by a Soret band centred at 413 nm ($\epsilon^{413} = 3.23 \times 10^5 \text{ M}^{-1} \text{ cm}^{-1}$) and a set of four weak Q bands ranging from 500 nm to 700 nm. It is noteworthy that the spectroscopic properties measured by this approach might slightly differ from the preliminary absorption data (Table 1) because of the different experimental conditions and of the fact that these data were derived from the electronic absorption spectra of the pure species that were calculated using statistical methods.⁴¹⁻⁴⁶ Upon pH decrease, the Soret band gradually underwent a bathochromic shift to λ_{max} of 435 ($\epsilon^{435} = 3.28 \times 10^5 \text{ M}^{-1} \text{ cm}^{-1}$).

Concomitantly, the four Q bands were altered to two bands, the more intense being centred at 645 nm ($\epsilon^{645} = 3.22 \times 10^4 \text{ M}^{-1} \text{ cm}^{-1}$). This spectral variation is consistent with the successive protonations of two nitrogens of the tetrapyrrolic moiety. It has been indeed shown that the absorption spectrum of diprotonated porphyrin consist of two Q-bands in addition to a red-shifted Soret band due to the symmetry alteration induced by the protonation of the tetrapyrrolic core. The absorption and potentiometric data have been processed⁴¹⁻⁴⁶ and allowed evaluating the two corresponding pK_a values ($\text{pK}_{a1} = 4.57 \pm 0.02$ and $\text{pK}_{a2} = 4.66 \pm 0.03$ in 0.1 M NaCl, Table 2) that are in agreement with previously reported data ($\text{pK}_{a1} = 4.6$ and $\text{pK}_{a2} = 5.2$ in 0.1 M NaCl). By contrast with the preliminary spectrophotometric approach (*i.e.*, pH buffers were used, Figure 1), no additional absorption centred at 490 nm was observed under our conditions in agreement. This J_B absorption corresponds to J -aggregates (sharp band - denoted as J_B band - that is red-shifted by 56 nm with respect to the Soret B band at 435 nm of **[TPPS.2H]²⁺** monomer)⁴⁷ that is prevented under our experimental conditions. This process was reported to occur under acidic pH ($\text{pH} < 4$) following protonations of the tetrapyrrolic core.^{47,48} The diprotonated species of **TPPS** therefore exists in the form of a zwitterionic compound with the four peripheral sites being negatively charged and the tetrapyrrolic core being positively charged.⁴⁹ The absorption electronic spectra of the protonated species of **TPPS** are given in ESI, while the distribution diagrams of the **TPPS** protonated species are depicted in Figure 3. At pH 4-5, the three protonated species coexist. Following these results, we anticipate that **Zn-TPPS** mainly predominates as a tetra-anionic species in a broad range of pH given the fact that the porphyrinic nitrogens are involved in the Zn(II) coordination.

Figure 2B illustrates then the spectral variation experienced by **TPPC** upon pH decrease. Under basic conditions, the fully deprotonated species is characterized by an intense Soret band at 414 nm ($\epsilon^{414} = 3.93 \times 10^5 \text{ M}^{-1} \text{ cm}^{-1}$) and four weakly absorptive Q bands lying between 480 nm and 700 nm (see ESI). **TPPC** mainly exist as a monomeric form ($\sim 80\%$) under our experimental conditions (3.5 μM) as it was shown that **TPPC** could lead to dimer at neutral pH with a dimerisation constant of $4.55 \times 10^4 \text{ M}^{-1}$.⁵⁰ Up to $\text{pH} \sim 5$, a weak hypochromic shift (*i.e.*, protonation of the carboxylate functions) concomitant to a partial protonation of the porphyrinic core could be observed in agreement with the classical bathochromic shift of the

Soret band. When the pH was further decreased, the Soret band faded and a broad, split and weak absorption centred at ~ 430 nm appeared. This feature likely suggests that further acido-basic reactions of **TPPC** led to protonated species that underwent aggregation in water. It has been indeed shown⁴⁶ that for $1 < \text{pH} < 4.5$, the Soret band of **[TPPC.6H]²⁺** is split into two components at about 444 (with a shoulder at 439) and 404 nm and this was assigned to the formation of a dimeric species. In the same report,⁴⁶ the pK_a s of the carboxylic functions and of the tetrapyrrolic protonated units were estimated to be at about 5. Due to the precipitation that occurred below $\text{pH} \sim 5$, only the spectra recorded from basic pH values to $\text{pH} 5.2$ were processed. The processing of the data allowed evaluating two pK_a values. The lowest deprotonation constant determined under these conditions ($\text{pK}_{a1} = 4.1 \pm 0.4$) is proposed to be related to deprotonations of one of the nitrogens of the tetrapyrrolic core (*i.e.*, the first deprotonation of the tetrapyrrolic core was not accessible due to precipitation of **TPPC**), while the deprotonations of the four peripheral benzoate units are characterized by an apparent deprotonation constant ($\text{pK}_{a2} = 5.4 \pm 0.5$). The distribution diagrams of the **TPPC** protonated species are given in Figure 3 and suggest that the dimerization is likely induced by the protonation in a narrow pH window of the benzoate functions giving to the neutral species that dimerizes. These observations are in agreement with the preliminary absorption spectrophotometric investigation (Figure 1) as well as published results.^{46,50}

To go even further in this approach, we have recorded the spectral variations of an aqueous solution of **Zn-TPPC** as a function of pH (see ESI). Similarly to **TPPC**, the metallated porphyrin **Zn-TPPC** was solubilised under basic conditions. The fully deprotonated species (*i.e.*, benzoate functions) is characterized by an intense Soret band at 422 nm ($\epsilon^{422} = 3.32 \times 10^5 \text{ M}^{-1} \text{ cm}^{-1}$) as well as two Q bands at 557 nm ($\epsilon^{557} = 1.16 \times 10^4 \text{ M}^{-1} \text{ cm}^{-1}$) and 597 nm ($\epsilon^{597} = 5.93 \times 10^3 \text{ M}^{-1} \text{ cm}^{-1}$). Upon acidification, the absorption bands experienced a gradual hypochromic shift and then a significant alteration of the absorption characteristics (at $\sim \text{pH} 5$) as seen previously for **TPPC** in water (*vide supra*). This confirmed that protonation of the benzoate units led to a species that underwent self-interaction in water (*i.e.*, most likely dimerization on the basis of similar spectral features). The pK_a value provided as a mere estimate was found to be at about 4.8. This is in line with the previous observations (Figure 1).

We finally examined the acido-basic properties of **TPPP** in water (Figure 2C). As for the two previous free-base porphyrins (*vide supra*), the fully deprotonated species predominates under basic conditions (Soret band at 416 nm, $\epsilon^{416} = 1.92 \times 10^5 \text{ M}^{-1} \text{ cm}^{-1}$ and four Q bands lying between 480 nm and 700 nm). The gradual pH decrease first led to a hypochromic shift of the Soret band up to $\text{pH} \sim 7$ with no evidence of protonation of the tetrapyrrolic core. This likely suggests that the phosphonate groups are being protonated. From $\text{pH} \sim 7$ to ~ 2.5 , the Soret band then experienced a significant bathochromic shift in agreement with the protonations of two nitrogens of the porphyrinic unit. Under these experimental conditions ($2.49 < \text{pH} < 10.73$, Figure 2C), each of the phosphonate units most likely undergo monoprotonation (*i.e.*, $\text{RPO}_3^{2-} + \text{H}^+ \leftrightarrow \text{RPO}_3\text{H}^-$) as suggested from the data measured on phenylphosphonic acid ($\text{pK}_{a1} = 1.68$ and $\text{pK}_{a2} = 7.021$)⁵¹ or other derivatives such as

nitrilo-*tris*(methylenephosphonic acid) ($pK_a < 2$ in $\text{CH}_3\text{OH}/\text{H}_2\text{O}$ 80/20).⁵⁰ Full protonation of the phosphonate units thus likely occurs under very acidic conditions ($\text{pH} < 1$). The statistical processing of the spectral and potentiometric data sets allowed calculating three protonation constants. The tetrapyrrolic core is associated to two deprotonation constants ($pK_{a1} = 4.1 \pm 0.2$ and $pK_{a2} = 5.7 \pm 0.1$) that are in agreement with those determined for the other investigated free-base porphyrinic systems (*i.e.*, **TPPS** and **TPPC**, *vide supra*, Table 2). An apparent protonation constant was also evidenced for the four phosphonate groups ($pK_{a^*} = 7.33 \pm 0.07$). The absorption electronic spectra of the protonated species of **TPPP** are available in the ESI, while the distribution diagrams of these species are given in Figure 3. At pH 4.5, two main negatively charged species predominates,

namely **[TPPP.5H]³⁻** and **[TPPP.6H]²⁻**.

To get a deeper understanding of our homogenous series of porphyrins, their acido-basic properties were also assessed in a mixed solvent made of 80 % of methanol and 20 % of water (by weight) containing 0.1 M of *n*-tetrabutylammonium perchlorate as the supporting salt. It has been shown that the optimal solubilisation of **TPPS** or **TPPC** was achieved for aqueous solutions containing 80 % of methanol.⁴⁸ Under these conditions aggregation was prevented and only the porphyrin monomers predominate. The UV-Vis absorption spectra of **TPPS**, **TPPC**, **TPPP**, **Zn-TPPS** and **Zn-TPPC** were recorded over a large span of pH values starting from acidic conditions and are depicted in Figure 4.

Table 2 Physico-chemical data measured for **TPPC**, **TPPS**, **TPPP**, **Zn-TPPC** and **Zn-TPPS**.

	$pK_a \pm 3\sigma$		
	Nitrogens of the tetrapyrrolic core	Peripheral ionisable sites	Aggregation occurred?
TPPS (water) ^a	$pK_{a1} = 4.57 \pm 0.02$ $pK_{a2} = 4.66 \pm 0.03$	$pK_{a(\text{sulfonate})} \ll 2$	No
TPPS ($\text{CH}_3\text{OH}/\text{H}_2\text{O}$) ^b	$pK_{a1} = 2.3 \pm 0.2$ $pK_{a2} = 2.7 \pm 0.1$	$pK_{a(\text{sulfonate})} \ll 2$	No
Zn-TPPS ($\text{CH}_3\text{OH}/\text{H}_2\text{O}$) ^b	na	$pK_{a(\text{sulfonate})} \ll 2$	No
TPPC (water) ^a	$pK_{a1} < 4$ $pK_{a2} = 4.1 \pm 0.4$	$pK_{a(\text{benzoate})}^* = 5.4 \pm 0.4$	Yes (dimerization)
TPPC ($\text{CH}_3\text{OH}/\text{H}_2\text{O}$) ^b	$pK_{a1} = 2.1 \pm 0.4$ $pK_{a2} = 2.4 \pm 0.2$	$pK_{a(\text{benzoate})}^* = 5.8 \pm 0.2$	No
Zn-TPPC ($\text{CH}_3\text{OH}/\text{H}_2\text{O}$) ^b	na	$pK_{a(\text{benzoate})}^* = 7.1 \pm 0.1$	No
Zn-TPPC (water) ^a	na	$pK_{a(\text{benzoate})}^* \sim 4.8$	Yes (dimerization)
TPPP (water) ^a	$pK_{a1} = 4.1 \pm 0.2$ $pK_{a2} = 5.7 \pm 0.1$	$pK_{a(\text{phosphonate})}^* = 7.33 \pm 0.07$	No
TPPP ($\text{CH}_3\text{OH}/\text{H}_2\text{O}$) ^b	$pK_{a2} + pK_{a3} = 4.8 \pm 0.3$	$pK_{a1(\text{phosphonate})} \ll 2$ $pK_{a4(\text{phosphonate})} = 3.8 \pm 0.3$ $pK_{a5(\text{phosphonate})} = 5.7 \pm 0.2$ $pK_{a6(\text{phosphonate})} = 9.77 \pm 0.06$	No

^a water, 0.1 M NaCl; ^b $\text{CH}_3\text{OH}/\text{H}_2\text{O}$ 80/20 w/w, 0.1 *n*-NBu₄ClO₄; na = not applicable. $T = 25.0 \pm 0.2$ °C.

As mentioned above, the peripheral sulfonic groups of **TPPS** are strong acids and were consequently found to be deprotonated within the pH range considered (*i.e.*, $pK_a < 1$).⁴⁷ Under acidic pH ($\text{pH} \sim 2$), the absorption spectrum of **TPPS** is characterized by an intense Soret band centred at 436 nm ($\epsilon^{436} = 4.13 \times 10^5 \text{ M}^{-1} \text{ cm}^{-1}$) as well as an intense Q_i band at 648 nm ($\epsilon^{648} = 4.46 \times 10^4 \text{ M}^{-1} \text{ cm}^{-1}$). These spectrophotometric features are in agreement with those determined in water (*vide supra*) and are characteristics of a protonated **TPPS** species with the two nitrogens of the tetrapyrrolic core being involved. By contrast with the preliminary approach in water (Figure 1), no additional absorption was found at 490 nm (*i.e.*, characteristic of an *J*-aggregation phenomenon)⁵² thus indicating

that this solvent system (*i.e.*, $\text{CH}_3\text{OH}:\text{H}_2\text{O}$ 80/20 w/w, $l = 0.1 \text{ M } n\text{-NBu}_4\text{ClO}_4$) prevents aggregation and ensures efficient solubilisation of all the protonated **TPPS** species. The increase of the medium acidity to pH 4 led to deprotonation of the **TPPS** chromophoric unit as shown by the hypsochromic shifts of the Soret band to 416 nm ($\epsilon^{416} = 3.14 \times 10^5 \text{ M}^{-1} \text{ cm}^{-1}$) (Figure 4). Above pH 4-5 no further absorption spectral variation was observed (Figure 4) in agreement with the absence of any other acido-basic equilibria. The processing⁴¹⁻⁴⁵ of the spectrophotometric and potentiometric data sets led to the evaluation of two acidic pK_a ($pK_{a1} = 2.3 \pm 0.2$ and $pK_{a2} = 2.7 \pm 0.1$) values that are related to the nitrogen atoms of the porphyrin moiety (Table 2).

These values were found to be more than two order lower than those determined in pure water ($pK_{a1} = 4.57 \pm 0.02$ and $pK_{a2} = 4.66 \pm 0.03$) and reflect the differences of solvation and dielectric constants of the chosen solvents (water *versus* methanol/water). The electronic absorption spectra and the distribution diagrams of the protonated species of **TPPS** are depicted in ESI and emphasize the nature and the pH range of the predominating charged species under these experimental conditions. With respect to the metallated **Zn-TPPS** system, no absorption variation was observed over a large pH range (see ESI) thus demonstrating that the tetra-anionic **Zn-TPPS** species is the main protonated species within the pH range examined. This species is characterized by an intense Soret band centred at 424 nm ($\epsilon^{424} = 5.90 \times 10^5 \text{ M}^{-1} \text{ cm}^{-1}$) as well as two Q bands at 558 nm ($\epsilon^{558} = 2.08 \times 10^4 \text{ M}^{-1} \text{ cm}^{-1}$) and 598 nm ($\epsilon^{598} = 7.79 \times 10^3 \text{ M}^{-1} \text{ cm}^{-1}$) in agreement with literature data.⁵³ This feature confirmed our hypothesis that **Zn-TPPS** also predominates as a tetra-anionic species in water over a broad pH range.

The absorption and potentiometric titration of **TPPC** in $\text{CH}_3\text{OH}/\text{H}_2\text{O}$ (80/20 w/w) ($2.22 < \text{pH} < 11.65$) is shown in Figure 4. Similarly to **TPPS** under acidic conditions, the Soret band at 438 nm ($\epsilon^{438} = 3.26 \times 10^5 \text{ M}^{-1} \text{ cm}^{-1}$) is accompanied by a series of Q bands whose Q¹ is the more intense ($\lambda_{\text{max}}^{\text{Q}1} = 648 \text{ nm}$, $\epsilon^{648} = 3.08 \times 10^4 \text{ M}^{-1} \text{ cm}^{-1}$), thus demonstrating that the free-base porphyrin **TPPC** is protonated on its tetrapyrrolic moiety. As for **TPPS**, no aggregation was observed under acidic conditions. Significant hypsochromic shift of the Soret band and marked alterations of the Q bands shape took place on increasing the pH to 4-5 as already seen for **TPPS**. These spectral variations could be ascribed to the deprotonation of the tetrapyrrolic nitrogens ($pK_{a1} = 2.1 \pm 0.4$ and $pK_{a2} = 2.4 \pm 0.2$). As for **TPPS**, The pK_a

values measured in $\text{CH}_3\text{OH}/\text{H}_2\text{O}$ were found to be much lower than those measured in water herein ($pK_{a1} = 4.5 \pm 0.2$ and $pK_{a2} = 5.5 \pm 0.3$, Table 2). Above pH 5, the pH variation had a significant impact on the absorption properties of **TPPC** as seen in Figure 4. This feature was attributed to the deprotonation of the peripheral benzoate-like groups. The successive deprotonation constants of the four ionisable sites could not be separated and only an apparent deprotonation constant was determined ($pK_{a(\text{benzoate})}^* = 5.8 \pm 0.2$) in $\text{CH}_3\text{OH}/\text{H}_2\text{O}$ (80/20 w/w).^{54,55} The determined value was found to be in agreement with data obtained for benzoic acid in methanol/water mixtures ($pK_a = 5.98$ in $\text{CH}_3\text{OH}:\text{H}_2\text{O}$ 60/40 w/w, Table 2)⁵⁶ and is higher than that in water ($pK_a^* = 3.4 \pm 0.3$, Table 2). While **TPPS** was shown to be a negatively charged species over a large span of pH in $\text{CH}_3\text{OH}/\text{H}_2\text{O}$ (80/20 w/w), **TPPC** was found to be a versatile system existing predominantly as a positively charged species under acidic conditions, a neutral species from pH ~ 3 to ~ 6.5 and a negatively charged system above pH ~ 6.5 (see ESI).

For the metallated Zn(II) porphyrin **Zn-TPPC**, the absorption spectrophotometric titration *versus* pH did not evidenced significant spectral change over a large pH range (see ESI) by contrast to what was observed for its free-base porphyrin homologue **TPPC** (see ESI). **Zn-TPPC** is characterized by an intense Soret absorption lying at 425 nm ($\epsilon^{425} = 2.79 \times 10^5 \text{ M}^{-1} \text{ cm}^{-1}$) in agreement with reported data.⁵⁷ The increase of pH had a weak hypochromic effect on the Soret band (*i.e.*, as observed for the free-base porphyrin **TPPC**, see ESI) and was attributed to the deprotonation of the benzoic units ($pK_{a(\text{benzoate})}^* = 7.1 \pm 0.1$). We finally turned our attention on **TPPP** that displays four phosphonic acids as peripheral ionisable sites (Figure 4).

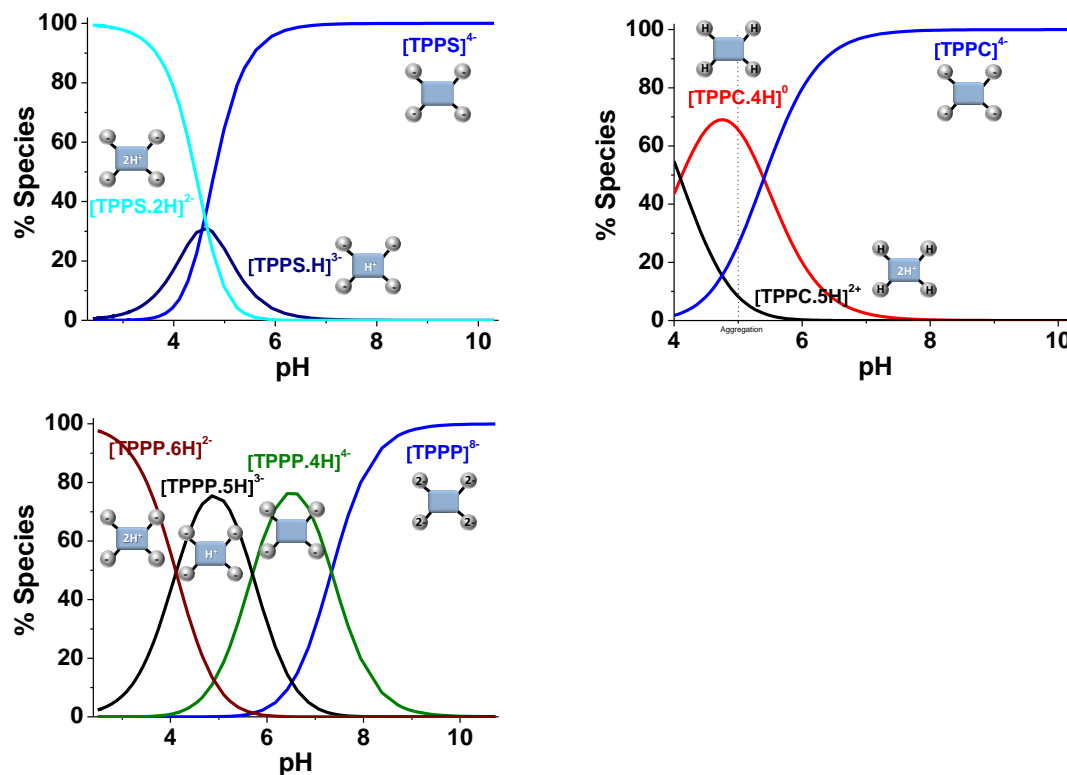


Figure 3 Distribution diagrams of the protonated species of the free-base porphyrins **TPPS**, **TPPC** and **TPPP**. Solvent: H_2O ; $I = 0.1 \text{ NaCl}$; $T = 25.0 \pm 0.2 \text{ }^\circ\text{C}$

Under acidic conditions, **TPPP** is characterized by an intense Soret band centred at 438 nm ($\epsilon^{438} = 1.0 \times 10^5 \text{ M}^{-1} \text{ cm}^{-1}$) and a set of two Q bands ($\lambda_{\text{max}} \text{ Q}^I = 651 \text{ nm}$, $\epsilon^{651} = 1.03 \times 10^4 \text{ M}^{-1} \text{ cm}^{-1}$) that clearly evidenced the diprotonated nature of a tetrapyrrolic core. Deprotonation of the porphyrinic core was easily monitored by the red-shift of the Soret band as well as the altered profile of the Q bands (*i.e.*, from two main absorptions to four bands upon deprotonation). A global acidic deprotonation constant was obtained ($\text{p}K_{\text{a}2} + \text{p}K_{\text{a}3} = 4.8 \pm 0.3$) and was found to be similar to those measured for **TPPS** ($\text{p}K_{\text{a}1} + \text{p}K_{\text{a}2} = 5.0$) and **TPPC** ($\text{p}K_{\text{a}1} + \text{p}K_{\text{a}2} = 4.5$) in $\text{CH}_3\text{OH}/\text{H}_2\text{O}$.

Further increase of the pH led to a hyperchromic shift of the Soret band (Figure 2) and was attributed to the stepwise deprotonation of the monoprotonated phosphonate units (*i.e.*, $\text{RPO}_3\text{H}^- \leftrightarrow \text{RPO}_3^{2-} + \text{H}^+$; $\text{p}K_{\text{a}4} = 3.8 \pm 0.3$, $\text{p}K_{\text{a}5} = 5.7 \pm 0.2$ and $\text{p}K_{\text{a}6} = 9.77 \pm 0.06$). The first deprotonation constant $\text{p}K_{\text{a}1}$ of the monoprotonated phosphonate units was estimated to be lower than 2 and could not be determined with good accuracy. The $\text{p}K_{\text{a}}$ separation of the phosphonate groups measured for **TPPP** was found to be in agreement with other polyphosphonated derivatives.⁵⁸ The distribution diagrams of the protonated species of **TPPP** is depicted in ESI.

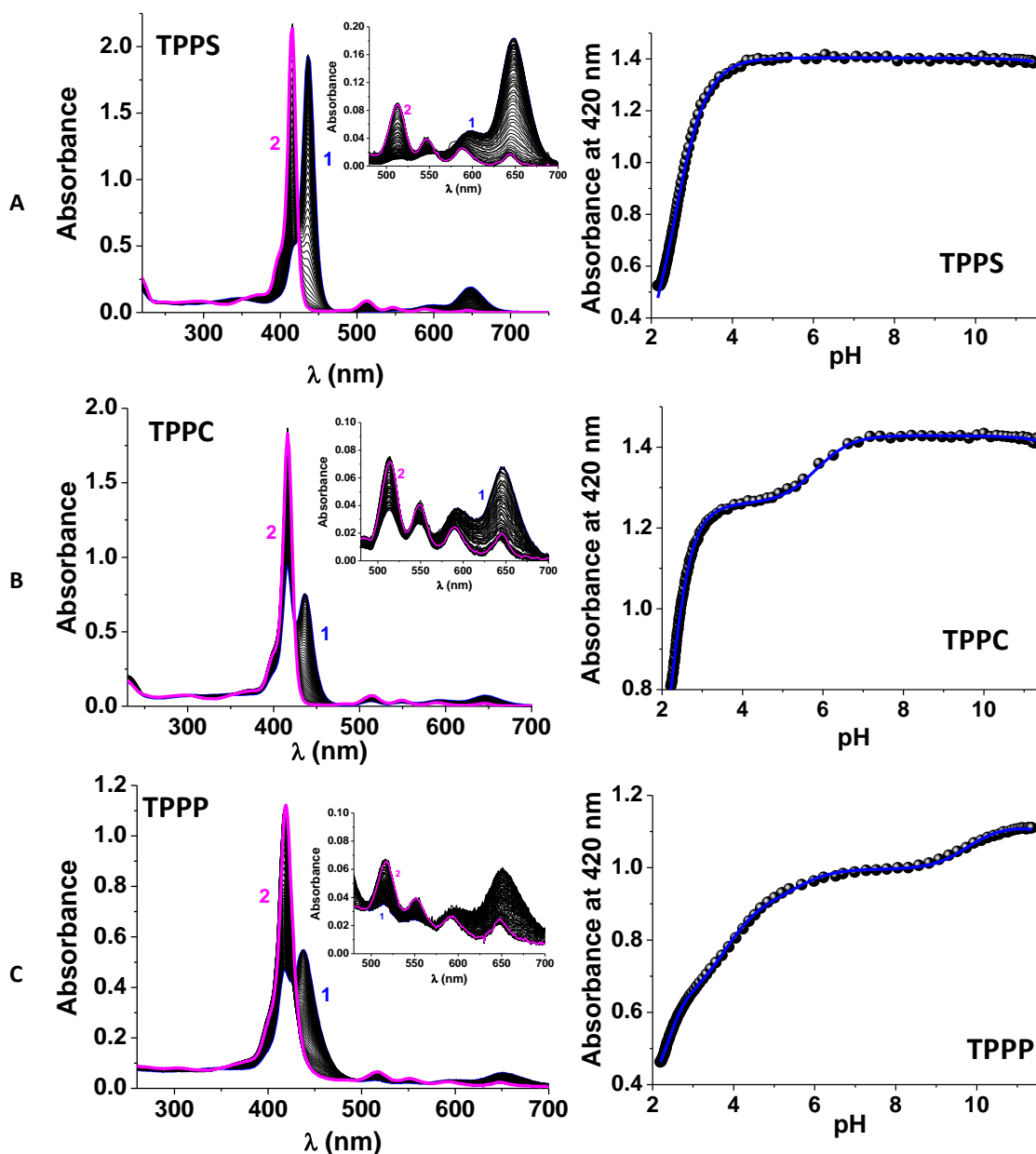


Figure 4 (left) UV-Visible absorption titrations *versus* pH of the free-base and zinc(II) porphyrins and (right) corresponding absorbance variations of the Soret band as a function of pH (*i.e.*, the blue solid line corresponds to the theoretical curve from the Specfit program). (A) **[TPPS]₀** = $7.18 \times 10^{-6} \text{ M}$; (1) pH = 2.16; (2) pH = 11.43; **porphyrin**: $\text{p}K_{\text{a}1} = 2.3 \pm 0.2$ and $\text{p}K_{\text{a}2} = 2.7 \pm 0.1$. (B) **[TPPC]₀** = $5.33 \times 10^{-6} \text{ M}$; (1) pH = 2.22; (2) pH = 11.65; **porphyrin**: $\text{p}K_{\text{a}1} = 2.1 \pm 0.4$ and $\text{p}K_{\text{a}2} = 2.4 \pm 0.2$ & **benzoate**: $\text{p}K_{\text{a}}^* = 5.8 \pm 0.2$. (C) **[TPPP]₀** = $6.90 \times 10^{-6} \text{ M}$; $l = 1 \text{ cm}$; (1) pH = 2.19; (2) pH = 11.36; **porphyrin**: $\text{p}K_{\text{a}2} + \text{p}K_{\text{a}3} = 4.8 \pm 0.3$ & **phosphonate**: $\text{p}K_{\text{a}1} < 2$, $\text{p}K_{\text{a}4} = 3.8 \pm 0.3$, $\text{p}K_{\text{a}5} = 5.7 \pm 0.2$, $\text{p}K_{\text{a}6} = 9.77 \pm 0.06$. Solvent: $\text{CH}_3\text{OH}/\text{H}_2\text{O}$ (80/20 by weight); $l = 0.1 \text{ n-NBu}_4\text{ClO}_4$; $T = 25.0 \pm 0.2^\circ\text{C}$, $l = 1 \text{ cm}$.

ROS production

To evaluate and compare the capacity of all studied porphyrins to generate ROS under light irradiation, Electron Paramagnetic Resonance (EPR) spectroscopy was used to detect the superoxide anion $O_2^{\cdot-}$ (produced after a photo-induced electron transfer, *i.e.* the so-called Type I process) and the singlet oxygen 1O_2 (produced through an energy transfer to dioxygen, *i.e.* the so-called Type II process), according to the method described by Riou *et al.*²⁸ As 1O_2 is non-radical and both 1O_2 and $O_2^{\cdot-}$ are short-lived species, experiments were performed in presence of specific scavengers (*e.g.* 2,2,6,6-tetramethyl-4-piperidone or TEMP, giving TEMPO in the presence of 1O_2 , and 5,5-dimethyl-1-pyrroline N-oxide, DMPO, giving DMPO-OOH in the presence of $O_2^{\cdot-}$). The results are summarized in Figure 5. No variation of the initial EPR signal was observed when the reaction mixture was measured without light irradiation or in the absence of a PS for both singlet oxygen and superoxide anion production monitoring. With respect to the singlet oxygen production, the metallated porphyrins herein investigated were immediately degraded, probably by 1O_2 itself, as depicted in Figure 5A. The same behaviour (*i.e.* degradation by singlet oxygen production) was already observed in our previous study for the metallated porphyrin investigated then (namely zinc(II) tetra-(*N*-methyl-pyridinium)-porphyrin tetrachloride) even if the degradation pattern was slower for this metalloporphyrin.²⁸ Concerning the free-base porphyrins, **TPPC** and **TPPS** were clearly shown to be more efficient in production of singlet oxygen than **TPPP**, although degradation was observed for **TPPC** after 20 minutes of accumulated irradiation.

Regarding $O_2^{\cdot-}$ production (Figure 5B), all compounds exhibited similar profiles, *i.e.* a rapid growth followed by a plateau (the most efficient being **TPPC**), except for **Zn-TPPS** which followed a quasi-linear progression. Interestingly, no correlation was noticed between ROS production and metalation state of the porphyrins. Indeed, if $O_2^{\cdot-}$ levels reached with **Zn-TPPC** were lower to those reached with **TPPC**, the opposite behaviour was observed for the **TPPS** series. As for 1O_2 production, **TPPP** was among the less efficient system.

However, all investigated compounds can generate ROS, by both type I and II processes for **TPPC**, **TPPS**, and **TPPP** and only by Type I process for **Zn-TPPC** and **Zn-TPPS**, the most efficient system being **TPPC**.

UV-Visible absorption properties in TBY-2 cells growth medium

As the growth medium for the TBY-2 cells, a modified Murashige and Skoog medium supplemented by 0.27 mg L⁻¹ of 2,4-dichlorophenoxyacetic acid and 10 mg mL⁻¹ of thiamine solutions was used.⁵⁹ Due to complexity of this medium, UV-Vis absorption spectra of all the investigated porphyrins were recorded in spent medium and compared to those obtained, at the same pH, in phosphate buffer (Figures 1 and 6). The value of pH was fixed at 4.5, the pH value of spent medium of growing cells⁶⁰ which were used in biological assay (*vide infra*). Hence, we believe it is the best way to mimic as faithfully as possible experimental conditions of biological assays. As one can see from Figure 6, no significant modification of the absorption profile with respect to the medium was observed for **Zn-TPPS** and **TPPP** whereas a hypochromic effect was noticed for **TPPS** when phosphate buffer was replaced by the growth medium. We supposed an effect of the complexity of the spent medium.⁶⁰ Altogether, these results and those obtained from the absorption spectrophotometric study (*vide supra*) evidenced that, as expected, in growth medium, **Zn-TPPS** predominates as a tetra anionic species ($[Zn-TPPS]^{4-}$), whereas **TPPP** likely exist under di-anionic or tri-anionic forms, the phosphonate groups being all mono-protonated and one ($[TPPP.5H]^{3-}$) or two nitrogens ($[TPPP.6H]^{2-}$) being protonated (Figure 3). The position of the Soret band and the presence of an intense Q band at about 650 nm strongly substantiate this hypothesis. In the case of **TPPS**, the species displaying protonated nitrogens (zwitterionic $[TPPS.H]^{3-}$ and $[TPPS.2H]^{2-}$ species) and the fully deprotonated tetra-anionic one ($[TPPS]^{4-}$) coexist at this pH as evidenced by the split Soret band (Figure 6). These observations are in excellent agreement with the data collected in this report (*i.e.*, these three species coexist in equivalent amounts, Figures 2 and 3).

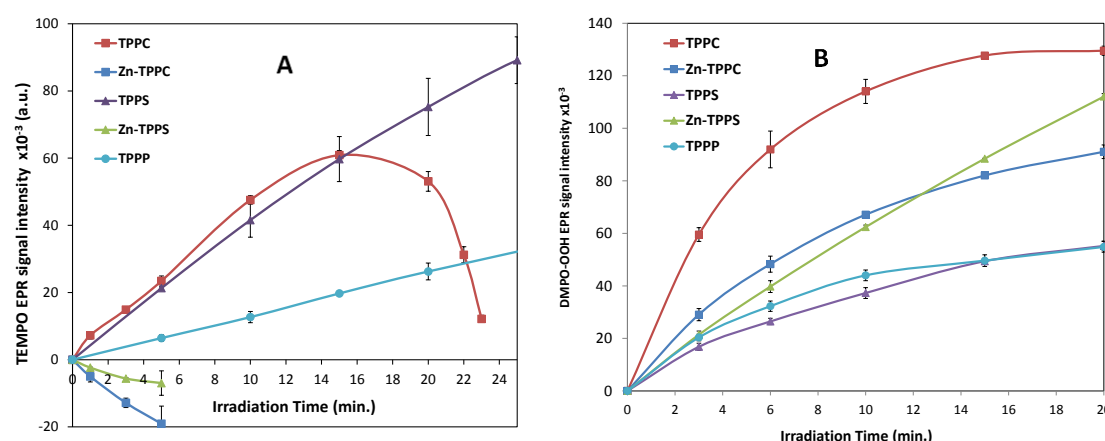


Figure 5 (A) EPR signal of TEMPO generation by irradiation of **TPPC**, **Zn-TPPC**, **TPPS**, **Zn-TPPS** and **TPPP**. ([TEMP] = 12.5 mM [Porphyrins] = 40 μ M in 0.01 M phosphate buffer, pH 7.4); (B) EPR signal of DMPO-OOH generated by irradiation of **TPPC**, **Zn-TPPC**, **TPPS**, **Zn-TPPS** and **TPPP**. ([DMPO] = 225 mMol [Porphyrins] = 50 μ M in DMSO). The irradiation was performed with white light (280 μ E.s⁻¹.m⁻² for experiments **A** and 70 μ E.s⁻¹.m⁻² for experiments **B**). The values represent the mean \pm S.D. obtained from 3 independent experiments (experiments were performed as described in ESI).

The behaviour of **TPPC** and **Zn-TPPC** depends more closely on the nature of the medium. It has been shown in the spectrophotometric approach conducted in water ($I = 0.1$ M NaCl) or in buffer that **Zn-TPPC** and **TPPC** might lead to dimerization at about pH 5 on protonation of the benzoate (*i.e.*, the neutral form likely dimerizes). This consequently led to significantly altered absorption spectra at pH 4.5 in the buffer solution. However, in the growth medium, the situation stands in an interesting contrast since no broad and split band that is characteristic of self-interaction could be seen. This would suggest that **TPPC** and **Zn-TPPC** mainly predominates as monomeric forms. For **TPPC**, protonation of the central nitrogen in the spent medium is negligible than in phosphate

buffer, as the intensity of the Q₁ band decreased and the B band is centred close to 415 nm. For **Zn-TPPC**, if the central protonation was not possible anymore, protonation of the carboxylic groups still occurred, even more than in phosphate buffer as evidenced by the disappearance of the Soret band at 423 nm (*i.e.*, specific of the non-protonated form, *vide supra*). The fact that the absorption of the Soret band is not markedly affected in the growth medium suggests that the neutral species ($[\text{Zn-TPPC.4H}]^0$) predominates and that subsequent dimerization is prevented. Table 3 summarizes the various acido-basic states that likely predominate for all compounds in spent medium at pH 4.5.

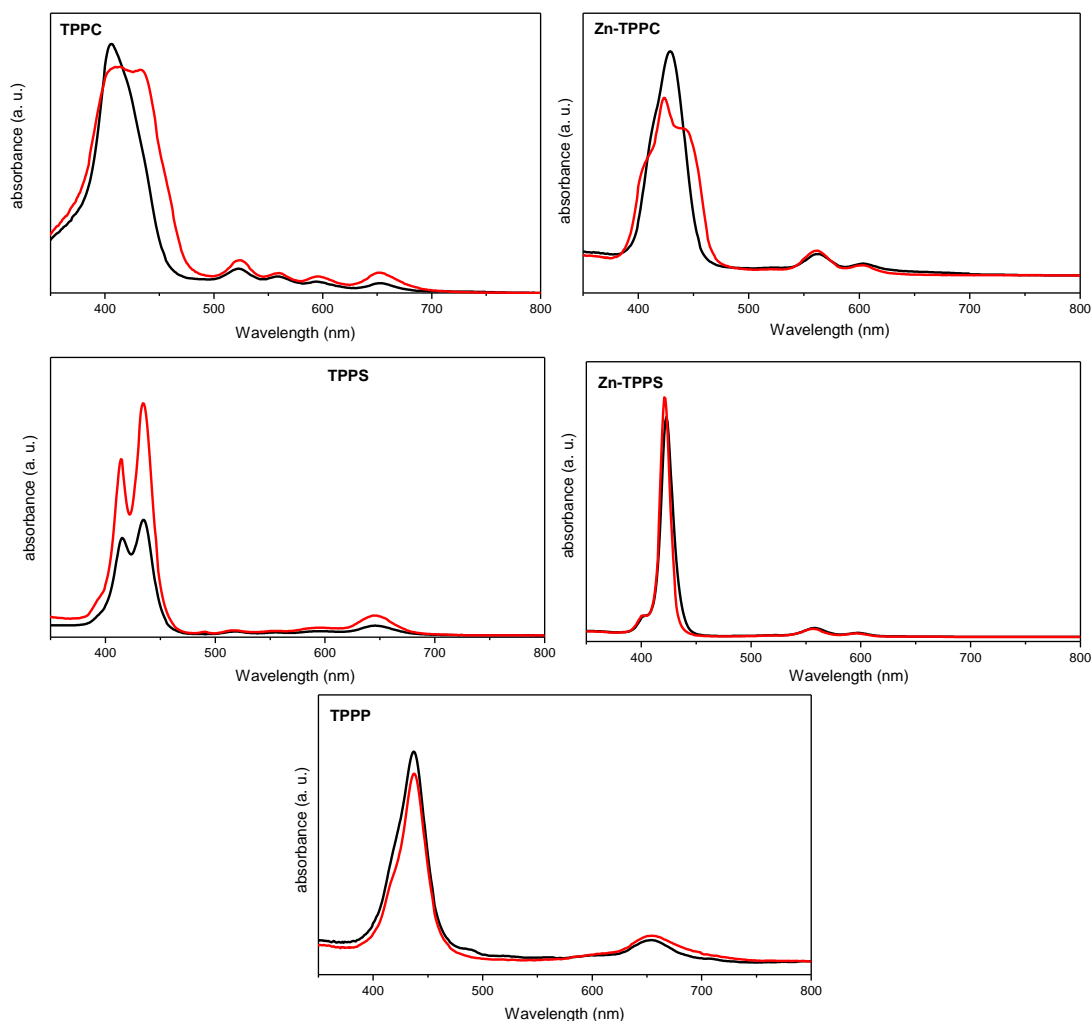


Figure 6 Effect of medium on porphyrin absorption spectra. Phosphate buffer in red; spent medium in black (298 K; pH = 4.5; [porphyrin] = 2 μ M).

Table 3 Main protonated forms of all compounds in the spent medium and phosphate buffer as deduced from their UV-Vis absorption profiles (298 K; pH = 4.5; value under bracket is the total charge of the compound).^a

		Fully anionic	Peripheral protonation	H ₂ -Porphyrin ²⁻	H-Porphyrin ³⁻	H-Porphyrin ⁺	Fully protonated
TPPC	phosphate buffer		X (Neutral)			X (+)	
	growth medium		X (Neutral)				
Zn-TPPC	phosphate buffer	X (4-)	X (Neutral)				
	growth medium	X (4-)	X (Neutral)				
TPPS	phosphate buffer	X (4-)		X (2-)	X (3-)		
	growth medium	X (4-)		X (2-)	X (3-)		
Zn-TPPS	phosphate buffer	X (4-)					
	growth medium	X (4-)					
TPPP	phosphate buffer			X (2-)	X (3-)		
	growth medium			X (2-)	X (3-)		

^a In the case of **TPPP**, only one protonation occurs on the phosphonate groups. **TPPP** still have 4 negative charges at the peripheral positions, not shown.

Photo-stability in TBY-2 cells growth medium

To check the photo-stability of these different porphyrins, and their capacity to reach the cells on the time scale of the experiment, their absorption spectra were recorded for different irradiation times under the same conditions (*i.e.* light, concentration) used for biological assay. The intensity of the Soret band was monitored as a function of irradiation time and allowed calculating a percentage of the non-degraded porphyrins. Indeed, except for **TPPP**, no other modification than the intensity of UV-Vis absorption spectra were

observed, thus indicating that **TPPC**, **TPPS** and their zinc counterpart did not undergo photo-transformation but only photo-bleaching. In the case of **TPPP**, the the λ_{max} of the Soret band oscillated between 427 and 434 nm (see ESI). This behaviour can be explained by the equilibrium, at this pH for two **TPPP protonated species**, namely the mono- and diprotonated on the central nitrogens (Figure 3). Hence, for this compound, the percentages were calculated for the maximum of absorption, whatever the wavelength, assuming that it will provide a good idea of the photo-stability of this compound. The results are summarized in Table 4.

Table 4 Photo-stability of **TPPC**, **TPPS**, **TPPP**, **Zn-TPPC**, **Zn-TPPS** in the growth medium (pH = 5.4, 298 K, 95 $\mu\text{E} \cdot \text{s}^{-1} \cdot \text{m}^{-2}$).^a

	T0	After 3h of dark incubation	1h under light	3h under light
TPPC (2 μM) ^b	100	54.08 \pm 7.85	18.02 \pm 4.82	7.95 \pm 6.67
TPPS (3.5 μM) ^b	100	94.89 \pm 0.76	89.25 \pm 1.94	84.07 \pm 3.52
TPPP (3.5 μM) ^b	100	94.29 \pm 1.34	64.98 \pm 4.84	39.57 \pm 6.02
Zn-TPPC (2 μM) ^c	100	70.46 \pm 11.99	10.41 \pm 0.58	4.10 \pm 1.52
Zn-TPPS (3.5 μM) ^c	100	97.00 \pm 1.50	48.60 \pm 0.50	11.90 \pm 1.40

^a Values were determined by monitoring the Soret band intensity at 416 nm for **TPPC**, 414 nm for **TPPS**, 423 nm for **Zn-TPPC** and 422 nm for **Zn-TPPS**. For **TPPP**, the maximum of absorption was recorded.

^b The value is the mean of at least 3 independent measurements.

^c The value is the mean of 2 independent measurements.

After dark incubation over 3h in the growth medium, we noticed a degradation of **TPPC** and its metallated counterpart (around 46 and 30 % respectively) whereas the others remained stable. As previously observed,²⁸ the metallated compounds are less stable than their free-base homologues. To sum up, the more stable were **TPPS** and **TPPP**, then **TPPC**, the metallated ones, **Zn-TPPS** and **Zn-TPPC**, being

the less stable species, especially **Zn-TPPC**, after one hour of light irradiation.

Biologic assays

In a previous work, we have shown that the anionic porphyrin **TPPS** was the most efficient to induce TBY-2 cell death compared to a

cationic one.²⁸ To get further insight into the importance of the nature of the anionic groups, we monitored the viability of TBY-2 cells after incubation and irradiation with the investigated porphyrins. For that purpose, TBY-2 cells were isolated at exponential growing phase, incubated with the different porphyrins for 3 hours under dark conditions, washed to eliminate the excess of porphyrins in the spent medium and placed under illumination (around 95 $\mu\text{E} \cdot \text{s}^{-1} \cdot \text{m}^{-2}$) for 3 hours.^{28,60} Cell viability was determined after treatment and a 20h incubation under dark. None of the porphyrins was cytotoxic under dark conditions as shown by comparison with control experiment realized with water instead of porphyrins (Figure 7).

When tested at 2 μM , **TPPC** and **Zn-TPPC** were the most efficient to induce cell death (around 70 and 50 % respectively) compared to **TPPP** and **TPPS**. Indeed, **TPPS** must be tested at 3.5 μM to reach the same percentage of cell death than **TPPC** whereas, even at this concentration, **TPPP** was poorly efficient. This behaviour is somewhat surprising since **TPPC** and **Zn-TPPC** were found to be less photo-stable in the growth medium than **TPPS** and **TPPP** (Table 3). This biological assay, in addition to the EPR data, are in favour in a type I reaction for the production of ROS (*i.e.*, by electron transfer to lead to formation of superoxide anion). On one hand, **Zn-TPPC** was indeed the most efficient cell death inducer but exhibited a very poor $^1\text{O}_2$ production (Figure 5). Conversely, **TPPS** as **TPPC** displayed very good and comparable $^1\text{O}_2$ generation levels whereas **TPPS** induced less cell death. On the other hand, **TPPS** exhibited low superoxide anion production whereas **TPPC** was the best producer. Whatever, the difference in ROS production is not sufficient to explain the whole biological assays results and the hypothesis of a favoured type I

mechanism compared to type II has to be confirmed by studies of the response to oxidative stress in cells. Moreover, in regard to their acido-basic forms (Table 3), it also appears that their efficiency was intimately linked to the charges carried by both the peripheral ionisable sites and central nitrogens as shown by **TPPC** that is neutral in the cell culture while **TPPS** and **TPPP** were found to be anionic. Further experiments with water soluble neutral porphyrins have to be performed to confirm this hypothesis.

Conclusions

With respect to biological application such as APDT, our work on anionic porphyrins efficiency and behaviour pointed out the importance of the combined factors such as photostability, ROS generation but also environment that played a critical role on their acido-basic properties. Indeed, although all those parameters make the study of these molecules in a complex medium and with biological material quite difficult to monitor, especially under light, it however allowed getting a better understanding of structure-activity relationships. Altogether, despite a low stability under dark conditions, our results demonstrated that **TPPC** was the best cell killer of the investigated porphyrins series. In addition, its low stability makes it a powerful and eco-friendly pesticide with a high degree of degradation.

Acknowledgements

We thank the French National Research Agency (ANR Porphy-Plant) for financial support and the Centre National de la Recherche

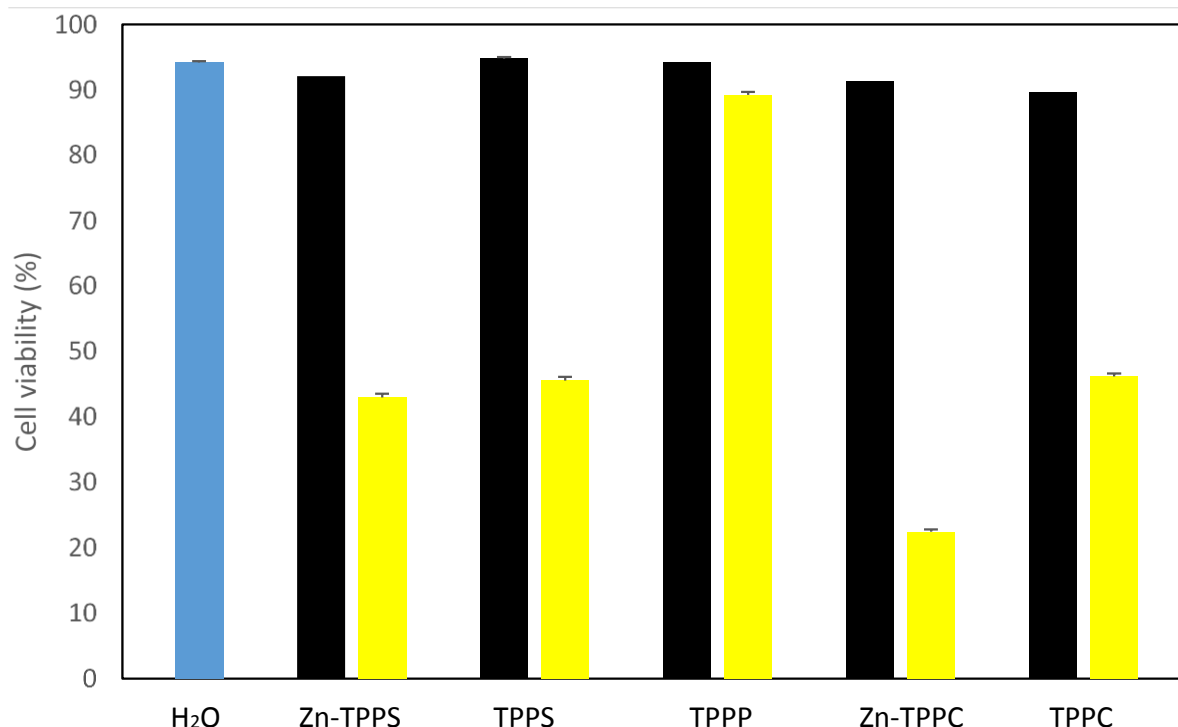


Figure 7 TBY-2 cell viability in response to photo-activated anionic porphyrins under dark conditions (black) and after 3 hours of illumination (yellow). **TPPS**, **Zn-TPPS** and **TPPP** were tested at 3.5 μM ; **TPPC** and **Zn-TPPC** were tested at 2 μM . H₂O corresponds to the control of experiments without porphyrins (same results under dark and irradiation). Results are the mean \pm sem of 3 independent experiments.

Scientifique (CNRS) and the University of Strasbourg (LIMA UMR 7042). We also want to warmly thank Pr. F. Fages for his advices and for having suggested this fruitful collaboration.

Note and references

- 1 K. M. Kadish, *The Porphyrin Handbook: Synthesis and organic chemistry*, Elsevier, 2000.
- 2 D. Mauzerall, in *Photosynthesis I*, eds. P. D. A. Trebst and P. D. M. Avron, Springer Berlin Heidelberg, 1977, pp. 117–124.
- 3 M. Danquah, Review of Handbook of Porphyrin Science with Application to Chemistry, Physics, Materials Science, Engineering, Biology and Medicine. Volume 40: Nanoorganization of Porphyrinoids, *J. Nat. Prod.*, 2017, **80**, 1232–1232.
- 4 S. Hiroto, Y. Miyake and H. Shinokubo, Synthesis and Functionalization of Porphyrins through Organometallic Methodologies, *Chem. Rev.*, 2017, **117**, 2910–3043.
- 5 M. O. Senge, Stirring the porphyrin alphabet soup—functionalization reactions for porphyrins, *Chem. Commun.*, 2011, **47**, 1943–1960.
- 6 A. R. Antonangelo, K. C. M. Westrup, L. A. Burt, C. Grazia Bezzu, T. Malewschik, G. S. Machado, F. S. Nunes, N. B. McKeown and S. Nakagaki, Synthesis, crystallographic characterization and homogeneous catalytic activity of novel unsymmetric porphyrins, *RSC Adv.*, 2017, **7**, 50610–50618.
- 7 Ö. Birel, S. Nadeem and H. Duman, Porphyrin-Based Dye-Sensitized Solar Cells (DSSCs): a Review, *J. Fluoresc.*, 2017, **27**, 1075–1085.
- 8 M. Jurow, A. E. Schuckman, J. D. Batteas and C. M. Drain, Porphyrins as Molecular Electronic Components of Functional Devices, *Coord. Chem. Rev.*, 2010, **254**, 2297–2310.
- 9 S. Lin, C. S. Diercks, Y.-B. Zhang, N. Kornienko, E. M. Nichols, Y. Zhao, A. R. Paris, D. Kim, P. Yang, O. M. Yaghi and C. J. Chang, Covalent organic frameworks comprising cobalt porphyrins for catalytic CO₂ reduction in water, *Science*, 2015, **349**, 1208–1213.
- 10 J. Barona-Castaño, C. Carmona-Vargas, T. Brocksom and K. de Oliveira, Porphyrins as Catalysts in Scalable Organic Reactions, *Molecules*, 2016, **21**, 310.
- 11 W.-B. Huang, W. Gu, H.-X. Huang, J.-B. Wang, W.-X. Shen, Y.-Y. Lv and J. Shen, A porphyrin-based fluorescent probe for optical detection of toxic Cd²⁺ ion in aqueous solution and living cells, *Dyes Pigments*, 2017, **143**, 427–435.
- 12 H. Huang, W. Song, J. Rieffel and J. F. Lovell, Emerging applications of porphyrins in photomedicine, *Front. Phys.*, , DOI:10.3389/fphy.2015.00023.
- 13 H. Kato, Y. Kato, R. Yoneyama, R. Ishikawa, M. Kojika, K. Miyajima, N. Takizawa and K. Furukawa, Review of PDT for lung cancer and future, *Photodiagnosis Photodyn. Ther.*, 2017, **17**, A30–A31.
- 14 M. Q. Almerie, G. Gossedge, K. E. Wright and D. G. Jayne, Photodynamic Therapy Use for Peritoneal Carcinomatosis: Systematic Review, *Photodiagnosis Photodyn. Ther.*
- 15 S. Pei, A. C. Inamadar, K. A. Adya and M. M. Tsoukas, Light-based therapies in acne treatment, *Indian Dermatol. Online J.*, 2015, **6**, 145–157.
- 16 E. Alves, M. A. F. Faustino, M. G. P. M. S. Neves, Â. Cunha, H. Nadais and A. Almeida, Potential applications of porphyrins in photodynamic inactivation beyond the medical scope, *J. Photochem. Photobiol. C Photochem. Rev.*, 2015, **22**, 34–57.
- 17 T. Ben Amor and G. Jori, Sunlight-activated insecticides: historical background and mechanisms of phototoxic activity, *Insect Biochem. Mol. Biol.*, 2000, **30**, 915–925.
- 18 C. Fabris, M. Soncin, G. Jori, A. Habluetzel, L. Lucantoni, S. Sawadogo, L. Guidolin and O. Coppellotti, Effects of a new photoactivatable cationic porphyrin on ciliated protozoa and branchiopod crustaceans, potential components of freshwater ecosystems polluted by pathogenic agents and their vectors, *Photochem. Photobiol. Sci. Off. J. Eur. Photochem. Assoc. Eur. Soc. Photobiol.*, 2012, **11**, 294–301.
- 19 O. Coppellotti, C. Fabris, M. Soncin, M. Magaraggia, M. Camerin, G. Jori and L. Guidolin, Porphyrin photosensitized processes in the prevention and treatment of water-and vector-borne diseases, *Curr. Med. Chem.*, 2012, **19**, 808–819.
- 20 A. Stallivieri, F. L. Guern, R. Vanderesse, E. Meledje, G. Jori, C. Frochot and S. Acherar, Synthesis and photophysical properties of the photoactivatable cationic porphyrin 5-(4-N-dodecylpyridyl)-10,15,20-tri(4-N-methylpyridyl)-21H,23H-porphyrin tetraiodide for anti-malaria PDT, *Photochem. Photobiol. Sci.*, 2015, **14**, 1290–1295.
- 21 E. T. Carrera, H. B. Dias, S. C. T. Corbi, R. A. C. Marcantonio, A. C. A. Bernardi, V. S. Bagnato, M. R. Hamblin and A. N. S. Rastelli, The application of antimicrobial photodynamic therapy (aPDT) in dentistry: a critical review, *Laser Phys.*, , DOI:10.1088/1054-660X/26/12/123001.
- 22 F. Le Guern, V. Sol, C. Ouk, P. Arnoux, C. Frochot and T.-S. Ouk, Enhanced Photobactericidal and Targeting Properties of a Cationic Porphyrin following the Attachment of Polymyxin B, *Bioconjug. Chem.*, 2017, **28**, 2493–2506.
- 23 G. B. Kharkwal, S. K. Sharma, Y.-Y. Huang, T. Dai and M. R. Hamblin, Photodynamic Therapy for Infections: Clinical Applications, *Lasers Surg. Med.*, 2011, **43**, 755–767.
- 24 Y. LIANG, L.-M. LU, Y. CHEN and Y.-K. LIN, Photodynamic therapy as an antifungal treatment, *Exp. Ther. Med.*, 2016, **12**, 23–27.
- 25 J. C. Gonzales, G. T. P. Brancini, G. B. Rodrigues, G. J. Silva-Junior, L. Bachmann, M. Wainwright and G. Ú. L. Braga, Photodynamic inactivation of conidia of the fungus *Colletotrichum abscissum* on Citrus sinensis plants with methylene blue under solar radiation, *J. Photochem. Photobiol. B*, 2017, **176**, 54–61.
- 26 L. Fracarolli, G. B. Rodrigues, A. C. Pereira, N. S. Massola Júnior, G. José Silva-Junior, L. Bachmann, M. Wainwright, J. Kenupp Bastos, G.U.L. Braga, Inactivation of plant-pathogenic fungus *Colletotrichum acutatum* with natural plant-produced photosensitizers under solar radiation, *Journal of Photochemistry & Photobiology, B: Biology*, 2016, **162**, 402-411..
- 27 D. Guillaumot, M. Issawi, A. Da Silva, S. Leroy-Lhez, V. Sol, C. Riou, Synergistic enhancement of tolerance mechanisms in response to photoactivation of cationic tetra (N-methylpyridyl) porphyrins in tomato plantlets, *Journal of Photochemistry and Photobiology, B, Biology*, 2016, **156**, 69-78.
- 28 C. Riou, C. A. Calliste, A. Da Silva, D. Guillaumot, O. Rezazgui, V. Sol and S. Leroy-Lhez, Anionic porphyrin as a new powerful cell death inducer of Tobacco Bright Yellow-2 cells, *Photochem. Photobiol. Sci.*, 2014, **13**, 621.

- 29 M. Issawi, D. Guillaumot, V. Sol, C. Riou, Responses of an adventitious fast-growing plant to photodynamic stress: comparative study of anionic and cationic porphyrin effect on *Arabidopsis thaliana*, *Physiologia Plantarum*, 2018, **162**, 379–390.
- 30 C. A. Rebeiz, A. Montazer-Zouhoor, H. J. Hopen and S. M. Wu, Photodynamic herbicides: 1. Concept and phenomenology, *Enzyme Microb. Technol.*, 1984, **6**, 390–396.
- 31 C. A. Rebeiz, K. N. Reddy, U. B. Nandihalli and J. Velu, Tetrapyrrole-Dependent Photodynamic Herbicides, *Photochem. Photobiol.*, 1990, **52**, 1099–1117.
- 32 S. O. Duke, J. Lydon, J. M. Becerril and T. D. Sherman, Weed Science Society of America, *Weed Sci.*, 1991, **39**, 465–473.
- 33 A. Villanueva, M. J. Hazen and J. C. Stockert, Photodynamic effect of the porphyrin derivative meso-tetra (4-N-methylpyridyl) porphine on sister chromatid exchanges in meristematic cells, *Experientia*, 1986, **42**, 1269–1271.
- 34 A. Villanueva, M. Cañete and M. J. Hazen, Uptake and DNA photodamage induced in plant cells in vivo by two cationic porphyrins, *Mutagenesis*, 1989, **4**, 157–159.
- 35 F. Odobel, E. Blart, M. Lagrée, M. Villieras, H. Boujtita, N. E. Murr, S. Caramori and C. A. Bignozzi, Porphyrin dyes for TiO₂ sensitization, *J. Mater. Chem.*, 2003, **13**, 502–510.
- 36 J. V. Hollingsworth, A. J. Richard, M. G. H. Vicente and P. S. Russo, Characterization of the self-assembly of meso-tetra(4-sulfonatophenyl)porphyrin (H₂)TPPS(4-) in aqueous solutions, *Biomacromolecules*, 2012, **13**, 60–72.
- 37 A. B. Ormond and H. S. Freeman, Effects of substituents on the photophysical properties of symmetrical porphyrins, *Dyes Pigments*, 2013, **96**, 440–448.
- 38 L. D. Freedman and G. O. Doak, The Preparation And Properties Of Phosphonic Acids, *Chem. Rev.*, 1957, **57**, 479–523.
- 39 J. R. Weinkauff, S. W. Cooper, A. Schweiger and C. C. Wamser, Substituent and Solvent Effects on the Hyperporphyrin Spectra of Diprotonated Tetraphenylporphyrins, *J. Phys. Chem. A*, 2003, **107**, 3486–3496.
- 40 V. S. Bhat and A. K. Srivastava, Ionic Conductivity in Binary Solvent Mixtures. 5. Behavior of Selected 1:1 Electrolytes in Ethylene Carbonate + Water at 25 °C, *J. Chem. Eng. Data*, 2001, **46**, 1215–1221.
- 41 R. A. Binsteadt and A. D. Zuberbühler, *SPECFIT: A program for global least squares fitting of equilibrium and kinetics systems using factor analysis and Marquardt minimisation*, Chapel Hill, NC, USA, 1998.
- 42 H. Gampp, M. Maeder, C. J. Meyer and A. D. Zuberbühler, Calculation of equilibrium constants from multiwavelength spectroscopic data—I: Mathematical considerations, *Talanta*, 1985, **32**, 95–101.
- 43 H. Gampp, M. Maeder, C. J. Meyer and A. D. Zuberbühler, Calculation of equilibrium constants from multiwavelength spectroscopic data—II, *Talanta*, 1985, **32**, 257–264.
- 44 H. Gampp, M. Maeder, C. J. Meyer and A. D. Zuberbühler, Calculation of equilibrium constants from multiwavelength spectroscopic data—IV: Model-free least-squares refinement by use of evolving factor analysis, *Talanta*, 1986, **33**, 943–951.
- 45 D. Marquardt, An Algorithm for Least-Squares Estimation of Nonlinear Parameters, *J. Soc. Ind. Appl. Math.*, 1963, **11**, 431–441.
- 46 M. Maeder and A. D. Zuberbühler, Nonlinear least-squares fitting of multivariate absorption data, *Anal. Chem.*, 1990, **62**, 2220–2224.
- 47 R. F. Pasternack, P. R. Huber, P. Boyd, G. Engasser, L. Francesconi, E. Gibbs, P. Fasella, G. Cerio Venturo and L. deC. Hinds, Aggregation of meso-substituted water-soluble porphyrins, *J. Am. Chem. Soc.*, 1972, **94**, 4511–4517.
- 48 J. Sobczyński, H. H. Tønnesen and S. Kristensen, Influence of aqueous media properties on aggregation and solubility of four structurally related meso-porphyrin photosensitizers evaluated by spectrophotometric measurements, *Pharm.*, 2013, **68**, 100–109.
- 49 M. Y. Choi, J. A. Pollard, M. A. Webb and J. L. McHale, Counterion-Dependent Excitonic Spectra of Tetra(p-carboxyphenyl)porphyrin Aggregates in Acidic Aqueous Solution, *J. Am. Chem. Soc.*, 2003, **125**, 810–820.
- 50 B. Spiess, E. Harraka, D. Wencker and P. Laugel, Complexing properties of nitrilotri(methylenephosphonic) acid with various transition and heavy metals in a 10:90 ethanol—water medium, *Polyhedron*, 1987, **6**, 1247–1249.
- 51 M. Wozniak and G. Nowogrocki, Phosphonate complexes. Part 6. Influence of steric effects, solvation, and chelation on stability, *J. Chem. Soc. Dalton Trans.*, 1981, **0**, 2423–2428.
- 52 D.-M. Chen, T. He, D.-F. Cong, Y.-H. Zhang and F.-C. Liu, Resonance Raman Spectra and Excited-State Structure of Aggregated Tetrakis(4-sulfonatophenyl)porphyrin Diacid, *J. Phys. Chem. A*, 2001, **105**, 3981–3988.
- 53 P. Neta, One-electron transfer reactions involving zinc and cobalt porphyrins in aqueous solutions, *J. Phys. Chem.*, 1981, **85**, 3678–3684.
- 54 H. N. Po and N. M. Senozan, The Henderson-Hasselbalch Equation: Its History and Limitations, *J. Chem. Educ.*, 2001, **78**, 1499.
- 55 J. Reijenga, A. van Hoof, A. van Loon and B. Teunissen, Development of Methods for the Determination of pK_a Values, *Anal. Chem. Insights*, 2013, **8**, 53–71.
- 56 J. Chatt and A. A. Williams, The nature of the co-ordinate link. Part IX. The dissociation constants of the acids p-R₃M-C₆H₄-CO₂H (M = C, Si, Ge, and Sn and R = Me and Et) and the relative strengths of σ - π -bonding in the M–Car bond, *J. Chem. Soc. Resumed*, 1954, **0**, 4403–4411.
- 57 J. Rochford, D. Chu, A. Hagfeldt and E. Galoppini, Tetrachelate Porphyrin Chromophores for Metal Oxide Semiconductor Sensitization: Effect of the Spacer Length and Anchoring Group Position, *J. Am. Chem. Soc.*, 2007, **129**, 4655–4665.
- 58 S. Abada, A. Lecointre, I. Déchamps-Olivier, C. Platas-Iglesias, C. Christine, M. Elhabiri and L. Charbonniere, Highly stable acyclic bifunctional chelator for ⁶⁴Cu PET imaging, *Radiochim. Acta Int. J. Chem. Asp. Nucl. Sci. Technol.*, 2011, **99**, 663–678.
- 59 T. Murashige and F. Skoog, A Revised Medium for Rapid Growth and Bio Assays with Tobacco Tissue Cultures, *Physiol. Plant.*, 1962, **15**, 473–497.
- 60 M. Issawi, M. Muhieddine, C. Girard, V. Sol and C. Riou, Unexpected features of exponentially growing Tobacco Bright

Journal Name

ARTICLE

Yellow-2 cell suspension culture in relation to excreted extracellular polysaccharides and cell wall composition, *Glycoconj. J.*, 2017, **34**, 585–590.

PUBLICATION 6: “Crossing the first threshold: New insights in the influence of chemical structure of anionic porphyrins from cell wall interactions to photodynamic cell death induction in TBY-2 suspension culture” (in preparation for submission to The Plant Journal)

Crossing the first threshold: New insights in the influence of chemical structure of anionic porphyrins from cell wall interactions to photodynamic cell death induction in TBY-2 suspension culture.

Mohammad Issawi, Stephanie Leroy-Lhez, Vincent Sol and Catherine Riou*

Laboratoire Peirene EA7500, avenue Albert Thomas, 87060 Limoges Cedex

*Corresponding author

Abstract (233 words)

In this study, our fundamental research interest was to understand how negatively charged porphyrins could be able to interact with plant cell wall and further act inside cells. Thus, three anionic porphyrins differing by their anionic external groups (carboxylates, sulfonates and phosphonates) were tested. Firstly, tobacco cell wall was isolated to monitor *in vitro* its interactions with the three different anionic porphyrins. Unexpectedly, these negatively charged molecules were able to bind to negatively charged cell wall probably by weak bounds such as H bonds and/or electrostatic interactions when tetrapyrrolic core was protonated. Moreover, we showed that, at the pH of spent cell culture medium (4.5), the neutrality of the carboxylated porphyrin (TPPC) facilitated its cell wall crossing while the diffusion of the two other sulfonated (TPPS) or phosphonated (TPPP) porphyrins that remained anionic was delayed. Once inside TBY-2 cells, TPPC induced higher production of both H₂O₂ and MDA compared to TPPS after illumination. That result was in good correlation to a strong cell death induction by photoactivated TPPC. Furthermore, ROS scavenging enzymes such as catalase, peroxidases and superoxide dismutase were also strongly down modulated in response to TPPC before 1 hour illumination while these enzymes were almost unchanged in response to photoactivated TPPS. To our knowledge, this is the first study that took in account the whole story from interactions of porphyrins with plant cell wall to their photodynamic activity inside the cells.

Abbreviations: APDT: antimicrobial photodynamic treatment; PDT: photodynamic therapy; PS; photosensitizer, ROS; reactive oxygen species, TPPC: tetrakis-carboxyphenyl porphyrin; TPPS: tetrakis-sulfonatophenyl porphyrin; TPPP: tetrakis-phosphonatopheny porphyrin

Introduction

In the past decade, photodynamic strategy as a powerful tool to kill harmful cells or organisms such as bacteria, fungi and cancer cells was intensively reported (Hamblin 2016). Whole process depends on the use of key molecules called photosensitizers (PS) that could be excited by light and subsequently interacts with other molecules such as molecular oxygen and/or biological substrates resulting in the generation of highly toxic reactive oxygen species (ROS) that lead to death.

Photodynamic treatment (PDT) was firstly developed against cancer and in various medical fields such as ophthalmology, odontology and dermatology (Babilas and Szeimies 2010, Rishi and Agarwal 2015). PDT was also used in order to inactivate microorganisms such as bacteria, yeast and fungi, the so-called photodynamic inactivation (PDI) or APDT for antimicrobial photodynamic treatment especially as a new tool against multidrug resistant microorganisms (Huang *et al.*, 2010). APDT applications were investigated from medicine domain to agriculture, water disinfection and food decontamination (Alves *et al.*, 2010).

Until now, cationic PS were described as the most efficient PS to induce cell death. Nevertheless, in a lesser extent, negatively charged PS were also able to induce cell death excepted on Gram negative bacteria (George *et al.*, 2009). Meanwhile, it was shown that anionic PS, when tested in combination with cell wall disrupting agents like EDTA, CaCl₂, polymyxin B, were really efficient to kill Gram negative bacteria (Le Guern *et al.*, 2017). The resistance of Gram negative bacteria to anionic PS was probably due to the structure of their cell wall that has an impermeable outer membrane surrounding a peptidoglycan layer inside which is located the plasma membrane whereas Gram positive bacteria have a thick porous permeable cell wall (Annex 1, Annex 2, Maisch *et al.*, 2004). Nevertheless, George *et al.*, (2009) pointed out the mechanism of uptake of anionic and cationic PS by Gram positive or Gram negative bacteria that possess negatively charged cell walls owing to the presence of teichoic acid residues and lipopolysaccharides in their cell wall, respectively. PS could cross easily the Gram positive cell wall through electrostatic interactions and protein transporters while cationic PS are taken up by Gram negative bacteria through self-promoted uptake . Furthermore, other factors such as PS charge distribution and amphiphilicity must be taken in consideration in PS and bacteria cell wall interactions (Reddi *et al.*, 2002, Kessel *et al.*, 2003, Lazerri *et al.*, 2004, Demidova *et al.*, 2005, Simoes *et al.*, 2005, Banfi *et al.*, 2006).

Fungi cell wall that is mostly composed of glucan-chitin complex and mannoproteins could be considered as an intermediate in term of permeability between Gram positive and Gram negative bacteria suggesting that fungi will be difficult to photoinactivate with anionic PS (Annex 1, Annex 2, Lipke and Ovalle 1998, Kashef *et al.*, 2017). Nevertheless, it is still unclear how the binding and uptake of PS in fungi occur. Several studies reported that the porphyrins cannot be uptaken by yeast and the photodynamic inactivation of fungal cells was mediated by unbound PS that are present in the extracellular medium (Bertolini *et al.*, 1987, 1989, Donnelly *et al.*, 2008). Other study showed that cationic, anionic or neutral porphyrins are able to bind and inactivate candida and saccharomyces yeasts (Oriel and Nitzan 2012, Moghnie *et al.*, 2017).

Studies on PS and insect cells have been also conducted. These cells have an outermost layer, called envelop, which is rich in neutral lipids, esterified fatty acids and proteins, and surround cuticle harboring fibrillar chitin. Investigations showed that PS were able to photoinactivate insects such as pest flies, anopheles, culex and aedes larvae (Ben Amor and Jori 2000, Lucantoni *et al.*, 2011, Moussian 2013, De Souza *et al.*, 2017). It was mediated by cationic PS like methylene blue and di-cis N-methyl pyridyl porphyrins and anionic PS like rose Bengal and hematoporphyrin but it was more pronounced using amphiphilic PS (Fairbrother *et al.*, 1981, Ben Amor and Jori 2000). Moreover, PS accumulate in the cuticle, midgut and malphigian tubes insects (Lucantoni *et al.*, 2011).

Only few studies focused on photodynamic inactivation of phototrophic organisms like green algae surrounding by a wall rich in cellulose, xyloglucan and negatively charged polymeric matrix (sulfated carbohydrates) or cyanobacteria (Synytsya *et al.*, 2015). Both organisms were significantly more sensitive to cationic PS like positively charged corrole-based PS, methylene blue, than anionic ones like nuclear fast red, negatively charged corrole-based PS, sulfonated phtalocyanine, sulfonated porphyrine, this being probably due to the unfavored interaction between anionic PS and phototrophic cells (McCullagh and Robertson 2006, Drabkova *et al.*, 2007, Pohl *et al.*, 2015). However, there is no direct investigation on interactions and binding of PS to phototrophic microorganisms or plant cell walls.

Only few studies on leaves, root cells or cell lines with exogenous natural or synthetic PS supply were reported (Annex 3, for review Issawi *et al.*, 2018, submitted). Orange tree leaves and flowers and kiwi leaves were not affected by either natural/synthetic photosensitizers whereas strawberry leaves were significantly damaged (De Menezes *et al.*, 2014a,b, Fracarolli *et*

al., 2016, Gonzales *et al.*, 2017, Jesus *et al.*, 2018, Issawi *et al.*, 2018 submitted). In previous work, we studied the effect of exogenous water-soluble cationic and anionic porphyrins on tomato and on *Arabidopsis thaliana* plantlets. Thus, we showed that anionic porphyrins did not inhibit growth even tested at high concentration (50 μ M) (Guillaumot, *et al.*, 2016, Issawi *et al.*, 2018). Intriguingly and in contrary, we demonstrated that anionic porphyrins were greatly more efficient to induce TBY-2 plant cell death compared to cationic ones (Riou *et al.*, 2014). Therefore, we focused our attention on the structure-activity relationship of anionic porphyrins that differ in the meso-substituted groups namely sulfonates (TPPS), carboxylates (TPPC) and phosphonates (TPPP) and their ability to induce TBY-2 photodynamic cell death.

Material and methods

Porphyrins

5,10,15,20-tetrakis(carboxyphenyl) porphyrin (TPPC) was purchased from Frontier Scientific (Carnforth, United Kingdom). 5,10,15,20-tetrakis(4-sulfonatophenyl) porphyrin TPPS as tetra ammonium salt and 5,10,15,20-tetrakis(4-phosphonatophenyl) porphyrin TPPP were purchased from PorphyChem (Dijon, France). Stock solutions (1mM) of porphyrins were prepared by dissolving the necessary mass of porphyrin in 300 μ L of 1 M NaOH for TPPC and directly in water for TPPP and TPPS.

A special phosphate buffer (0.1 M, pH 4.5) was prepared by mixing K_2HPO_4 in deionized water and addition of H_3PO_4 according to Hollingsworth *et al.*, 2012. The pH variation as a function of H_3PO_4 addition was monitoring with a Mettler Toledo Five EasyTM FE20 pH-meter.

TBY-2, suspension culture

TBY-2 cells were cultured according to Issawi *et al.*, 2017. The spent medium corresponds to the native medium (pH 4.5) of growing cells at the beginning of the exponential phase (3 and 4-day old cells). The new medium corresponds to a freshly prepared medium (pH 5.4 after autoclaving).

Cell wall interactions with porphyrins

TBY-2 cell wall was isolated as described in Issawi *et al.*, 2017. 2.5 mg of isolated and lyophilized cell wall was stirred 24h in 0.1M phosphate buffer at pH = 4.5. Porphyrin solution was then added to reach a final concentration of 2 μ M. Cell wall and porphyrin solution was stirred for 3h under dark conditions and then centrifuged at 4500 rpm for 5 min at room

temperature. Supernatant was discarded. 5 mL of phosphate buffer (pH 4.5) was added to the pellet and solution was centrifuged again. This was performed twice. Supernatants were used to evaluate the quantity of free porphyrin not retained by the cell wall. Deionized water (5 mL) and 10 μ L of 1 M NaOH were added to the pellet (final pH 6.4). This solution was stirred 1h under dark and then centrifuged at 4500 rpm for 5 min at room temperature. Supernatant was discarded. Deionized water (5 mL) and 10 μ L of 1 M NaOH were added to the pellet and the solution was stirred overnight under dark conditions and then centrifuged at 4500 rpm for 5 min at room temperature. Supernatant was removed. 5 mL of water was added to the pellet and solution was centrifuged again. This was done twice. Supernatants were used to evaluate the quantity of porphyrin initially retained by the wall but released at this pH value. Pellet was suspended in 2.5 mL of water in order to check that all porphyrin was released. Concentration of porphyrin was monitored by UV-visible absorption. UV-vis spectra were recorded on a Specord 210 (Analytik Jena) double-beam spectrophotometer equipped with a Peltier temperature-controlled cell holder (air-cooled, Analytika Jena).

Confocal microscope analysis

Four day-old TBY-2 cells were incubated with porphyrins for 3 hours under dark, rinsed 3 times with new TBY-2 culture medium before observations under a Zeiss confocal microscope LSM510META. For spectral acquisition, samples were excited at 405 nm and fluorescence peak was followed at around 640 nm for the three porphyrins. For observation and pictures, we performed both spectral and mode acquisitions.

H₂O₂ quantification and lipid peroxidation assays

The H₂O₂ production and MDA generation that was associated to lipid peroxidation were quantified as described in Guillaumot *et al.*, 2016 and Issawi *et al.*, 2018.

Determination of proline content

Proline content was assayed according to Issawi *et al.*, 2018

Ascorbate (ASH/DHA), glutathione (GSH/GSSG) and pyridine nucleotide (NADPH/NADP⁺) assays

All assays were conducted by adapting microplate to Eppendorf tube protocol according to Noctor *et al.*, 2007. Redox states were calculated according to Locato *et al.*, 2015 as reduced forms/reduced forms + oxidized forms.

Enzymatic assays

Guaiacol and ascorbate peroxidases (GPOX and APX), catalase (CAT) and superoxide dismutase (SOD) enzymatic specific activities were determined as described in Guillaumot *et al.*, 2016 and Issawi *et al.*, 2018. Dehydroascorbate reductase (DHAR) and glutathione reductase (GR) activities were monitored according to Murik *et al.*, 2013.

Determination of caspase-like (CLK) protease activities

CLK-1 and CLK-3 activities were measured according to Mlejnek and Procházka 2002 with modifications. TBY-2 cells were ground in nitrogen liquid and homogenized in caspase buffer containing 50 mM HEPES pH7.2, 1 mM EDTA, 0.2% CHAPS, 5 mM DTT, and proteinase inhibitor cocktail for 15 min at 4 °C. Lysates were centrifuged for 45 min, 18000 rpm and then filtered through a nitrocellulose filter, pore size 0.2 µm. Clarified lysates were mixed with 1 ml of caspase assay buffer pH7.2 containing 50 mM PIPES-KOH, 5 mM EGTA, 2 mM MgCl₂, 5 mM DTT and reactions were initiated by adding a specific substrate (100 µM). Samples were incubated 1 h at 30 °C before reading the fluorescence by spectrofluorimeter at appropriate excitation and emission wavelengths (380 nm and 445 nm respectively). Acetyl-Tyr-Val-Ala-Asp-aminomethylcoumarin (Ac-YVAD-AMC) and acetyl-Asp-Glu-Val-Asp-aminomethylcoumarin (Ac-DEVD-AMC) served as substrates for CLK-1 and CLK-3 proteases, respectively. A no specific residual substrate cleavage was determined in the presence of 100 µM Ac-YVAD-CHO (for CLK-1) or 100 µM Ac-DEVD-CHO (for CLK-3) and was subtracted from every measured value of activity. Ac-YVAD-AMC, Ac-DEVD-CHO and Ac-DEVD-AMC were purchased from Sigma-Aldrich (France) and Ac-YVAD-CHO from VWR

DNA fragmentation

DNA isolation from 500 µl of treated or control TBY-2 cells was performed following manufacturer's advice (Nexttec™, Hilgertshausen, Germany). DNA was resuspended in 80 µL of H₂O and kept overnight at 4°C. 40 µL of aqueous DNA was tested on 1.8 % agarose gel (50 V, 8 h migration).

Statistical analysis

All biological experiments were performed at least three times independently. Results were expressed as mean ± SD (Standard Deviation). Data were analyzed by *t*-student test and one-way ANOVA using the PAST free software. Mean values were expressed as 100% in comparison to dark condition as reference excepted for ascorbate, glutathione and NADP that have conjugate species.

Results

I-Cytotoxicity of anionic porphyrins in TBY-2 cells

As the first step of our study and because it was also described in literature for cationic porphyrins, we decided to test the cytotoxicity of the three porphyrins of interest at high concentration. No significant effect on TBY-2 cell was observed for TPPC and TPPP and only a low cytotoxic or genotoxic effect was determined for TPPS (Fig.1). Thus, we concluded that further effect that we will be able to show after irradiation, will only depend on their ability to be photo-activated and produce deleterious ROS in TBY-2 cells.

II-Photoactivated TPPC is the most efficient to induce TBY-2 cell death

Upon 3 h light exposure, TPPC tested at 2 μ M and TPPS at 3.5 μ M strongly induced TBY-2 cell death (around 60 % cell death) whereas TPPP, even tested at 10 μ M, weakly did it (around 20 %) (Fig. 2). This result was unexpected because TPPC was unstable under dark conditions and further photo-degraded and/or photo-bleached whereas the two other porphyrins were more stable even under light conditions (Leroy-Lhez *et al.*, 2018, submitted). As the three porphyrins are anionic and share the same tetrapyrrolic cycle (Fig 9), we hypothesized that their differential power as plant cell death inducer depends on four relevant factors that could act alone or in combination : medium composition, interaction with plant cell wall and its crossing, ROS production (singlet oxygen and superoxide anion or H₂O₂). Furthermore, Leroy-Lhez (2018) showed that, following the pH of the medium (water, methanol/water, phosphate buffer, growth or spent TBY-2 medium), the three porphyrins presented differential charge pattern as shown in Fig.9. Therefore, this factor (charge pattern) must be also considered but must be related to the interaction with plant cell wall. Moreover, Issawi *et al.*, 2017 described a complex composition of spent medium of TBY-2 cells compared to the new one. Indeed, TPPC was even more efficient to induce cell death in new medium than in spent medium (Fig.2). We supposed that a putative interaction with secreted molecules such as polysaccharides could prevent TPPC interaction with cell wall making it less efficient (Fig.2). Nevertheless, this explanation did not work for TPPP and TPPS that did not display any difference as cell death inducer in the new medium (Fig.2). Fortunately, our result relative to cell death induction in presence of TPPC and TPPS were well correlated to previous study that showed that TPPC and TPPS were the most efficient to produce ROS compared to TPPP (Leroy-Lhez *et al.*, 2018). In addition, TPPC was mainly observed within cell wall of TBY-2 cells with a spotty pattern whereas TPPS and TPPP

localizations were very diffuse and weak (Fig. 3). *In situ* localizations could explain the difference as death inducer between the three porphyrins. Nevertheless, based only on this experiment, it was quite difficult to understand the difference in cell death induction between TPPS and TPPP. Moreover, while TPPP did not strongly trigger cell death even at 10 μ M it was shown that TPPP was also able to produce ROS (Fig.2, Leroy-Lhez *et al.*, 2018). Thus, we supposed that as a first step to enlarge our understanding, plant cell wall interaction with the three different porphyrins should be a key factor to explore.

III- Relationship between chemical structure of anionic porphyrin and cell wall

To gain insight into relative efficiency of anionic porphyrins to induce TBY-2 cell death (Fig.2, 3), we monitored to work on isolated cell wall in presence of porphyrins. We showed that porphyrins interacted differentially with TBY-2 isolated cell wall basing on their chemical structure (Fig. 4). After 3h incubation of TBY-2 cell wall with porphyrins at pH 4.5, we observed a strong retention of the three anionic porphyrins by the cell wall, TPPS being the most retained (100%) whereas TPPP showed the lowest interactions (92% and 77% respectively). This result partially supported our hypothesis suggesting that TPPP was not able to firmly interact and/or cross cell wall as also shown in Fig. 3. In contrary TPPS tightly interacted with plant cell wall and thus should take longer time to cross it. Moreover, in all case, the increase of the pH value above 6 brought about the release of all trapped porphyrins. Finally, while TPPS strongly interacted with cell wall, TPPC was spared from its trapping and cross it very rapidly (Fig. 4). TPPC was fully uncharged at the tested pH (Fig. 9). This result suggested that neutrality assisted the crossing of plant cell wall. The two other porphyrins took more time owing to electrostatic interactions. According to our result and surprisingly, we showed that in a negatively charged plant cell wall, anionic porphyrins were able to bind and cross it despite negative charges.

IV- Porphyrin Photoactivation consequences into TBY-2 cells

1) Photoactivated TPPS and TPPC induce a huge oxidative burst in TBY-2 cells

For further investigations concerning oxidative stress we gave up TPPP because its inefficiency to induce cell death under light (Fig. 2). TPPS and TPPC at 3.5 μ M and 2 μ M respectively, after photo activation into cells, induced an excessive oxidative stress. Thus, we measured the amount of the most stable ROS, namely H₂O₂ and showed that its level increased significantly over 3 h illumination (Fig 5A). In parallel, the quantity of MDA that is the final product of bio-membrane lipid peroxidation increased markedly under 3 h illumination (Fig 5B). Proline as a stress marker

showed a higher amount in cells treated with both porphyrins (Fig 5C). H₂O₂ production, MDA generation and proline were more pronounced in TBY-2 cells treated with TPPC than with TPPS that was in good correlation with cell death induction (Fig.2).

2) Antioxidant enzymes activities were inhibited in TBY-2 cells subjected to photodynamic stress

Different patterns of antioxidant enzymes inhibition were shown in TBY-2 cells treated with photoactivated porphyrins. TPPS at 3.5 μM induce an inactivation of APX whereas GPOX and SOD were not changed. The increase in CAT activity during 1 h illumination indicated that CAT is possibly acting in the dismutation of the excess H₂O₂ (Fig 6A). However, TPPC at 2 μM triggered complete inhibition of the enzymatic machinery with exception of CAT activity that remained constant (Fig 6B).

3) The redox hub was altered in TBY-2 cells undergoing photodynamic treatment

Photodynamic stress induced fluctuations in the level of the components of ascorbate-glutathione cycle over illumination time. TBY-2 cells treated with 3.5 μM TPPS showed decrease in ASH and DHA contents whereas they remained nearly unchanged in cells treated with 2 μM TPPC (Fig 7 A). In fact, over 2h illumination, a significant decrease in ascorbate redox state for TPPC treated cells was observed due to an increase in DHA relative to ASH (from 0.71 to 0.59, data not shown). While GSH amount was quite constant in TPPS-treated cells, it decreased significantly in TBY-2 cells treated with TPPC (Fig. 7 B). The oxidized form of glutathione (GSSG) content remained very low in TBY-2 cells after TPPS and TPPC photoexcitation leading to a perfect stabilization of glutathione redox state (0.99) (Fig 7 B). Pyridine nucleotide phosphate quantification showed a 4 fold increase in NADP⁺ content in cells treated with TPPC and a lower increase for TPPS since NADPH level in response to both porphyrins slightly decreased (Fig 7). In response to TPPS, ascorbate recycling enzyme DHAR activity was inhibited and GR clearly up regulated after 1h light exposure (Fig. 7D). In response to TPPC and by comparison to TPPS situation, DHAR and GR were differentially regulated leading to a significant decrease in GR activity after 1 hour treatment (Fig. 7D). Remarkably DHAR remained constant explaining why total ascorbate remained also constant (Fig. 7A,D). This suggested that cells were not able to defend themselves after this point under TPPC phototreatment in agreement to TPPC high efficiency to induce cell death (Fig.2).

TPPS and TPPC photoactivation induce apoptosis-like cell death in TBY-2 cells

TBY-2 cells undergoing photodynamic stress presented membrane shrinkage which is a hallmark of apoptosis (Fig 8A). To gain insight into the type of cell death mediated by photoactivated porphyrins in TBY-2 cells, we assayed caspase-like activities and DNA fragmentation. We showed that CLK-1 and CLK-3 activities were significantly involved in the mediation of cell death in TBY-2 cells treated with both porphyrins. CLK-1 and CLK-3 activities increased around 2-fold excepted CLK-3 in TPPC-treated cells which increased three times in comparison to control cells incubated in dark conditions (Fig 8 A and B). In addition, genomic DNA fragmentation assay showed low-molecular-weight internucleosomal DNA degradation in fragments of nearly 250 bp (Fig 8 C).

Discussion

In this study, we covered mechanisms that occurred in TBY2 cells upon anionic porphyrin treatment from cell wall interactions to photodynamic responses and cell death. Basing on previous studies that outlined the efficacy of photoactivated anionic porphyrins over cationic ones to kill TBY-2 cells, we tested three different anionic porphyrins differing by their external groups that bear negative charges (carboxylates, sulfonates and phosphonates) (Riou *et al.*, 2014; Leroy-Lhez *et al.*, 2018, submitted). Furthermore, in Leroy-Lhez *et al.*, (2018), we determined and predicted accurately the global charge of these PS that interact with cells at the beginning of exponential phase at acidic pH (4.5) of spent medium (Annex 4).

As we wanted to be exhaustive regarding cellular mechanisms that occurred from outside to inside of TBY-2 cells upon photodynamic treatment, the first step was to decipher how such complex molecules interact with cell wall polysaccharides and consequently are able to cross it. TBY-2 cell line is quite a very special cell suspension with a high growth rate and only primary cell wall. In a previous work following growth rate curve, TBY-2 cell wall composition and its corresponding spent medium were established and showed that the spent medium (pH and composition) varied in function to cell suspension age (Issawi *et al.*, 2017). We monitored all our experiments with TBY-2 cells isolated at the beginning of exponential growth phase (3 or 4 days after dilution) when spent medium is at pH 4.5. Plant primary cell wall is an extremely complex structure in which cellulose and hemicellulose network is embedded in a matrix of pectic polysaccharides with a protein set. Plant primary cell wall architecture has been widely studied

for fundamental knowledge while studies on chemical interaction (drugs, herbicides, growth factors) with plant cell wall, are still very difficult to access *in situ* (Caffal and Mohnen 2009, Chen et al 2010, Jarvis 2011, Liu et al 2013, Martinez-Sanz et al 2015). In our case, the emission of fluorescence properties of TPPC, TPPS and TPPP ($\lambda_{em} = ca. 640 \text{ nm}$), allows to follow them with confocal microscope coupled to spectrophotometer. Nevertheless, the *in situ* result that we described in this paper was not sufficient to understand their cell wall interaction and crossing. Thus, we performed an *in vitro* experiment with isolated TBY-2 pectin-rich cell wall and anionic porphyrins. Until now, two modes of porphyrin-sugar recognition were analyzed. The first involved covalent linkage between boronic acid-conjugated porphyrins and saccharides and the second mode was based on coordination bonding and non-covalent interactions including H bonds, electrostatic, and hydrophobic interactions (Kralova et al 2014). Here, we pointed out that TPPC and TPPS showed perfect binding to the cell wall whereas TPPP had weaker retention pattern at the same concentration (2 μM). Furthermore, according to our biological results on TBY-2 cell death in response to photoactivated porphyrins, we supposed that TPPC rapidly got inside the cells than TPPS. According to Leroy-Lhez *et al.*, 2018, external carboxylic acid groups were protonated at pH 4.5 in spent medium, leading to a neutral TPPC while TPPS remained totally anionic with one or two positive charges on the central nitrogens of porphyrin unit and 4 anions charge on the side groups (Fig 9). Therefore, three species of TPPS co-existed in spent medium. Thus, we supposed that TPPC formed H bonds with pectin carboxyl groups whereas TPPS established two types of chemical bounds represented by electrostatic interaction between positively charged tetrapyrrolic core and anionic pectin-rich wall in addition to sulfonate H acceptor groups. This could also explain why TPPC cell wall crossing was faster than TPPS that remained longer time in cell wall. TPPP did not strongly interact with TBY-2 cell wall. For the same reason as TPPS, it should stay longer time in cell wall compartment. Furthermore, two species of TPPP coexisted as tri-anionic or di-anionic due to core protonation suggesting a strong electrostatic interaction that delayed its crossing as TPPS. Moreover, as TPPP and TPPS are very similar in term of molecular weight (around 1000 Da) greater than TPPC (around 791 Da), a potential steric hindrance could also explain this delay. Thus, to explain the difference between TPPP and TPPS, the strongest ROS production of TPPS remained the more valuable hypothesis. In apoplast according to its pH comprised between 5 and 6, two acid-base species (neutral and tetra-anionic) of TPPC should coexisted. Hence, we could imagine that the negatively charged

TPPC got inside the cytoplasm via bulk endocytosis as argued for TPPS that remained anionic regardless of pH. The symmetrical and neutral form of TPPC triggered lipid peroxidation mediated permeation supported by MDA quantification after light exposure. This mode of diffusion via phospholipid disruption was envisaged basing on a study on the interaction in liposomal membrane mimicking system of meso-tetrahydroxyphenyl chlorine (m-THPPC) that shares similarities with TPPC (Mojzisoava et al 2009).

Thus, according to our results, the main issue to explain the force of anionic PS to induce TBY-2 cell death is the global charge of the PS, the less anionic it is, the strongest is the effect, neutral form being the best cell death inducer. Further investigations should be monitored to explore this hypothesis based on the use of known neutral porphyrins such as tetrakis-hydroxyphenyl porphyrin or glycosylated porphyrins. Nevertheless, molecular size, ROS production and photostability should always be kept in mind.

Porphyrins were reported as cytotoxic and DNA binders depending on their tested concentration (Villanueva et al 1989, Shi et al 2017). In agreement to these previous studies, TPPS was indeed cytotoxic when tested at very high concentration (100 μ M). Nevertheless, tested at a concentration 30 times lower, TPPS was not anymore cytotoxic. Intriguingly and in contrast to TPPS, TPPC and TPPP did not show any significant dark toxicity when tested at 100 μ M. According to TPPP localization and its weaker cell wall interaction, this result was not surprising although it was for TPPC. Nevertheless, TPPC was never found in the nucleus suggesting that the nuclear envelop plays a physical barrier that prevents TPPC entry. Indeed, TPPS was reported to interact with DNA only *in vitro*. Moreover, TPPS was shown to be relocalized to the nucleus upon photosensitization via protein translocators. (Kessel 1997, Liao 2009, Patito and Malik 2001).

Once inside cells, porphyrins exerted their photodynamic function via the generation of superoxide anion ($O_2^{\cdot-}$) hydrogen peroxide (H_2O_2) and hydroxyl radical ($\cdot OH$) by electron transfer (type I process) or singlet oxygen (1O_2) by energy transfer to molecular oxygen (type II process). All these ROS damage vital cellular constituents such as carbohydrates, nucleic acids, proteins, lipids leading to cell death (Gill and Tuteja 2010, Demidchik 2015, Czarnocka et al, 2017). As expected after TPPS and TPPC photoactivation, an excessive amount of H_2O_2 were produced in TBY-2 cells mainly through type I photochemical reaction. Consequently, biomembranes should be disrupted as also shown by lipid peroxidation. Moreover, the setting up

of photodynamic stress was marked by the important production of proline that is well known as stress marker (De Lacerda et al, 2013, Yaish 2015).

In the other side, TB_Y-2 cells and plantlets responded to such photodynamic treatment (Guillaumot *et al.*, 2016; Issawi *et al.*, 2018). Plant cells are equipped with defense systems assigned to enzymatic and molecular defense in order to keep ROS under control (Racchi 2013, You and Chan 2015). While enzymatic activities such as APX, GPOX were rapidly and strongly inhibited (50 % and 30 % for GPOX and APX respectively after 1h light in presence of TPPC, it was obviously less strong in the case of TPPS even after 3h treatment (Fig. 6). The increase in CAT activity monitored after 1 h illumination under TPPS treatment indicated that this enzyme plays a major role in H₂O₂ dismutation ascribed as early responses to photodynamic stress. Such response was also reported in TB_Y-2 cells under nickel stress (Pompeu et al 2008) (Fig. 5A). Indeed, this could also explain why TPPS was a less powerful cell killer because cells were able to defend themselves under TPPS action and not upon TPPC treatment. A similar situation was reported in TB_Y-2 cells subjected to abiotic stress such as boron deprivation and heat shock (Hoque 2007, Koshiba et al 2008, De Pinto et al 2013, Van Doorn and Ketsa 2014). Altogether, the first line of defense through peroxidases GPOX and APX and CAT demonstrated that molecular mechanisms of defense were not regulated in the same way for both porphyrins proving that cells were more able to defend themselves against TPPS than TPPC. We hypothesized that TPPS endocytosis that is known as a slow mechanism and compartmentalization in endocytic vesicles delayed its photodynamic effect into cell while free TPPC could act directly on biological targets after photoactivation

The second line of defense was relative to antioxidant molecules such as ascorbate and glutathione implemented in Foyer-Halliwel-Asada cycle that also engages four enzymes : APX, MDHAR, DHAR, and GR in addition to the reducing agent NADPH (Potters et al 2010). Indeed, TPPC and TPPS showed opposite patterns regarding the evolution of ASH/DHA couple. Concerning glutathione, the redox state of glutathione did not change suggesting that the glutathione was maintained in its reduced form despite the rise of oxidative load. However, the amount of NADP⁺ in TPPC and TPPS treated cells increased significantly suggesting the high redox cycling of GSH pool that occurred through the ascorbate-glutathione cycle and corresponded to the decrease in NADPH content that was converted to NADP⁺ in cells treated with both porphyrins. That high amount of GSH was linked to GR activity especially in TPPS-

treated cells. Taken together redox homeostasis was drastically overwhelmed in photodynamically stressed cells despite the stability of glutathione redox state as stated in TBY2 under salt stress and ophiobilin A toxicity (Hoque et al 2007, Locato et al 2015)

The ultimate outcome of porphyrin-mediated photodynamic stress was cell death. The hallmarks of apoptosis-like in TBY-2 treated with TPPC and TPPS were obvious : membrane shrinkage, increase in caspase-like activities and DNA fragmentation. These morphological and biochemical features of programmed cell death were reported in TBY-2 cells exposed to cadmium, isopentyladenosine and acrolein witnessing therefore the occurrence of apoptosis-like cell death in plant cells (Mlejnek and Prochazka 2002, Kuthanova et al 2008, Biswas and Mano 2016).

Conclusion and perspectives

Our aim was to dissect the mechanisms that occurred from outside to inside TBY2 cells upon anionic porphyrin phototreatment. We showed that different anionic porphyrins that are negatively charged were able to interact and cross plant cell wall that bears anionic polysaccharides. Thus we tried to mimic plant cell wall interactions with our molecules in phosphate buffer with a pH closed to the spent medium but also to follow *in situ* their localization. Quite unexpectedly, we showed that negatively charged molecules were able to bind to negatively charged cell wall probably by weak bounds such as H bonds and/or electrostatic bonds when core was protonated. Moreover, we also showed that the neutrality of the molecule such as TPPC at the tested pH played a crucial role in the rate of cell wall crossing. These results constituted a corpus of data that could be enlarged to water soluble charged molecules such as pesticides in the agronomic domain relative to plants. To our knowledge, this is the first study that took in account all the story or fate of a molecule from its interaction to its activity within cells.

Acknowledgements

Mohammad Issawi was granted by the municipality of Sharkieh (Lebanon).

References

- Alves, E., Faustino, M.A.F., Neves, M.G.P.M.S., Cunha, Â., Nadais, H. and Almeida, A.** (2015) Potential applications of porphyrins in photodynamic inactivation beyond the medical scope. *J. Photochem. Photobiol. C: Photochemistry Reviews*, **22**, 34–57.
- Babilas, P., Schreml, S., Landthaler, M. and Szeimies, R.-M.** (2010) Photodynamic therapy in dermatology: state-of-the-art. *Photodermatol. Photoimmunol. Photomed.* **26**, 118–132.
- Banfi, S., Caruso, E., Buccafurni, L., Battini, V., Zazzaron, S., Barbieri, P. and Orlandi, V.** (2006) Antibacterial activity of tetraaryl-porphyrin photosensitizers: An in vitro study on Gram negative and Gram positive bacteria. *J. Photochem. Photobiol. B: Biology*, **85**, 28–38.
- Ben Amor, T. and Jori, G.** (2000) Sunlight-activated insecticides: historical background and mechanisms of phototoxic activity. *Insect Biochem Mol Biol.* **30**, 915–925.
- Bertoloni, G., Reddi, E., Gatta, M., Burlini, C. and Jori, G.** (1989) Factors influencing the haematoporphyrin-sensitized photoinactivation of *Candida albicans*. *Microbiology*, **135**, 957–966.
- Bertoloni, G., Zambotto, F., Conventi, L., Reddi, E. and Jori, G.** (1987) Role of specific cellular targets in the hematoporphyrin-sensitized photoinactivation of microbial cells. *J. Photochem. Photobiol.* **46**, 695–698.
- Biswas, M.S. and Mano, J.** (2016) Reactive Carbonyl Species Activate Caspase-3-Like Protease to Initiate Programmed Cell Death in Plants. *Plant Cell Physiol.* **57**, 1432-1442.
- Caffall, K.H. and Mohnen, D.** (2009) The structure, function, and biosynthesis of plant cell wall pectic polysaccharides. *Carbohydr. Res.* **344**, 1879–1900.
- Chen, R., Ratnikova, T.A., Stone, M.B., Lin, S., Lard, M., Huang, G., Hudson, J.S. and Ke, P.C.** (2010) Differential Uptake of Carbon Nanoparticles by Plant and Mammalian Cells. *Small*, **6**, 612–617.
- Chen, Z. and Gallie, D.R.** (2006) Dehydroascorbate Reductase Affects Leaf Growth, Development, and Function. *Plant Physiol.* **142**, 775–787.
- Czarnocka, W. and Karpiński, S.** (2018) Friend or foe ? Reactive oxygen species production, scavenging and signaling in plant response to environmental stresses. *Free Radic. Biol.*
- De Lacerda, C.F., Cambraia, J., Oliva, M.A., Ruiz, H.A. and Prisco, J.T.** (2003) Solute accumulation and distribution during shoot and leaf development in two sorghum genotypes under salt stress. *Environ. Exper. Bot.* **49**, 107–120.
- De Menezes, H.D. de, Pereira, A.C., Brancini, G.T.P., Leão, H.C. de, Massola Júnior, N.S., Bachmann, L., Wainwright, M., Bastos, J.K. and Braga, G.U.L.** (2014a) Furocoumarins and coumarins photoinactivate *Colletotrichum acutatum* and *Aspergillus nidulans* fungi under solar radiation. *J. Photochem. Photobiol. B.* **131**, 74–83.

- De Menezes, H.D., Rodrigues, G.B., Teixeira, S.P., Massola, N.S., Bachmann, L., Wainwright, M. and Braga, G.U.L. (2014b).** In Vitro Photodynamic Inactivation of Plant-Pathogenic Fungi *Colletotrichum acutatum* and *Colletotrichum gloeosporioides* with Novel Phenothiazinium Photosensitizers. *Appl. Environ. Microbiol.* **80**, 1623–1632.
- Demidchik, V. (2015)** Mechanisms of oxidative stress in plants: From classical chemistry to cell biology. *Environ. Exper. Bot.* **109**, 212–228.
- Demidova, T.N. and Hamblin, M.R. (2005)** Effect of Cell-Photosensitizer Binding and Cell Density on Microbial Photoinactivation. *Antimicrob. Agents Chemother.* **49**, 2329–2335.
- De Lacerda, C.F., Cambraia, J., Oliva, M.A., Ruiz, H.A. and Prisco, J.T. (2003)** Solute accumulation and distribution during shoot and leaf development in two sorghum genotypes under salt stress. *Environ. Exper. Bot.* **49**, 107–120.
- Donnelly, R.F., McCarron, P.A. and Tunney, M.M. (2008)** Antifungal photodynamic therapy. *Microbiol. Res.* **163**, 1–12.
- Doorn, W.G. van (2011)** Classes of programmed cell death in plants, compared to those in animals. *J. Exp. Bot.* **62**, 4749–4761.
- Drábková, M., Maršálek, B. and Admiraal, W. (2007)** Photodynamic therapy against cyanobacteria. *Environ. Toxicol.* **22**, 112–115.
- Fairbrother, T.E., Essig, H.W., Combs, R.L. and Heitz, J.R. (1981)** Toxic effects of rose bengal and erythrosin B on three life stages of the face fly, *Musca autumnalis*. *Ecol. Entomol.* **10**, 506–510.
- Foyer, C.H. and Noctor, G. (2011)** Ascorbate and Glutathione: The Heart of the Redox Hub. *Plant Physiol.* **155**, 2–18.
- Fracarolli, L., Rodrigues, G.B., Pereira, A.C., Massola Júnior, N.S., Silva-Junior, G.J., Bachmann, L., Wainwright, M., Bastos, J.K. and Braga, G.U.L. (2016)** Inactivation of plant-pathogenic fungus *Colletotrichum acutatum* with natural plant-produced photosensitizers under solar radiation. *J. Photochem. Photobiol. B: Biology*, **162**, 402–411.
- Gadjev, I., Stone, J.M. and Gechev, T.S. (2008)** Programmed Cell Death in Plants: new insights into redox regulation and the role of hydrogen peroxide. *Int. Rev. Cell Mol. Biol.* **270**, 87-144.
- George, S., Hamblin, M.R. and Kishen, A. (2009)** Uptake pathways of anionic and cationic photosensitizers into bacteria. *Photochem. Photobiol. Sci.* **8**, 788-795.
- Gill, S.S. and Tuteja, N. (2010)** Reactive oxygen species and antioxidant machinery in abiotic stress tolerance in crop plants. *Plant Physiol. Biochem.* **48**, 909–930.

- Gonzales, J.C., Brancini, G.T.P., Rodrigues, G.B., Silva-Junior, G.J., Bachmann, L., Wainwright, M. and Braga, G.Ú.L.** (2017) Photodynamic inactivation of conidia of the fungus *Colletotrichum abscissum* on *Citrus sinensis* plants with methylene blue under solar radiation. *J. Photochem. Photobiol. B: Biology*, **176**, 54–61.
- Guillaumot, D., Issawi, M., Da Silva, A., Leroy-Lhez, S., Sol, V. and Riou, C.** (2016) Synergistic enhancement of tolerance mechanisms in response to photoactivation of cationic tetra (N-methylpyridyl) porphyrins in tomato plantlets. *J. Photochem. Photobiol. B: Biology*, **156**, 69–78.
- Hamblin, M.R.** (2016) Antimicrobial photodynamic inactivation: a bright new technique to kill resistant microbes. *Curr. Opin. Microbiol.* **33**, 67–73.
- Hollingsworth, J.V., Richard, A.J., Vicente, G.H., and Russo, P.S.** (2012). Characterization of the Self-Assembly of meso-Tetra(4-sulfonatophenyl)porphyrin (H₂TPPS₄⁻) in Aqueous Solutions. *Biomacromolecules*. **13**, 60–72
- Hoque, M.A., Banu, M.N.A., Okuma, E., Amako, K., Nakamura, Y., Shimoishi, Y. and Murata, Y.** (2007) Exogenous proline and glycinebetaine increase NaCl-induced ascorbate–glutathione cycle enzyme activities, and proline improves salt tolerance more than glycinebetaine in tobacco Bright Yellow-2 suspension-cultured cells. *Plant Physiol.* **164**, 1457–1468.
- Huang, L., Huang, Y.-Y., Mroz, P., et al.,** (2010) Stable Synthetic Cationic Bacteriochlorins as Selective Antimicrobial Photosensitizers. *Antimicrob. Agents Chemother.* **54**, 3834–3841.
- Issawi, M., Guillaumot, D., Sol, V. and Riou, C.** (2018) Responses of an adventitious fast-growing plant to photodynamic stress: comparative study of anionic and cationic porphyrin effect on *Arabidopsis thaliana*. *Physiol. Plant.* **162**, 379–390.
- Issawi, M., Muhieddine, M., Girard, C., Sol, V. and Riou, C.** (2017) Unexpected features of exponentially growing Tobacco Bright Yellow-2 cell suspension culture in relation to excreted extracellular polysaccharides and cell wall composition. *Glycoconj J.* **34**, 585–590.
- Issawi, M., sol, V., and Riou, C.** (2018) Plant photodynamic stress: what’s new? (Submitted to *Frontiers in plant science*).
- Jarvis, M.** (2011) Plant cell walls: Supramolecular assemblies. *Food Hydrocoll.* **25**, 257–262.
- Jesus, V., Martins, D., Branco, T., et al.,** (2018) An insight into the photodynamic approach versus copper formulations in the control of *Pseudomonas syringae* pv. *actinidiae* in kiwi plants. *Photochem. Photobiol. Sci.* **17**, 180–191.
- Kashef, N., Huang, Y.-Y. and Hamblin, M.R.** (2017) Advances in antimicrobial photodynamic inactivation at the nanoscale. *Nanophotonics*, **6**, 853-879.
- Kessel, D.** (1997) Subcellular Localization of Photosensitizing Agents Introduction. *Photochem. Photobiol.* **65**, 387-388.

- Kessel, D., Luguya, R. and Vicente, M.G.H.** (2003) Localization and photodynamic efficacy of two cationic porphyrins varying in charge distribution. *J. Photochem. Photobiol.*, **78**, 431–435.
- Konopka, K. and Goslinski, T.** (2007) Photodynamic Therapy in Dentistry. *J. Dent. Res.* **86**, 694–707.
- Koshiha, T., Kobayashi, M. and Matoh, T.** (2009) Boron Nutrition of Tobacco BY-2 Cells. V. Oxidative Damage is the Major Cause of Cell Death Induced by Boron Deprivation. *Plant Cell Physiol.* **50**, 26–36.
- Králová, J., Kejík, Z., Bříza, T., Kaplánek, R., Záruba, K., Martásek, P., and Král, V.** (2014) Design, Synthesis, Selective Recognition Properties and Targeted Drug Delivery Application in *Handbook of Porphyrin Science With Applications to Chemistry, Physics, Materials Science, Engineering, Biology and Medicine. Volume 33: Applications — Part II* (Kadish, K.M., Smith, K.M., and Guillard, R. eds.), pp. 1-75.
- Kuthanova, A., Fischer, L., Nick, P. and Opatrny, Z.** (2008) Cell cycle phase-specific death response of tobacco BY-2 cell line to cadmium treatment. *Plant Cell Environ.* **31**, 1634–1643.
- Larissa Marila de Souza, Natalia Mayumi Inada, Sebastião Pratavieira, Juliano José Corbi, Cristina Kurachi and Vanderlei Salvador Bagnato** (2017) Efficacy of Photogem® (Hematoporphyrin Derivative) as a Photoactivatable Larvicide against *Aedes aegypti* (Diptera: Culicidae) Larvae. *Life Sci.* **11**, 74-81.
- Lazzeri, D., Rovera, M., Pascual, L., and Durantini, E.N.** (2004) Photodynamic studies and photoinactivation of *Escherichia coli* using meso-substituted cationic porphyrin derivatives with asymmetric charge distribution. *Photochem. Photobiol.* **80**, 286-293.
- Le Guern, F., Sol, V., Ouk, C., Arnoux, P., Frochot, C. and Ouk, T.-S.** (2017) Enhanced Photobactericidal and Targeting Properties of a Cationic Porphyrin following the Attachment of Polymyxin B. *Bioconjugate Chem.* **28**, 2493–2506.
- Leroy-lhez, S., Rezazgui, O., Issawi, M., Elhabiri, M., Calliste, C.A., Riou, C.** (2018) Characterization of pH dependent charge states and physico-chemical properties of anionic porphyrins. (Submitted to Photochemical & Photobiological Sciences).
- Liao, B., He, B., Liu, R. and Huang, Y.** (2009) Induced Circular Dichroism of Anionic Porphyrin TPPS Aggregates in DNA Solutions. *Polymer Journal*, **41**, 739–743
- Lipke, P.N. and Ovale, R.** (1998) Cell wall architecture in yeast: new structure and new challenges. *J. Bacteriol.* **180**, 3735–3740.
- Liu, Q., Zhang, X., Zhao, Y., Lin, J., Shu, C., Wang, C. and Fang, X.** (2013) Fullerene-Induced Increase of Glycosyl Residue on Living Plant Cell Wall. *Environ. Sci. Technol.* **47**, 7490–7498.

- Locato, V., Uzal, E.N., Cimin, S., Zonno, M.C., Evidente, A., Micera, A., Foyer, C.H. and De Gara, L.** (2015) Low concentrations of the toxin ophiobolin A lead to an arrest of the cell cycle and alter the intracellular partitioning of glutathione between the nuclei and cytoplasm. *J.Exp.Bot.* **66**, 2991-3000.
- Lucantoni, L., Magaraggia, M., Lupidi, G., Ouedraogo, R.K., Coppellotti, O., Esposito, F., Fabris, C., Jori, G. and Habluetzel, A.** (2011) Novel, Meso-Substituted Cationic Porphyrin Molecule for Photo-Mediated Larval Control of the Dengue Vector *Aedes aegypti* P. Kittayapong, ed. *PLoS Negl. Trop. Dis.* **5**, e1434.
- Maisch, T., Szeimies, R.-M., Jori, G. and Abels, C.** (2004) Antibacterial photodynamic therapy in dermatology. *Photochem. Photobiol. Sci.* **3**, 907-917.
- Martínez-Sanz, M., Gidley, M.J. and Gilbert, E.P.** (2015) Application of X-ray and neutron small angle scattering techniques to study the hierarchical structure of plant cell walls: A review. *Carbohydr. Polym.* **125**, 120–134.
- McCullagh, C. and Robertson, P.K.J.** (2006) Photosensitized Destruction of *Chlorella vulgaris* by Methylene Blue or Nuclear Fast Red Combined with Hydrogen Peroxide under Visible Light Irradiation. *Environ. Sci. Technol.* **40**, 2421–2425.
- Mlejnek, P. and Procházka, S.** (2002) Activation of caspase-like proteases and induction of apoptosis by isopentenyladenosine in tobacco BY-2 cells. *Planta*, **215**, 158–166.
- Moghnie, S., Tovmasyan, A., Craik, J., Batinic-Haberle, I. and Benov, L.** (2017) Cationic amphiphilic Zn-porphyrin with high antifungal photodynamic potency. *Photochem. Photobiol. Sci.* **16**, 1709–1716.
- Moussian, B.** (2013) The Arthropod Cuticle. In A. Minelli, G. Boxshall, and G. Fusco, eds. *Arthropod Biology and Evolution*. Berlin, Heidelberg: Springer Berlin Heidelberg, pp. 171–196.
- Oriel, S. and Nitzan, Y.** (2012) Mechanistic Aspects of Photoinactivation of *Candida albicans* by Exogenous Porphyrins†. *J. Photochem. Photobiol.*, **88**, 604–612.
- Patito, I.A., Rothmann, C. and Malik, Z.** (2001) Nuclear transport of photosensitizers during photosensitization and oxidative stress. *Biology of the Cell*, **93**, 285–291.
- Pohl, J., Saltsman, I., Mahammed, A., Gross, Z. and Röder, B.** (2014) Inhibition of green algae growth by corrole-based photosensitizers. *J. Appl. Microbiol.* **118**, 305–312.
- Pompeu, G.B., Gratão, P.L., Vitorello, V.A. and Azevedo, R.A.** (2008) Antioxidant isoenzyme responses to nickel-induced stress in tobacco cell suspension culture. *Sci. Agric.* **65**, 548–552.
- Potters, G., Horemans, N. and Jansen, M.A.K.** (2010) The cellular redox state in plant stress biology – A charging concept. *Plant Physiol Biochem.* **48**, 292–300.
- Racchi, M.** (2013) Antioxidant Defenses in Plants with Attention to *Prunus* and *Citrus* spp.

Antioxidants, **2**, 340–369.

Rantong, G. and Gunawardena, A.H.L.A.N. (2015) Programmed cell death: genes involved in signaling, regulation, and execution in plants and animals. *Botany*, **93**, 193–210.

Reddi, E., Cecon, M., Valduga, G., Jori, G., Bommer, J., Elisei, F., Latterini, L. and Mazzucato, U. (2002) Photophysical properties and antibacterial activity of meso-substituted cationic porphyrins, *Photochem. Photobiol.* **75**, 462-470.

Riou, C., Calliste, C.A., Da Silva, A., Guillaumot, D., Rezazgui, O., Sol, V. and Leroy-Lhez, S. (2014) Anionic porphyrin as a new powerful cell death inducer of Tobacco Bright Yellow-2 cells. *Photochem. Photobiol. Sci.* **13**, 621-625.

Rishi, P., and Agarwal, V. (2015) Current Role of Photodynamic Therapy in Ophthalmic Practice. *Sci. J. Med. & Vis. Res. Foun.* **33**, 97-99.

Shi, L., Jiang, Y.-Y., Jiang, T., Yin, W., Yang, J.-P., Cao, M.-L., Fang, Y.-Q. and Liu, H.-Y. (2017) Water-soluble Manganese and Iron Mesotetrakis(carboxyl)porphyrin: DNA Binding, Oxidative Cleavage, and Cytotoxic Activities. *Molecules*, **22**, 1084-1101.

Simões, C., Gomes, M.C., Neves, M.G.P.M.S., Cunha, Â., Tomé, J.P.C., Tomé, A.C., Cavaleiro, J.A.S., Almeida, A. and Faustino, M.A.F. (2016) Photodynamic inactivation of *Escherichia coli* with cationic meso-tetraarylporphyrins – The charge number and charge distribution effects. *Catal. Today*, **266**, 197–204.

Synystsyia, A., Čopíková, J., Kim, W.J. and Park, Y.I. (2015) Cell Wall Polysaccharides of Marine Algae. In: *Handbook of Marine Biotechnology* (Kim, S.K., eds) Springer, Berlin, Heidelberg, pp. 543-590.

Villaneuva, A., canete, M., and Hazen, M.J. (1989). Uptake and DNA photodamage induced in plant cells *in vivo* by two cationic porphyrins. *Mutagenesis* **4**, 157-159.

Yaish, M.W. (2015) Proline accumulation is a general response to abiotic stress in the date palm tree (*Phoenix dactylifera* L.). *Genet. Mol. Res.* **14**, 9943–9950.

You, J. and Chan, Z. (2015) ROS Regulation During Abiotic Stress Responses in Crop Plants. *Front. Plant Sci.* **6**, 1092-1105.

Figure Legends

Figure 1 Anionic porphyrins are not cyto and/or genotoxic for TBV-2 cells under dark conditions. Cells isolated at the beginning of exponential cell phase were incubated with TPPS, TPPC and TPPP each tested at 100 μ M under dark for three hours. H₂O corresponded to the control without any porphyrin. Results are the means \pm sem of 3 independent experiments (no significant effect for TPPC and TPPP compared to control, for TPPS * $p < 0.05$)

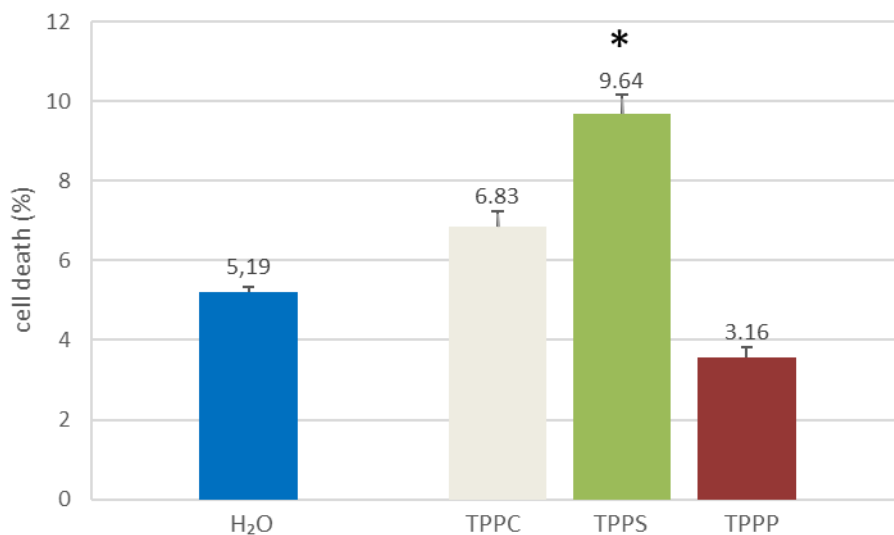


Figure 2 Photoactivated anionic porphyrins induce TBV-2 cell death. The three PS were tested under dark (black box) and light (yellow and brown boxes) conditions as described in material and methods. 3 hour-incubations with the tested porphyrins were performed in the spent TBV-2 cell medium (pH 4.5; yellow box) and in new TBV-2 cell medium (pH 5.38 ± 0.14; brown box), respectively. Porphyrin concentrations were reported on the graph. Results are the means ± sem of 4 independent experiments

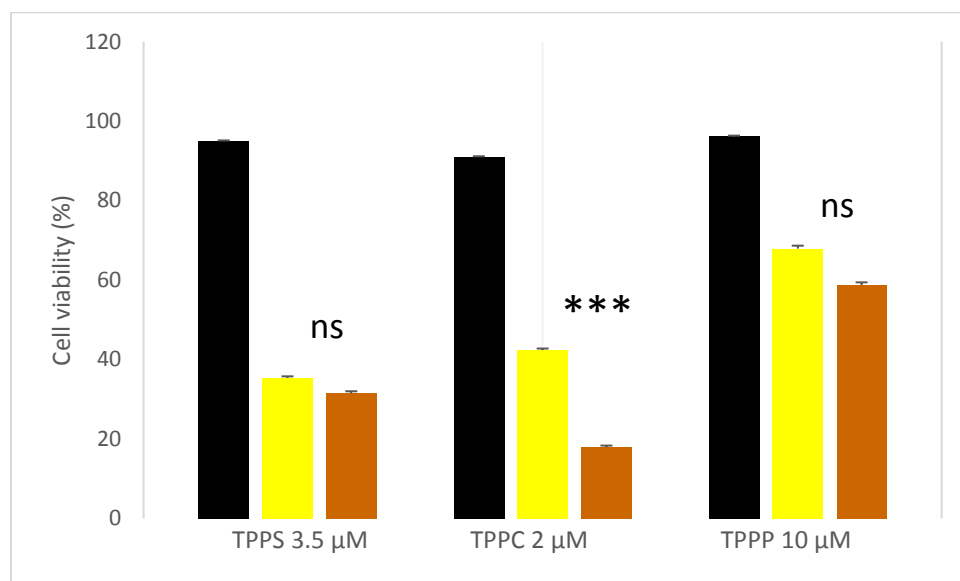


Figure 3 Differential localization of the three porphyrins in cell wall and cytoplasm of TBY-2 cells. 4 day-old TBY-2 cells were plasmolysed for 1h then incubated 3h with PP under dark in plasmolysis medium, rinsed and observed under Zeiss confocal microscope. PP were tested at 3.5 μM for TPPC (A) and TPPS (B) and 5 μM for TPPP (C). Left panel corresponds to λ emission from 640 to 680 nm (spectral detection) and right panel : bright field (channel mode).

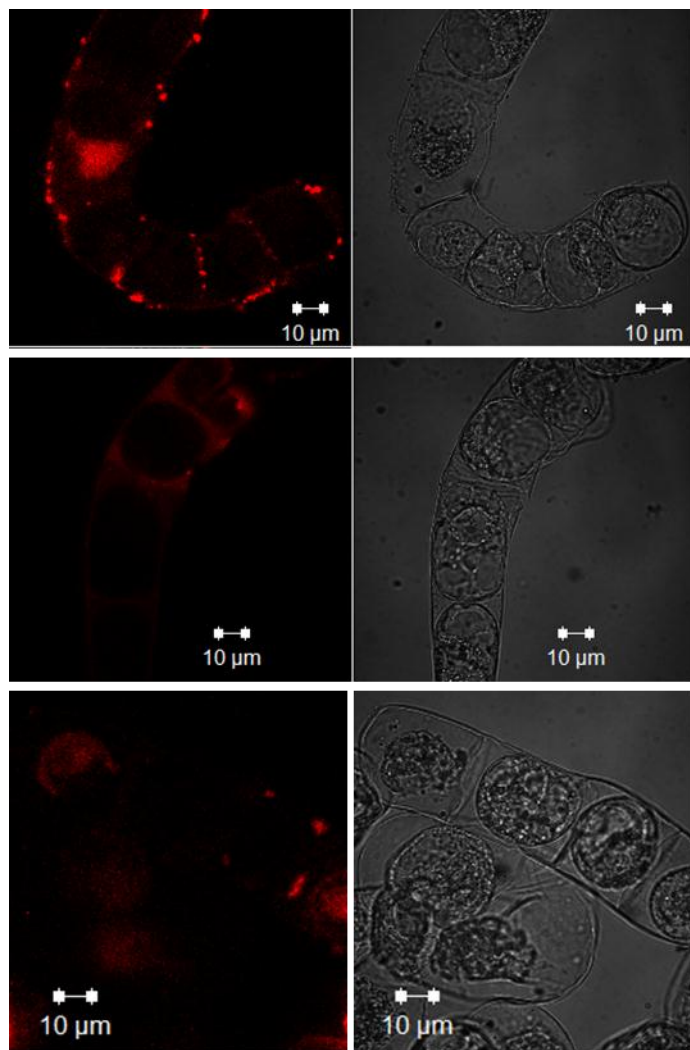


Figure 4 *In vitro* interaction of porphyrins TPPS, TPPC and TPP with isolated cell wall. Each porphyrin was tested at 2 μ M and incubated with isolated TBV-2 cell wall for 3 hours. Cell wall and porphyrins were washed as described in mat and meth. The retention rate was determined after spectrophotometer under UV measurements. Results are the means \pm SD of 3 independent experiments

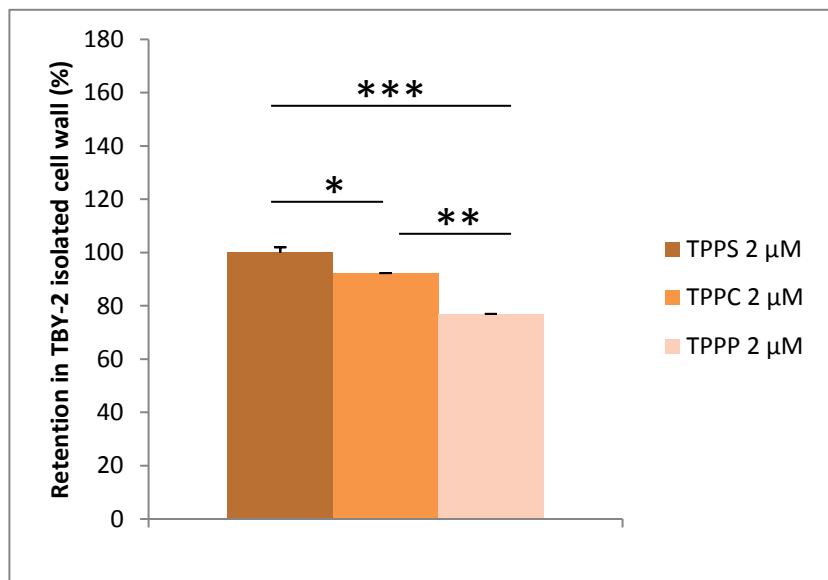


Figure 5 Responses of TBY-2 cells subjected to photo-activation of TPPS and TPPC. TPPS was tested at 3.5 μM and TPPC at 2 μM . **A)** H_2O_2 production. **B)** lipid peroxidation assay through MDA.quantification. **C)** Stress response determination via proline quantification. Ratio calculation was determined from control not-treated cells that arbitrary corresponds to 100.

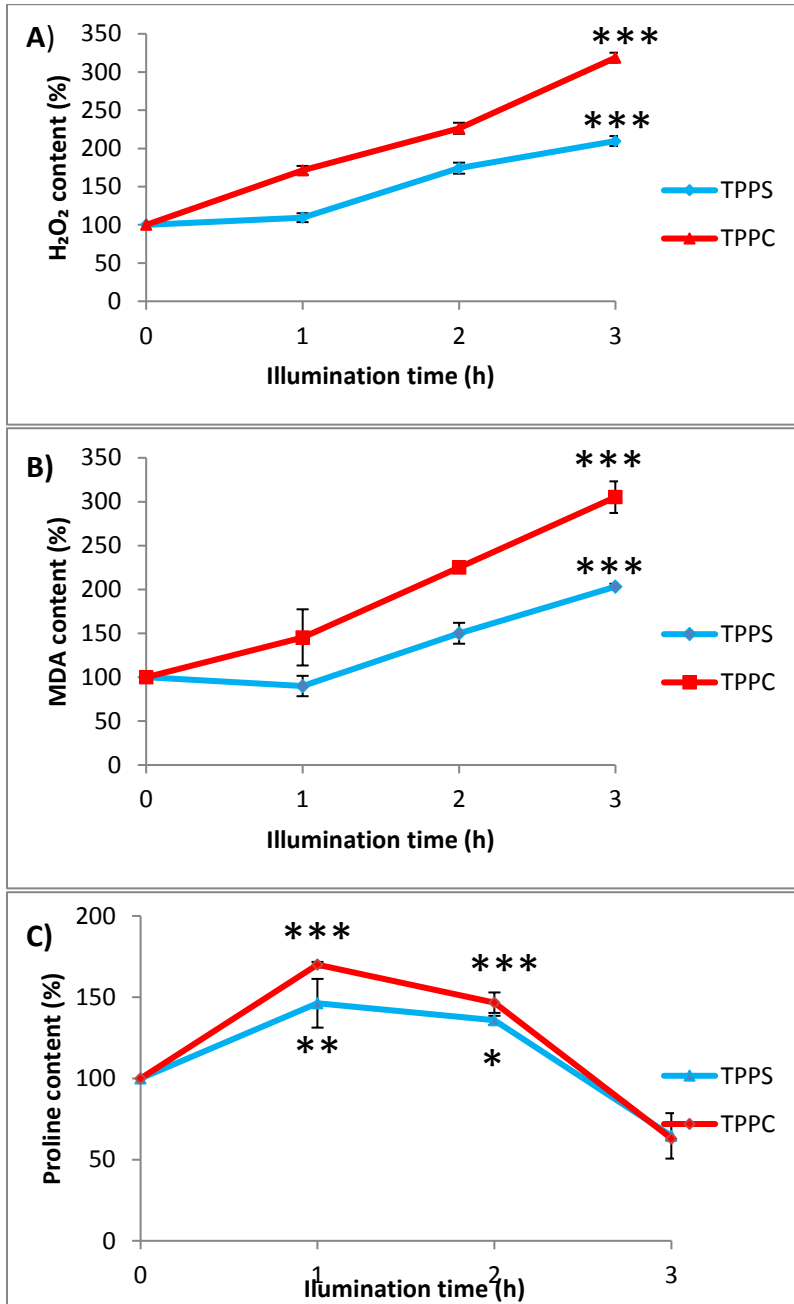


Figure 6 Antioxidant enzyme activities in TBY-2 cells treated with **A)** TPPS (3.5 μ M) and **B)** TPPC (2 μ M) over illumination time. APX: ascorbate peroxidase, GPOX guaiacol peroxidase, CAT catalase, SOD superoxide dismutase. Results are the mean \pm SD of three independent experiments.

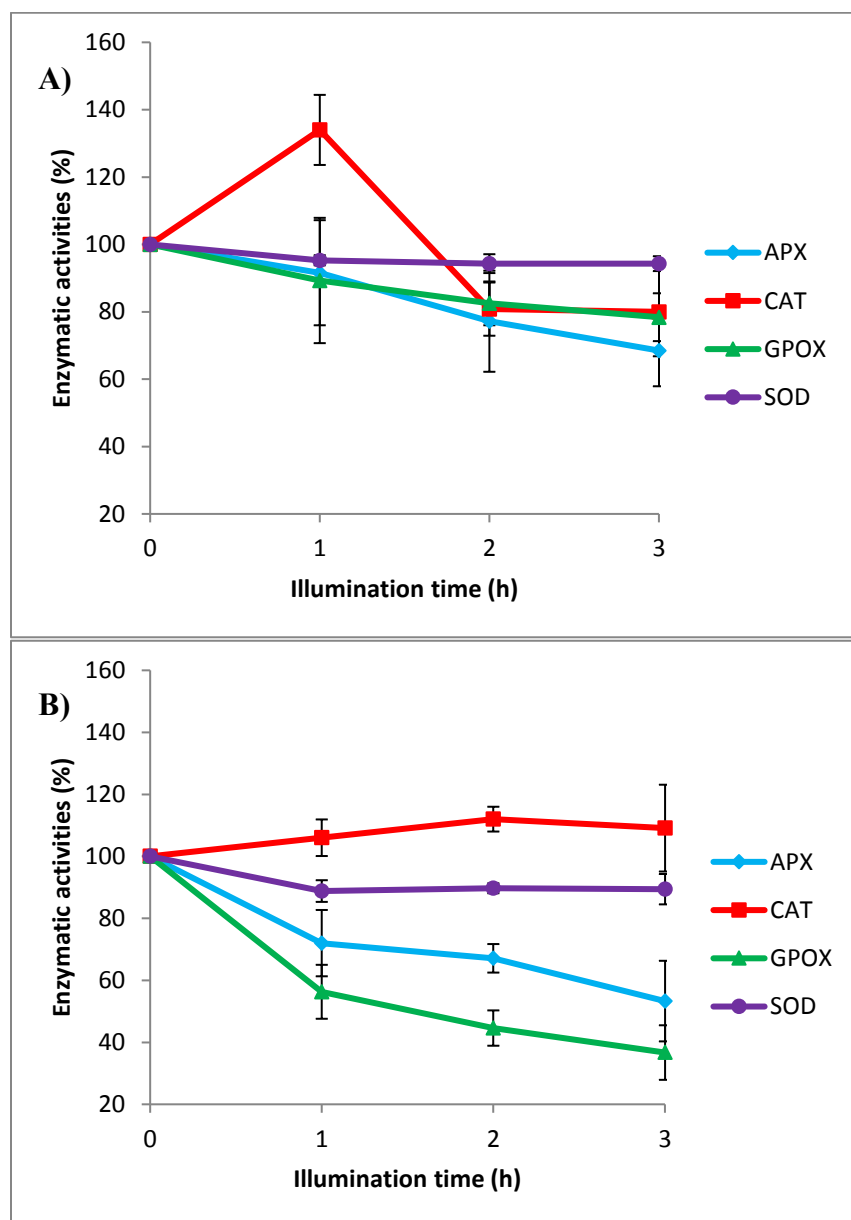


Figure 7 Measurement of Foyer-Halliwell-Asada cycle components in TBY-2 treated with photoactivated TPPS at 3.5 μM and TPPC at 2 μM following illumination time. Measurement of A) oxidized and reduced forms of ascorbate, B) glutathione, C) pyridine nucleotide phosphate as well as D) enzymatic activities of dehydroascorbate reductase (DHAR) and glutathione reductase (GR). Blue lines (dotted and continuous) correspond to TPPS treatment and red lines (dotted and continuous) to TPPC. Results are the mean of three experiments \pm SD.

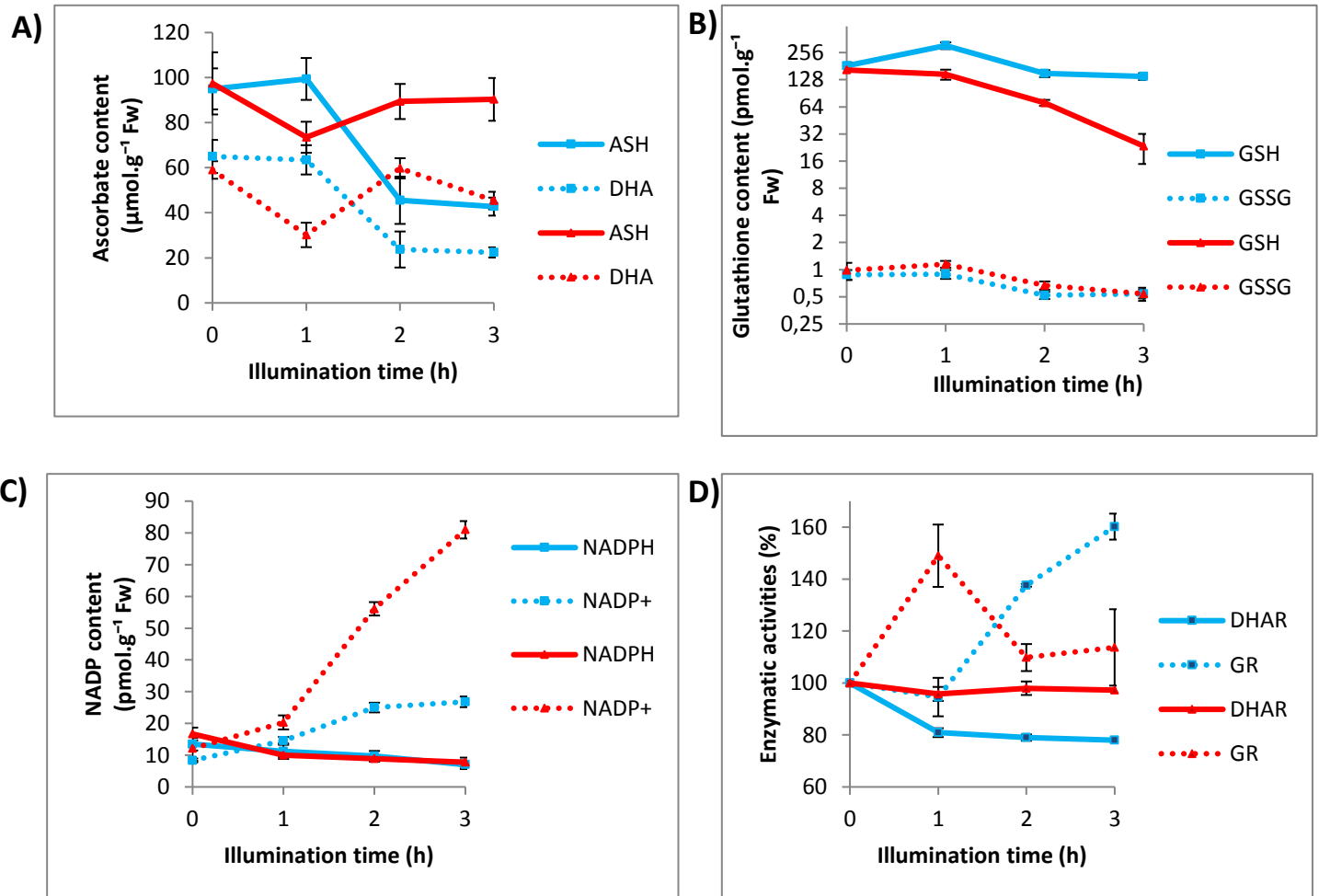


Figure 8 Apoptosis-like cell death induction in TBY-2 cells treated with photoactivated TPPS and TPPC. Caspase-like protease activities **A)** morphological marker. **B)** CLK-1 and CLK-3 activities. **C)** Genomic DNA fragmentation. Lines 1 and 4: DNA from dark treated cells, lines 2 and 5: Fragmented DNA from light treated cells, Lines 3 and 6 DNA size ladder. Lines 1 and 2 and Lines 4 and 5 correspond to TPPS and TPPC, respectively Arrow indicated the typical 250 pb fragment scale.

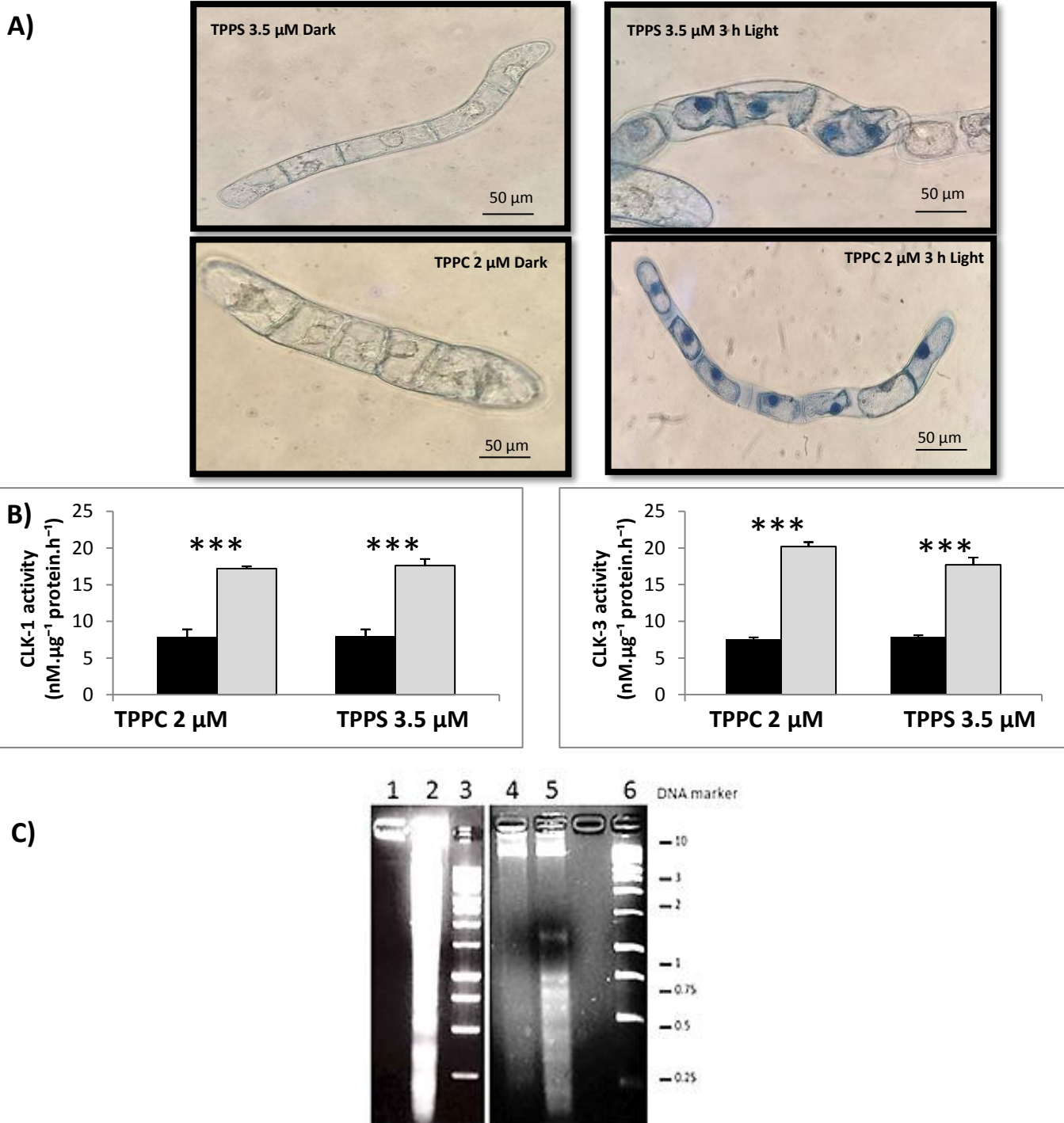


Figure 9 Schematic representation of chemical structure and charge of anionic porphyrins and their interaction and cross from cell wall to cytoplasm of TBY-2 cells in regard to crucial importance of pH change from spent medium to cytoplasm. Carboxylate groups of TPPC, sulfonate groups of TPPS and phosphonate groups of TPPP are shown in green, red and purple respectively. At the pH of the spent medium (4.5), TPPC was fully neutral whereas 3 species of TPPS coexisted as tetra-anionic, tri-anionic (with 2 positive charges at nitrogens of the core) and di-anionic (with 2 positive charges at the N of the core). TPPP coexisted by means of two species as tri-anionic and di-anionic as described for TPPS. In the apoplast, at weak acidic pH, TPPC can be deprotonated to yield tetra-anionic species. While at neutral pH, TPPC should be completely anionic in the cytoplasm. Phosphonate groups of TPPP have more complicated acido-basic properties. Hence, TPPP could be more and more anionic in the apoplast as well as in the cytoplasm (hydrogens represented in orange as -OH can lose protons). The three arrows (pink) ascribed for TPPC indicate the fast cell wall crossing whereas one arrow suggest that the diffusion of TPPS and TPPP was delayed. The tetra-anionic form of TPPC and TPPS and TPPP got inside cytoplasm by endocytosis whereas the fully neutral TPPC diffuse through phospholipids disruption upon photosensitization.

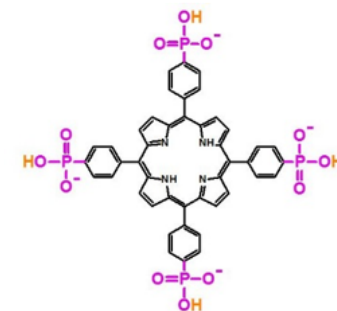
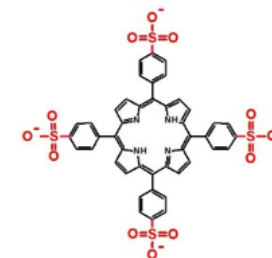
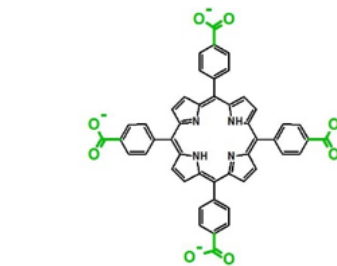
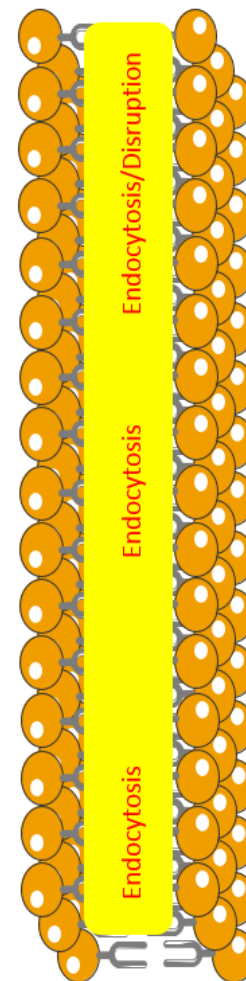
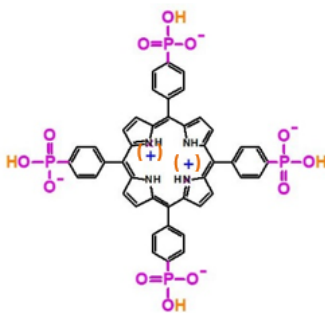
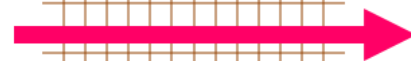
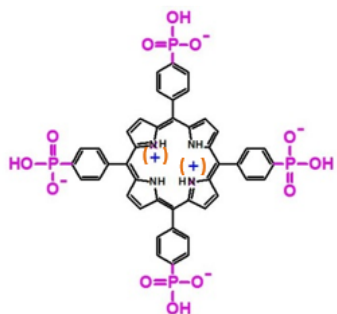
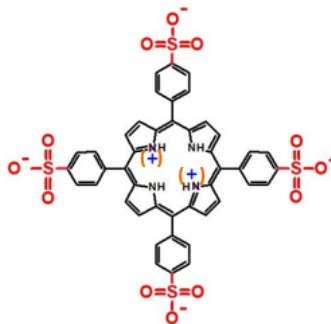
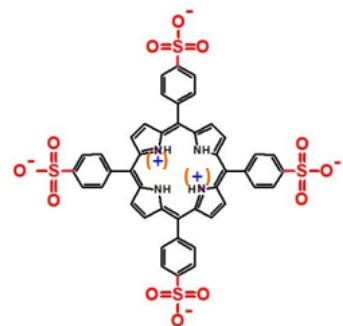
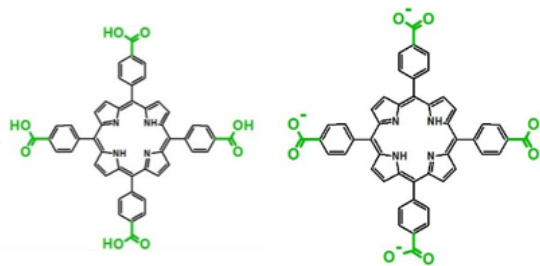
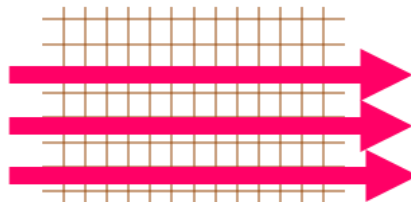
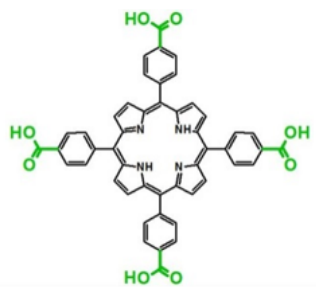
Spent medium
(pH=4.5)

Cell wall

Apoplast
(pH=5-6)

Plasma membrane

Cytoplasm
(pH=7)



Discussion and perspectives

Chapter II provided a dynamic study concerning plant photodynamic stress at cellular level. For all the experiments, we isolated TBY-2 cells at the beginning of exponential growth phase when cell spent medium reached a pH at 4.5 (Publication 4). As we discussed, such medium is very complex and contained minerals, phytohormones, vitamins, carbohydrates, proteins, organic acids. We also determined the chemical composition of TBY-2 outermost layer known as the cell wall which is exposed to extracellular microenvironment. We showed that cell wall from exponential growing cells was rich in pectin (around 55%) defined as galacturonic acid-rich polymers assigning therefore cell wall negative charge (Table 2).

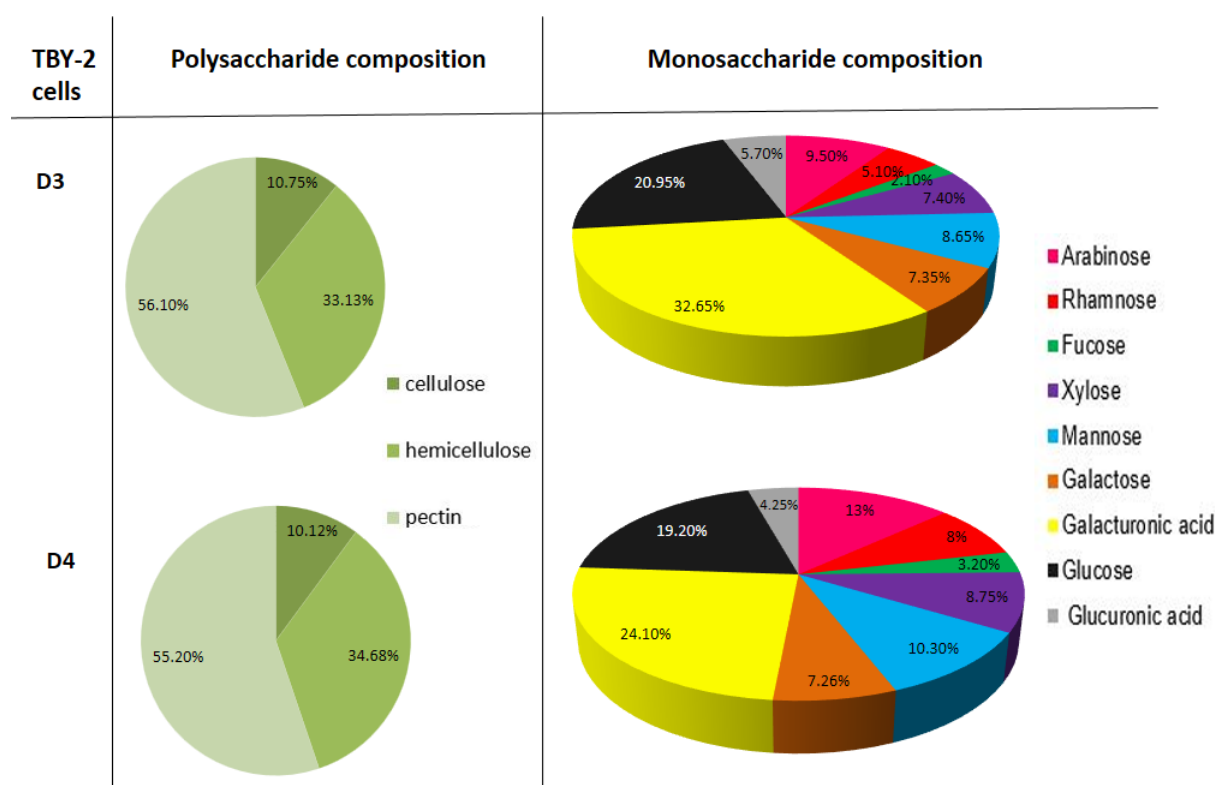


Table 2. Cell wall composition of TBY-2 cells.

The cell wall of young TBY-2 cells at the beginning of exponential phase (the growth phase at which we treat them with porphyrins) was isolated and analysed. D3 and D4 cells were similar as they were rich in galacturonic acid-rich pectin polymers and poor in cellulose. D3: 3 day-old cells, D4: 4 day-old cells.

In parallel, basing on the precedent data on cell wall, we monitored porphyrin spectrum in the spent medium and performed titration experiment in methanol/water, phosphate buffer and water in order to determine the precise structure of porphyrins at the time when they just interact with the TBY-2 cells (Annex 4, Publication 5).

All that insightful findings allowed us to decipher the interaction porphyrin-cell wall, discussed in Publication 6. Strikingly, TPPC was fully neutralized at pH=4.5 and it seems that it across the porous cell wall with a high diffusion rate interacting with surrounding polymers via hydrogen bonds. Since sulfonic acid group is a very strong acid, TPPS remained anionic at the peripheral side. However, its core showed protonation on the nitrogen atoms and its absorption spectrum suggests that three species coexisted in the spent medium. We expected that TPPS formed electrostatic interactions with negatively charged pectins without excluding H bonds. In the other hand, TPPP showed the weakest interaction with cell wall. In addition, TPPP-treated cells seen under confocal microscopy exhibited a very weak signal suggesting that TPPP barely cross the cell wall. Indeed, TPPP have interesting binding properties as they bear a strong H bond acceptor known for its biological role (P=O), in addition to an extra H bond donor (P-OH) comparing to TPPS. Therefore, we think that TPPP interacted with surrounding molecules in the spent medium before reaching the cell wall. (Kubat 2004; Kralova 2014). Cell wall form a continuum with the apoplast, the compartment between cell wall and plasma membrane where the pH fluctuates between 5 and 6 (Villiers and Kwak 2013). Facing the plasma membrane, TPPS was reported to get into the cytoplasm by endocytosis whereas the aspect of TPPC is ambiguous at the pH range of the apoplasm. TPPC side groups can be neutralized. Thus, two species must coexist bearing either neutral carboxylic acid or anionic carboxylate groups. One hypothesis is that anionic species could be internalized via endocytosis whereas neutral forms remained trapped at the plasma membrane due to their symmetric, non-polar and hydrophobic features. However, they could reach the cytoplasm upon photosensitization-mediated porous formation within plasma membrane triggering phospholipids loss. That was supported by the increase in MDA level. Altogether, we emphasized a dynamic trafficking of porphyrins within cellular barriers concluding that it is highly linked to their chemical structures and behaviours.

Upon crossing cellular barriers, TPPS and TPPC were able to induce an oxidative burst and overcome defense components as well as cause homeostasis disturbance by means of membrane peroxidation, ROS generation, antioxidative enzyme inhibition and alteration of buffering capacity. We finally discussed the ultimate outcome of photodynamic treatment and determined the mode of cell death although plant cell death is clearly questionable (Gadjev et al 2008, Reape and McCabe, 2010, Van Doorn, 2011, Vartapetian et al 2011, Rantong and Gunawardena 2015, Locato and De Gara 2018). Basing on morphological, biochemical and molecular hallmarks, we revealed that photodynamic cell death in porphyrin-treated TBY-2 is

in agreement with apoptosis-like plant cell death as we outlined the evidence of membrane shrinkage, caspase-like activities and DNA fragmentation.

Taken together, novel information concerning structure-activity relationship, interaction with plant cell wall, cellular photodynamic mechanisms were gathered. Our study will be valuable for drug-cell interaction, rather it constitutes the first step for photosensitizers application on plants or in the context of an agronomic APDT.

IV. General conclusion

In my PhD work, I conducted in parallel two studies to validate the possibility to use APDT in agricultural domain. The first approach was performed on two unrelated plant species: Arabidopsis and tomato to explore a possible agronomic application and the second one on TBY-2 cells to explore the fundamental aspect of the photodynamic stress induced by anionic porphyrins. Our great question was: is it possible to imagine APDT strategy as a valuable, eco-friendly and alternative approach in agriculture from both sides: plants and plant pathogens? According to my work on the “green” side, the answer is yes, APDT could be a reality. Nevertheless, further investigations on plant pathogens, adventices, soil wildlife and water quality should be required to validate this approach. Some aspects of this tremendous work will be monitored by Veronica Ambrosini (PhD student). Thus, our presented study on plants is just the beginning of a promising story. Indeed, APDT applied to the field of agriculture is may be still a dream but could be pretty soon a reality.

V. Perspectives and outlook

Some specific points must be considered to achieve this work on TBY-2 cell and PS interactions and validation of APDT approach.

As molecular biologist, it is of importance now to decipher signaling process and/or regulation of gene expression influenced by ROS generation underlying the differential responses upon TPPC and TPPS photodynamic treatments in TBY-2 cells using molecular tools such as transcriptomic profiling and/or proteomic approach. Indeed, as TBY-2 cells share some common features with tumor cells and microorganisms such as high proliferation rate and active metabolisms, such genetic studies will be meaningful for PDT applied to cancerology.

According to our biological and chemical studies (Chapter II), porphyrin characterization and TBY-2 cell wall interaction supported the involvement of structural neutrality (carried by TPPC) in the interaction with plant cell barriers and the crossing towards cytosolic compartment. To gain insight in neutrality hypothesis, we tested Tetrakis(4-hydroxyphenyl) prophyrine (THPP) at very low concentration (0.1 μ M) that led to a very important cell death (47% cell death after 3h light exposure, data not shown). This neutral porphyrin soluble in water is for the moment the strongest that we never tested, and it is in favour to our hypothesis relative to the power of PS and its neutrality. Further experiments are to be made to confirm this finding.

As cellular biologist working hand by hand with chemist, it will be amazing to follow porphyrin traffic inside the cells. As we showed *in planta* or TBY-2 we can already follow porphyrins by confocal microscopy under spectral acquisition. Nevertheless, porphyrin fluorescence emission at around 640 nm remains very weak and quite difficult to detect. In order to overcome such drawback, molecular dyads were synthesized before I started my PhD. It consists in porphyrin conjugation with fluorophores as fluorescein resulting in a stronger fluorescence when light excited (Rezazgui et al. 2016). However, these smart constructs were not water-soluble and then not suitable for common use in biology (Figure 11).

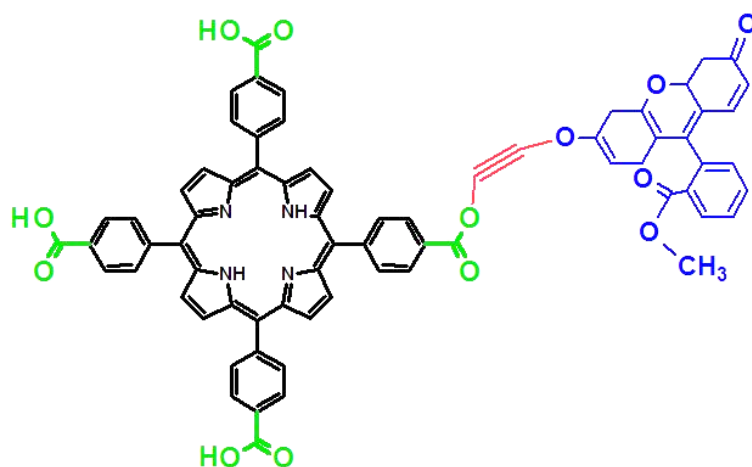


Figure 11. Structure of molecular dyad coupling TPPC with fluorescein via alkyne linker.

The linker is shown in red and fluorescein moiety is shown in blue.

Recently, nanoparticles have drawn so much interest in medical domain owing to their ability to drug delivery through a controlled manner in the optimum dose, minimizing drug side effects and drug vectorization to its target site. Furthermore, poorly water-soluble drugs are encapsulated in nanocarriers as biopolymer-based nanoparticles (cellulose, lignin and proteins nanodevices) or mesoporous silica nanoparticles to become soluble in water (Wilczewska et al. 2012, Gary-Bobo et al. 2012, Nitta and Numata 2013). Therefore, we think that encapsulation of dyads with such nanocarriers could overcome their lipophilicity.

As our previous work (Chapter I) demonstrated an eradication of Arabidopsis plantlets, porphyrins could also be considered as weed killer, in other terms herbicides. Thus, it would be interesting and informative to test them on a large panel of different noxious species or adventices like dandelion, quackgrass, common ragweed, bindweed. Our secondary challenge could be also to destroy the unwanted flora in fields. Taking into account both APDT and herbicidal effect, a double target strategy based on the use of a photoactivated, but also photodegradable and degradable porphyrin could be reasonably proposed. In the aim to enlarge our PS study that should not be restricted to porphyrin molecules, a larger panel of PS including phenothiazinium dyes as methylene blue, phenalenones, phthalocyanines, hyericin should be tested on plant and plant cells.

Finally, although several studies have been carried so far (2014-2018) involving ex vivo, in vitro and in vivo photodynamic inactivation of fungal and bacterial pathogens in

addition to PS spotting on their corresponding host leaves, host responses as well as evaluation of PS administration methods are missing. Until now, these studies are restricted to perennial plants that hindered PS activity due to their anatomical strength excepted for the herbaceous low-growing strawberry that were damaged upon sunlight-activated coumarins and furocoumarins (De Menezes et al. 2014a). Our group will focus its study on the grey mold *Botrytis cinerea* and its corresponding hosts (grapevine and potato plantlets) (V. Ambrosini, PhD).

References

- Abrahamse, H., and Hamblin, M.R. 2016. New photosensitizers for photodynamic therapy. *Biochemical Journal* **473**: 347–364.
- Agostinis, P., Berg, K., Cengel, K.A., Foster, T.H., Girotti, A.W., Gollnick, S.O., Hahn, S.M., Hamblin, M.R., Juzeniene, A., Kessel, D., et al. 2011. Photodynamic therapy of cancer: an update. *CA: A Cancer Journal for Clinicians* **61**: 250–281.
- Almeida, A., Cunha, A., Faustino, M.A.F., Tomé, A.C., and Neves, M.G.P.M.S. 2011. Porphyrins as Antimicrobial Photosensitizing Agents In: Hamblin, M.R., and G. Jori, Eds., *Comprehensive Series in Photochemical & Photobiological Sciences*. Cambridge: Royal Society of Chemistry, pp. 83–160.
- Alves, E., Faustino, M.A.F., Neves, M.G.P.M.S., Cunha, Â., Nadais, H., and Almeida, A. 2015. Potential applications of porphyrins in photodynamic inactivation beyond the medical scope. *Journal of Photochemistry and Photobiology C: Photochemistry Reviews* **22**: 34–57.
- Arrojado, C., Pereira, C., Tomé, J.P.C., Faustino, M.A.F., Neves, M.G.P.M.S., Tomé, A.C., Cavaleiro, J.A.S., Cunha, Â., Calado, R., Gomes, N.C.M., et al. 2011. Applicability of photodynamic antimicrobial chemotherapy as an alternative to inactivate fish pathogenic bacteria in aquaculture systems. *Photochemical & Photobiological Sciences* **10**: 1691–1701.
- Azizullah, A., Rehman, Z.U., Ali, I., Murad, W., Muhammad, N., Ullah, W., and Häder, D.-P. 2014. Chlorophyll derivatives can be an efficient weapon in the fight against dengue. *Parasitology Research* **113**: 4321–4326.
- Azzouzi, A.R., Barret, E., Moore, C.M., Villers, A., Allen, C., Scherz, A., Muir, G., Wildt, M. de, Barber, N.J., Lebdai, S., et al. 2013. TOOKAD[®] Soluble vascular-targeted photodynamic (VTP) therapy: determination of optimal treatment conditions and assessment of effects in patients with localised prostate cancer. *BJU International* **112**: 766–774.
- Babilas, P., Schreml, S., Landthaler, M., and Szeimies, R.-M. 2010. Photodynamic therapy in dermatology: state-of-the-art. *Photodermatology, Photoimmunology & Photomedicine* **26**: 118–132.
- Babu, P.S.S., Manu, P.M., Dhanya, T.J., Tapas, P., Meera, R.N., Surendran, A., Aneesh, K.A., Vadakkancheril, S.J., Ramaiah, D., Nair, S.A., et al. 2017. Bis(3,5-diiodo-2,4,6-trihydroxyphenyl) squaraine photodynamic therapy disrupts redox homeostasis and induce mitochondria-mediated apoptosis in human breast cancer cells. *Scientific Reports* **7**: 42126–42140.
- Baptista, M.S., Cadet, J., Di Mascio, P., Ghogare, A.A., Greer, A., Hamblin, M.R., Lorente, C., Nunez, S.C., Ribeiro, M.S., Thomas, A.H., et al. 2017. Type I and type ii photosensitized oxidation reactions: guidelines and mechanistic pathways. *Photochemistry and Photobiology* **93**: 912–919.
- Barker, C.A., Zeng, X., Bettington, S., Batsanov, A.S., Bryce, M.R., and Beeby, A. 2007. Porphyrin, phthalocyanine and porphyrazine derivatives with multfluorenyl substituents as

efficient deep-red emitters. *Chemistry - A European Journal* **13**: 6710–6717.

Bartolomeu, M., Reis, S., Fontes, M., Neves, M., Faustino, M., and Almeida, A. 2017. Photodynamic Action against Wastewater Microorganisms and Chemical Pollutants: An Effective Approach with Low Environmental Impact. *Water* **9**: 630-647.

Bassham, J.A. 1959. Photosynthesis. *Journal of Chemical Education* **36**: 549-554.

Beale, S.I. 1990. Biosynthesis of the tetrapyrrole pigment precursor, δ -aminolevulinic acid, from glutamate. *Plant Physiology* **93**: 1273–1279.

Benov, L. 2015. Photodynamic Therapy: Current Status and Future Directions. *Medical Principles and Practice* **24**: 14–28.

Berg, K., Selbo, P.K., Weyergang, A., Dietze, A., Prasmickaite, L., Bonsted, A., Engesaeter, B., Angell-petersen, E., Warloe, T., and Frandsen, N. 2005. Porphyrin-related photosensitizers for cancer imaging and therapeutic applications. *Journal of Microscopy* **218**: 133–147.

Brzezowski, P., Richter, A.S., and Grimm, B. 2015. Regulation and function of tetrapyrrole biosynthesis in plants and algae. *Biochimica et Biophysica Acta (BBA) - Bioenergetics* **1847**: 968–985.

Buchovec, I., Lukseviciute, V., Marsalka, A., Reklaitis, I., and Luksiene, Z. 2016. Effective photosensitization-based inactivation of Gram (–) food pathogens and molds using the chlorophyllin–chitosan complex: towards photoactive edible coatings to preserve strawberries. *Photochemical & Photobiological Sciences* **15**: 506–516.

Buck, S.T.G., Bettanin, F., Orestes, E., Homem-de-Mello, P., Imasato, H., Viana, R.B., Perussi, J.R., and Silva, A.B.F. da 2017. Photodynamic Efficiency of Xanthene Dyes and Their Phototoxicity against a Carcinoma Cell Line: A Computational and Experimental Study. *Journal of Chemistry* **2017**: 1–9.

Carvalho, C.M., Tome, J.P., Faustino, M.A., Neves, M.G., Tome, A.C., Cavaleiro, J.A., Costa, L., Alves, E., Oliveira, A., and Cunha, A. 2009. Antimicrobial photodynamic activity of porphyrin derivatives: potential application on medical and water disinfection. *Journal of Porphyrins and Phthalocyanines* **13**: 574–577.

Costa, L., Alves, E., Carvalho, C.M.B., Tomé, J.P.C., Faustino, M.A.F., Neves, M.G.P.M.S., Tomé, A.C., Cavaleiro, J.A.S., Cunha, Â., and Almeida, A. 2008. Sewage bacteriophage photoinactivation by cationic porphyrins: a study of charge effect. *Photochemical & Photobiological Sciences* **7**: 415-423.

Dąbrowski, J.M., and Arnaut, L.G. 2015. Photodynamic therapy (PDT) of cancer: from local to systemic treatment. *Photochemical & Photobiological Sciences* **14**: 1765–1780.

Dąbrowski, J.M., Pucelik, B., Regiel-Futyra, A., Brindell, M., Mazuryk, O., Kyzioł, A., Stochel, G., Macyk, W., and Arnaut, L.G. 2016. Engineering of relevant photodynamic processes through structural modifications of metallotetrapyrrolic photosensitizers. *Coordination Chemistry Reviews* **325**: 67–101.

Dagani, R. 1992. fullerenes in nature: C60 and C70 found in ancient Russian rock. *Chemical & Engineering News* **70**: p. 6.

References

- Daub, M.E. 1982. Cercosporin, a photosensitizing toxin from *Cercospora* species. *Phytopathology* **72**: 370-374.
- Daub, M.E., Herrero, S., and Chung, K.-R. 2005. Photoactivated perylenequinone toxins in fungal pathogenesis of plants. *FEMS Microbiology Letters* **252**: 197–206.
- Davies, K.S., Linder, M.K., Kryman M.W., and Detty, M.R. 2016. Extended rhodamine photosensitizers for photodynamic therapy of cancer cells. *Bioorganic & Medicinal Chemistry* **24**: 3908–3917.
- Delcanale, P., Montali, C., Rodríguez-Amigo, B., Abbruzzetti, S., Bruno, S., Bianchini, P., Diaspro, A., Agut, M., Nonell, S., and Viappiani, C. 2016. Zinc-substituted myoglobin is a naturally occurring photo-antimicrobial agent with potential applications in food decontamination. *Journal of Agricultural and Food Chemistry* **64**: 8633–8639.
- De Menezes, H.D., Pereira, A.C., Brancini, G.T.P., Leão, H.C., Massola Júnior, N.S., Bachmann, L., et al. 2014a. Furocoumarins and coumarins photoinactivate *Colletotrichum acutatum* and *Aspergillus nidulans* fungi under solar radiation. *Journal of photochemistry and Photobiology B: Biology* **131**: 74–83.
- De Menezes, H.D., Rodrigues, G.B., Teixeira, S.P., Massola, N.S., Bachmann, L., Wainwright, M., et al. 2014b. In vitro photodynamic inactivation of plant-pathogenic fungi *Colletotrichum acutatum* and *Colletotrichum gloeosporioides* with novel phenothiazinium photosensitizers. *Applied and Environmental Microbiology* **80**: 1623–1632.
- De Menezes, H.D., Tonani, L., Bachmann, L., Wainwright, M., Braga, G.U.L., Marcia Regina Kress, M.R.V.Z. 2016. Photodynamic treatment with phenothiazinium photosensitizers kills both ungerminated and germinated microconidia of the pathogenic fungi *Fusarium oxysporum*, *Fusarium moniliforme* and *Fusarium solani*. *Journal of Photochemistry and Photobiology B: Biology* **164**: 1-12.
- DiCosmo, F., Towers G.H.N. and Lam, j. 1982. Photo-induced fungicidal activity elicited by naturally occurring thiophene derivatives. *Journal of Pest science* **13**: 589-594.
- Ding, H., Yu, H., Dong, Y., Tian, R., Huang, G., Boothman, D.A., Sumer, B.D., and Gao, J. 2011. Photoactivation switch from type II to type I reactions by electron-rich micelles for improved photodynamic therapy of cancer cells under hypoxia. *Journal of Controlled Release* **156**: 276–280.
- Drogat, N., Barrière, M., Granet, R., Sol, V., and Krausz, P. 2011. High yield preparation of purpurin-18 from *Spirulina maxima*. *Dyes and Pigments* **88**: 125–127.
- Drogat, N., Gady, C., Granet, R., and Sol, V. 2013. Design and synthesis of water-soluble polyaminated chlorins and bacteriochlorins with near-infrared absorption. *Dyes and Pigments* **98**: 609-614.
- Dumoulin, F., Durmuş, M., Ahsen, V., and Nyokong, T. 2010. Synthetic pathways to water-soluble phthalocyanines and close analogs. *Coordination Chemistry Reviews* **254**: 2792–2847.
- Durantini, A.M., Heredia, D.A., Durantini, J.E., and Durantini, E.N. 2018. BODIPYs to the

rescue: Potential applications in photodynamic inactivation. *European Journal of Medicinal Chemistry* **144**: 651–661.

Ebermann, R., Alth, G., Kreitner, M., and Kubin, A. 1996. Natural products derived from plants as potential drugs for the photodynamic destruction of tumor cells. *Journal of Photochemistry and Photobiology B: Biology* **36**: 95–97.

Evstigneev, V.B. 1965. On the mechanism of photosensitizing action of chlorophyll. *Photochemistry and Photobiology* **4**: 171–182.

Fayyaz, F., Rahimi, R., Rassa, M., and Yaghoobi, R.Z. 2015. Photodynamic Antimicrobial Chemotherapy, A Pathway for Photo-Inactivation of Bacteria by Porphyrin Compounds In: Proceedings of the 1st International Electronic Conference on Molecular Science, Sciforum Electronic Conference Series.

Feese, E., Sadeghifar, H., Gracz, H.S., Argyropoulos, D.S., and Ghiladi, R.A. 2011. Photobactericidal porphyrin-cellulose nanocrystals: synthesis, characterization, and antimicrobial properties. *Biomacromolecules* **12**: 3528–3539.

Fracarolli, L., Rodrigues, G.B., Pereira, A.C., Massola Júnior, N.S., Silva-Junior, G.J., Bachmann, L., et al. 2016. Inactivation of plant-pathogenic fungus *Colletotrichum acutatum* with natural plant-produced photosensitizers under solar radiation. *Journal of Photochemistry and Photobiology B: Biology* **162**: 402–411.

Gadjev, I., Stone, J.M., and Gechev, T.S. 2008. Programmed cell death in plants. In: International Review of Cell and Molecular Biology. Elsevier, pp. 87–144.

Gary-Bobo, M., Hocine, O., Brevet, D., Maynadier, M., Raehm, L., Richeter, S., Charasson, V., Looock, B., Morère, A., Maillard, P., et al. 2012. Cancer therapy improvement with mesoporous silica nanoparticles combining targeting, drug delivery and PDT. *International Journal of Pharmaceutics* **423**: 509–515.

Glueck, M., Schamberger, B., Eckl, P., and Plaetzer, K. 2017. New horizons in microbiological food safety: Photodynamic Decontamination based on a curcumin derivative. *Photochemical & Photobiological Sciences* **16**: 1784–1791.

Gonzales, J.C., Brancini, G.T.P., Rodrigues, G.B., Silva-Junior, G.J., Bachmann, L., Wainwright, M., et al. 2017. Photodynamic inactivation of conidia of the fungus *Colletotrichum abscissum* on *Citrus sinensis* plants with methylene blue under solar radiation. *J. Photochemistry and Photobiology B: Biology*. **176**: 54–61.

Grimm, B. 1998. Novel insights in the control of tetrapyrrole metabolism of higher plants. *Current Opinion in Plant Biology* **1**: 245–250.

Guldi, D.M., Mody, T.D., Gerasimchuk, N.N., Magda, D., and Sessler, J.L. 2000. Influence of Large Metal Cations on the Photophysical Properties of Texaphyrin, a Rigid Aromatic Chromophore. *Journal of the American Chemical Society* **122**: 8289–8298.

Guillaumot, D., Issawi, M., Da Silva, A., Leroy-Lhez, S., Sol, V., and Riou, C. 2016. Synergistic enhancement of tolerance mechanisms in response to photoactivation of cationic

tetra (N-methylpyridyl) porphyrins in tomato plantlets. *Journal of Photochemistry and Photobiology B: Biology* **156**: 69–78.

Häder, D.-P., Schmidl, J., Hilbig, R., Oberle, M., Wedekind, H., and Richter, P. 2016. Fighting fish parasites with photodynamically active chlorophyllin. *Parasitology Research* **115**: 2277–2283.

Hager, B., Strauss, W.S.L., and Falk, H. 2009. Cationic Hypericin Derivatives as Novel Agents with Photobactericidal Activity: Synthesis and Photodynamic Inactivation of *Propionibacterium acnes*. *Photochemistry and Photobiology* **85**: 1201–1206.

Hazen, M.J., Villaneuva, A., and Stockert, J.C. 1987. Induction of sister chromatid exchanges in *Allium cepa* meristematic cells exposed to meso-tetra (4-pyridyl) porphine and hematoporphyrin photoradiation. *Journal of Photochemistry and Photobiology B: Biology* **46**: 463–467.

Hazen, M.J., and Gutierrez-Gonzalvez, M.G. (1988). UV-mediated toxic bioactivity of harmine in the meristematic cells of *Allium cepa*. *Mutagenesis* **3**: 333–335.

Henderson, B.W., Sumlin, A.B., Owczarczak, B.L., and Dougherty, T.J. 1991. Bacteriochlorophyll-a as photosensitizer for photodynamic treatment of transplantable murine tumors. *Journal of Photochemistry and Photobiology B: Biology* **10**: 303–313.

Hill, R. 1937. Oxygen Evolved by Isolated Chloroplasts. *Nature* **139**: 881–882.

Huang, H.C., and Hasan, T. 2014. The nano world in photodynamic therapy. *Austin Journal of Nanomedicine & Nanotechnology* **2**: 4–8.

Hong, E.J., Choi, D.G., and Shim, M.S. 2016. Targeted and effective photodynamic therapy for cancer using functionalized nanomaterials. *Acta Pharmaceutica Sinica B* **6**: 297–307.

Horne, T.K., and Cronjé, M.J. 2014. Novel Porphyrazine Derivatives show Promise for Photodynamic Therapy despite Restrictions in Hydrophilicity. *Photochemistry and Photobiology* **90**: 648–658.

Huang, L., Huang, Y.-Y., Mroz, P., Tegos, G.P., Zhiyentayev, T., Sharma, S.K., Lu, Z., Balasubramanian, T., Krayner, M., Ruzie, C., et al. 2010. Stable synthetic cationic bacteriochlorins as selective antimicrobial photosensitizers. *Antimicrobial Agents and Chemotherapy* **54**: 3834–3841.

Hohmann-Marriott, M.F., and Blankenship, R.E. 2011. Evolution of photosynthesis. *Annual Review of Plant Biology* **62**: 515–548.

Hsu, Y.-C., Chiang, C.-P., Chen, J.W., Lee, J.-W., and How, M.-H. 2010. Topical chlorophyll-pheophytin derivative-mediated photodynamic therapy for DMBA-induced hamster buccal pouch premalignant lesions: an in vivo study In: Kessel, D.H., Ed., pp. 755118–755127.

Issawi, M., Muhieddine, M., Girard, C., Sol, V. and Riou, C. 2017. Unexpected features of exponentially growing Tobacco Bright Yellow-2 cell suspension culture in relation to excreted extracellular polysaccharides and cell wall composition. *Glycoconjugate Journal*

References

34: 585-590.

Issawi, M., Guillaumot, D., Sol, V., and Riou, C. 2018. Responses of an adventitious fast growing plant to photodynamic stress: comparative study of anionic and cationic porphyrin effect on *Arabidopsis thaliana*. *Physiologia Plantarum* **162**: 379-390.

Jesus, V., Martins, D., Branco, T., Valério, N., Neves, M.G.P.M.S., Faustino, M.A.F., et al. 2018. An insight into the photodynamic approach *versus* copper formulations in the control of *Pseudomonas syringae* pv. *actinidiae* in kiwi plants. *Photochemical and Photobiological Sciences*. **17**: 180-191.

Josefsen, L.B., and Boyle, R.W. 2008. photodynamic therapy and the development of metal-based photosensitisers. *Metal-Based Drugs* **2008**: 267109–267132.

Joshi, P., and Saenz, C. 2013. Recent Advances in developing improved agents for photodynamic therapy, in Handbook of Photomedicine, 2011, pp. 227-267.

Junqueira, J.C., Ribeiro, M.A., Rossoni, R.D., Barbosa, J.O., Querido, S.M.R., and Jorge, A.O.C. 2010. Antimicrobial photodynamic therapy: photodynamic antimicrobial effects of malachite green on *Staphylococcus*, Enterobacteriaceae, and *Candida*. *Photomedicine and Laser Surgery* **28**: 67–72.

Juzenienne, A. 2009. Chlorin e6-based photosensitizers for photodynamic therapy and photodiagnosis. *Photodiagnosis and Photodynamic Therapy* **6**: 94-96.

Kataoka, H., Nishie, H., Hayashi, N., Tanaka, M., Nomoto, A., Yano, S., and Joh, T. 2017. New photodynamic therapy with next-generation photosensitizers. *Annals of Translational Medicine* **5**: 183–183.

Kessel, D., and Oleinick, N.L. 2018. Cell Death Pathways Associated with Photodynamic Therapy: An Update. *Photochemistry and Photobiology* **94**: 213–218.

Kharkwal, G.B., Sharma, S.K., Huang, Y.-Y., Dai, T., and Hamblin, M.R. 2011. Photodynamic therapy for infections: Clinical applications: PHOTODYNAMIC THERAPY FOR INFECTIONS. *Lasers in Surgery and Medicine* **43**: 755–767.

Konopka, K., and Goslinski, T. 2007. Photodynamic Therapy in Dentistry. *Journal of Dental Research* **86**: 694–707.

Králová, J., Kejík, Z., Bříza, T., Kaplánek, R., Záruba, K., Martásek, P., and Král, V. (2014) Design, Synthesis, Selective Recognition Properties and Targeted Drug Delivery Application in Handbook of Porphyrin Science With Applications to Chemistry, Physics, Materials Science, Engineering, Biology and Medicine. Volume 33: Applications — Part II (Kadish, K.M., Smith, K.M., and Guillard, R. eds.) pp. 1-75.

Krasnovsky, A.A., and Brin, G.P. 1947. Photosensitizing agent of Mg-phtalocyanine and chlorophyll in solution.

Krieger-Liszkay, A. 2004. Singlet oxygen production in photosynthesis. *Journal of Experimental Botany* **56**: 337–346.

Kubat, P., Lang, K., and Azenbacher Jr., P. 2004. Modulation of porphyrin binding to swrum

References

Mohammad ISSAWI | Thèse de doctorat | Université de Limoges | 2018

Licence CC BY-NC-ND 3.0

albumin by pH. *Biochimica et Biophysica Acta* **1670**: 40-48.

Lhotáková, Y., Plíštil, L., Morávková, A., Kubát, P., Lang, K., Forstová, J., and Mosinger, J. 2012. Virucidal Nanofiber Textiles Based on Photosensitized Production of Singlet Oxygen. *PLoS ONE* **7**: 11-20.

Liu, Y.C., Tu, S.Y., Lin, H.Y. 2015. Evaluation of the practicality of melanin as a photodynamic-inactivation agent photosensitizer by its nanonization. *Journal of Photopolymer Science and Technology* **28**: 739-746.

Locato, V., and De Gara, L. 2018. Programmed Cell Death in Plants: An Overview, in: De Gara, L., and V. Locato, Eds., Plant Programmed Cell Death. New York, NY: Springer New York, pp. 1–8.

Luksiene, Z., and Brovko, L. 2013. Antibacterial photosensitization-based treatment for food safety. *Food Engineering Reviews* **5**: 185–199.

Lukšienė, Ž., Danilčenko, H., Tarasevičienė, Ž., Anusevičius, Ž., Marozienė, A., and Nivinskis, H. 2007. New approach to the fungal decontamination of wheat used for wheat sprouts: Effects of aminolevulinic acid. *International Journal of Food Microbiology* **116**: 153–158.

Maisch, T., Szeimies, R.-M., Lehn, N., and Abels, C. 2005. Antibacterial photodynamic therapy. A new treatment for bacterial skin diseases? *Der Hautarzt* **56**: 1048–1055.

Maisch, T., Eichner, A., Späth, A., Gollmer, A., König, B., Regensburger, J., and Bäumler, W. 2014. Fast and effective photodynamic inactivation of multiresistant bacteria by cationic riboflavin derivatives. *PLoS ONE* **9**: 1-18.

Mandal, A.K., Sahin, T., Liu, M., Lindsey, J.S., Bocian, D.F., and Holten, D. 2016. Photophysical comparisons of PEGylated porphyrins, chlorins and bacteriochlorins in water. *New Journal of Chemistry* **40**: 9648–9656.

Master, A., Livingston, M., and Sen Gupta, A. 2013. Photodynamic nanomedicine in the treatment of solid tumors: Perspectives and challenges. *Journal of Controlled Release* **168**: 8-40.

Matsubara, T., Kusuzaki, K., Matsumine, A., Murata, H., Marunaka, Y., Hosogi, S., Uchida, A., and Sudo, A. 2010. Photodynamic therapy with acridine orange in musculoskeletal sarcomas. *Bone & Joint Journal* **92**: 760–762.

McCoy, C.P., O’Neil, E.J., Cowley, J.F., Carson, L., De Baróid, Á.T., Gdowski, G.T., Gorman, S.P., and Jones, D.S. 2014. Photodynamic antimicrobial polymers for infection control. *PLoS ONE* **9**: 108500-108511.

McCullagh, C. and Robertson, P.K.J. 2006. Photosensitized Destruction of *Chlorella vulgaris* by Methylene blue or nuclear fast red combined with hydrogen peroxide under visible light irradiation. *Environmental Science & Technology* **40**: 2421–2425.

Molero, M.L., and Hazen, M.J. 1988. Photodynamic effect of acridine orange, eosin Y and orcein in a plant system in vivo measured by the sister chromatid exchanges test. *Journal of Plant Physiology* **132**: 636–637.

References

Mohammad ISSAWI | Thèse de doctorat | Université de Limoges | 2018

Licence CC BY-NC-ND 3.0

Molero, M.L., Hazen, M.J., and Stockert, J.C. 1985. Photodynamic effect of berberine sulfate on the growth rate of *Allium cepa* roots. *Journal of Plant Physiology* **120**: 91–94.

Monteiro, J.S.C., Oliveira, S.C.P.S. de, Pires Santos, G.M., Pires Sampaio, F.J., Pinheiro Soares, L.G., and Pinheiro, A.L.B. 2017. Effectiveness of antimicrobial photodynamic therapy (AmPDT) on *Staphylococcus aureus* using phenothiazine compound with red laser. *Lasers in Medical Science* **32**: 29–34.

Montoya, S.C.N., Comini, L.R., Sarmiento, M., Becerra, C., Albesa, I., Argüello, G.A., and Cabrera, J.L. 2005. Natural anthraquinones probed as Type I and Type II photosensitizers: singlet oxygen and superoxide anion production. *Journal of Photochemistry and Photobiology B: Biology* **78**: 77–83.

Mroz, P., Yaroslavsky, A., Kharkwal, G.B., and Hamblin, M.R. 2011. Cell Death Pathways in Photodynamic Therapy of Cancer. *Cancers* **3**: 2516–2539.

Muehler, D., Sommer, K., Wennige, S., Hiller, K.-A., Cieplik, F., Maisch, T., and Späth, A. 2017. Light-activated phenalen-1-one bactericides: efficacy, toxicity and mechanism compared with benzalkonium chloride. *Future Microbiology* **12**: 1297–1310.

Nagata, T., Nemoto, Y., and Hasezawa, S. 1992. Tobacco BY-2 cell line as the “Hela” cell in the cell biology of higher plants. *International Review of Cytology* **132**: 1-31.

Nazir, M., El Maddah, F., Kehraus, S., Egereva, E., Piel, J., Brachmann, A.O., and König, G.M. 2015. Phenalenones: insight into the biosynthesis of polyketides from the marine alga-derived fungus *Coniothyrium cereale*. *Organic & Biomolecular Chemistry* **13**: 8071-8080.

Nitta, S., and Numata, K. 2013. Biopolymer-Based Nanoparticles for Drug/Gene Delivery and Tissue Engineering. *International Journal of Molecular Sciences* **14**: 1629–1654.

Ogawa, K., and Kobuke, Y. 2008. Recent advances in two-photon photodynamic therapy. *Anti-Cancer Agents in Medicinal Chemistry (Formerly Current Medicinal Chemistry-Anti-Cancer Agents)* **8**: 269–279.

Orlob, G.B. 1967. Inactivation of purified plant viruses and their nucleic acids by photosensitizing dyes. *Virology* **31**: 402–413.

Ormond, A., and Freeman, H. 2013. Dye Sensitizers for Photodynamic Therapy. *Materials* **6**: 817–840.

Plaetzer, K., Berneburg, M., Kiesslich, T., and Maisch, T. 2013. New applications of photodynamic therapy in biomedicine and biotechnology. *BioMed Research International* **1**–3.

Pohl, J., Saltsman, I., Mahammed, A., Gross, Z. and Röder, B. 2014. Inhibition of green algae growth by corrole-based photosensitizers. *Journal of Applied Microbiology* **118**: 305–312.

Rantong, G., and Gunawardena, A.H.L.A.N. 2015. Programmed cell death: genes involved in signaling, regulation, and execution in plants and animals. *Botany* **93**: 193–210.

References

Reape, T.J., and McCabe, P.F. 2010. Apoptotic-like regulation of programmed cell death in plants. *Apoptosis* **15**: 249–256.

Rezazgui, O., Trouillas, P., Qiu S.H., Siegler, B., Gierschner, J., Leroy-Lhez, S. 2016. Synthesis and conformation of a novel fluorescein-Zn-porphyrin dyad and intramolecular energy transfer. *New Journal of Chemistry* **40**: 3843-3856.

Richter, A.S., and Grimm, B. 2013. Thiol-based redox control of enzymes involved in the tetrapyrrole biosynthesis pathway in plants. *Frontiers in Plant Science* **4**: 1-11.

Ringot, C., Sol, V., Barrière, M., Saad, N., Bressollier, P., Granet, R., Couleaud, P., Frochot, C., and Krausz, P. 2011. Triazinyl Porphyrin-Based Photoactive Cotton Fabrics: Preparation, Characterization, and Antibacterial Activity. *Biomacromolecules* **12**: 1716–1723.

Riou, C., Calliste, C.A., Da Silva, A., Guillaumot, D., Rezazgui, O., Sol, V., et al. 2014. Anionic porphyrin as a new powerful cell death inducer of Tobacco Bright Yellow-2 cells. *Photochemical and Photobiological Sciences* **13**: 621-625.

Rishi, P., and Agarwal, V. 1972. Current Role of Photodynamic Therapy in Ophthalmic Practice. *Lancet* **2**: 1175–7.

Robertson, C.A., Evans, D.H., and Abrahamse, H. 2009. Photodynamic therapy (PDT): A short review on cellular mechanisms and cancer research applications for PDT. *Journal of Photochemistry and Photobiology B: Biology* **96**: 1–8.

Rodionov, D.A., Vitreschak, A.G., Mironov, A.A., and Gelfand, M.S. 2003. Comparative Genomics of the Vitamin B₁₂ Metabolism and Regulation in Prokaryotes. *Journal of Biological Chemistry* **278**: 41148–41159.

Salci, A., and Toprak, M. 2017. Spectroscopic investigations on the binding of Pyronin Y to human serum albumin. *Journal of Biomolecular Structure and Dynamics* **35**: 8–16.

Senge, M.O., MacGowan, S.A., and O'Brien, J.M. 2015. Conformational control of cofactors in nature – the influence of protein-induced macrocycle distortion on the biological function of tetrapyrroles. *Chemical Communications* **51**: 17031–17063.

Senge, M., Ryan, A., Letchford, K., MacGowan, S., and Mielke, T. 2014. Chlorophylls, Symmetry, Chirality, and Photosynthesis. *Symmetry* **6**: 781–843.

Sessler, J.L., and Miller, R.A. 2000. Texaphyrins: new drugs with diverse clinical applications in radiation and photodynamic therapy. *Biochemical Pharmacology* **59**: 733–739

Shin, H., Yoon, J.-S., Koh, W., Kim, J.Y., Kim, C.-H., Han, K.M., Kim, E.J., and Kwon, O. 2016. Nonpigmented hair removal using photodynamic therapy in animal model: nonpigmented hair removal using photodynamic therapy. *Lasers in Surgery and Medicine* **48**: 748–762.

Sieber, F., Krueger, G.J., O'Brien, J.M., Schober, S.L., Sensenbrenner, L.L. and Sharkis S.J. 1989. Inactivation of Friend Erythroleukemia Virus and Friend Virus-Transformed Cells by Merocyanine 540-Mediated Photosensitization *Blood* **73**: 45-350.

Skwor, T.A., Klemm, S., Zhang, H., Schardt, B., Blaszczyk, S., and Bork, M.A. 2016.

References

Mohammad ISSAWI | Thèse de doctorat | Université de Limoges | 2018

Licence CC BY-NC-ND 3.0

Photodynamic inactivation of methicillin-resistant *Staphylococcus aureus* and *Escherichia coli*: a metalloporphyrin comparison. *Journal of Photochemistry and Photobiology B: Biology* **165**: 51–57.

Song, R., Feng, Y., Wang, D., Xu, Z., Li, Z., and Shao, X. 2017. Phytoalexin phenalenone derivatives inactivate mosquitolarvae and root-knot nematode as type-ii photosensitizer. *Scientific Reports* **7**: 42058-42067.

Spaeth, A., Graeler, A., Maisch, T., and Plaetzer, K. 2017. CureCuma—cationic curcuminoids with improved properties and enhanced antimicrobial photodynamic activity. *European Journal of Medicinal Chemistry*.

Tanaka, R., and Tanaka, A. 2007. Tetrapyrrole Biosynthesis in Higher Plants. *Annual Review of Plant Biology* **58**: 321–346.

Tanaka, M., Kinoshita, M., Yoshihara, Y., Shinomiya, N., Seki, S., Nemoto, K., Hirayama, T., Dai, T., Huang, L., Hamblin, M.R., et al. 2012. Optimal Photosensitizers for Photodynamic Therapy of Infections Should Kill Bacteria but Spare Neutrophils. *Photochemistry and Photobiology* **88**: 227–232.

Tegos, G.P., Demidova, T.N., Arcila-Lopez, D., Lee, H., Wharton, T., Gali, H., and Hamblin, M.R. 2005. Cationic fullerenes are effective and selective antimicrobial photosensitizers. *Chemistry & Biology* **12**: 1127–1135.

Thandu, M., Comuzzi, C., and Goi, D. 2015. Phototreatment of water by organic photosensitizers and comparison with inorganic semiconductors. *International Journal of Photoenergy* 1–22.

Thomas, A.P., Saneesh Babu, P.S., Asha Nair, S., Ramakrishnan, S., Ramaiah, D., Chandrashekar, T.K., Srinivasan, A., and Radhakrishna Pillai, M. 2012. *meso*-Tetrakis (*p*-sulfonatophenyl) N-Confused Porphyrin Tetrasodium Salt: A Potential Sensitizer for Photodynamic Therapy. *Journal of Medicinal Chemistry* **55**: 5110–5120.

Tripathy, B.C., Sherameti, I., and Oelmüller, R. 2010. Siroheme: an essential component for life on earth. *Plant Signaling & Behavior* **5**: 14–20.

Uebelhoer, N.S., and Dover, J.S. 2005. Photodynamic therapy for cosmetic applications. *Dermatologic Therapy* **18**: 242–252.

Valicsek, Z., and Horváth, O. 2013. Application of the electronic spectra of porphyrins for analytical purposes: The effects of metal ions and structural distortions. *Microchemical Journal* **107**: 47–62.

Van Doorn, W.G. 2011. Classes of programmed cell death in plants, compared to those in animals. *Journal of Experimental Botany* **62**: 4749–4761.

Van straten, D., Mashayekhi, V., Bruijn, H. de, Oliveira, S., and Robinson, D. 2017. Oncologic Photodynamic Therapy: Basic Principles, Current Clinical Status and Future Directions. *Cancers* **9**: 19-73.

Villiers, F., and Kwak, J.M. 2013. Rapid apoplasmic pH measurement in *Arabidopsis* leaves using a fluorescent dye. *Plant Signaling & Behavior* **8**: 22587-22590.

References

Mohammad ISSAWI | Thèse de doctorat | Université de Limoges | 2018

Licence CC BY-NC-ND 3.0

- Wilczewska, A.Z., Niemirowicz, K., Markiewicz, K.H., and Car, H. 2012. Nanoparticles as drug delivery systems. *Pharmacological Reports* **64**: 1020–1037.
- Wilson, B.C., and Patterson, M.S. 2008. The physics, biophysics and technology of photodynamic therapy. *Physics in Medicine and Biology* **53**: 61–109.
- Yoshida, A., Sasaki, H., Toyama T., Araki M., Fujioka, J., Tsukiyama, K., Hamada, N., and Yoshino, F. 2017. Antimicrobial effect of blue light using *Porphyromonas gingivalis* pigment. *Scientific reports* **7**: 5225-5234.
- Yin, R., Agrawal, T., Khan, U., Gupta, G.K., Rai, V., Huang, Y.-Y., and Hamblin, M.R. 2015. Antimicrobial photodynamic inactivation in nanomedicine: small light strides against bad bugs. *Nanomedicine* **10**: 2379–2404.
- Yoon, H.E., Oh, S.H., kim, S.A., Yoon, J.H., and Ahn, S.G. 2014. Pheophorbide a-mediated photodynamic therapy induces autophagy and apoptosis via the activation of MAPKs in human skin cancer cells. *Oncology Reports* **31**: 137-144.
- Zhao, J., Wu, W., Sun, J., and Guo, S. 2013. Triplet photosensitizers: from molecular design to applications. *Chemical Society Reviews* **42**: 5323.

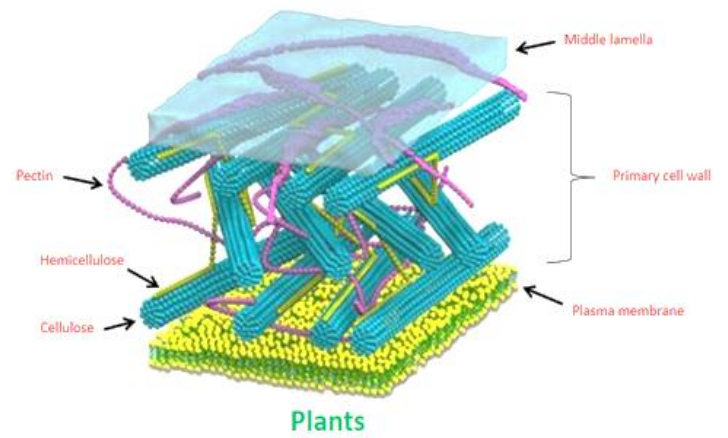
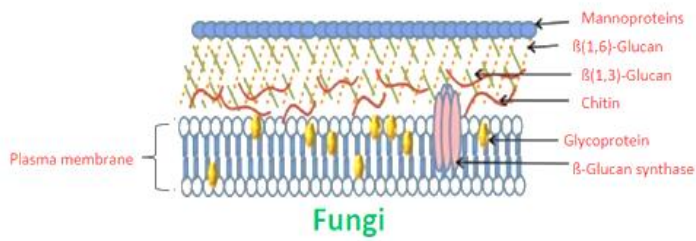
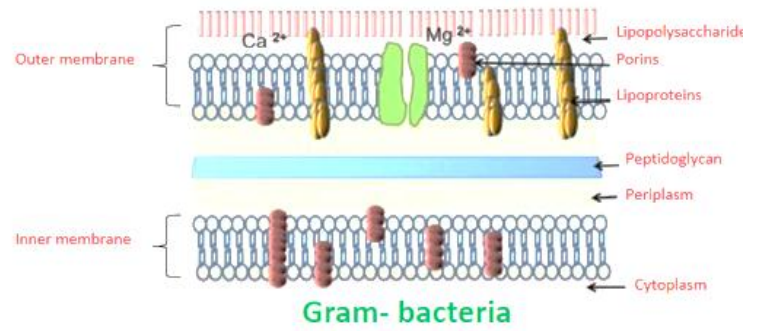
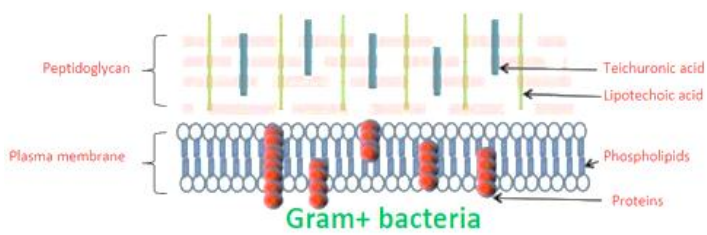
Annex 1

Cell wall composition of microorganisms *Porosity represents the hole size of peptidoglycan in bacterial cell wall, chitin-glucan matrix in fungal cell wall and pectin in plant cell wall. Porosity of fungal cell wall is highly variable and depends to species. It can vary from 1 to 400 nm. As well, molecular sieving tightly depends on fungal species and vary between 5 and 270 kDa.

	Gram+ bacteria	Gram- bacteria	Fungi	Plants
Thickness	20-80 nm	10-15 nm	45 nm	0.2 μ m
Composition	Peptidoglycan + teichuronic and lipoteichoic acids	Peptidoglycan + outer-membrane of phospholipids and lipopolysaccharides	Chitin-glucan + mannoproteins	Pectin + hemicellulose + cellulose
Charge	negative	negative	negative	negative
Porosity (nm) *	2.12	2.06	Variable	3-20
Nature of sieved molecules	Polysaccharides, glycopeptides, antimicrobials	Hydrophilic compounds	Polysaccharides, proteins, lipids	Ions, water - soluble molecules
Size limit of sieved molecules*	30000-57000 Da	< 600-700 Da	Variable	300000-60000 Da

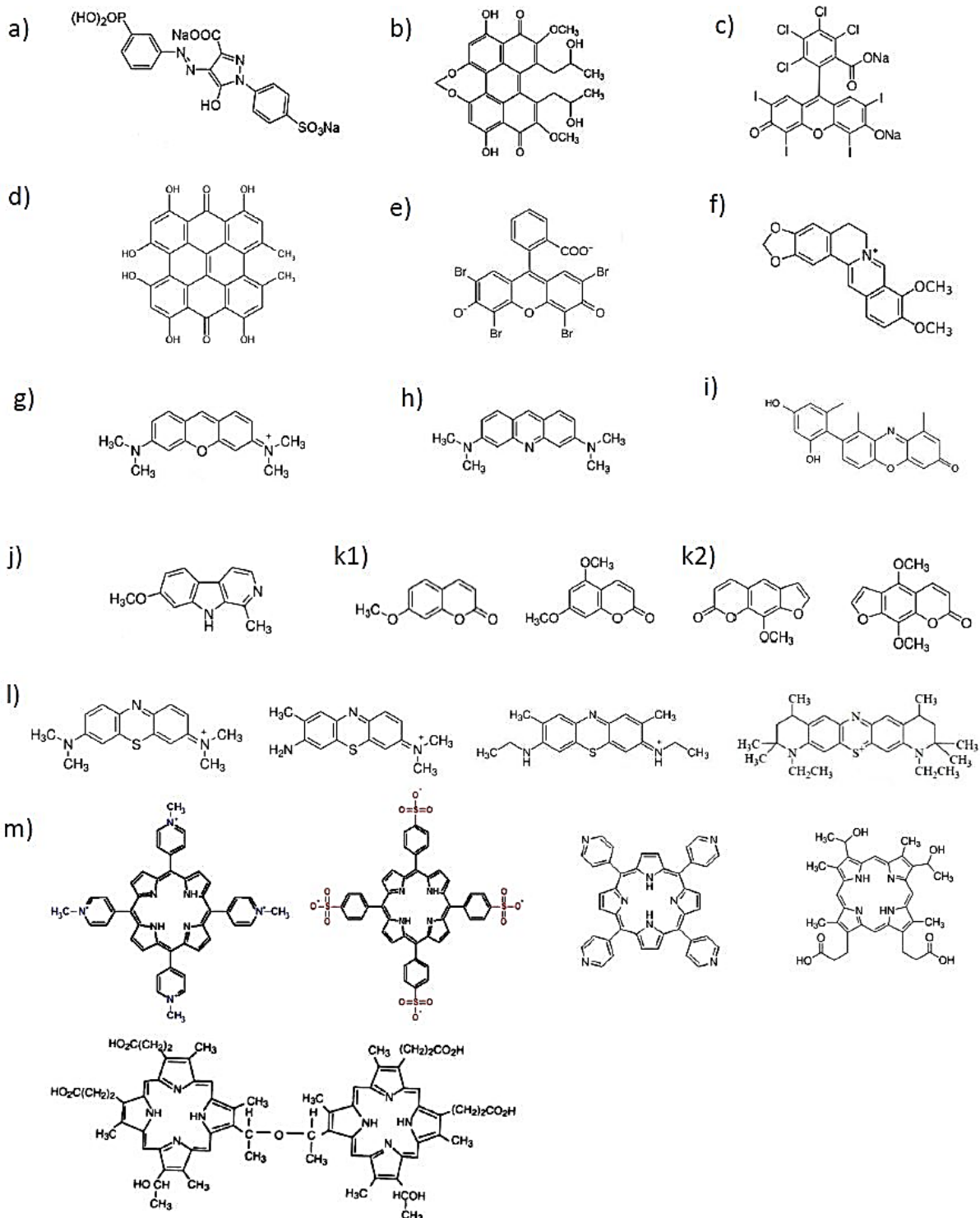
Annex 2

Cell wall structure of Gram+, Gram- bacteria, Fungi and plants.



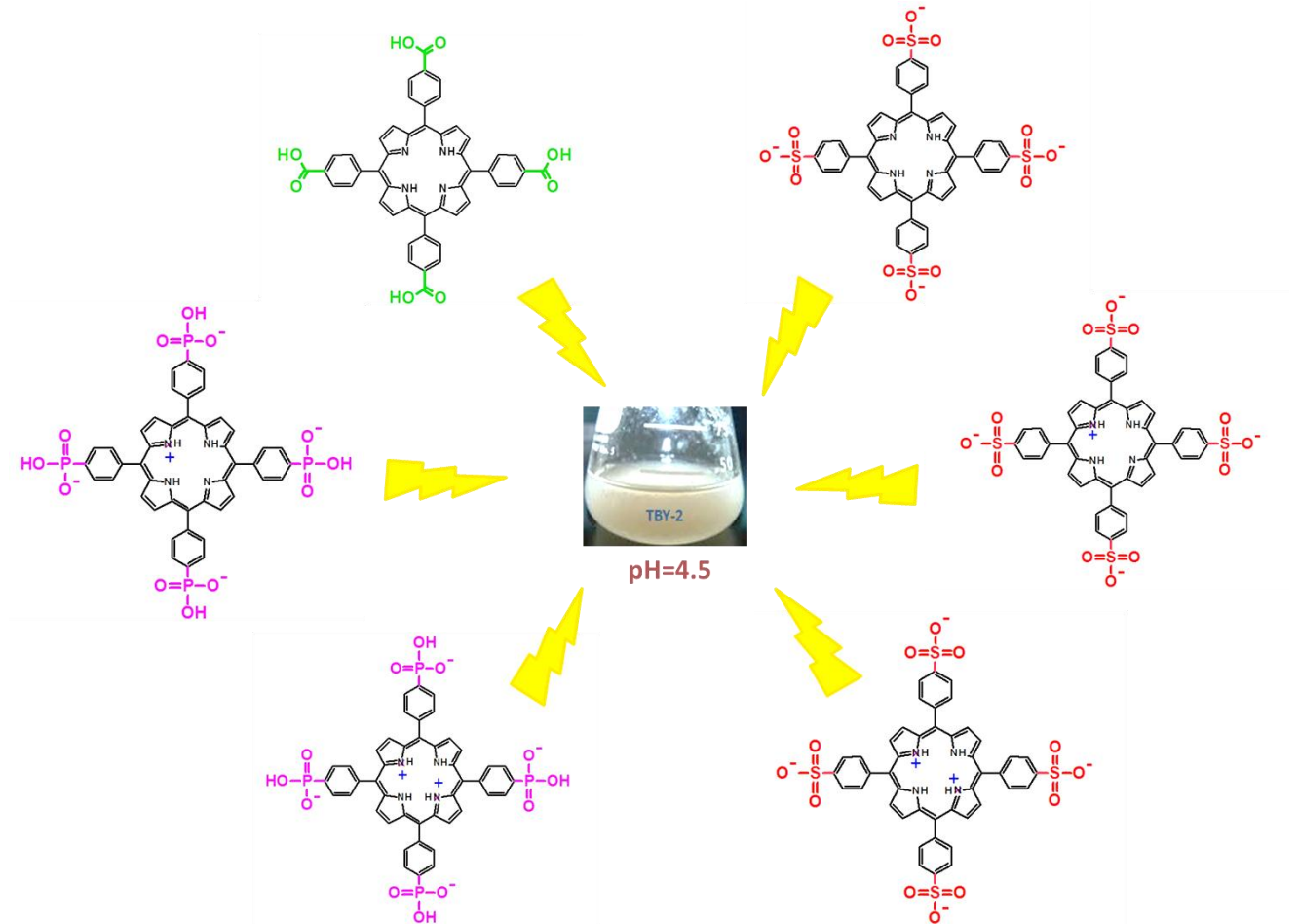
Annex 3

Structures of exogenous PS supplied to plant materials. a) Procion yellow. b) Cercosporin. c) Rose Bengal. d) Hypericin. e) Eosin Y. f) Berberine. g) Pyronin Y. h) Acridin orange. i) Orcein. j) Harmine k1) Coumarins and k2) Fucocoumarins. l) Phenothiazinium dyes. m) Porphyrins (upper panel: TMPyP, TPPS, TPyP, HP; lower panel: HPD).



Annex 4

Structures of porphyrins at the time they interact with exponential growing TBY-2 cells (pH=4.5). TPPC is shown in green, TPPS species are shown in red, TPPP species are shown in purple, positive charges that indicate protonation of the core are shown in blue.



MOHAMMAD ISSAWI

🏠 13, Petit Faubourg Manigne 87000, Limoges-France
📅 09/01/1991, Beirut-Lebanon
❤️ Single
✉️ mohammad.issawi@unilim.fr
☎️ +33624483373
📄 Researchgate.net/profile/Mohammad_Issawi
🚗 Driving licence B



LANGUAGES

Arabic ●●●●●
French ●●●●●
English ●●●●●

INFORMATICS

Microsoft office, statistic tools (SPSS, OiginPro, R programming, PAST software), bio-informatic tools, Image processing (Image J, Photoshop).

TECHNICS

Molecular Biology, Cellular Biology and Physiology, Biochemistry, *In Vitro* culture.

COMMUNICATION AND LEADERSHIP SKILLS

Good teamwork integrations, strategical thinking, problem solving, and master's student supervision.

HOBBIES

Football, literature, music, travelling.

CAREER PATH

- 2009 — High school diploma in Life science, with Distinction - Education and teaching high school, Lebanon.
2012 — Bachelor's degree in general biology (Average 73.23/100) – Lebanese University, Lebanon
2012 — DELF B2 “Diplôme en langue française” (70/100) – French institute of Beirut, Lebanon
2012/2013 — Master 1 Plant biology and environment, with Distinction - Lebanese University, Lebanon
2013/2014 — Master 2 (research) Applied plant biotechnology with highest honors - Lebanese University, Lebanon.
2014 — M2 Internship entitled “Response of lignification to drought and salinity stresses through cinnamyl alcohol dehydrogenase enzyme in Barley” - Shahid Beheshti University, Iran.
2015-2018 — PhD in Plant physiology entitled « Plant photodynamic stress: study of molecular and cellular mechanisms in plant and plant cells upon porphyrin treatment» - University of Limoges, France.

PUBLICATIONS

- **Mohammad Issawi**, Vincent Sol and Catherine Riou (2018) Plant photodynamic stress: what's new? *Frontiers in Plant Science* DOI: 10.3389/fpls.2018.00681 (IF 4.29).
- **Mohammad Issawi**, Damien Guillaumot, Vincent Sol and Catherine Riou (2018) Responses of an adventitious fast-growing plant to photodynamic stress: comparative study of anionic and cationic porphyrin effect on *Arabidopsis thaliana*. *Physiologia Plantarum* DOI: 10.1111/ppl.12666 (IF 3.33)
- **Mohammad Issawi**, Mohammad Muhieddine, Céline Girard, Vincent Sol and Catherine Riou (2017) Unexpected features of exponentially growing Tobacco Bright Yellow-2 cell suspension culture in relation to excreted extracellular polysaccharides and cell wall composition. *Glycoconjugate Journal* DOI: 10.1007/s10719-017-9782-7 (IF 2.2).
- Damien Guillaumot, **Mohammad Issawi**, Anne Blondeau, Stephanie Lhez, Vincent Sol and Catherine Riou (2016) Synergistic enhancement of tolerance mechanisms in response to photoactivation of cationic tetra (N-methylpyridyl) porphyrins in tomato plantlets. *Journal of Photochemistry and Photobiology B Biology* DOI: 10.1016/j.jphotobiol.2016.01.015 (IF 2.96).
- **Mohammad Issawi**, Stéphanie Leroy-Lhez, Vincent Sol and Catherine Riou “Crossing the first threshold: New insights in the Influence of chemical structure of anionic porphyrins from cell wall interactions to photodynamic cell death induction in TBY-2 suspension culture”. (Ongoing)
- Stéphanie Leroy-Lhez, Olivier Rezazgui, **Mohammad Issawi**, Mourad Elhabiri, Claude Calliste and Catherine Riou “Characterization of pH dependent charge states and physico-chemical properties of anionic porphyrins” Submitted to *Photochemical and Photobiological Sciences* (IF 2.34).
- **Mohammad Issawi**, Veronica Ambrosini, Vincent Sol and Catherine Riou “Starchy surprise: new ability of TBY-2 cells to synthesize an amylose-rich starch in presence of auxin.” (Ongoing)

CONGRESS ATTENDED

- (IPA 2017) ● International photodynamic association - Coimbra, Portugal. Contribution: poster presentation entitled: Photoactivation of cationic tetra (N-methylpyridyl) porphyrin dramatically altered *Arabidopsis thaliana* plantlet development.
- (SFBV 2016) ● Société française de biologie végétale - Angers, France. Contribution: oral presentation entitled: Comparative study of three anionic porphyrins in Tobacco Bright Yellow-2 cells: from cell wall interaction and localization to phototoxic damage and cell defense.

Réponses des plantes et des cellules végétales au stress photodynamique induit par les porphyrines

Le traitement photodynamique antimicrobien (acronyme anglais APDT) est apparu comme une solution alternative pour lutter contre les microorganismes multi-résistants. Cette méthode basée sur l'utilisation de photosensibilisateurs dont les porphyrines, fonctionne aussi contre les agents pathogènes des plantes ce qui nous a conduit à proposer une approche de type APDT dans le domaine de l'agriculture. Au cours de ce travail de thèse, nous nous sommes intéressés au côté « vert » de la mise en place de cette approche en réalisant une étude approfondie sur des plantules de deux espèces végétales: *Arabidopsis thaliana* et *Lycopersicon esculentum* (tomate) et sur une suspension cellulaire de tabac (TBY-2). Des porphyrines anioniques et cationiques hydrosolubles ont été testées. Nous avons montré qu'aucune de ces porphyrines testées à forte concentration ($\geq 80 \mu\text{M}$) n'était cytotoxique à l'obscurité sur les plantules ou la suspension. Par contre sous photopériode (16h), les porphyrines cationiques testées à faible concentration (3,5 μM) se sont révélées létales pour les plantules d'*Arabidopsis* alors qu'elles n'ont fait que ralentir la croissance des plantules de tomate. Étonnamment, les porphyrines anioniques même testées à forte concentration n'ont pas (ou très peu) induit d'altérations de croissance des plantules. Cette situation se trouve inversée dans les cellules TBY-2 qui sont beaucoup plus sensibles aux porphyrines anioniques photoactivées qui induisent leur mort par apoptose. Ce modèle cellulaire nous a permis de comprendre i) les mécanismes d'interaction porphyrines anioniques avec la paroi cellulaire et ii) quels mécanismes étaient mis en place dans les cellules en réponse au stress photodynamique. En conclusion, ces études préliminaires sur le végétal laissent sérieusement entrevoir la possibilité de développer l'APDT en agriculture ciblée aux pathogènes de plantes et sans effet notable sur les plantes d'intérêt agronomique et les microorganismes du sol.

Mots-clés : Porphyrines, Photosensibilisateurs, stress photodynamique des plantes, *Arabidopsis thaliana*, *Lycopersicon esculentum*, cellules TBY-2, agriculture.

Responses of plants and plant cells to porphyrin-induced photodynamic stress

Antimicrobial photodynamic treatment (APDT) has emerged as an alternative modality to strive against multidrug-resistant microorganisms. This method, based on the use of photosensitizers including porphyrins, has also shown substantial efficiency to kill plant pathogens. This led us to propose an APDT approach in the field of agriculture. During this thesis work, we were interested in the "green" side of this approach. Thus, we performed an in-depth study on two plant species: *Arabidopsis thaliana* and *Lycopersicon esculentum* (tomato) and on Tobacco Bright Yellow-2 suspension culture (TBY-2 cells) using anionic and cationic water-soluble porphyrins. We have shown that none of these porphyrins tested at high concentration ($\geq 80 \mu\text{M}$) was cytotoxic on plantlets or suspension cells under dark conditions. On the other hand, the cationic porphyrins tested at low concentration (3.5 μM) were lethal for *Arabidopsis* while they only slowed the growth of tomato plantlets under 16 h photoperiod. Surprisingly, the same anionic porphyrins tested at high concentrations did not induce growth alterations of both plantlets. This situation is reversed in TBY-2 cells, which are much more sensitive to photoactivated anionic porphyrins that induce apoptosis-like cell death. TBY-2 cells allowed to understand i) the interactions of anionic porphyrins with the cell wall and ii) the induced cellular and molecular mechanisms in response to photodynamic stress. In conclusion, these preliminary studies on the plants and plant cells suggest the possibility of developing APDT in agriculture. It will be targeted to plant pathogens without any side effects on plants of agronomic interest and soil microorganisms.

Keywords: Porphyrins, photosensitizers, plant photodynamic stress, *Arabidopsis thaliana*, *Lycopersicon esculentum*, TBY-2 cells, agriculture.

